# Real Time Computer Controlled Adaptive Active Suspension: An Analytical and Experimental Investigation

Satya Srinivas Vallurupalli

A Thesis
in
The Department
of
Mechanical Engineering

Presented in Partial Fulfillment of the Requirements
for
the Degree of Doctor of Philosophy
at
Concordia University
Montreal, Quebec, Canada

February 1996

ISBN 0-612-18452-8

Canada

# Abstract

## Real Time Computer Controlled Adaptive Active Suspension: An Analytical and Experimental Investigation

Satya Srinivas Vallurupalli

Suspensions play a crucial role in optimizing a vehicle for stability and ride comfort. Suspension design has always been a critical factor, and is becoming even more important due to increasing customer demands for safety and comfort. The wider use of automobiles in the transportation sector increases demand for a comfortable ride, however this demand runs counter to vehicle highway safety. This reduction of vehicle highway safety itself runs counter to the raising of or complete removal of speed limits. Hence it is all the more important to examine the vehicle suspension as an optimization problem involving handling and comfort. The application of active chassis control systems such as Antilock Brake Systems (ABS), Automatic Stability Control plus Traction (ASC+T), Electronic damping control and Directional Stability Control (DSC) has raised the performance targets for traction, braking and lateral stability control. Research in the past has indicated that positive benefits can be attained by using active suspension either independently or by integrating it with the above mentioned systems. The conventional control schemes involving fixed gains used for the active suspension could not effectively be modulated to achieve improved performance over a wide range of vehicle operating conditions. Adaptive control of active suspensions can be applied to achieve an optimal performance even under rapid changes in the input (different road profiles and velocities) and operational vehicle parameter variations during longitudinal manoeuvres thereby reducing nose dive and squat. This dissertation presents an analytical and experimental investigation of the new concept of adaptive active suspension to achieve the above specified target regarding optimal performance.

Adaptive control for the single degree of f- edom (SDOF) nonlinear time vary ing (NTV) vehicle failsafe active suspension model has been formulated in a contin uous and discrete time domain. Simulation results indicate that an optimal per formance and static equilibrium maintenance has been achieved irrespective of large dynamic parameter variations at different road profiles by adapting to the sky hook ref erence model. A comparative study of the model reference adaptive control (MRAC) approach and the stochastic optimal control approach has also been made. Adaptive control approach for the general multi-degree of freedom (MDOF) NTV suspension model has been presented by extending the MRAC approach using feedforward, feed back and auxiliary controller parameters. Adaptive control of an active suspension for a half-car model MDOF system has been formulated based on discrete model ref erence adaptive control (DMRAC) with recursive least square estimation and covari ance modification. Deterministic auto-regressive moving average (DARMA) models for a linearized half-car and for a dual skyhook reference model have been devel oped. A modified version of the least square estimation in which the parameters are updated as a matrix which thereby reduces the order of the projection operator ma trix and consequently the computational efforts is presented. Computer simulation results indicate that the concept achieves the optimal reference model performance and maintains static equilibrium position, thereby eliminating nose dive and squat during braking and acceleration manoeuvres respectively. Experimental validation of the concept has been performed by modelling a full scale (1:1) SDOF failsafe ac tive suspension model of a Porsche 928 car and fabricating the setup. A generalized discrete adaptive active suspension simulator software has been developed. The test results indicate good adaptation and validate the feasibility of the concept. Various automotive applications for potential use of the concept are discussed.

# Acknowledgement

Jotting the final drops of ink after getting through the tough but jolly times, I would like to acknowledge many people who made this possible.

First and foremost I would like to thank my supervisors Dr.M.O.M.Osman and Dr.R.V.Dukkipati for their supervision and financial support without which this endeavor would not have been possible. I appreciate their support and high standards in terms of the goal of the project "to develop a new and advanced concept that takes the research community small strides ahead". Special thanks are extended to Dr.S.Rakheja and Dr.R.V.Patel even in their busy schedules were able to squeeze in a few valuable moments for me. I am very thankful to my supervisors for the financial support. *Natural Sciences and Engineering Research Council (NSERC) Canada, Grant Nos. A5181, A36332 and La Formation de cherecheurs et d'action concertee of the gouvernment of Quebec, Grant No. 042-110* are also acknowledged.

I would like to thank the people responsible for resources at CONCAVE Research Center, Fluid Dynamics Lab., Computer Center and Machine Shop. I take this glorious moment to acknowledge and thank the following people for sharing their expertise and helping me get over the big hurdle of experimental validation. Dale Rathwell and Danny Juras for those long days at CONCAVE Research Center. John Elliot, Wesley Fitch, Joseph Hulet and Henry for hardware and computer resources. Thanks to Hans, Paul Scheiwiller, George and Mike Brennan for turning and grinding the metal for me.

A special word of thanks for my wife Rani and for my friend Singu Babu for their help in being part of the balancing act between thesis completion and my work at Chrysler Corporation. I would also like to thank my brother "thannu" and sister-in-law "Sudha" for their help in many ways. I appreciate all the help and glorious moments I had with my friends at Concordia.

**SPECIAL THANKS**

to my wife *Rani*

for her support and understanding.

**DEDICATED**

to my *Parents*

for their support.

# Contents

# List of Figures

## Chapter 3

## Chapter 4

## Chapter 5

## Chapter 6

## Chapter 7

## Chapter 8



## Appendix D

# Nomenclature

| | |
|---|---|
| $a$ | Acceleration of the vehicle ($\frac{m}{s^2}$) |
| $A(\omega)$, $B(\omega)$ | Fourier integral constants |
| $A(q^{-1}), \cdots$ *etc.* | Polynomial representation in the left difference operator |
| *c.g.* | Centre of gravity |
| $C(t)$ | Constant of Proportionality in linear damping ($\frac{Ns}{m}$) [SDOF model] |
| $C_v(t)$ | Constant of proportionality in nonlinear orifice damping ($\frac{Ns^2}{m^2}$) [SDOF model] |
| $C_l^*$, $C_t^*$ | Nominal damping constant at leading and trailing nonlinear orifice dampers ($\frac{Ns^2}{m^2}$) [Half-car model] |
| $C_{m_l}$, $C_{m_t}$ | Equivalent linear damping constant of proportionality at the leading and trailing ends of reference model ($\frac{Ns}{m}$) [Half-car model] |
| $C_p$, $C_s$ | Damping constant of proportionality of the primary and secondary nonlinear orifice damping ($\frac{Ns^2}{m^2}$) [2 DOF Bounce model] |
| $d$, $\dot{d}$, $\ddot{\mathrm{d}}$ | Time delay in discrete model ($s$) |
| $d_1$ | Distance between the nominal position of c.g. and the leading axle ($m$) [Half-car model] |
| $d_2$ | Distance between the nominal position of c.g. and the trailing axle ($m$) [Half-car model] |
| $D$ | Allowable suspension deflection ($m$) |
| $D_{m_l}$, $D_{m_t}$ | Skyhook damper linear constant of proportionality at the leading and trailing ends of reference model ($\frac{Ns}{m}$) [Half-car model] |
| $D_{m_p}$, $D_{m_s}$ | Skyhook damper linear constant of proportionality for the primary and secondary masses ($\frac{Ns}{m}$) [2 DOF Bounce model] |
| $D_m$ | Skyhook damper linear constant of proportionality ($\frac{Ns}{m}$) [SDOF car model] |
| $E_{P.E}$, $E_{K.E}$, $E_{D.E}$, $E_L$ | Potential, Kinetic, Damping and Lagranges Energy terms |

| | |
|---|---|
| $E, \dot{E}$ | Error vector in model following |
| $D$, $\dot{D}$ | Large numbers compared to $D$ used in the Fourier integrals |
| $F_l$, $F_t$ | Longitudinal force applied at the leading and trailing wheel/road interface ($N$) |
| $F_k(t)$ | Stiffness force due to the suspension springs ($N$) |
| $F(t)$ | Coulomb friction constant ($N$) |
| $F_c(t)$ | Coulomb friction force ($N$) |
| $F_d(t)$ | Damping force ($N$) |
| $F_s(t)$ | Elastic limit stop force ($N$) |
| $F_{cont}$ | Control force evaluated by the controller ($N$) |
| $F_{act}$ | Actuator force signal given to the actuator ($N$) |
| $f(x)$, $g(x)$ | Functional representation |
| $g$ | Acceleration due to gravity ($\frac{m}{s^2}$) |
| $G(s)$ | Suspension transfer function |
| $G_m(s)$ | Reference model transfer function |
| $h$ | Height of the c.g. of car body above the road surface ($m$) |
| $\breve{h}$ | Sampling time interval in the discrete domain ($s$) |
| $H(\omega)$ | Linear filter transfer function |
| $\lvert H_{XW} \rvert$ | System gain factor of X with respect to W |
| $\imath$ | Complex number $\sqrt{-1}$ |
| $I_{MI}$, $I_{m_{MI}}$ | Mass moment of inertia about the c.g. of the Half-car model and the reference model ($kgm^2$) |
| $K_l(t)$, $K_t(t)$ | Stiffness constant of the leading and trailing suspension springs ($\frac{N}{m}$) [Half-car model] |
| $K(t)$ | Stiffness constant of the suspension springs ($\frac{N}{m}$) [SDOF model] |
| $K_p$, $K_s$ | Stiffness constant of the Primary and Secondary suspension springs ($\frac{N}{m}$) [2 DOF Bounce model] |
| $K_l^*$, $K_t^*$ | Nominal stiffness constants for the leading and trailing suspension ($\frac{N}{m}$) [Half-car model] |
| $K_{tire}$ | Tire stiffness ($\frac{N}{m}$) |

| | |
|---|---|
| $K_{es}(t)$ | Stiffness constant of the elastic stops $(\frac{N}{m})$ |
| $K_{es_l}, K_{es_t}$ | Stiffness constant of the leading and trailing elastic stops $(\frac{N}{m})$ |
| $K_{m_l}, K_{m_t}$ | Stiffness constants at the leading and trailing ends of reference model $(\frac{N}{m})$ [Half-car model] |
| $K_m$ | Stiffness constant for the reference model $(\frac{N}{m})$ [SDOF model] |
| $K_{m_{tire}}$ | Tire stiffness of the reference model $(\frac{N}{m})$ |
| $L$ | Total wheel base $(m)$ |
| $M_s(t)$ | Total sprung mass of the vehicle $(kg)$ [Half car model] |
| $M_s^*$ | Nominal design value of the total sprung mass of the vehicle $(kg)$ [Half-car model] |
| $M_l(t), M_t(t)$ | Load distributed onto the leading and trailing suspension of the vehicle $(kg)$ [Half-car model] |
| $M_l^*, M_t^*$ | Load distributed onto the leading and trailing suspensions due to the total nominal sprung mass $(kg)$ [Half-car model] |
| $M_{u_l}, M_{u_t}$ | Unsprung mass of the leading and trailing suspensions $(kg)$ [Half car model] |
| $M_{m_s}$ | Total sprung mass of the reference model $(kg)$ [Half-car model] |
| $M_{m_{u_l}}, M_{m_{u_t}}$ | Unsprung mass at the leading and trailing axles of the reference model $(kg)$ [Half-car model] |
| $M_p(t), M_s(t)$ | Primary and Secondary Suspension masses $(kg)$ [2 DOF Bounce Model] |
| $M(t)$ | Sprung mass $(kg)$ [SDOF model] |
| $M_m$ | Time invariant reference model sprung mass $(kg)$ [SDOF model] |
| $m, n$ | Matrices indices |
| $q^{-1}()$ | Backward shift operator |
| $q()$ | Forward shift operator |
| $R(s), S(s), T(s)$ | |
| $Q(s), Q_I(s), V(s)$ | Controller polynomials in $s$ domain |
| $P(s), M(s), W(s)$ | Transfer function polynomials in $s$ domain |
| $sgn()$ | Sign function (Nonlinear discontinuous functions) |
| $S^*()$ | Nonlinear discontinuous function in elastic stops |
| $u(t)$ | Actuator force [SDOF model] |

| | |
|---|---|
| $u_p(t), u_s(t)$ | Primary and Secondary actuator force [2DOF Bounce model] |
| $u_l(t), u_t(t)$ | Leading and Trailing actuator force [Half-car model] |
| $v$ | Longitudinal velocity of the vehicle ($\frac{m}{s}$) |
| $w(t)$, $w(t-\tau)$ | Displacement road excitation at leading and trailing wheels with a time delay of $\tau$ ($m$) [Half-car model] |
| $W_l$, $W_t$ | Total normal load at the leading and trailing wheel/road interface ($kg$) [Half-car model] |
| $x_b$ | Bounce degree of freedom of the sprung mass ($m$) [Half-car model] |
| $x_{l_1}$, $x_{t_1}$ | Bounce sprung mass DOF at the leading and trailing suspension attachment to the half-car model ($m$) [Half-car model] |
| $x_{l_2}$, $x_{t_2}$ | Bounce unsprung mass DOF at the leading and trailing axles of half-car model ($m$) [Half-car model] |
| $x_{m_b}$ | Bounce DOF of the reference model ($m$) [Half-car model] |
| $x_{m_{l_1}}$, $x_{m_{t_1}}$ | Bounce sprung mass DOF at the leading and trailing suspension attachment to the reference model ($m$) [Half-car model] |
| $x_{m_{l_2}}$, $x_{m_{t_2}}$ | Bounce unsprung mass DOF at the leading and trailing axles of the reference model ($m$) [Half-car model] |
| $x$ | Bounce DOF of the sprung mass ($m$) [SDOF model] |
| $x_m$ | Bounce DOF of the sprung mass of the reference model ($m$) [SDOF model] |
| $x_1$, $x_2$ | Bounce DOF of the two DOF bounce model ($m$) [2 DOF bounce and Chapter 2] |
| $X$, $X_m$ | State variable vector of the state space representation of the plant and reference model |
| $Y$, $Y_m$ | Output vector of the state space representation of the plant and reference model |
| $z$, $z_m$ | Relative displacement or suspension working space (Rattle space) of model and reference model ($m$) [SDOF model] |
| $\pi$ | Constant [$4 \times tan^{-1}(1)$] |
| $\aleph$ | Numerically high value |
| $\omega$ | Frequency ($Hz$) |

| | |
|---|---|
| $\vartheta_0 \cdots \vartheta_6$ | Coefficients of third order linear filter equation for random input |
| $\mu_1 \cdots \mu_5$ | Characteristic coefficients of different random road profiles |
| $\tau$ | Input time delay between leading and trailing road input ($sec.$) |
| $\Delta_{st_l}$, $\Delta_{st_t}$ | Initial static deflections at the leading and trailing suspensions due to nominal load ($m$) [Half-car model] |
| $\delta_{st_l}$, $\delta_{st_t}$ | Static deflections due to dynamic load shifts at the leading and trailing suspension ($m$) [Half-car model] |
| $\delta_{st}$ | Static deflection due to dynamic load shifts for SDOF model (m) |
| $\delta_{t_l}$, $\delta_{t_t}$ | Static tire deflection due to dynamic load shifts at the leading and trailing wheel hub ($m$) [Half-car model] |
| $\theta$, $\theta_m$ | Pitch degree of freedom of the car body ($deg.$) |
| $\Theta$ | Controller parameter vector/matrix |
| $\hat{\Theta}$ | Estimation of controller parameter vector/matrix |
| $\omega_p$, $\omega_m$ | Plant and reference model natural frequency for SDOF model ($\frac{rad}{sec}$) |
| $\eta_p$, $\eta_m$ | Damping ratio for a SDOF suspension and reference model |
| $\lambda_i$, $i = 1, m$ | Eigen values |
| $\varepsilon[\ ]$ | Mean Value |
| $\rho_1, \rho_2$ | Weighing Constants in the Performance Index ($\mathcal{PI}$) |
| $\phi_c$ | Controllability matrix |
| $\phi_o$ | Observability matrix |
| $\alpha_0 \cdots \alpha_6$ | Constants |
| $\acute{\alpha}_0 \cdots \acute{\alpha}_6$ | Constants |
| $\beta_0 \cdots \beta_6$ | Constants |
| $\acute{\beta}_0 \cdots \acute{\beta}_6$ | Constants |
| $\varepsilon_0 \cdots \varepsilon_5$ | Constants |
| $\varpi_1 \cdots \varpi_5$ | Constants |
| $\chi_1 \cdots \chi_3$ | Constants |
| $\varrho, \varphi$ | Constants |
| $\xi$, $\dot{\xi}$, $\ddot{\xi}$ | White noise derivatives for random input filter |

| | |
|---|---|
| $\mathcal{PI}$ | Performance Index |
| $\mathcal{A}$, $\mathcal{B}$, $\mathcal{C}$, $\cdots$ | Calligraphic letters represents matrix notation |
| $\mathcal{I}_m$ | Identity matrix of order $m$ |
| $\mathcal{Q}$, $\mathcal{F}$, $\mathcal{F}_1$, $\mathcal{F}_2$ | Matrices in discrete domain |
| $\mathcal{Q}_m$, $\mathcal{F}_m$ | Matrices in discrete domain of reference model |
| $\mathcal{OP}$ | Operating point of the nonlinear function |
| $\mathcal{FN}$ | Represents *"function of"* |
| $\mathcal{P}[k]$ | Estimator matrix |
| $\mathcal{V}$ | Lyapunov function |
| $\mathcal{S}(\omega)$ | Power Spectral Density function $(\frac{m^2}{Hz})$ |
| $\mathcal{S}_0$ | Power spectral density of white noise input $(\frac{m^2}{Hz})$ |
| $(t)$ | Continuous time domain representation |
| $[k]$ | Discrete time domain representation |
| $(\ )^{'}$ | Transpose |

# Chapter 1

# Introduction

## 1.1 General

Suspension design is very critical in vehicle design as it has to cater simultaneously to all of the following requirements, namely support the vehicle weight, provide guidance along the road/track, keep continuous contact between wheel and road/track to provide traction at all times, isolate carbody and passengers or freight from disturbances like road/track irregularities and external forces (like windgust, load variations) etc.. It plays a crucial role in vehicle design in providing both the stability and ride comfort at the same time. An ideal suspension system should simulate the soft suspension characteristics of luxury cars for high frequency wheel motion and the stiff response of sports cars for low-frequency body motion induced by braking and steering inputs.

## 1.2 Perspective

Contemporary suspension systems containing passive control elements such as dampers and springs have been developed to such an extent that the suspension performance would not improve unless some radical changes are made to the basic principle of sus-

pension operation. Passive suspension systems have been extensively analyzed and used to the maximum extent of their capabilities. An active suspension would either replace or act in parallel to the passive components with actuators which continuously supply and modulate the flow of energy by generating forces on the basis of a control law to achieve the required performance. An active suspension would enable the vehicle to have a lower sprung mass frequencies which would result in a better ride comfort and would also reduce suspension travel at lower frequencies, but maintains high frequency isolation characteristics of a passive suspension. The implication here is that the sprung mass frequencies can be made lower without sacrificing the static stiffness required to resist body and manoeuvring forces. The control law can contain information of any kind obtained from any where in the vehicle. The controller evaluates the control force signal on the basis of the required performance and signals from various transducers. Hence these can adapt to various levels of external forces and track irregularities to simultaneously appear hard to guidance forces and soft to road/track irregularities. The bandwidth attainable by such an active suspension is limited by the frequency response of the actuator and the control components.

Active suspensions of different forms have been pursued as an alternative for a long time and an excellent review has been published on ground transportation by Goodall and Kortüm [1], on road vehicle suspensions by Sharp and Crolla [2] and on railway vehicle active suspensions by Hedrick [3].

Chassis design has come a long way from the conventional mechanical point of view to the present electronic control systems integration. Various control systems that are being studied for vehicle performance modifications are Antilock Brake System (ABS), Automatic Stability Control (ASC), Automatic Stability Control plus Traction (ASC+T), electronic damping control, etc.. Active suspension and lateral stability monitoring (DSC) are two other systems that are still under development. Reference [4] describes how the sensory information necessary for various control systems described above could be duplicated within those systems. The results presented

in this reference also indicate that addition of active suspension would increase the effectiveness of any of the above basic systems. At the same time addition of the above described control systems to the basic active suspension may not give any added advantage. The results imply that an active suspension can be a feasible solution for replacement of many of the other independent control systems. For example, a combination of active suspension and ABS gives shorter braking distances and increased yaw stability through modulation of wheel loads.

## 1.3 Review of Active Controls in Vehicle Systems

The term active controls is used to imply the application of advanced control techniques based on micro-computer technology to the design of an overall stable system, there by liberating the designers from the restrictions on the inherent stability/unstability of the controlled system. Active controls in ground transportation are becoming successful in theoretical studies, simulation, and implementation in spite of late introduction in the field compared to other modes of transport like air and on water. The potential for active control is promising due to knowledge from the exhaustive study of passive systems, reliable and efficient software, improved computer techniques and less expensive hardware. Application of advanced controls based on micro-computer technology to motor vehicles has become a major interest to automotive control engineers. The following sections describe a general review of active controls with particular emphasis on active suspension.

### 1.3.1 Vehicular Active Controls (other than suspension)

It is natural that state of the art micro-computers and sensors should be applied to motor vehicle control to improve the dynamics, when they become available for practical application. The micro-computers were initially applied to control accessories

such as air conditioners, auto devices, displays, and later applied to control engines, transmissions, brakes and finally to control steering and suspension. This section briefly describes some examples incorporating active controls.

Active steering systems can be used to provide stability with a simple actuator to give a positive steering effect. A vehicle should have the characteristics of slight understeer to maintain directional stability at high speed. It is normally undesirable to have rear wheel steering which may reduce the rigidity of rear suspension in the lateral direction which is very important for directional stability of motor vehicles. However, power steering has come into wide use in cars and this increases the torsional rigidity of the steering system by reducing the reaction torque transmitted to the steering wheel from the front wheels, generating cornering forces. This power steering or these power actuators make the rear wheels steerable without reducing the lateral rigidity of the suspension. The active control steering could also be used for compensation of various external forces caused by lateral wind gust or lateral slope of the road which would disturb the stable travel of vehicles along their course. Iguchi [5] describes how a vehicle traveling on a straight road that slopes to the right hand side would compensate for the lateral component of the gravitational force. To maintain a straight course, the four wheels must have cornering forces to balance the lateral external force by generating the appropriate side slip angles at each wheel. A conventional car would rotate in the yaw plane to compensate while compromising comfortable driving. But an active control four-wheel steering system would steer the rear wheels to eliminate the yaw motion.

Public service buses and sight-seeing buses which run at low to medium speed in urban localities require that the steering effort at low speed be reduced and steering stability at high speed be improved. Thus to cope with this, a vehicle speed sensing power steering system has been developed which is becoming more common in passenger cars, buses and trucks [6]. This incorporates an active control that needs less steering effort at low speed and greater effort at higher speeds.

Active safety system has been another area where active controls are being applied at a wider range. Automotive safety can be secured only when humans, vehicles and their environment are well balanced [5]. To cope with the increase in the gross vehicle weight, operating speeds and traffic its very important that active controls be implemented in the braking system. Antilock braking system (ABS) are to be standardized and become the legal requirement. Also auxiliary brakes like compression engine brakes and exhaust brakes [7] are becoming more widely used.

Active controls are being implemented for accident prevention equipment such as drowsiness warning device [8], in which a micro-computer judges the degree of sudden fatigue spasmodic motions, steering wheel operation patterns such as high frequency steering wheel operation that are specific to drivers who are not completely awake. By comparing this data with stored-in data the system would detect abnormal driving to fairly high accuracy. Radar collision warning devices which would detect an object in front of the vehicle by a radar sensor and sound an alarm when the distance reduces to a predetermined value are being designed using active control systems [9]. The radar systems could also be used to sense the drivers blind spot and flash a warning.

### 1.3.2 Semi-active Suspension

The semi-active suspension device is a variable damper which is considered to provide a force equal to that which a fully active system with a good control law would give, except that when the semi-active system need to act as an energy supplier it switches off. In these systems the bandwidth is limited by the control strategy. Semi-active system behavior has been studied by Crosby and Karnopp [10], Karnopp et al. [11] and Margolis [12]. Rakheja and Sankar [13] compared the concept of an on-off damper for semi-active system employing the relative displacement and relative velocity feedback signals with the one designed by Karnopp which uses the sign of absolute velocity. Sharp and Hassan [14] considered a dissipative semi-active suspension system with

two types of control laws based on the linear optimal control. Fig.1.1 shows the semi-active system with a spring in parallel to the dissipative damper. Sharp and Hassan [15] studied the relative performance capabilities of passive, active and semi-active systems in terms of fully and partial feed-back active systems. The results indicate that the semi-active systems are not much worse in performance than the fully active

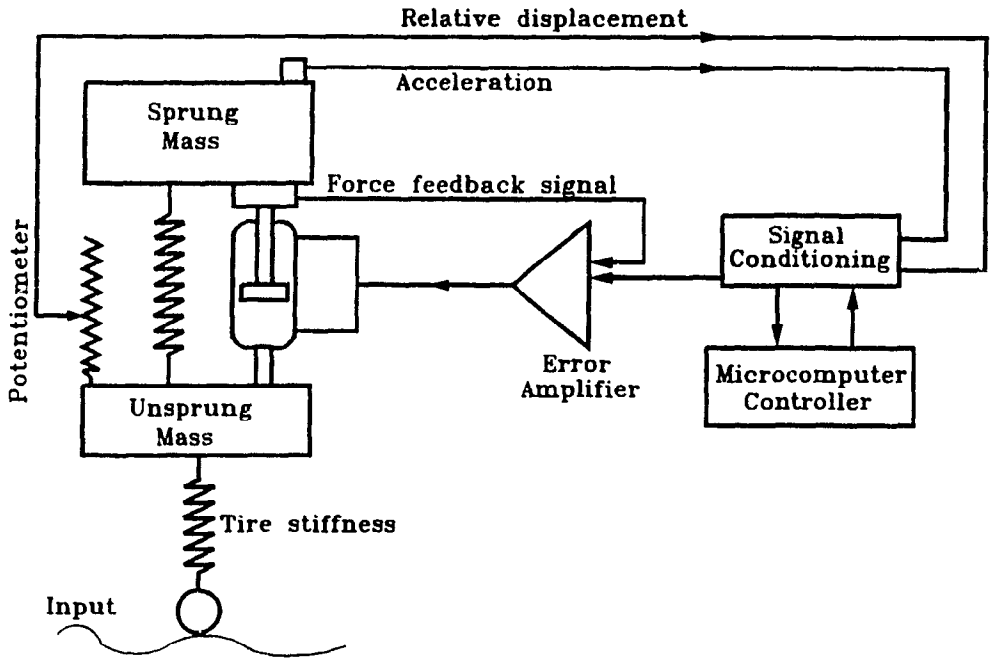


Fig.1.1: Semi active suspension system.

systems. Given the capacity to vary the control law parameters in the manner of an active system, they are capable of very good behavior over a realistic range of operating conditions. Semi-active system needs most of the measurement requirements of an active system but allow the replacement of hydraulic pump, accumulator, high performance filters, hoses, actuator and servo-valve by a rapidly adjustable damper. Simplified versions of the dissipative semi-active suspension concept are commercially available on cars as described in Refs.[16] and [17]. Here the dampers are switched

between soft and hard settings depending on the control signals from sensors monitoring vehicle speed, steer wheel angle, velocity, stop lamp switch, throttle position and acceleration.

Even though the results of semi-active and active systems show considerable advantages over the passive system, the performance would not be much enthusiastic for off-road vehicles which are enclosed with more working space relative to the road roughness. A semi-active system was developed for a single-wheel using a hydraulic strut by Automotive Products Limited (AP) and was implemented for a complete vehicle as described in Ref.[18] by Crolla et. al. The application of AP suspension for ten degree of freedom (DOF) farm transport vehicle is also discussed in Ref.[18].

The success of practical implementation of fully active and semi-active suspensions is further enhanced by autonomous low-loss hydraulic struts which make the system operate at or near zero rate as developed by Clerk [19]. Dominy [20] discusses a semi-active suspension that is capable of withstanding very high downward forces generated by "ground effect" aerodynamics while remaining soft to rapid road inputs for a Formula 1 racing car. An active damper could be defined as a subclass of semi-active suspension in which only damping forces are generated on the basis of some control law with the compliance element kept passive and passivity restriction on the damper force relaxed. A semi-active dissipating damper is found to closely track an active-damper for statistical random input by Elmadany and Abduljabbar [21].

### 1.3.3 Active Suspension

The six degrees of freedom (namely vertical, lateral and longitudinal translational motions and the rotations of yaw, roll and pitch) of a rigid body like a motor car would interact with each other. The vertical force due to weight and longitudinal manoeuvres, tire tangential force due to traction or braking and lateral force due to

cornering which are produced at the tire and road interface lead to motions in various degrees of freedom. The total vehicle weight is distributed as vertical forces, and in turn the frictional and cornering forces are mainly dependent on the vertical force at the tire patch. The distribution of vertical forces is disturbed by rolling, pitching and other motions. Hence, an active suspension which comes between the vehicle body and point of application of forces (tire contact patch) could be actively controlled to monitor the forces and achieve the required stability and control of vehicles. Review of active suspension in ground vehicles is divided into general review of active suspension, review of control strategies in active suspension which is followed by adaptive control of active suspension. The schematics of a two DOF fully active suspension system, failsafe active suspension system and slow-active suspension system are shown in Figs. 1.2, 1.3 and 1.4 respectively.

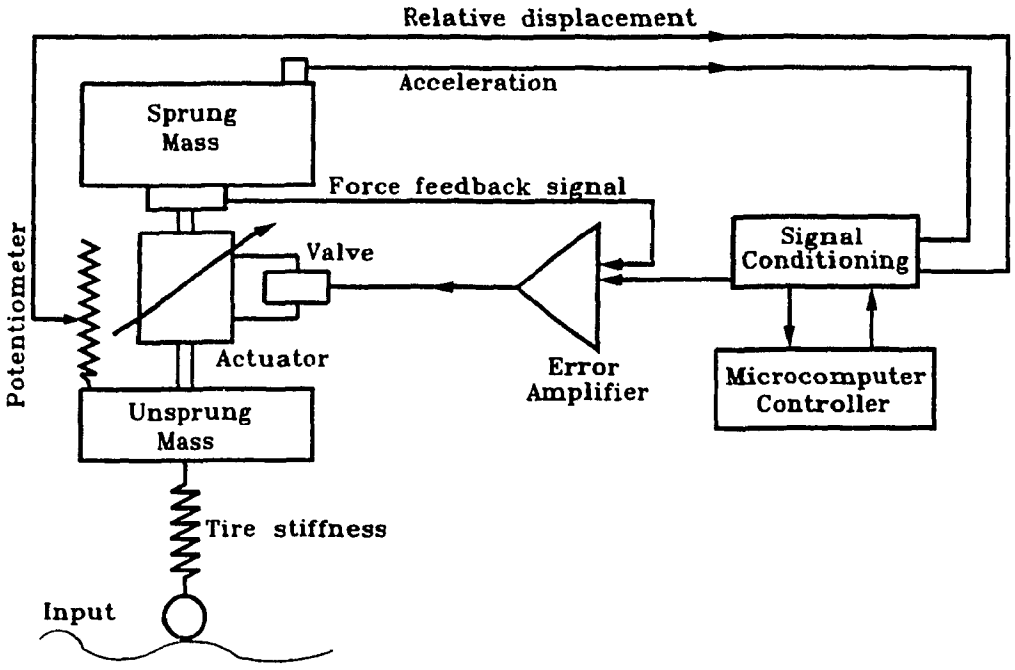


Fig.1.2: Fully active suspension system.

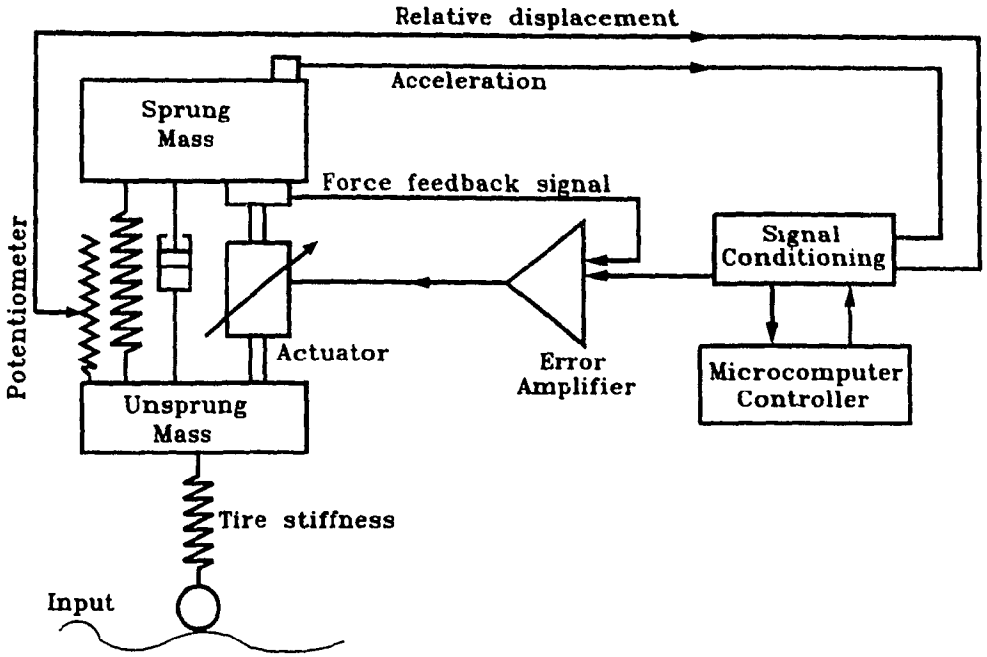


Fig.1.3: Failsafe active suspension system.

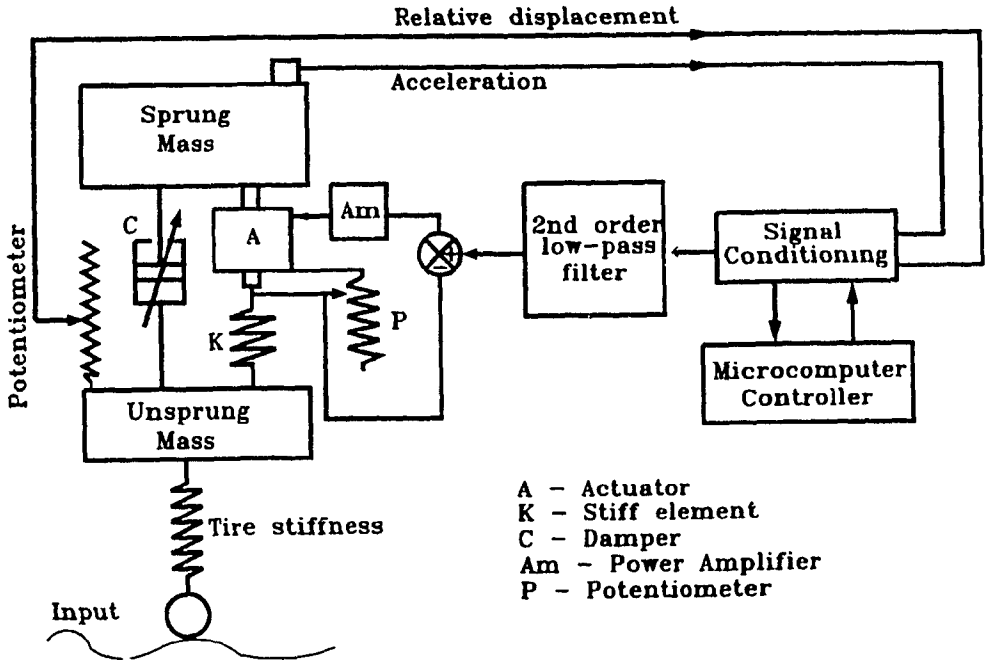


Fig.1.4: Slow active suspension system.

## Unguided Vehicles

There are two principal techniques for design of suspension namely, the analysis procedure and the synthesis procedure. The analysis procedure is based on first specifying the practical configuration of equipment and then analyzing the dynamic characteristics using mathematical techniques. This limits the procedure to a particular system defined and is confined to few degrees of freedom. But the synthesis method is designed through the modern control theory based on optimal control theory and modal control theory. In the modal synthesis design method an open-loop suspension is initially defined in terms of forces acting and the open-loop is controlled in such a way that eigen values of the open-loop are replaced by assigned eigen values. Synthesis and experimental setup is described by Sutton in [22] and [23]. The pole placement approach which studies the effects of closed loop poles in the "$s$" plane to the performance of the system are illustrated by Hall and Gill in [24], where the results of various active systems are compared.

Theoretical investigation of active seat suspension for a wheeled tractor with a simple active suspension system constituting a servo-hydraulic cylinder, a servo-valve and energy source is discussed in [25]. A seven DOF model is analyzed by Chalasani [26] to evaluate ride isolation, road-holding and suspension travel for both random and deterministic roadway disturbances. The results are then compared with a simple quarter-car analysis. This study showed an improvement of 15% in ride quality when compared with a soft passive suspension while maintaining comparable levels of suspension travel and tire deflections. A fully active suspension system has been developed by Lotus Cars Ltd. and implemented on Formula racing cars. More recently, a high performance road car (Esprit) which uses an electro-hydraulic control technology is described in [27]. A brilliant combination of electronic sensing and hydraulic actuation which led to actual implementation of the active suspension on Formula 1 car is also described in [28] and [29]. An interesting work on electronics

was done at Williams Grand Prix Engineering [30] to help solve active suspension implementation problems. The success of active suspension achieved so far on racing cars could widen the application to four different categories. First, for vehicles where the laden/unladen weight ratio is too high for conventional suspensions to be satisfactory for both these conditions, secondly for off-road vehicles including the high speed military vehicles where it is necessary to keep all the wheels on the ground for traction and to provide a stable platform. The third category is comprised of earthmovers and tractors in which the absence of suspension leads to resonance of their soft lightly damped tires. An active suspension control system would prevent any undesired attitude changes due to high external loads. And finally the ambulance, where the maintenance of level platform and good isolation despite of necessary fast cornering and traffic negotiations is very important.

Control bandwidth of actuators in active suspension extends substantially beyond the wheel hop frequency determined by the unsprung mass and tire stiffness. The slow active suspension systems defined in [2] could be described as shown in Fig.1.1 These systems differ from active systems in their control bandwidth being restricted to the normal range of body resonant frequencies in various degrees of freedom but not extending beyond the wheel hop frequencies. In these cases the actuators can be designated to perform in two different ways beyond body resonant frequency when the slow active suspension is inactive. They can act as a flexible spring when inactive in the control sense as in the case of pneumatic actuators in which case they can support the body weight or act in parallel with a spring. Secondly as a rigid body as in the case of electric motor/irreversible lead screw actuators or spool valve controlled hydraulic actuators which have to be mounted in series with a spring. This rigid type of actuator acts as a displacement producer and hence the error in the control loop is based on the displacement parameter. It was shown by Sharp and Hassan in [31] that a slow-active system with 3 Hz bandwidth actuator and variable damping will give excellent ride quality over wide range of road roughness conditions. A further detailed study has to be made in all aspects in order to apply the slow-active system

as a substitute for a fully active system.

## Guided Vehicles

High speed ground transportation using guided vehicles is looked upon as part of a solution for todays transportation problems. Wheel-rail systems and to a lesser extent magnetic levitation are being used world wide to achieve higher speeds. Refs.[1] and [3] incorporate an extensive review on the rail vehicle active suspension. Active suspension concepts for guided vehicles have come a long way since being initiated by Osben and Pertman [32] for US-DOT and followed by Sarma and Kozin [33], Hullender et al. [34], Jeffcoat and Wormley [35] and Sinha et al. [36]. The complete analytical design which includes the actuators and sensors required is presented by Celinkar and Hedrick [37]. They were experimentally implemented for secondary lateral suspension of AMTRAK passenger cars by Cho and Hedrick [38]. Pollard and Simons examined various methods of assessing passenger comfort and made proposals for acceptable vibration levels in railway vehicles [39]. Advantages and disadvantages of various active suspension actuators have been clearly tabulated by Hedrick in [3]. Performance of some experimentally verified actuators for rail vehicles are also discussed. Actuators for active suspension should have a large bandwidth (unless one wants to compromise by using slow-active systems), but at the same time should be rugged and reliable.

Most studies on active suspension system deal with heave-only, one or two DOF models. These simple models form the basics and are easy to analyze and are very useful in understanding the concept. On designing a full suspension system the heave only model could be used for each of the vehicle modes namely heave, pitch, roll and warp, but these could not explain the coupling between various modes like in the cases of heave and pitch and handling characteristics in case of roll and wrap. This model also would not be able to reflect the effect of the control strategy on the normal load distribution which is one of the important performance characteristics

of the suspension. Malek and Hedrick [40] considered a full vehicle model with seven DOF to reflect the coupling between various DOF, and analyzed the effect of suspension design on wheel load distribution. It was shown that full interconnection allows arbitrary and independent specification of all the suspension parameters and also the degree of coupling between various modes. The decoupling of heave and pitch modes reduced the body pitch transmissibility due to heave input and absolute body damping was found to reduce fore-aft wheel load transfer. By decoupling and controlling the actuator at each end of the vehicle independently, we can idealize the bounce and pitch DOF according to the required performance.

## Active Suspension for Various Applications

A wheeled robotic mechanism is considered to be best suited for high speed locomotion among various robotic vehicle mechanisms. But this high energy efficient method is restricted to even road surfaces. As described in Ref.[41] an active suspension is designed to accommodate the road unevenness. An experimental setup with a vehicle and road simulator is used to achieve a high performance vehicle body stability by suspension control during a run on the uneven road surface. Comparison of performance of wheeled robot for PID and optimal discrete control is described in Ref.[42]. An active suspension for a vehicular model travelling on flexible beams with an irregular surface has also been analyzed in Ref.[43].

An electromagnetic suspension to support and influence the vibration of a rotor simultaneously without any contact has been described in [44]. Here, a closed loop control of a reduced order model is analyzed and experimentally verified. Active suspension of a bearing for rotor dynamics is also discussed in Refs.[45], [46] and [47]. A linear optimum multi-dimensional system for control of active magnetic suspension of a rigid rotor along with test results for an experimental high speed motorized spindle are presented in [48]. An active magnetic suspension for an electric motor is described in [49].

### 1.3.4 Review of Control Strategies for Active Suspension

A vehicle system with an active suspension is predominantly a fairly complex dynamic system with control loops added to monitor and modify its basic characteristics. It has been established over the years by considerable research throughout the world that positive cost-benefits could be achieved by advances in the active suspension. Design of a robust and reliable control scheme poises an equally important problem as that of mechanical design. A complete system with full complexities of vehicle dynamics and suspension control would be a very large model which is difficult to analyze and validate with experimental results. Hence it was correctly proposed by Goodall et al. [50] to pursue parallel courses taking a full dynamic analysis of the vehicle with a simplified control system and a full control system analysis active on a simplified suspension. The general closed loop vehicle dynamics system can be represented as shown in Fig.1.5 with design process as shown in Fig.1.6 [50]. The closed loop system can be complex as in the case of magnetically levitated vehicle where an active suspension is considered to be the most preferred solution as a secondary suspension to compensate for the absence of primary damping in the system. The control system should also be able to position the vehicle within tight limits. The complexity can be demonstrated by the way a two part complementary control system is designed to follow the track and minimize secondary suspension deflection at low frequencies and to isolate the body from high frequency random roughness. Review on Maglev systems in Refs. [1], [50], [51] along with the study by North on Birmingham airport-Maglev in [52] should give an extensive idea on these systems. In perspective of the complexity of using advanced control concepts for a full vehicle dynamic model as discussed in these references, various simplified strategies as described in Fig.1.5 have been used in this dissertation. This dissertation starts with a simple but detailed suspension model single degree of freedom nonlinear time varying (SDOF-NTV) without any details of the actuator but involves a complicated adaptive control strategy. Complicated detailed models with a larger number of DOFs have been studied with detailed control strategies in the later chapters. The over all

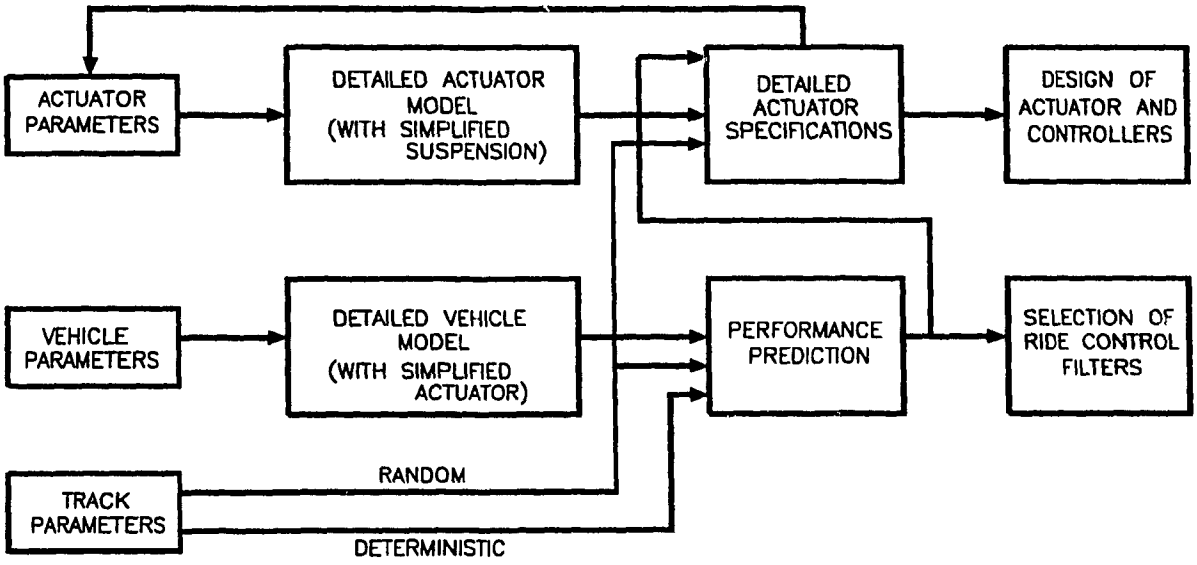


Fig.1.5: General vehicle dynamics control system [50].

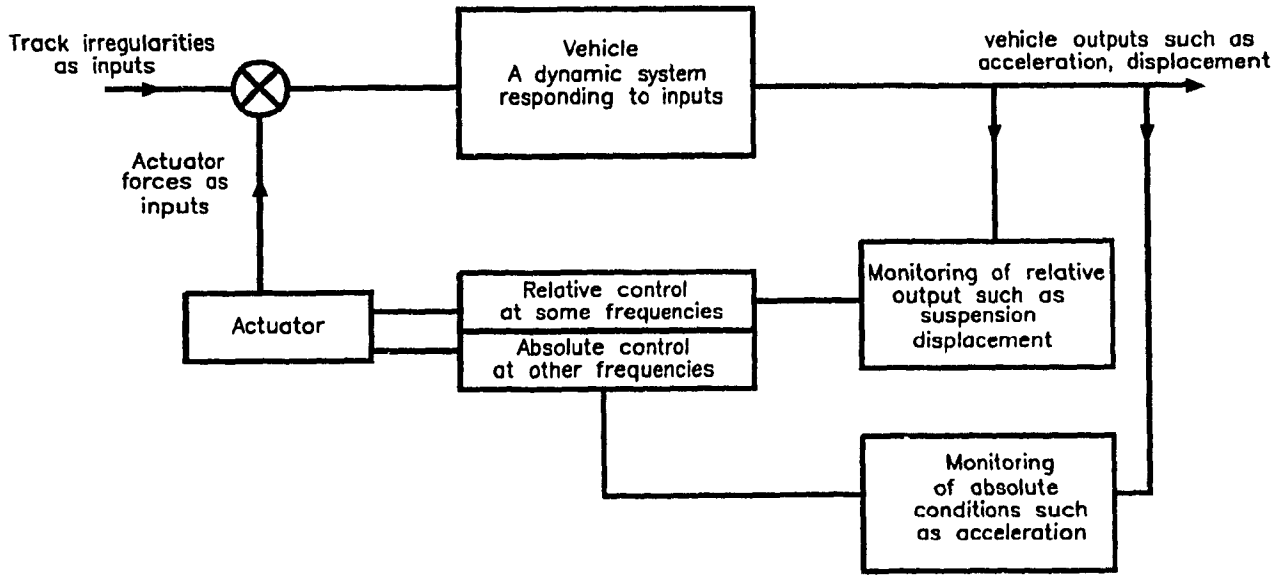


Fig.1.6: Simplified design process [50].

system could be represented as shown in Fig.1.6, where the absolute conditions are taken care of as the skyhook reference model.

Control laws for active systems would replace the passive suspension components constants in terms of the coefficients of feedback control law. These coefficients are controller parameters and need not be physically realizable compared to the spring stiffness and damping coefficients in the passive system. Hence they are less constrained within the operation bandwidth of actuators. The active suspension control systems can be designed on the basis of classical frequency response techniques and linear optimal control theory. A relevant question about active suspensions being optimal or classical was poised and discussed by Williams in [53].

Linear optimal control theory emerged as a systematic approach and has been used as both tracking and stochastic disturbance problem. In this, a performance index containing the weighted sum of mean square values of system output like acceleration, rattle space and control force is minimized to obtain the required feedback gain matrix. The feedback control is implemented by various state sensors including a road height sensor [54]. A compromise between optimality attainable and hardware realization for measurements of all states is discussed by Thompson in [55], where a suboptimal linear active suspension is proposed. Here position feedback relative to the axle rather than with respect to the road is considered. State estimation of the unmeasurable state variables has also been analyzed in [56] and [57]. A further improvement to the performance index was made with the addition of derivative constraints which make the suspension infinitely stiff towards static loading or body forces and soft with respect to the road inputs. Thompson and Davis derived dynamic controllers which use integrators ahead of the control input which in turn eliminates steady state error due to system step or ramp input. The additional integrators introduce an extra state variable and increase the order of the system, hence it complicates the analysis of multi-degree of freedom system. The system with integrators

was transformed to limited state feedback system using the Ferguson and Rekasius method to achieve zero steady state response to both static body forces and ramp road inputs in Refs.[58] and [59]. The optimal solution is also widely derived using linear stochastic optimal control theory with system input as white noise or filtered white noise. Wilson et al. [60] examines the relation between the theory of linear stochastic regulator and Thompson's derivation of the optimal control laws on the basis of full or partial state feedback systems. The theory has been applied successfully for wide range of different types of vehicles. Suspension optimization of two DOF bounce model has been described by Hac in [61]. Stochastic optimal control for the active lateral suspension to a track/vehicle system incorporating Gaussian track irregularity and noise in the state measurements along with the state estimation using Kalman filter is discussed in [62]. Stochastic optimal control of bounce vehicle model and eleven DOF highway truck model incorporating the bending modes of the body are considered by Hac in [63] and Elmadany in [64] respectively.

For a straight line motion and for cornering with large radius of rotation the rear input is a time delayed version of that at the front. This correlation between the front and rear axles and other time delays have been neglected to avoid some problems with the optimization techniques. The covariance matrix consisting of controlled system states which describe the average performance of stochastic optimal control system depends on the intensity of the input noise. If the time delays are considered, then the off diagonal elements of intensity matrix comes into effect and the controller matrix could not be explicitly stated. To allow the linear controller techniques, the time delay was included in the disturbance model as a Pade approximation of fourth order which was discussed by Frühauf et al. in Ref.[65]. Discrete linear quadratic regulator theory has been applied in [66] for a half-car four DOF system where the time delay disturbance entering the front and rear wheels is taken into account. Here a preview control appears naturally in the optimization process and the non-preview part behaves as if rear and front inputs are uncorrelated. The performance index has been improved by more than 25% for vehicle speeds up to 29 $\frac{m}{s}$ but beyond

this, the improvements are less. The time delays of multi-axle excitation inputs are considered while designing active suspension for heavy duty trucks using optimal control theory [67]. The validation of these approaches by practical implementation has to be explored. Limiting the power requirement and consequently the complexity of the active suspension has been another important factor that has to be considered seriously. A qualitative solution for limiting the power absorption has been made in [68] and [69]. A systematic approach that uses a tandem active-passive system and evaluates the passive constants by minimizing the power required by the active system using an optimal control procedure has been dealt by Corriga et al. in [70].

Williams discusses the comparison of experimental performance of classical and optimal controllers in [53]. Classical control was found to translate theory to practice much better than compared to the optimal control. Physical realization of the classical control systems gave less problems as compared to the design of a realistic optimal controller, since the vehicle model had to be reduced, rationalized and designed heavily on the experience of classical systems. Commissioning the classical control systems was straight forward due to modular nature of their design compared to that of observers in the optimal control. Experimental comparison of the performance of classical skyhook damper, position controller and optimal controllers was also analyzed. It was found that simple skyhook damper gave the biggest improvement in ride and was easiest to optimize because it is immune to imperfection in the model. Position control theoretical results proved difficult to be achieved practically. Even though the performance of optimal controller with modal observers was not as expected, the performance could be improved with more experience with optimal control theory. Karnopp [71] discusses two contrasting versions of the optimal active vehicle suspension designed according to two different performance criteria, and concludes that the results are not necessarily comparable and it may not be fair to compare an optimal suspension with a conventional one unless all aspects of suspension performance are considered simultaneously. This argument is quite appropriate but some sort of reference criteria for comparison is required, hence design of a global

comparison criteria is necessary.

The use of dynamic controller with integrators would be ineffective when adequate damping of the wheel-bounce mode is not present. This could be well tackled by applying damped vibration absorbers to the unsprung masses. An optimization of vehicle suspension with a damped absorber has been dealt by Ghoneim and Metwalli in [72] and the performance was compared with that of optimal active suspension. Optimum damped absorber suspension is found to be superior when ride comfort is considered but controllability is found to be better in the case of optimal active suspension. Later Thompson et al. [73] considered active suspension along with a vibration absorber. A preview suspension system and one without relative displacement measurement were considered and the overall system with vibration absorber was found to give 10% reduction in the Performance Index ($\mathcal{PI}$). A further reduction in bandwidth of the body reference along with steady state errors in ramp and static load conditions can be achieved by dynamic optimal control with integrated feedback applied to an active suspension with vibration absorber as discussed in [74]. The effect of tire damping on the performance of vibration absorber in an active suspension has been studied by Thompson in [75]. It was observed that damping of the bounce mode for the active system with the vibration absorber is comparatively low and large transient overshoot may be produced by isolated road obstructions. Further research has to be done for improving the performance of the vibration absorber by incorporating partial damping force control or using two or more absorbers.

One of the difficulties in the Linear quadratic regulator control method for vibration isolation is the choice of representative form of the performance index and also in deciding which variables need to be more heavily penalized than others to give best dynamic characteristics. Human tolerance to vibration is a function of mode of vibration, frequency and exposure time. Human sensitivity to vibration could be incorporated into the optimal control problem by choosing a frequency shaped cost function. The design and results of this approach for a quarter car model both with

and without vibration absorber is discussed by Allen et al. in [76] and [77]. Discrete-time frequency-shaping parametric linear quadratic control approach applied for a seat suspension is presented in [78]. A control approach based on reducing the order of the problem using the presence of fast and slow modes in the suspension system has been performed by Salman et al. [79].

## 1.4 Adaptive Control of Active Suspension

### 1.4.1 Nonlinear Time Varying Vehicle Model

Even though active suspension has become very popular, it is very important to look into the reliability and actuator power requirements. This led to the more appropriate failsafe active suspension which incorporates the conventional passive components and the more advanced active part. This type of concept can give good reliability and safety in ad-hoc conditions when the active suspension fails and also reduces the power consumption. A failsafe system also reduces the complex circuitry, initial and operating costs. Hence invariably compliance elements of the form of leaf or coil springs, torsion bars and springs using rubber, liquids or gases along with the absorbing elements like viscous dampers (shock absorbers) are always encountered in vehicular suspension designs. Presence of these elements leads to nonlinear and time varying behavior as their parameters vary with respect to operating conditions and the period they were in operation. A general model which is made up of various contiguous bodies has large number of degrees of freedom (DOF) and is NTV in nature. The NTV characteristics of the vehicle arise from many factors such as uncertainties in vehicle parameters and external disturbances, nonlinear characteristics of the components, signal noise, load variations etc.. Inadequate analytical treatment of nonlinear characteristics of components and imprecise knowledge of inertial properties further contribute to the NTV characteristics of the system. Also when the vehicle undergoes various critical manoeuvres like acceleration and deceleration or describing

curves, it creates a load shift from one side to other. This leads to the suspensions being imposed by various time varying loading conditions. All these factors make the general vehicle model highly nonlinear and time varying and quite different from the model normally assumed for analysis.

The following description defines the original idea of adaptive control and its various modes of functionality. This part of the section is introduced to bring forward the definition and remove the vagueness created by some publications reviewed later on.

Adaptation in general can be defined as the ability of self-adjustment or self-modification in accordance with changing conditions of environment or structure. In a more technical sense it can be defined as the process of changing the parameter structure and possibly the controls of a system on the basis of information obtained during the control period. This optimizes (from one point of view or another) the state of a system when the operating conditions are either defined incompletely or changed [80]. This can be explained as an adaptive system which measures a certain Index of Performance using the inputs, the states and the output of the adjustable system. From the comparison of the measured ($\mathcal{PI}$) values and a set of given ones, the adaptation mechanism modifies the parameters of the adjustable system or generates an auxiliary input in order to maintain the ($\mathcal{PI}$) values close to the set of given ones.

Here the adjustable system is defined to be capable of adjusting its performance by modifying its parameters or internal structure or by modifying its input signals. The general adaptive systems can be classified as

**Passive adaptation** In which the design for operation is based on wide variations in parameters and operating conditions, like robust high gain control which is useful when the uncertainties are unstructured and known in advance. In this case the system achieves adaptation without system parameter changes.

**Input signal adaptation:** Systems which adjust their parameters in accordance with input signal characteristics.

**System-variable adaptation:** Systems which base self-adjustment on measurement of system variables.

**System characteristic adaptation:** Systems which make self-adjustment based on measurement of transfer characteristics.

**Extremum adaptation:** Systems which self-adjust based on a maximum or minimum of a system variable.

### 1.4.2 Relevance of Adaptive Control to Active Suspension

The concept of adaptation for active controls in vehicular technology was poised as an open problem in the survey papers which were discussed in the previous sections. With the rapid advances made in power semiconductor devices, new concepts used in micromechanics for advanced electric motors, pneumatic and hydraulic actuators, hydraulic pumps, accumulators etc. could be applied to deliver highly efficient controlled power. The advances made in microprocessor based digital control hardware could be associated with a sophisticated servo-valve which could respond to very high frequency signals to achieve very fine delivery of required forces. Its very implicative that usage of these advanced and expensive hardware would become more meaningful only if an appropriate control scheme has been designed to incorporate various active control functions to deliver the best out of the whole system.

The conventional control schemes designed would assume the system to be Linear Time Invariant (LTI), where the gains are constants and cannot cope with the changing dynamics and operating conditions. The advanced adaptive control concepts which have been widely used in fields as robotics, flight control systems, navigational applications, servomechanisms, machining operations etc. could be extended to the

active controls in vehicle technology. The general vehicle suspension design is very complicated as in this case the adaptation has to be with respect to various:

1. changes in the input, like road (asphalt, paved, dirt) or off-road and with respect to vehicle velocity,
2. the nonlinear dynamics exhibited by various suspension components,
3. the dynamic time varying properties like load shifts during operation,
4. the static varying properties like laden/unladen load in the commercial vehicles,
5. variations in the operating conditions like vehicle speed etc.,
6. unknown vehicle parameters and their variation with operating period and
7. various static and dynamic body forces that apply on the vehicle due to environmental and operating conditions.

These variations indicate that the adaptive control in the case of vehicular active control overlaps most of the previously described general classifications of adaptive control. The following examples indicate various situations where the need of adaptive control is generally felt and could be designed to achieve better performance of the vehicle.

EXAMPLE 1: In the case of braking and cornering, priority should be given to handling of the vehicle compared to ride quality. This is necessary due to predominant longitudinal and transverse accelerations. An adaptive active suspension system adapts the gains to compensate for braking and cornering tilt in the carbody and minimizes the centrifugal forces acting on the passengers. Once this manoeuvre is over, this system can resume normal operation.

EXAMPLE 2: In the case of active control of steering, the control laws investigated use a linear optimal control (Ricatti design) and pole-assignment to give

command signal to change the wheel angle using a hydraulic servo system. A constant gain controller cannot be sensitive to parameter changes in friction between tire and road, radii of curvature, vehicle loading condition and compressibility of the hydraulic fluid. A robust control with high gains can be designed to accommodate variations in speed, mass and friction coefficient but this may not be optimal at all changing model parameters. Hence an adaptive controller with variable gains can be designed to accommodate the varying dynamics and inputs.

EXAMPLE 3: In the case of active suspension, the controller gives the command signal to the suspension actuator to obtain the required performance. As described above a controller designed on the basis of optimal control or high gain robust controller would not be able to take care of the changing parameters and nonlinearities of various components of the vehicle. Even in this case an adaptive controller could be realized to make the system robust and give optimal performance for wide range of operating conditions.

EXAMPLE 4: An adaptive active suspension could be designed so that it varies the controller gains to compensate for the squat and nose dive of the vehicle during the critical longitudinal acceleration and deceleration manoeuvres.

EXAMPLE 5: An automatic load leveling active suspension could be designed to take care of the maintenance of static equilibrium level due to static load variations.

If an equally successful adaptive control scheme as in the case of various other fields as robotics and flight control systems could be developed for active suspension, then the practical implementation and hardware realization of the active suspension concept would be more meaningful.

### 1.4.3 Review of General Adaptive Control Applications

The term adaptive system in control theory represents a control system that monitors its performance and adjusts the parameters in the direction of better performance even without accurate knowledge of the complete system dynamics. Model Reference Adaptive Control System (MRAC) is one of the categories into which most of the adaptive control theory falls under. Refs.[81] and [82] gives a wide review on various applications using MRAC over the past. To make it concise we review the advances in MRAC over the past few years only.

The aircraft industry has been the foremost field where MRAC has been applied in 1958. Since then the field has seen quite a lot of applications based on adaptive control in general. Recently a robust controller which uses a command-general-tracking adaptive control technique to force a complex aircraft model (like B1 Bomber) with unmodelled dynamics to follow a reduced order model has been developed by Sanchez and Edgar in [83]. The results indicate that the adaptive controller is robust and can force flexible aircraft to follow rigid body responses even with a lot of complex unmodelled dynamics. Kruise and Stein [84] studied a general adaptive control structure that takes care of controller parameter errors and measured the signal errors for a missile problem.

Control of robotic manipulators has poised a challenging problem due to its highly nonlinear and coupled nature. In the last two decades this problem has been well tackled by various authors using MRAC techniques. Ref.[85] reviews the most recent work in robotics. Software development and practical implementation of MRAC for a PUMA 560 robot are referred in [86]. Ref.[87] deals with more complex industrial robots which are highly nonlinear and whose parameters like inertia are unknown. A more general nonlinear adaptive control for a N-link robot with unknown load and computation time delay has been discussed by Han et al. in [88]. The above references indicate the error stability due to adaptive control algorithms even under

large dynamic variations. To enhance the controller performance, discrete models of MRAC technique based on hyperstability theory has been performed for industrial robotic manipulators [89]. Skowronski [90] has considered a nonlinear extension of MRAC technique to a double arm nonlinearizable robot manipulators with flexible links.

Adaptive control has entered into the area of process control which until recent past has been mainly dependent on fixed controllers. Unbehaven [91] reviews adaptive systems for process control which shows that the adaptive control applications are no more secluded only for pilot projects but are also being applied in the industrial units. Hahn et al. discusses few applications of an unified theory based on both multi-variable Adaptive Generalized Minimum Variance (AGMVC) and MRAC in [92]. The examples illustrate that these techniques have reached a high degree of maturity and can become a powerful tool in process control applications. MRAC successfully applied to binary distillation column, combustion control of a power unit boiler and control of thermostatic chamber has been discussed in [93], [94] and [95] respectively.

Advance in adaptive control technology together with reduction in the cost of hardware electronics could be successfully used to find less expensive and robust substitutes for more expensive and complicated devices. This point can be well illustrated [96] by the usage of MRAC technique for solenoid valves which can be substituted for complicated and precision involved hydraulic servo mechanisms. MRAC has also become a widely used tool in power engineering as the case of control of Thyristor driven DC motor systems, adjustable speed DC motor drives and electrohydraulic servo systems as explained in [97], [98] and [99].

Production engineering has been another area where adaptive control is being actively applied to obtain better performance with the existing hardware conditions. Ulsoy in [100] and Daneshmend and Pak in [101] discuss the application of MRAC for the control of feed force in metal cutting operation. Cascaded model reference adap-

tive controller is also used as an inner loop to improve the performance of Computer Numerically Controlled (CNC) lathes to achieve constant-horse power in cutting by adaptively controlling the spindle speeds [102]. MRAC controller was found to be stable over wide range of cutting conditions and at the same time perform the force control more effectively than the conventional fixed gain controller for end milling operations as discussed in [103]. However, the MRAC adaptive controller was found to outcast conventional controllers in performance but was found difficult to implement due to various factors such as measurement noise etc. as discussed in [104]. MRAC systems are gaining momentum in fields like welding which are predominantly manual, as continuous visual inspection is required. Suzuki and Hardt [105] have discussed real time control using MRAC for the control of highly nonlinear and nonstationary weld geometry dynamics with process-noise-contamination and time dependent dynamic parameter variations. The results presented in [105] show that adaptive control is capable of modifying incorrect initial plant parameters but was found not to perform well when plant dead band was introduced intentionally.

Finally coming down to the recent advances in MRAC both in theory and for practical implementation, it is expected that reduced hardware costs and improvements in electronic devices should give a helping hand for real time control. Discrete time MRAC which could ease the complications of practical implementation are discussed in [106] and [107]. A new approach called Data model reference adaptive control in which a simple data model is formed from some discrete data of controlled plant's step response. This data model is used to evaluate the output of the adaptive controller. This method presented by Li et al. in [108] is limited to linear system characteristics. An adaptive control software package which utilizes distributed processing (multiple computers) and based on partial state MRAC technique has been discussed in [109]. Adaptive control has been practically implemented and the experimental results are presented in [110] and [111]. Recently a new technique called as Learning Adaptive Control (LAC), in which some decision rules are incorporated to choose the required adaptive control strategies on the basis of trend in the disturbances is

discussed in [112].

### 1.4.4 State of the Art in Adaptive Active Suspensions

An adaptive active suspension may be interpreted as any suspension type like semi-active, slow-active and fully-active suspension which is capable of varying its parameters (for example, spring stiffness and damping coefficient for the hardware and feedback constants in the controller) to suit for different input conditions, operating conditions (forward velocity etc.) and unmodelled and time varying dynamic parameters. Section (1.4.2) discusses the relevance and importance of adaptive control technology applied to active suspension. The previous section already demonstrated the capabilities of adaptive control in general and MRAC in particular. Adaptive control of active suspension has been an area where little work has been done until now. As reviewed in section 1.3.4 relating to various active control algorithms for a suspension, the control processes including optimal control is based on the non-varying parameters of vehicle model and operating conditions. Although this analysis was found to operate well over a small range of speeds and road conditions [15], they have to be adaptive in nature in the sense that they should operate well for different vehicle speeds, road/track roughness and varying dynamics.

Adaptation of passive systems has been worked out by Sharp and Hassan [113] where, a supervisory strategem for controlling the passive stiffness and damping parameters is discussed. Here passenger discomfort, suspension working space and dynamic tire loading parameters are calculated for combinations of spring stiffness and damping coefficients for realistic random input of different quality and for different velocities. A good adaptation of both stiffness and damping governed by proper control program should give a less expensive and high performance suspension system that is capable of taking care of various road/speed conditions and other manoeuvres. The development of high speed remote electrically/pneumatically adjustable dampers along with reasonably fast adjustable springs governed by microprocessor

based controller (as developed by Yokaya et al. in [16] and by Mitzuguchi et al. in [17]) should give a boost to the variable passive suspension. The above references also indicate development of inexpensive sensors and a microprocessor that are required for control of suspension parameters. Micro-processor based adaptive passive suspension has also been discussed by Poyser in [114]. Redfield and Karnopp discussed the optimal performance comparison of various variable component suspensions in [115]. Here, active damping and full state feedback were studied and important conclusions were drawn in various suspension requirements. Ref.[115] presents three dimensional plots of acceleration-rattlespace-contact force optimization for both passive and active damping systems. Even though the results presented are for linear analysis they could be extended for nonlinear suspension components. Tuning of passive, semi-active and fully active suspension systems for different velocity/road combination and disturbance force to the sprung mass is studied in [116]. The tuning of vehicle suspension for the required performance has been implemented by real time computer control in the form of Computer Optimized Adaptive Suspension Technology (COAST) as presented in [117]. As described in this reference the patented COAST process provides simultaneous real-time optimum control of all of the parameters of suspension movements such as roll, pitch, sprung and unsprung natural frequencies, height control and energy supplied. The damping, energy storage and controller units that are used to achieve high performance of the COAST suspension unit are also discussed. The reference does not indicate any results of the actual implernentation of the COAST unit.

Karnopp and Margolis [118] analyze a class of basically passive suspension whose parameters are varied in response to various measured signals of the vehicle. In this, the adaptive suspension is based on simultaneous variation of damping and spring stiffness depending on measured performance and manual over rides or over rides based on manoeuvrability inputs such as steering, braking or throttle changes incorporating different vehicle velocities and road inputs. Here an adaptation in the sense of controlling the stiffness and damping properties is discussed.

A computerized active suspension system which is complimented with an "adaptive control" for heavy commercial and military vehicles has been developed by Sachs [119]. Here an optimal parameter matrix based on Power Spectral Density (PSD) data of previewed terrains and different forward speeds is stored on an on-board mini-computer. In Ref.[120] Hac discusses a similar "adaptive active suspension" with a clear statement that adaptation is oriented towards the compensation in excitation characteristics rather than the changes in vehicle model parameters. Here the control gain vector is calculated off-line for various velocities and types of road/terrain inputs and are stored as a look-up table on an on-board computer to be used up with the controller in actual implementation. The control gains are evaluated by optimal control assuming the vehicle model as linear time invariant. Here the variance of sprung mass acceleration for a two DOF "adaptive suspension" compared with a constant gain active suspension as functions of the weighing factors for suspension deflection and tire deflection of an active suspension is presented. A different mode of "adaptive suspension" system is proposed in [121] by Yeh based on modern discrete optimal control theory. Here two different weighting function sets are stored for different manoeuvrabilities, for instance, if the vehicle moves on a straight path then feedback loop adjusts the gains for high frequency isolation but if it changes lanes or makes turn then gains are adjusted for better road holding. The signal from steering wheel angle is used for switching to different modes by the microprocessor. Another similar arrangement has been proposed by Armstrong Patents Company Limited called as "Adaptive Suspension Control" [122]. It varies the stiffness according to the static load conditions as a self leveling device and also switches damping settings between extreme values depending on the control signals from various sensors monitoring suspension displacement, steering wheel angle, vehicle speed etc..

The adaptive control as defined in section 1.4.1 and reviewed in section 1.4.3 should be capable of accommodating the variations in operating dynamics of vehicle, inaccuracies in modelling and operating conditions. The approaches discussed earlier assume that the vehicle parameters are completely known and controller gains are not

updated on real time basis but are only pi ,ed up from the look-up table. The second set of adaptive active suspensions are based on the concept that a priori knowledge of complete vehicle dynamics and parameters along with operating conditions are not known. The control input given to the active suspension actuator dictates the performance obtained by the suspension. The idea of forcing any suspension to give the desired optimal performance depends on how the gains are evaluated in the control law. If the actual vehicle model is NTV and its complete dynamics are not known then optimal performance can be obtained in two different ways. First we can assume the model to be LTI over small operating period and use the advanced concepts like stochastic optimal control to attain the control gain vector to implement the control law. The model could be updated for evaluation of gains at every instant but it does not make it adaptive since we assume that parameter variations are known a priori. The papers reviewed earlier in this section fall under this category. Stochastic optimal control designed for a particular linear time invariant model cannot be robust for large dynamic variations. But the optimal controller could be designed to be robust towards parameter variations, modelling errors and time delays by designing bounds on the perturbations. An estimate of the bounds for the nonlinear time varying perturbations has to be made and then they have to be used up in the quadratic performance index [123]. Bounds had to be laid on various perturbations involving plant parameters, forward velocity and different inputs. The robust controllers developed are generally not applicable over a very wide range of plant parameter variations, hence they are applicable to limited bounds on variations. But an adaptive controller does not need any knowledge of the perturbations and by adapting gains we could attain less rattle space and expend less amount of actuator work for the required isolation. In the second approach we assume a LTI optimal reference model and then adaptive laws are derived to update the gains to take care of the varying operating parameters of the vehicle, operating conditions and unmodelled dynamics.

In the past, active vibration isolation for flexible payloads has been discussed by Leatherwood and Dixon in [124]. An interesting problem of the protection of space

craft payload which is subjected to low frequency vibration along with the changing acceleration field normally from 1g-5g during launch has been discussed. An adaptive controller that can adjust its gains to achieve the required vibration isolation, damp the transient response and minimize the isolator static deflections has also been designed for the flexible payloads. An experimental investigation has been carried out as discussed in Ref.[124]. Cheok et al. present an optimal model-following suspension with variable damping force governed by a microcomputer in [125]. The control input to the actual system is imposed by varying a damping parameter using a microcomputer. An optimal suspension with microcomputer-controlled parameter optimizing variable damper which could perform as an optimal suspension with inertial reference damping has been studied. An experimental setup has been implemented and the results shown in the reference indicate convincing performance of the suspension based on this technique. The paper does not indicate the performance of the system for any model parameter variations.

Different approaches in the same line of MRAC has been proposed in parallel by Sunwoo et al. and Vallurupalli et al.. In these the adaptive laws vary the gains on line according to the changing operating parameters and operating conditions without a priori knowledge of complete dynamics. A multi-degree of freedom adaptive controller that would follow an optimal reference model in each degree of freedom was proposed in Ref.[126]. Various other results for SDOF and various MDOF models that has been developed by the author et al. has been presented in this dissertation.

Sunwoo discusses the MRAC of active suspension for a single degree of freedom model in [127]. The adaptive laws are derived from the Lyapunov function which is based on the error in model following and controller parameters. Here the derivative of Lyapunov function is found to be nonpositive hence the design is just stable. Also the derivative of Lyapunov function does not involve the errors in controller parameters. Hence the convergence of controller parameters is not ensured. Sunwoo [164] addressed the concept of adaptive active suspension based on two different control

schemes using Model Reference Adaptive Control and Self-Tuning Adaptive Control. The problem has been solved in a different approach in parallel to the above reference using hyperstability theory and error augmentation which leads to asymptotic stability as discussed in Ref.[130]. The details of various results for different models and control algorithms as presented in this dissertation and are published in the references [128], ..., [137].

The complexity of adaptive suspension design was further increased by the application of neural network techniques on the basis of Lyapunov stability theory and MRAC. Cheok and Huang [138] derived supervised training and unsupervised learning algorithms for model following of semiactive suspension. Here the actual suspension with unknown dynamics was made to follow a neural model by learning from past experience. The analysis was supported by simulation results. One other new concept in the active suspension is the control of active suspension subjected to random component failures. Given the complicated status of active suspension this forms a step in the right direction. The fully active suspension can be made a failsafe active suspension with introduction of passive components, this along with robust adaptive control laws should be able to take care of any of component failures to some extent. But to avoid the cumulative failures by accumulation of errors which could be checked by fault tolerant algorithms based on certainty equivalence and dual control approximations as described in [139]. Here an approach to the problem of fault tolerant control in which the control of the system based on identification of the component failures (diagnosis) and the regulation of the process outputs (control) is discussed. Simulation results based on eleven operating modes like disconnected sensors, increased sensor-noise, hydraulic actuator leaks etc. are discussed to show the effectiveness of the approach. Results are achieved by solving a large algebraic Ricatti equation based on observed date and involves a nonlinear filter.

## 1.5 Scope and Layout of the Thesis

The previous extensive review can be encapsulated into three different sections. The first capsule contains the review of active controls in vehicles in general and semiactive and active suspension in particular. The second capsule contains various control strategies applied in active suspensions and general adaptive control applications. The third capsule amalgamates the active suspension with adaptive control concepts and reviews the adaptive active suspensions. The previous sections 1.4.1 and 1.4.2 indicated how the vehicle model and its performance can be complex in nature and hence the relevance of application of adaptive control concepts to active suspensions. Although some earlier studies as described in section 1.4.4 have put forward the term *"adaptive control"* in relation to the active suspension, they fail to use the full potential of the concept as defined in section 1.4.1 and its applications in various other fields as enumerated in section 1.4.3.

The primary objectives of the research in this dissertation are thus formulated to investigate the potential for application of complex adaptive control concepts to active suspensions. The detailed objectives of the study are:

1. to study and develop analytical models for nonlinear and time varying vehicle parameters during normal operations of the vehicle,
2. to develop an adaptive controller to maintain static equilibrium position during the vehicle operation for the first time,
3. to develop a continuous time domain adaptive control for a single degree of freedom suspension model,
4. to develop a discrete time domain adaptive controller for practical realization of an adaptively controlled active suspension,

5. analytical comparison of a stochastic optimal controller with adaptive control concepts,

6. to study the application of continuous time MRAC for a general suspension model,

7. development of discrete adaptive controller with estimation for pitch and bounce control of a half-car model,

8. to investigate the hardware realization and experimental validation of a SDOF adaptive active suspension and

9. to develop an adaptive active suspension along with a software package involving simulation, animation and control algorithms.

Chapter 2 discusses the assumptions regarding the nonlinearity properties and their linearization for various vehicle suspension components. The dynamic parametric variations and various road inputs that are generally encountered in the vehicle operation are described in chapter 2. The respective models are also derived in chapter 2. Two different modes of parametric variations and excitations are recognized for hardware and simulation purposes. A continuous time domain adaptive controller for SDOF failsafe active suspension is presented in chapter 3. Chapter 4 discusses development of a discrete domain adaptive controller that takes into account the time delays involved in hardware implementation and reasonable assumptions about the feedback signals available for practical implementation. To show the enhanced performance of the active suspension using the adaptive controller over the stochastic optimal controller, they are both compared under similar conditions in chapter 5. Chapter 6 describes the application of a generalized MDOF continuous time adaptive controller for two DOF bounce suspension. A discrete time domain MDOF adaptive controller for a half-plane model that involves the pitch control of the vehicle in acceleration and braking conditions is presented in chapter 7. Here a modified version

of the least squares estimation that updates the controller parameters as a matrix rather than a vector is newly developed.

Experimental validation of adaptive controller for full scale vehicular SDOF active suspension is discussed in chapter 8. The setup is built from the scratch and tested in each stage to obtain reliable results. A separate horizontal static test rig is built to initially implement position and force control. The force actuator unit is initially used to obtain position control through interfacing with the computer. Then a force feedback control is implemented. The force actuator is installed with a full scale passive suspension to form a failsafe suspension. This forms a real time computer controlled system with an in house built software (written in C language and Window programming) that is used for parameter selection and monitoring. The software also shows the simulation results and animates the suspension performance. Conclusions along with suggestions for future work are described in chapter 9.

# Chapter 2

# Excitation, Parameter Variations and Various Nonlinearity Assumptions

## 2.1 General

Vehicles in general will be required to operate under a typical range of loading conditions and to run at different speeds on road surfaces of widely differing roughness. As described in section 1.4.1 the linear models generally assumed for analysis are quite different from the actual vehicle with failsafe suspension which is highly nonlinear and time varying. This chapter describes various global assumptions that are made and are used throughout the dissertation. The assumptions deal with the type of excitation input both deterministic and stochastic considered for the evaluation of the suspension performance. Different types of parametric variations that the model is subjected to simulate closely to the time varying properties of the vehicle are discussed in section 2.2. Various nonlinearities that are considered to model the suspension as close as possible to the actual hardware are discussed next. Here linearization of the nonlinearities is also discussed which would be used to derive a nonlinear analytic model.

## 2.2 Excitation Input

Any vehicle in its general operating conditions is subjected to a random input that is a function of the profile of the roadbed it is traversing on and the speed of operation. In this dissertation the analytical models along with the controller designed are subjected to two different types of inputs namely deterministic input and more general stochastic input.

### 2.2.1 *Excitation mode I*

The real time simulation results presented in this dissertation in time domain representation are achieved by assuming that a vehicle is subjected to a deterministic input. A sinusoidal input describes excitation at one predominant frequency. The combination of sines is a amalgamation of inputs at various predominant frequencies and different amplitudes. This gives an approximation of road profile of a given spectra but in the deterministic model. A half sinusoidal or bump input represents a typical off road profile or a road under construction. The models could also be subjected to various other deterministic inputs such as round pulse, oscillatory step and round step which represents various shock excitations as used by Rakheja and Sankar [140]. These inputs can be used individually or in sequence to simulate various excitation conditions in real time simulations.

### 2.2.2 *Excitation mode II*

Since validation of the simulation results is to be performed in real time, random inputs corresponding to various road profiles (such as asphalt, paved road and dirt road) are to be generated in the time domain. The random input is generated online by modifying the method presented by Hac in Ref. [120]. A good approximation of road/terrain profile PSD function derived from experimental studies is presented in

Eq. 2.1 as described by Hac in Ref. [120].

$$\mathcal{S}(\omega) = \left(\frac{\mu_4}{\pi}\right)\left[\frac{\mu_1 v}{\omega^2 + \mu_1{}^2 v^2}\right] + \left(\frac{\mu_5}{\pi}\right)\left[\frac{\mu_2 v\left(\omega^2 + \mu_2{}^2 v^2 + \mu_3{}^2 v^2\right)}{\left(\omega^2 + \mu_2{}^2 v^2 - \mu_3{}^2 v^2\right)^2 + 4\mu_2{}^2 \mu_3{}^2 v^4}\right] \tag{2.1}$$

where, $\omega$ denotes the angular frequency, $v$ the vehicle velocity and the coefficients $\mu_1, \mu_2, \mu_3, \mu_4, \mu_5$ depend upon the type of road or terrain the vehicle is moving on. Experimental road measurements have been made by various authors in the past as indicated in Refs.[142] and [143].

The required input is generated by filtering a white noise input using a linear filter whose transfer function is of the form $H(\omega)$. The required PSD ($\mathcal{S}(\omega)$) in Eq.2.1 is considered as the output of the filter $H(\omega)$ which is subjected to a white noise input of PSD ($\mathcal{S}_0$). From the stochastic analysis of a linear system, this can be represented as

$$\mathcal{S}(\omega) = |H(\omega)|^2 \mathcal{S}_0 \tag{2.2}$$

The linear filter in the time domain is represented as a third order differential equation of the form

$$\vartheta_0 \dddot{w} + \vartheta_1 \ddot{w} + \vartheta_2 \dot{w} + \vartheta_3 w = \vartheta_4 \ddot{\xi} + \vartheta_5 \dot{\xi} + \vartheta_6 \xi \tag{2.3}$$

where, $\vartheta_0, \cdots, \vartheta_6$ represent the coefficients and $\xi, \dot{\xi}, \ddot{\xi}$ denote the white noise random input displacement, velocity and acceleration values respectively. Eq.2.2 can be written in the form as

$$\mathcal{S}(\omega) = \frac{\vartheta_4{}^2\omega^4 + \left(\vartheta_5{}^2 - 2\vartheta_6\vartheta_4\right)\omega^2 + \vartheta_6{}^2}{\vartheta_0{}^2\omega^6 + \left(\vartheta_1{}^2 - 2\vartheta_2\vartheta_0\right)\omega^4 + \left(\vartheta_2{}^2 - 2\vartheta_3\vartheta_1\right)\omega^2 + \vartheta_3{}^2}\mathcal{S}_0 \tag{2.4}$$

Equating the coefficients of various powers of $\omega$ on both the sides we obtain

$$\begin{aligned}
\vartheta_0 &= 1 \\
\vartheta_1 &= \varepsilon_1 + \sqrt{\varepsilon_2 + 2\varepsilon_0} \\
\vartheta_2 &= \varepsilon_0 + \varepsilon_1\sqrt{\varepsilon_2 + 2\varepsilon_0} \\
\vartheta_4 &= \sqrt{\tfrac{\varepsilon_5}{S_0\pi}} \\
\vartheta_5 &= \sqrt{\tfrac{\varepsilon_5}{S_0\pi}\left(\varepsilon_4 + 2\varepsilon_3\right)} \\
\vartheta_6 &= \sqrt{\tfrac{\varepsilon_5}{S_0\pi}\left(\varepsilon_3{}^2\right)}
\end{aligned} \tag{2.5}$$

where,

$$
\begin{aligned}
\varepsilon_0{}^2 &= v^4\mu_3{}^2\left(\mu_3{}^2+2\mu_2{}^2\right)\\
\varepsilon_1 &= \mu_1 v\\
\varepsilon_2 &= 2v^2\left(\mu_2{}^2-\mu_3{}^2\right)\\
\varepsilon_3{}^2 &= \left[\mu_4\mu_1\mu_3{}^2\left(2\mu_2{}^2+\mu_3{}^2\right)+\mu_5\mu_1{}^2\mu_2\left(\mu_2{}^2+\mu_3{}^2\right)\right]\frac{v^5}{\varepsilon_5^3}\\
\varepsilon_4 &= \left[2\mu_4\mu_1\left(\mu_2{}^2-\mu_3{}^2\right)+\mu_5\mu_2\left(\mu_1{}^2+\mu_2{}^2+\mu_3{}^2\right)\right]\frac{v^3}{\varepsilon_5}\\
\varepsilon_5 &= \left(\mu_4\mu_1+\mu_5\mu_2\right)v
\end{aligned}
$$

The coefficients derived in Eq.2.5 are found to vary from those derived by Hac in Ref.[120]. The linear third order equation of the form in Eq.2.3 is represented as a state space form and solved in the time domain by substituting the coefficients derived above and by a random input which is generated on line.

Fig.2.1 shows the frequency spectra for asphalt road and dirt road input at a vehicle velocity of 20 $\frac{m}{s}$. The coefficients used in Eq.2.5 to generate the asphalt road and dirt road signals in the time domain are taken as ($Asphalt$ : $\mu_1 = 0.2m^{-1}$, $\mu_2 = 0.05m^{-1}, \mu_3 = 0.6m^{-1}, \mu_4 = 7.65\,e^{-6}m^2, \mu_5 = 1.35\,e^{-6}m^2$) and ($Dirt$ : $\mu_1 = 0.8m^{-1}, \mu_2 = 0.5m^{-1}, \mu_3 = 1.1m^{-1}, \mu_4 = 7.4\ e^{-4}m^2, \mu_5 = 2.5\ e^{-4}m^2$) [120]. The continuous line in Fig. 2.1 indicates the PSD function described in Eq.2.1. The dotted line is obtained by converting time domain data by solving the filter equation Eq.2.3 using the Coolev-Tukey procedure. The road spectra obtained was found to be independent of the magnitude of white noise random input in Eq.2.4. Fig. 2.1 shows that the frequency spectra of the random input which the suspension model is subjected to closely coincides with that of actual road input obtained experimentally and from which the PSD curve in Eq.2.1 is derived.

## 2.3 Dynamic Parameter Variations

The basic idea of implementing an adaptive controller as discussed in section 1.4.2 and cited in various examples is that an adaptive active suspension achieves the required dynamic performance for large and unknown variations of system parameters. The

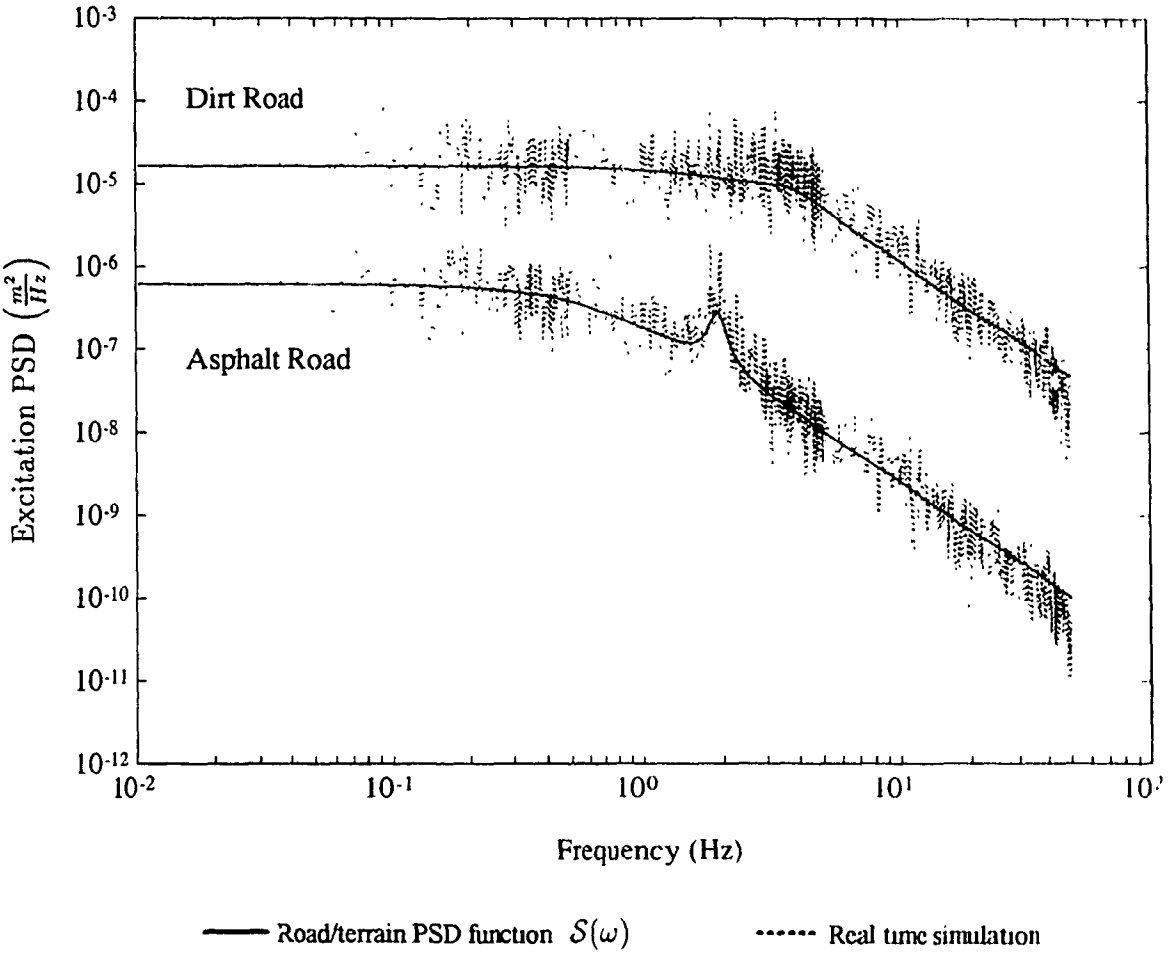


Fig.2.1: Asphalt and dirt road excitation power spectral density (PSD) curves.

adaptive controller should be able to take care of these parameter variations without any a priori knowledge. Two types of dynamic parameter variations are incorporated to test the controller throughout the dissertation.

### 2.3.1 *Parameter variations mode I*

Model parameters could vary with respect to time as the vehicle is operated. Let us consider the case of acceleration/deceleration of the vehicle in which case the rear and front suspensions would be subjected to dynamic load changes.

Figure 2.2 shows a passively suspended in plane half-car model which incorporates pitch and bounce degrees of freedom. Let the total sprung mass $M_s$ of the vehicle vary about the nominal design value of $M_s^*$. Due to the noncentric location of the c.g. the load distribution on the front and rear suspension are unequal and represented as $M_l$ and $M_t$ respectively. From the force and moment equilibrium we could express the load distribution as

$$\begin{aligned} M_l g &= \frac{d_2 M_s^* g}{L} \\ M_t g &= \frac{d_1 M_s^* g}{L} \end{aligned} \tag{2.6}$$

Using the nominal values of the front and rear stiffnesses $K_l^*$ and $K_t^*$ and assuming static equilibrium conditions, we obtain the initial static deflections $\triangle_{st_l}$ and $\triangle_{st_t}$ as

$$\begin{aligned} \triangle_{st_l} &= \frac{M_s^* d_2 g}{L K_l^*} \\ \triangle_{st_t} &= \frac{M_s^* d_1 g}{L K_t^*} \end{aligned} \tag{2.7}$$

These equations would give the acceptable initial static deflections at the leading and trailing axles. The leading and trailing suspension stiffnesses are chosen so that the initial static deflection is assumed to be same at both the wheels. But when the mass and stiffness parameters vary from the nominal values $(M_s^*, K_l^*, K_t^*)$ to $(M_s(t), K_l(t), K_t(t))$ the initial static deflection would be different.

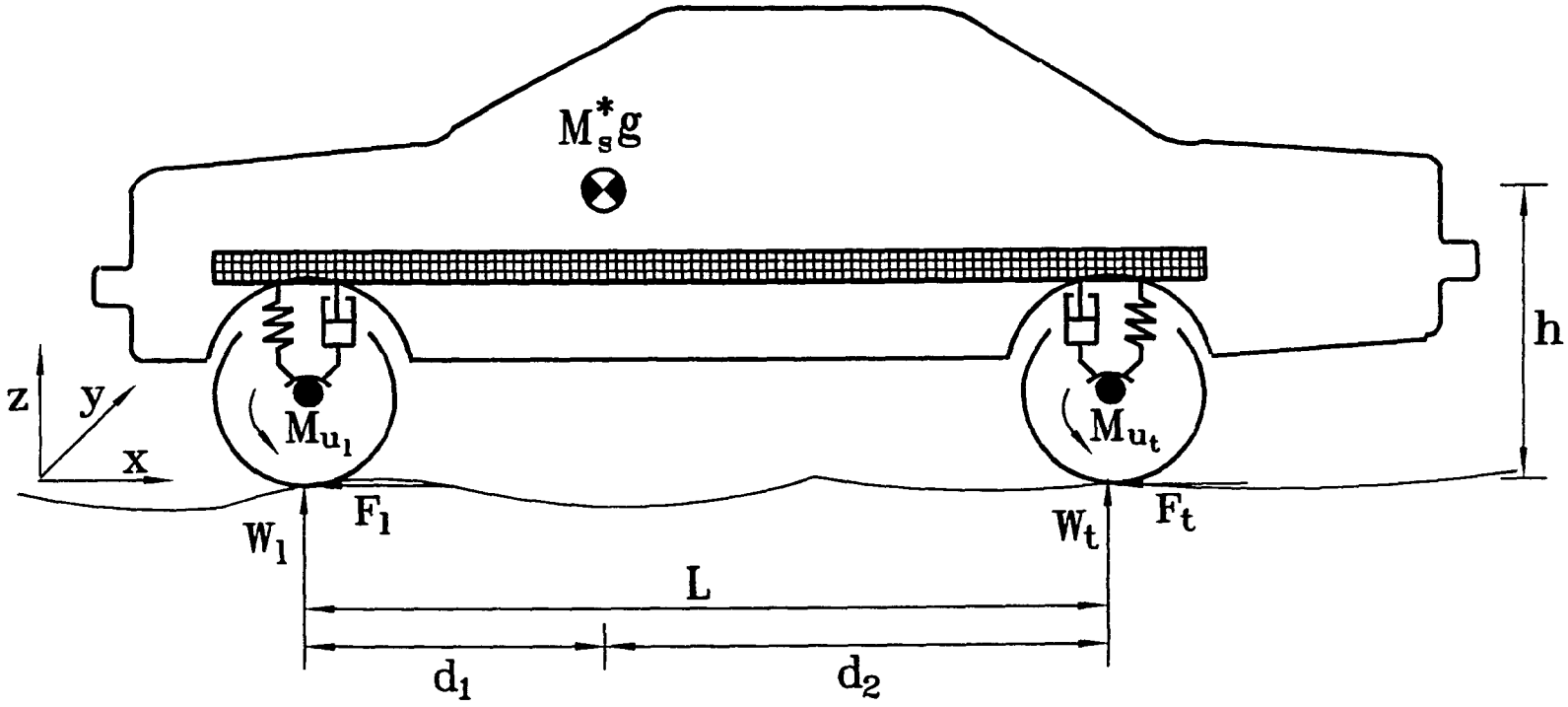


Fig.2.2: Inplane vehicle model at constant velocity.

As shown in Figure 2.3, an additional load variation due to acceleration and deceleration would vary the total load acting on the front and rear suspensions. For example when the vehicle accelerates, the force balance in the longitudinal direction gives

$$(M_s^* + M_{u_l} + M_{u_t})\, a = F_l + F_t \tag{2.8}$$

By taking moments about the front and rear tire road interfaces and neglecting other resistances, the total normal reaction forces at the tire patches are given as

$$\begin{aligned} W_l &= M_{u_l} g + M_s^* g \frac{d_2}{L} - M_s^* a \frac{h}{L} \\ W_t &= M_{u_t} g + M_s^* g \frac{d_1}{L} + M_s^* a \frac{h}{L} \end{aligned} \tag{2.9}$$

where, $h$ represents the height of the c.g. and "$a$" is the acceleration of the vehicle. The load shift force would change its direction when the vehicle decelerates which is achieved by substituting "$-a$" for "$a$". The static load which causes the static deflection in the suspension would exert equal vertical load on the tire causing a static tire deflection. Assuming the same nominal stiffness $K_{tire}^*$ for both front and rear tires we could extend the equilibrium equations as

$$\begin{aligned} \frac{M_s^* g d_2}{L} &= K_l^* \delta_{st_l} \\ \frac{M_s^* g d_1}{L} &= K_t^* \delta_{st_t} \end{aligned} \tag{2.10}$$

The total suspension deflection is the sum of the initial static deflections and deflections due to dynamic load shifts $(\delta_{st_l} + \triangle_{st_l})$ and $(\delta_{st_t} + \triangle_{st_t})$ on the leading and trailing wheels respectively. The total tire deflections on the leading and trailing wheels is given as $\frac{W_l}{K_{tire}}$ and $\frac{W_t}{K_{tire}}$ respectively. Since the initial static deflections are generally considered in the initial tuning of the suspension, the deflections due to dynamic load transfers are to be compensated adaptively. Simulation results are illustrated for acceleration and deceleration manoeuvres encountered most frequently by the vehicle. Figure 2.4 shows typical accelerating and braking conditions the vehicle is subjected for real time control simulation purposes. This figure shows the

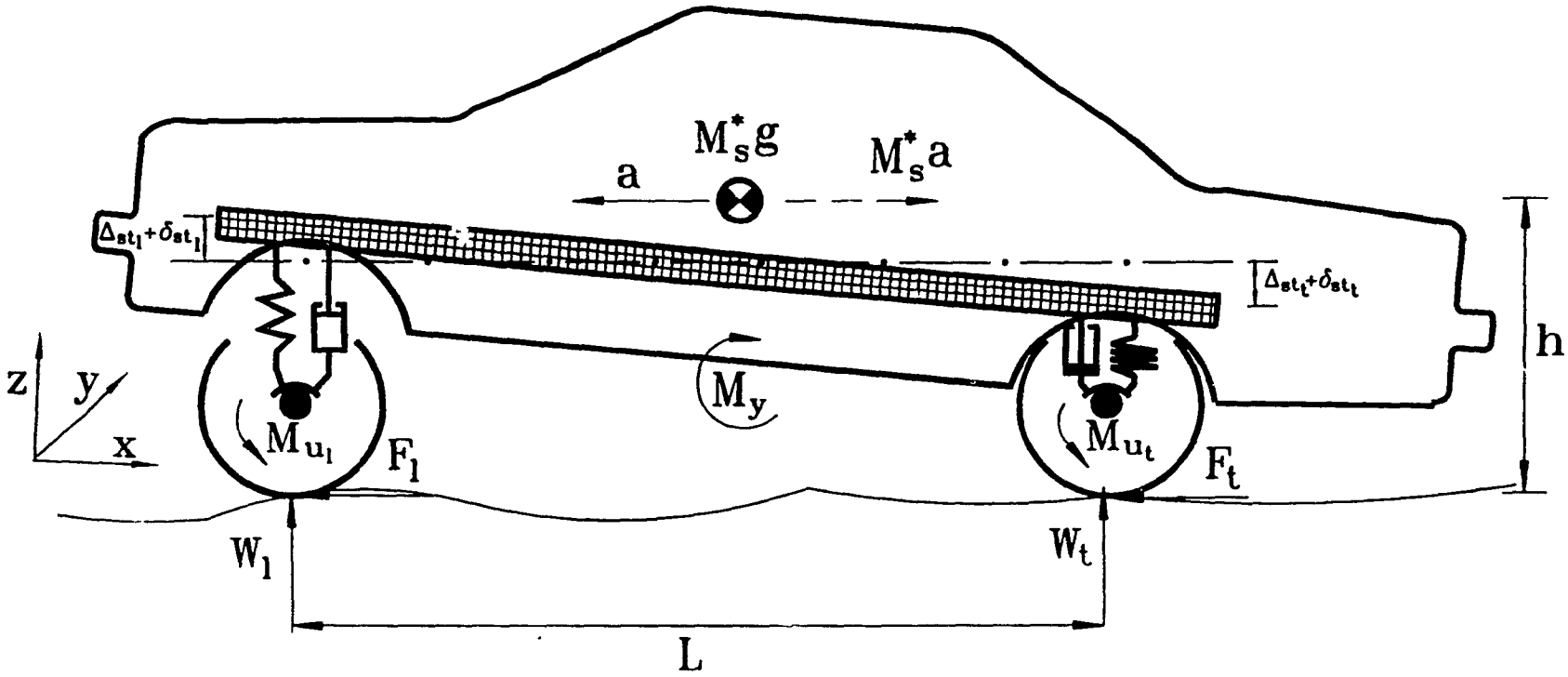


Fig.2.3: Inplane vehicle model when accelerating.

manoeuvre involving acceleration at the rate of 4.0 $\frac{m}{s^2}$ for 8 secs. from a stationary condition to 115 kmph. This figure also shows the influence of sudden deceleration of 7.0 $\frac{m}{s^2}$ for 2 secs. representing a typical braking condition by reducing the velocity from 115 kmph to 65 kmph. Fig.2.5 and 2.6 shows the load shifts to the leading and trailing wheels for a typical half-car model with the following nominal parameter values $M_s^* = 500\,Kg$, $K_l^* = K_t^* = 17000\ \frac{N}{m}$, $C_l^* = C_t^* = 2500\ \frac{Ns}{m}$, $I_{MI} = 500 * (1.5)^2\,kgm^2$, $K_{tire} = 100000\ \frac{N}{m}$, $d_1 = d_2 = 1.5\ m$. These figures indicate a load shift to the order of 60% over the normal operating conditions.

The suspension stiffness and damping properties could be assumed to be varying during the time of operation either due to operational failure or gradual wear out. For example as shown in Figs. 2.7 and 2.8, a gradual change of air spring stiffness with temperature and blow-off of the shock absorber valves is assumed. These variations in stiffness and damping parameters are used for the purpose of testing the adaptive capabilities of the controller designed. The analysis could be extended to other vehicle manoeuvres like roll of the vehicle during turning, etc..

### 2.3.2 *Parameter variations mode II*

The second type of parameter variations to which the controller is subjected is based on the assumption that the actual values of the system parameters are not known a priori. The suspension parameters such as loading condition, damping coefficients and suspension stiffness might vary about the nominal design values before the start of operation. These variations are assumed to be static parameter variations as they would differ from the nominal design values and remain constant during the simulation period. These variations are incorporated along with the stochastic road input to test the performance of the system during simulation and experimental studies. It is assumed that the load acting on the suspension has increased by 40% and the stiffness constant and damping coefficient have decreased by 10% of the nominal values.

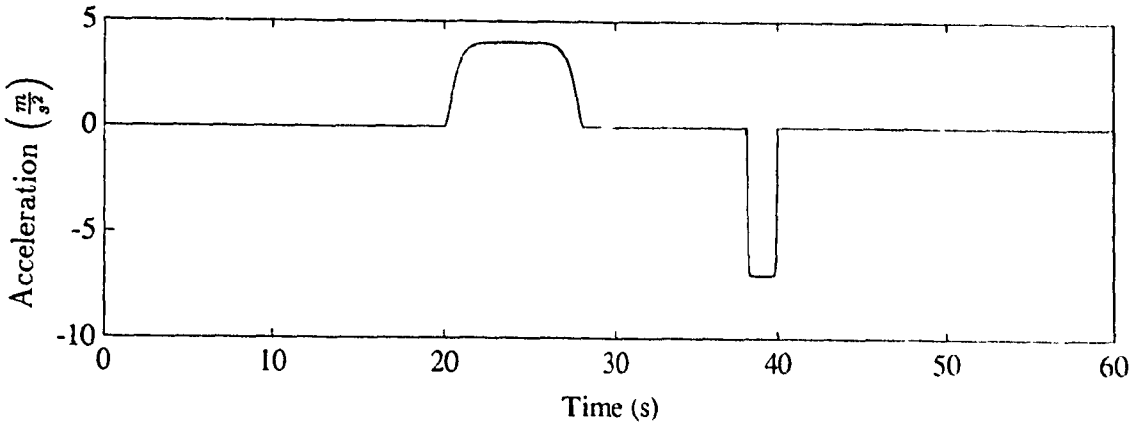


Fig.2.4: Simulated acceleration and braking conditions.

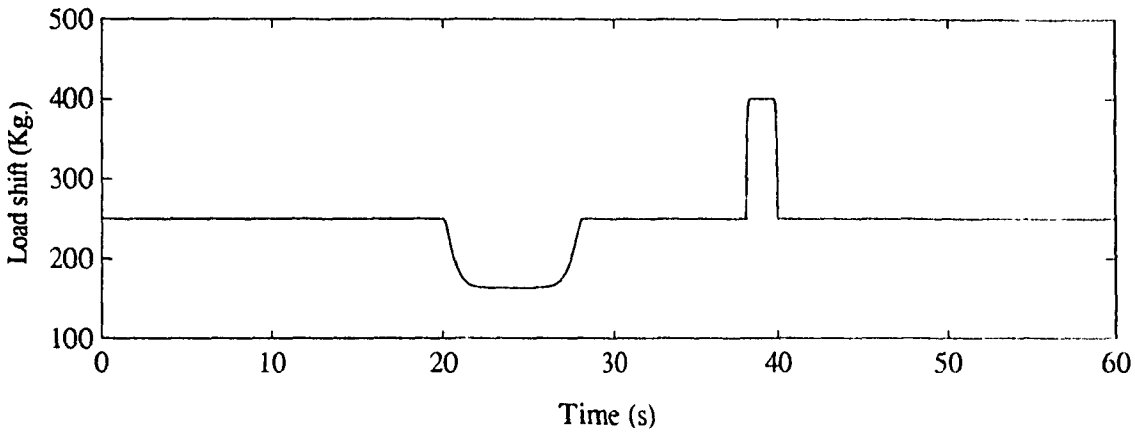


Fig.2.5: Load shift on to the leading suspension.

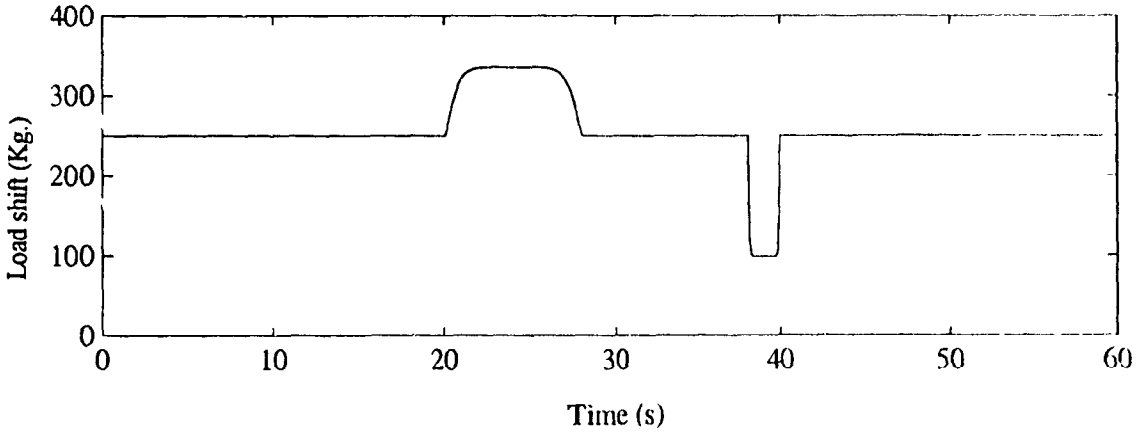


Fig.2.6: Load shift on to the trailing suspension.

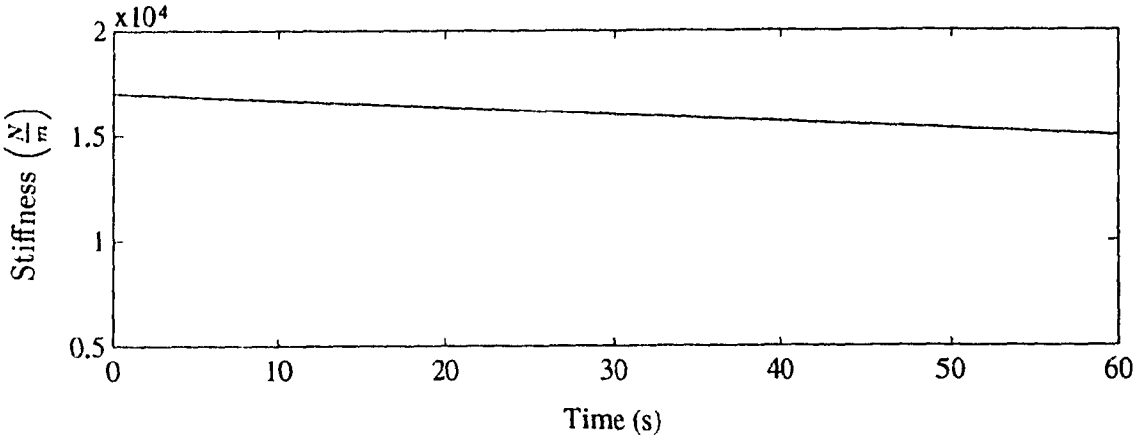


Fig.2.7: Simulated stiffness parameter variations.

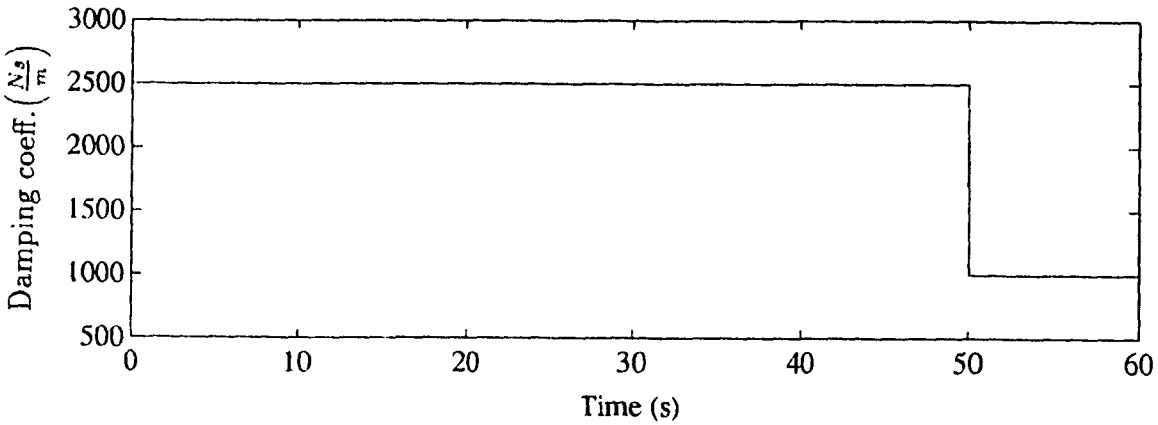


Fig.2.8: Simulated damping parameter variations.

## 2.4 Suspension Components

A class of vehicle subsystems, specifically suspension systems invariably include non linearities in the form of complaince elements as leaf or coil springs, torsion bars and springs using rubber, liquids or gases along with the energy dissipating elements like viscous dampers etc.. Since linear systems are easier and more economical to analyze than nonlinear ones, most of the studies conducted so far have examined models that are linear. In this dissertation, the study is extended to include the nonlinearities which are mostly encountered in the vehicle suspension systems so that the application of advanced concepts such as adaptive control would be more meaningful.

Figure 2.9 shows a half-car model that involves a failsafe active suspension with various nonlinear and time varying properties such as Coulomb friction, Stiffness, Velocity squared viscous damping and Elastic limit stops. Analysis on vehicle suspension system involving such nonlinearities has been discussed by Rakheja et al. in Ref.[141]. The various nonlinear properties of components and the analytic models which we will be using later on are described in this section.

### 2.4.1 Damping Properties

At the low velocity operating conditions the damping property of a shock absorber (fluid forced through an orifice) could be characterized as velocity squared damping. The damping force expression could be written as [141]

$$\begin{aligned} F_d &= C(t)\,(\dot{x}_2 - \dot{x}_1)^2\, sgn\,(\dot{x}_2 - \dot{x}_1) \\ &= C(t)\,(\dot{x}_2 - \dot{x}_1)\,|\dot{x}_2 - \dot{x}_1| \end{aligned} \tag{2.11}$$

where, $C(t)$ is the constant of proportionality due to the orifice flow that could vary with time of operation. Since this gives a nonlinear but continuous or analytic damping characteristics, it could be linearized at various operating points using the Taylor series.

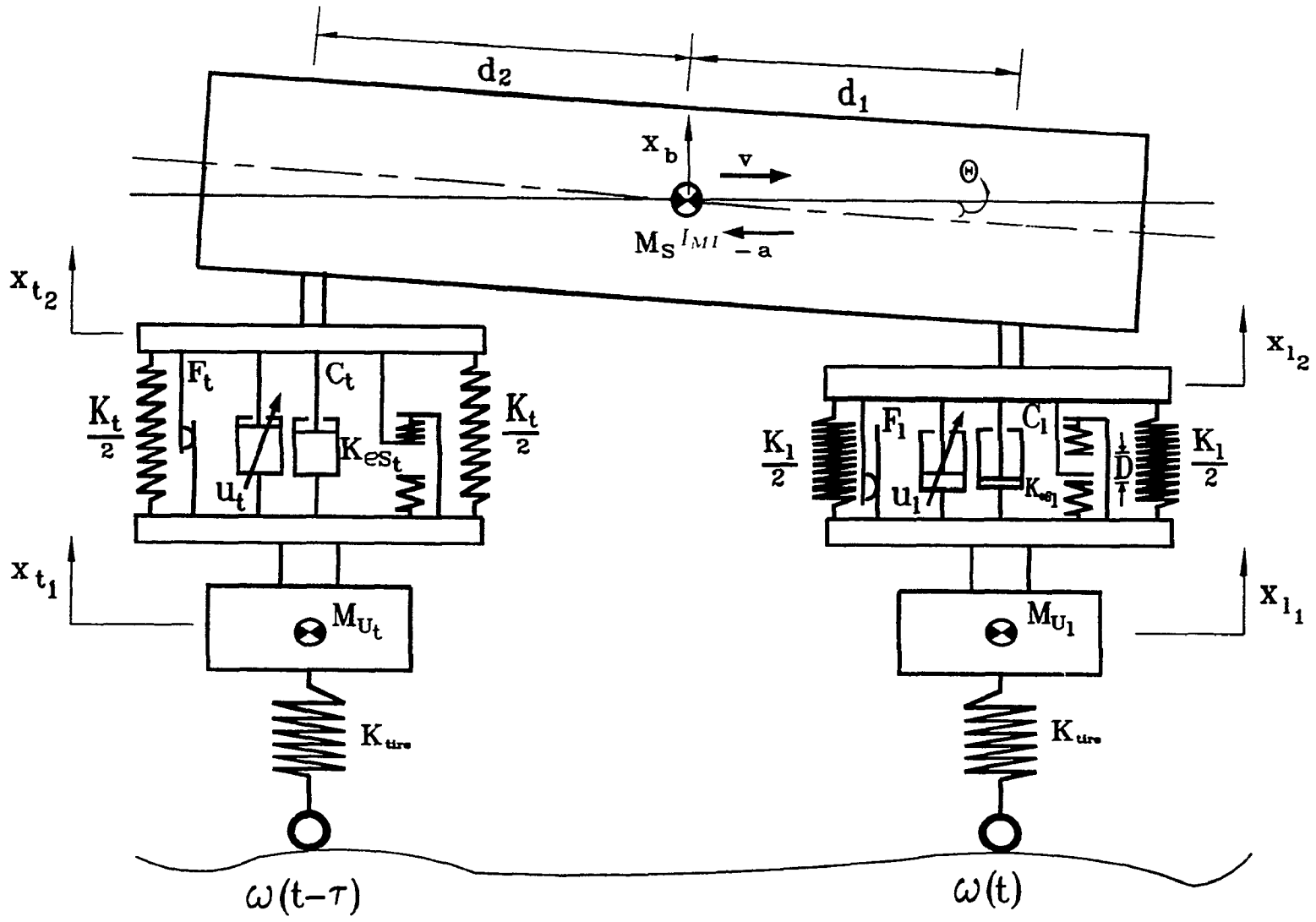


Fig.2.9: Half-car model with nonlinear time varying failsafe active suspension.

### 2.4.2 Elastic Limit Stops

Even though the elastic limit stops/jounce bumpers look unimportant, they play a crucial role in the performance of a suspension system. The limit stop forces could be represented by the equation of the form [141]

$$\begin{aligned} F_s = \quad & K_{es}(t)S^* \left[(x_2 - x_1) - \tfrac{D}{2} sgn\,(x_2 - x_1)\right] \\ where,\ S^* = & \begin{cases} 0 & if\ |x_2 - x_1| \leq \frac{D}{2} \\ 1 & otherwise \end{cases} \end{aligned} \tag{2.12}$$

where $D$ is the allowable suspension travel and $K_{es}(t)$ the stiffness due to the limit stops that could vary with the time of operation, due to factors such as temperature. This forcing function involves two types of nonlinear discontinuous functions as $S^*$ and $sgn\,(x_2 - x_1)$. The nonlinear discontinuous terms are modified to nonlinear and analytic functions to apply the Taylor series and linearize the dynamic model as follows. The discontinuous function $S^*$ is written in a simplified function form as

$$\begin{aligned} f(x) = & \begin{cases} 0 & if \quad |x| \leq \frac{D}{2} \\ 1 & otherwise \end{cases} \\ & where,\ x\ is\ (x_2 - x_1) \end{aligned} \tag{2.13}$$

The Theorem [144] on Fourier integrals as quoted below has been used.

---

If a non periodic function $f(x)$ is piecewise continuous in every finite interval and has right and left hand derivatives at every point and if the integral $\int_{-\infty}^{\infty} |f(x)|\,dx$ exists, then the function can be represented as a Fourier integral of the form

$$f(x) = \int_0^{\infty} [A(\omega)cos\,(\omega x) + B(\omega)sin\,(\omega x)]\,dw \tag{2.14}$$

where, the coefficients are given as

$$A(\omega) = \frac{1}{\pi}\int_{-\infty}^{\infty} f(u)cos\,(\omega u)\,du$$

$$B(\omega) = \frac{1}{\pi}\int_{-\infty}^{\infty} f(u)sin\,(\omega u)\,du$$

Since the function in Eq.2.13 does not satisfy the necessary condition for the Fourier integral, it could be written as $g(x) = 1 - f(x)$ where, $\int_{-\infty}^{\infty} |g(x)|\,dx$ exists. Using the Fourier integral for the function $g(x)$

$$g(x) = \begin{cases} 1 & if \quad x \leq \frac{D}{2} \\ 0 & otherwise \end{cases} \tag{2.15}$$

as

$$g(x) = \int_0^{\infty} [A(\omega)cos\,(\omega x) + B(\omega)sin\,(\omega x)]\,dw \tag{2.16}$$

where, the coefficients are given as

$$A(\omega) = \frac{1}{\pi}\int_{-\infty}^{\infty} g(u)cos\,(\omega u)\,du$$
$$B(\omega) = \frac{1}{\pi}\int_{-\infty}^{\infty} g(u)sin\,(\omega u)\,du$$

On simplification of the above coefficients, we obtain

$$A(\omega) = \frac{2sin\left(\omega\frac{D}{2}\right)}{\pi\omega}$$
$$B(\omega) = 0 \tag{2.17}$$

Hence on substituting the Fourier coefficients from the above equation into Eq.2.14 and Eq.2.16, we obtain the analytic function of the form

$$S^* = 1 - \frac{2}{\pi}\int_0^{\infty} \frac{sin\left(\omega\frac{D}{2}\right)cos\,[\omega\,(x_2 - x_1)]}{\omega}d\omega \tag{2.18}$$

Generally it is not necessary for the limit of $\omega$ in the above equation to trend towards $\infty$, but could be restricted towards a numerically large value ($\aleph$) for all practical purposes. Hence, the nonlinear and discontinuous function in the elastic stops ($S^*$) is converted to a nonlinear and continuous (analytic) function cf the form

$$S^* = 1 - \frac{2}{\pi}\int_0^{\aleph} \frac{sin\left(\omega\frac{D}{2}\right)cos\,[\omega\,(x_2 - x_1)]}{\omega}d\omega \tag{2.19}$$

The second nonlinear discontinuous term $sgn\,(x_2 - x_1)$ is made continuous by adapting the same procedure. The nonlinear term given as

$$sgn\,(x_2 - x_1) = \begin{cases} -1 & if \quad (x_2 - x_1) \leq 0 \\ 1 & otherwise \end{cases} \tag{2.20}$$

is expressed in the simpler form as

$$f(x) = \begin{cases} -1 & if \quad x \leq 0 \\ 1 & otherwise \end{cases} \qquad (2.21)$$
$$where, \quad x = (x_2 - x_1)$$

The above function does not satisfy the necessary condition for the Fourier integral $\int_{-\infty}^{\infty} |f(x)|\, dx$. Since the relative displacement $(x_2 - x_1)$ in the Eq.2.21 does not exceed the value $D$ (the maximum suspension deflection), the function $f(x)$ is restricted to have the form as

$$g(x) = \begin{cases} -1 & if \; -\acute{D} < x \leq 0 \\ 1 & 0 < x < \acute{D} \\ 0 & x > \acute{D} \;\; or \;\; x < -\acute{D} \end{cases} \qquad (2.22)$$
$$where, \quad x = (x_2 - x_1)$$

$\acute{D}$ is a number very much larger than $D$. Evaluating the Fourier coefficients by substituting the limits in the Fourier equations we have

$$g(x) = \frac{2}{\pi} \int_0^{\infty} \left[ \frac{1}{\omega} - \frac{cos\left(\omega \acute{D}\right)}{\omega} \right] sin\left[\omega\left(x_2 - x_1\right)\right] \quad d\omega \qquad (2.23)$$

Limiting the upper limit of integration to a large numerically feasible number we obtain the analytic function written as

$$g(x) = \frac{2}{\pi} \int_0^{\aleph} \left[ \frac{1}{\omega} - \frac{cos\left(\omega \acute{D}\right)}{\omega} \right] sin\left[\omega\left(x_2 - x_1\right)\right] \quad d\omega \qquad (2.24)$$

Figures 2.10 and 2.11 show the approximated continuous function compared with the actual discontinuous functions for $S^*$ and $sgn(x_2 - x_1)$ which are derived by following the above procedure.

### 2.4.3 Coulomb Friction

In the Coulomb damping, the force resisting motion is assumed to be proportional to the normal force between the sliding surfaces and is independent of velocity except for the sign. The nonlinear Coulomb damping force is given as

$$F_c = \quad F(t) sgn\left(\dot{x}_2 - \dot{x}_1\right)$$
$$where, \quad sgn\left(\dot{x}_2 - \dot{x}_1\right) = \begin{cases} -1 & if\left(\dot{x}_2 - \dot{x}_1\right) \leq 0 \\ 1 & otherwise \end{cases} \qquad (2.25)$$

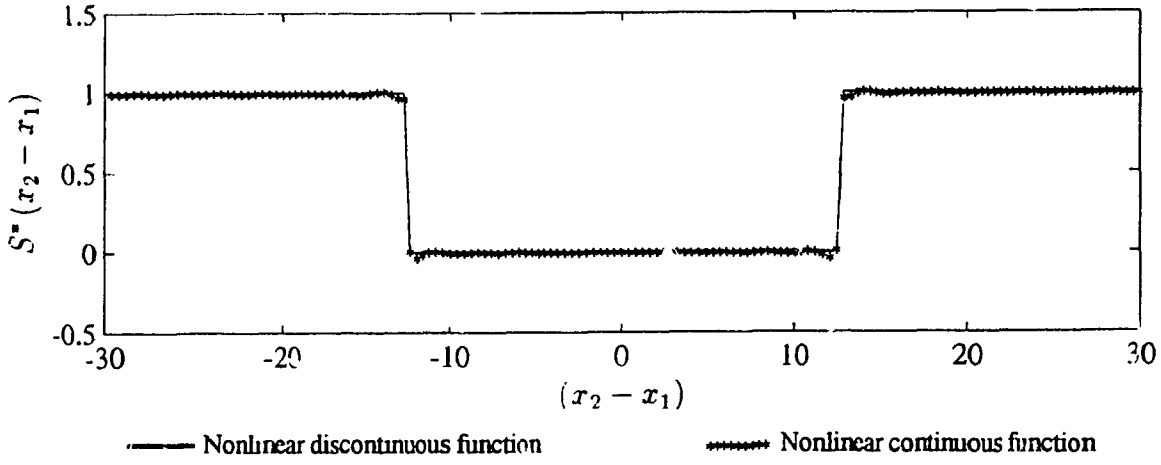


Fig.2.10: Approximated [$S^*(x_2\text{-}x_1)$] function compared with actual discontinuous function.

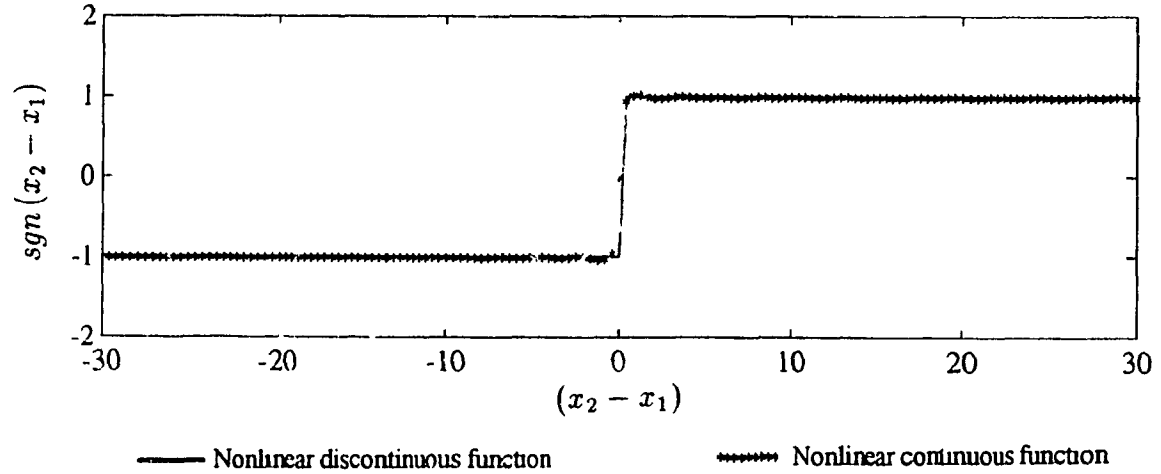


Fig.2.11: Approximated [$sgn(x_2\text{-}x_1)$] function compared with actual discontinuous function.

$F(t)$ is the magnitude of the friction force that could vary with the time of operation. Using the Fourier integrals as before, the nonlinear discontinuous $sgn\,(\dot{x}_2 - \dot{x}_1)$ function could be made continuous to obtain the final analytic function of the form

$$F_c = F(t)\frac{2}{\pi}\int_0^{\infty}\left[\frac{1}{\omega} - \frac{cos\left(\omega\grave{D}\right)}{\omega}\right] sin\left[\omega\left(\dot{x}_2 - \dot{x}_1\right)\right] \quad d\omega \tag{2.26}$$

where, $\grave{D}$ is a number much larger than $D$.

### 2.4.4 Stiffness Properties

Since suspension springs have a reasonable linear range under most operating conditions, it is assumed that the stiffness is constant with respect to deflection but as described earlier, it varies with the time of operation. The stiffness force is assumed to be of the form

$$F_k = K(t)\left(x_2 - x_1\right) \tag{2.27}$$

Since this model is linear in the operating range it is analytic at all operating points.

## 2.5 Summary

This chapter enumerated various assumptions that are made and frequently referred to throughout the dissertation. The first section described various modes of excitation that the analytical models are subjected for validation of the approach. Here, an approach adapted to extract the real time road excitation is presented. Section 2.3 presented the realistic real time and static parameter variations which were assumed to test the performance of the controller. Section 2.4 described various nonlinear and discontinuous suspension component properties that were assumed to make the model as close as possible to the actual hardware. A Fourier integral approach that was used to achieve approximation of discontinuous functions to an analytic form was also presented.

# Chapter 3

# Single Degree of Freedom Continuous Time Adaptive Active Suspension

## 3.1 General

The following chapters discuss the development of analytical models of an adaptive active suspension which achieve the objectives stated in section 1.4.2. To study the feasibility and viability of an adaptively controlled active suspension subjected to various highly demanding assumptions as indicated in chapter 2, a single degree of freedom nonlinear time varying (SDOF-NTV) model is considered. The study of a SDOF-NTV is the prime pivot of the dissertation as it provides the fundamental concepts and is best suited for experimental validation in the laboratory environment. It is also felt that it is highly logical to develop this new concept for a SDOF model before tackling the more complex multi-degree of freedom models.

This chapter involves the development of a continuous time adaptive controller based on model reference adaptive control (MRAC). Since the control theory is well developed analytically in the continuous time, an initial attempt is made to design

the adaptive control of SDOF-NTV model in the continuous time domain.

A model following problem is defined, as the parameters of the system are adjusted to achieve a required performance that is defined by a reference model. Here the adjustable parameters of the controller are varied either directly or through parameter adjustment rules such that the closed loop transfer function will be close to a prescribed reference model. The error in model following depends on the system model and the control command signal. For perfect model following the error between the system performance and the reference model would trend towards zero for all command signals and variations in the system parameters. MRAC systems are generally designed based on the following approaches [145]: the Gradient approach, the Lyapunov approach and the Passivity approach. The gradient approach is based on the assumption that the parameter changes are slower than the other variables in the system. Here the system is treated as quasi-stationary and sensitivity derivatives are evaluated for the adaptation mechanism. This approach does not necessarily lead to a stable closed loop system.

## 3.2 Dynamic System Model

A single input single output(SISO) vehicle-suspension model which could be either a front or rear suspension of the vehicle model as assumed in section 2.3.1 and as shown in Figure 2.3 is considered. Figure 3.1 shows a SISO failsafe time varying vehicle suspension model. Here the dynamic parameter variations as discussed in section 2.3 are assumed and the adaptation to counteract the static deflections are also addressed for the first time. The suspension model considered, includes a conventional passive shock absorber appended with an actuator to make it a failsafe active suspension. This simpler model would also facilitate the discussions on comparison of the adaptive active suspension with stochastic optimal control.

The dynamic equations involving the static deflection for a SISO failsafe time varying vehicle-plant shown in Fig.3.1 is derived as

$$M(t)\ddot{x} + C(t)(\dot{x} - \dot{w}) + K(t)(x - w) + M(t)g - K(t)\delta_{st} - F_{act}(t) = 0 \qquad (3.1)$$

$$M^*g = K^*\delta_{st} \qquad (3.2)$$

where $M(t)$, $K(t)$ and $C(t)$ denote the flexible load suspended and time varying stiffness and damping parameters. For simplicity a linear range of the damping performance is considered and the damping force is considered to be a linear function. The term $\delta_{st}$ in Eq.3.2 denotes the static deflection of the nominal mass $M^*$ when suspended by the nominal stiffness $K^*$. At the nominal operating conditions the second equation is satisfied to maintain the static equilibrium. The multiplication factor ' $g$ ' denotes the acceleration due to gravity. $F_{act}(t)$ is the force applied by the actuator. For the analysis of a control problem, Eq.3.1 is written as

$$M(t)\ddot{x} + C(t)\dot{x} + K(t)x = F_{cont}(t) \qquad (3.3)$$

where, the control force $F_{cont}(t)$ is given as

$$F_{cont}(t) = F_{act}(t) + C(t)\dot{w} + K(t)w - M(t)g + K(t)\delta_{st} \qquad (3.4)$$

A fully active suspension as shown in Fig.3.2 can be derived from Eqs.3.3 and 3.4 by substituting $C(t) = 0$ and $K(t) = 0$. Assuming the vehicle model as LTI for the purpose of derivation of adaptive control laws, Eq.3.3 can be expressed in the form of a SISO transfer function as

$$G(s) = \frac{X(s)}{F_{cont}(s)} = \frac{1}{Ms^2 + Cs + K} \qquad (3.5)$$

The actuator force that has to be imposed on the suspension can be derived from the controller output as follows

$$F_{act}(t) = F_{cont}(t) - C^*\dot{w} - K^*w + M^*g - K^*\delta_{st} \qquad (3.6)$$

where, $M^*$, $K^*$ and $C^*$ represent the nominal parameters and could be updated using an estimator.

A skyhook damper Linear Time Invariant (LTI) model as shown in Fig.3.3 is chosen as a reference model to describe the optimal performance required by the suspension. It is established in the literature that a skyhook suspension whose damping force is proportional to the absolute velocity would give an optimal performance between the isolation and the rattle space. The equation of motion of LTI reference model shown in Fig.3.3 can be written as

$$M_m\ddot{x}_m + D_m\dot{x}_m + K_m(x_m - w) = 0 \tag{3.7}$$

The model transfer function is given as

$$G_m(s) = \frac{X_m(s)}{W(s)} = \frac{{\omega_m}^2}{s^2 + 2\zeta_m\omega_m s + {\omega_m}^2} \tag{3.8}$$

$$where, \qquad {\omega_m}^2 = \frac{K_m}{M_m} \qquad and \qquad \zeta_m = \frac{D_m}{2M_m\omega_m}$$

$\zeta_m$ and $\omega_m$ represents the damping and natural frequency of the specified reference model.

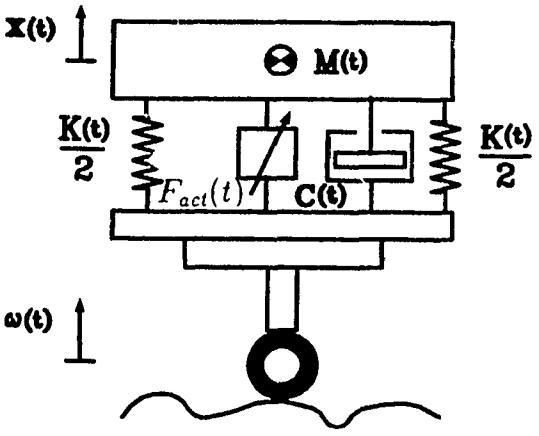


Fig.3.1: Single degree of freedom failsafe active suspension model.

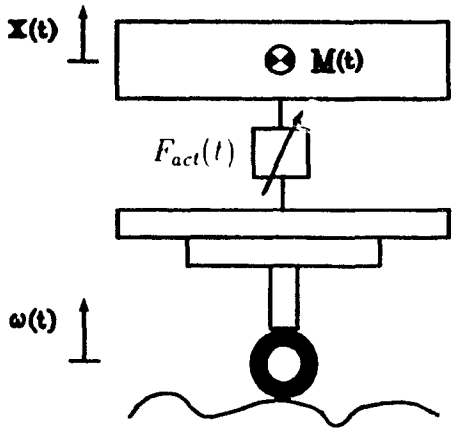


Fig.3.2: Single degree of freedom fully active suspension model.

## 3.3 Direct Model Reference Adaptive Control System Design

The LTI plant model in Eq.3.5 is represented as

$$G(s) = \frac{X(s)}{F_{cont}(s)} = \frac{1}{Ms^2 + Cs + K} = \frac{\frac{1}{M}}{s^2 + 2\zeta_p\omega_p s + {\omega_p}^2}$$

$$where, \qquad {\omega_p}^2 = \frac{K}{M} \qquad and \qquad \zeta_p = \frac{C}{2M\omega_p}$$

$$\Rightarrow \qquad \frac{X(s)}{F_{cont}(s)} = \frac{B}{A} = \frac{\frac{1}{M}}{s^2 + 2\zeta_p\omega_p s + \omega_p^2} \tag{3.9}$$

Eq.3.9 represents the required vehicle model that has to be controlled to achieve the optimal performance.

Let the LTI model transfer function in Eq.3.8 be represented as

$$\frac{X_m(s)}{W(s)} = \frac{B_m}{A_m} = \frac{{\omega_m}^2}{s^2 + 2\zeta_m\omega_m s + {\omega_m}^2} \tag{3.10}$$

where $A$, $A_m$ are the polynomials in differential operator s.

### 3.3.1 Regulator Structure Design

To design a suitable regulator structure we assume initially that the vehicle model in Eq.3.9 is known. As evident from Eq.3.9 the $deg(A) \geq deg(B)$, hence the system is proper and polynomial A is monic i.e. the coefficient of highest power of s is unity. Pole placement technique is used for the design of the regulator structure[145]. A general linear controller of the form

$$RF_{cont} = TW - SX \tag{3.11}$$

as shown in Fig.3.4 is chosen. Where R, S, T are chosen as polynomials in $s$ as

$$R(s) = s + r_1$$

$$S(s) = s_0 s + s_1$$

$$T(s) = t_0 s + t_1 \tag{3.12}$$

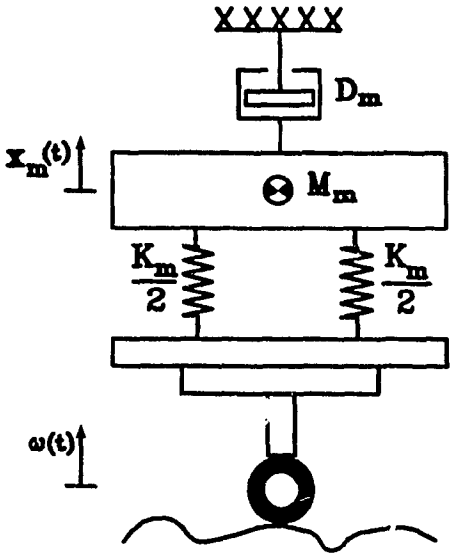


Fig.3.3: Single degree of freedom linear time invariant reference model.

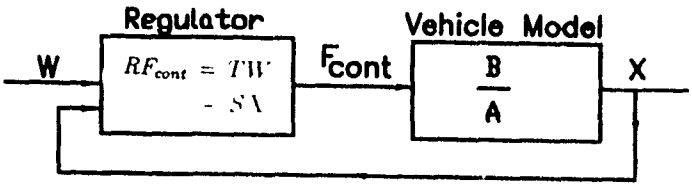


Fig.3.4: Simple degree of freedom regulator structure.

This control law denotes a feed-forward transfer function $\frac{T}{R}$ and a feed-back transfer function $(-\frac{S}{R})$. From Eqs.3.9 and 3.11 the closed-loop transfer function can be derived as

$$\frac{X(s)}{W(s)} = \frac{BT}{AR + BS} \tag{3.13}$$

For perfect model following, the controller structure is designed such that the closed-loop transfer function in Eq.3.13 should be equal to the model transfer function in Eq.3.10. The numerator of the vehicle-plant transfer function B is a constant $(\frac{1}{M})$. In general pole placement design B is split into $B^+$ and $B^-$ which represents factors that can be canceled with the closed-loop poles and the remaining factors of B respectively. In this problem

$$B = B^+B^- = 1 \times b_0 \quad where, \qquad b_0 = (\frac{1}{M}) \tag{3.14}$$

To obtain the desired closed-loop response $A_m$ should divide $(AR + BS)$ in Eq.3.13

This implies $(AR + BS)$ can be written as

$$AR + BS = B^{+}A_0A_m \qquad (Diophantine\ or\ Bezout\ equation) \tag{3.15}$$

where, $A_0$ is called the observer polynomial and $B^{+}$ is unity
The observer polynomial of the following form of degree 1 is chosen.

$$A_0 = s + a_0 \tag{3.16}$$

The choice of $A_0$ satisfies the following necessary conditions for a solution to the regulator problem to exist, namely

$$deg(A_0) \geq 2deg(A) - deg(A_m) - deg(B^{+}) - 1$$
$$deg(A_m) - deg(B_m) \geq deg(A) - deg(B)$$
$$deg(A_0) = 1;\ deg(A) = 2;\ deg(A_m) = 2;\ deg(B^{+}) = 0;$$
$$deg(B_m) = 0;\ deg(B) = 0$$

Since the second condition, which states that poles excess of reference model is equal to pole excess of the plant is satisfied, this avoids any differentiators in the control law. From the pole placement design the regulator structure can be derived as given in [145].

1. It follows from Eq.3.15 that $B^{+}$ should divide R such that

$$R_1 = \frac{R}{B^{+}}; \qquad since\ B^{+} = 1,\ R_1 = R \tag{3.17}$$

from Eqs.3.14, 3.15 and 3.17 we derive

$$AR + b_0S = A_0A_m \tag{3.18}$$

2. Also for perfect model following, $B^{-}$ should divide $B_m$

$$i.e. \quad \dot{B}_m = \frac{B_m}{b_0} \quad and \quad T = \frac{A_0B_m}{b_0} \tag{3.19}$$

Regulator parameters as coefficients of Eq.3.12 can be evaluated with complete knowledge of the vehicle model as described below. Diophantine Equation as derived in Eq.3.15 can be solved linearly to obtain coefficients of $R(s)$ and $S(s)$ as

$$r_1 = a_0 + 2\zeta_m\omega_m - 2\zeta_p\omega_p$$
$$s_0 = \left(\omega_m{}^2 + 2a_0\zeta_m\omega_m - \omega_p{}^2 - 2r_1\zeta_p\omega_p\right)/b_0$$
$$s_1 = \left(a_0\omega_m{}^2 - r_1\omega_p{}^2\right)/b_0$$

The regulator Eq.3.19 can be solved to obtain coefficients of $T(s)$ as

$$t_0 = \frac{\omega_m{}^2}{b_0}\ ; \quad t_1 = \frac{a_0\omega_m}{b_0} \tag{3.20}$$

Regulator parameters derived in the above equations are in terms of vehicle model parameters which can be evaluated only on complete knowledge of $\zeta_p$ and $\omega_p$, which would ensure perfect model following. But in the actual case, the vehicle model parameters in Eq.3.9 are not known. Hence regulator parameters are estimated to realize an adaptive controller.

### 3.3.2 Error Model Design

The Diophantine Eq.3.18 can be written as

$$ARx + b_0Sx = A_0A_mx$$

Substituting from Eqs.3.9 and 3.14 in the above equation we obtain

$$b_0\left(F_{cont}R + Sx\right) = A_0A_mx \tag{3.21}$$

On expressing the Eq.3.10 as $A_0B_mw = A_0A_mx_m$ and substituting Eq.3.19, we can derive

$$b_0Tw = A_0A_mx_m \tag{3.22}$$

subtracting Eq.3.22 from Eq.3.21 we obtain the error equation of the form

$$A_0A_m\left(x - x_m\right) = b_0\left(F_{cont}R + Sx - Tw\right)$$
$$\Rightarrow \qquad e = \frac{b_0}{A_0A_m}\left(F_{cont}R + Sx - Tw\right) \tag{3.23}$$

If the transfer function $\frac{b_0}{A_0 A_m}$ in the error model is strictly positive real (SPR) and stable, then the error ($e$) would go to zero asymptotically as $t \rightarrow \infty$. As described below, the transfer function $\frac{b_0}{A_0 A_m}$ is not SPR, hence a filtered error model is attained by multiplying with a compensator transfer function of form $\frac{Q(s)}{P(s)}$.

The transfer function $D(s) = \frac{b_0}{A_0 A_m}$ is checked for SPR as described in Ref. [115]. Substituting various polynomials, this function can be expanded as

$$D(s) = \frac{b_0}{(s+a_0)(s^2 + 2\zeta_m \omega_m s + {\omega_m}^2)} = \frac{b_0}{(s+a_0)(s^2 + z_1 s + z_2)}$$
$$where \qquad z_1 = 2\zeta_m \omega_m, \quad and \quad z_2 = {\omega_m}^2$$

The transfer function $D(s)$ would be positive real if only if it satisfies all of the following conditions.

1. *$D(s)$ is real for all real values of $s$* $\mapsto$ SATISFIED

2. *The denominator polynomial of $D(s)$ is stable.*

   This condition depends on parameters of the model chosen. Choosing the value of $a_0 = 2$, (which is always positive) and the model parameters $K_m = 5000 \frac{N}{m}$, $M_m = 250\ kg$. for an overdamped system as

   $$z_2 = {\omega^2}_m = \frac{K_m}{M_m} = 20 \left(\frac{rad}{s}\right)^2; \ and$$
   $$z_1 = 2\zeta_m \omega_m = 49.19 \frac{rad}{s}$$

   Then zero's of denominator are $-2$, $-0.41$, $-48.77$. The denominator polynomial has at least one zero close to the positive real axis (unstable region).

3. *The real part of $G(s)$ is non-negative along the $j\omega$ axis, i.e. $Re(G(j\omega)) \geq 0$.*

   For the specified model parameters

   $$Re(G(j\omega)) = b_0(-51.19\omega^2 + 40)$$

   Plotting this equation with respect to $\omega$ would show that this condition is not satisfied along the $j\omega$ axis.

Since all the above conditions are not satisfied, the transfer function $\frac{b_0}{A_0 A_m}$ is not SPR for the specified model parameters. This transfer function varies depending on the model parameters. Hence it is a conservative design to assume it is not SPR

To make the function $\frac{b_0}{A_0 A_m}$ as SPR, two polynomials $P(s)$ and $Q(s)$ are chosen such that $Q = A_0 A_m$ and $P = P_1 P_2$. Where $P_2$ is a stable monic polynomial of same degree as R such as $A_0$ and $P_1 = A_m$. Then the error equation 3.23 can be written as

$$e_f = \frac{b_0 Q}{A_0 A_m} \left( \frac{R}{P} F_{cont} + \frac{S}{P} x - \frac{T}{P} w \right) \tag{3.24}$$

where $\frac{b_0 Q}{A_0 A_m}$ is a constant $b_0$, which is SPR. Filtered error Eq.3.24 can be written in the form

$$e_f = \frac{b_0 Q}{A_0 A_m} \left( \frac{1}{P_1} F_{cont} + \frac{R - P_2}{P} F_{cont} + \frac{S}{P} x - \frac{T}{P} w \right) \tag{3.25}$$

Let $\ominus^0$ denote the nominal regulator parameter vector as

$$\ominus^0 = \{r_1, s_0, s_1, t_0, t_1\}^T \tag{3.26}$$

Let $\varphi$ represent a vector of the filtered command, input and output signal as

$$\varphi = \left( \frac{F_{cont}}{P(s)}, \frac{sx}{P(s)}, \frac{x}{P(s)}, \frac{-sw}{P(s)}, \frac{-w}{P(s)} \right)^T \tag{3.27}$$

On substituting the vectors in Eqs. 3.26 and 3.27, Eq.3.25 can be written as

$$e_f = \frac{b_0 Q}{A_0 A_m} \left( \frac{1}{P_1} F_{cont} + \varphi^T \ominus^0 \right) \tag{3.28}$$

Since the transfer function $\frac{b_0 Q}{A_0 A_m}$ is SPR and stable, the error $e_f$ goes to zero asymptotically as $t \to \infty$. Equating Eq.3.28 to zero the control law can be derived as

$$\frac{F_{cont}}{P_1} + \varphi^T \ominus^0 = 0 \qquad \Rightarrow \quad F_{cont} = -P_1 (\varphi^T \ominus)$$

where, $\ominus$ is the adjustable regulator parameters vector. To avoid derivatives of the regulator parameters, a control law of the form

$$F_{cont} = -\ominus^T (P_1 \varphi) \tag{3.29}$$

can be considered with $\varphi$ defined as in Eq.3.27. The vehicle-plant transfer function has a pole excess larger than 1, hence error augmentation has to be performed for the filter derived in Eq.3.27 [145]. To enhance the tracking of the reference model, a velocity error term is added to the filtered error ($e_f$). Then the total filtered error term is derived on substituting Eq.3.29 in Eq.3.28 to obtain

$$e_f = \frac{b_0 Q}{A_0 A_m}\left(\varphi^T \Theta^0 - \frac{1}{P_1}\Theta^T (P_1\varphi)\right) + K_v \dot{e}$$

$$e_f = \frac{b_0 Q}{A_0 A_m}\left(\varphi^T \Theta^0 - \varphi^T \Theta - \frac{1}{P_1}\theta^T (P_1\varphi) + \varphi^T \Theta\right) + K_v \dot{e} \qquad (3.30)$$

Error augmentation ($\eta$) is defined as equal to

$$\eta = \frac{1}{P_1}\Theta^T (P_1\varphi) - \varphi^T \Theta = -\left(\frac{1}{P_1} F_{cont} + \varphi^T \Theta\right) \qquad (3.31)$$

Then the augmented error ($\varepsilon$) can be derived from Eqs.3.30 and 3.31 as

$$\varepsilon = e_f + \frac{b_0 Q}{A_0 A_m}\eta + K_v \dot{e}$$

$$\varepsilon = \frac{Q}{P} e + \frac{b_0 Q}{A_0 A_m}\eta + K_v \dot{e} \qquad (3.32)$$

where the control velocity gain $K_v$ is defined as equal to $(-K_v')$. From Eq.3.31 we can also derive that

$$\varepsilon = \frac{b_0 Q}{A_0 A_m}\varphi^T \left(\Theta^T - \Theta\right) \qquad (3.33)$$

Since the augmented error model is linear in parameters and the transfer function $\frac{b_0 Q}{A_0 A_m}$ is SPR, it satisfies the requirements needed for the error to go to zero asymptotically. Once this condition is satisfied the regulator parameters could be updated by the following parametric adjustment law [145].

### 3.3.3 Parameter Adjustment Law

The regulator parameters ($\Theta$) in control law (Eq.3.29) are updated by the adjustment law of the form

$$\frac{d\Theta}{dt} = \gamma \varphi \varepsilon \quad or \quad \frac{d\Theta}{dt} = \gamma \frac{\varphi \varepsilon}{\alpha + \varphi \varphi^T} \qquad (3.34)$$

where, $\gamma$ denotes the adaptation gain that can be specified to achieve the required adaptation. On integrating the Eq.3.27, the vectors $\varphi$ and $P\varphi$ can be evaluated.

### 3.3.4 Estimation of $b_0$

The only vehicle-plant parameter that is needed for the whole control approach is $b_0$, which is $(\frac{1}{M})$. This value is estimated using a gradient estimator of the form

$$\frac{db_0^*}{dt} = \gamma \left(F_{cont}^* + \varphi^{*T} e\right) \hat{\varepsilon} \tag{3.35}$$

where, $b_0^*$ is the estimate of $b_0$ and

$$F_{cont}^* = \frac{Q}{A_0 A_m P_1} F_c \; ; \qquad \varphi_f^* = \frac{Q}{A_0 A_m} \varphi$$

and $\hat{\varepsilon}$ is the prediction error of the form $\hat{\varepsilon} = e_f - b_0^* \left(F_{cont}^* + \varphi^{*T} \cdot \right)$

### 3.3.5 Block Diagram Representation of Adaptive Controller

The control algorithm described above is represented as a block diagram in Fig.3.5 Vehicle model block represents the actual NTV vehicle model that has to be controlled. Sky-hook reference model block is the optimal model that describes the required suspension performance. The control law derived in Eq.3.29 would give the control signal $F_{cont}(t)$ in Eq.3.6 from which the actual force signal needed for the actuator $F_{act}(t)$ is evaluated. The nominal parameters described in the previous section could be used in Eq.3.6 to obtain the actuator force. But as shown in Fig.3.5 a parameter estimation could be done and the estimated values over a longer interval of time could also be used for achieving better results. Simulation results show good adaptation with the approximation of $M^*$, $C^*$ and $K^*$ as the initial design values. The adaptive controller takes care of the error due to this approximation for reasonable variation of plant dynamics. When the suspension is fully active, then $F_{act}(t) = F_{cont}(t)$ and no estimation is necessary, but a fully active suspension needs more energy and the reliability of the whole system would reduce. The block labelled *filter*, generates $\varphi$ and $P_1\varphi$ signals from $w, F_{cont}, x$ by simple trapezoidal integration

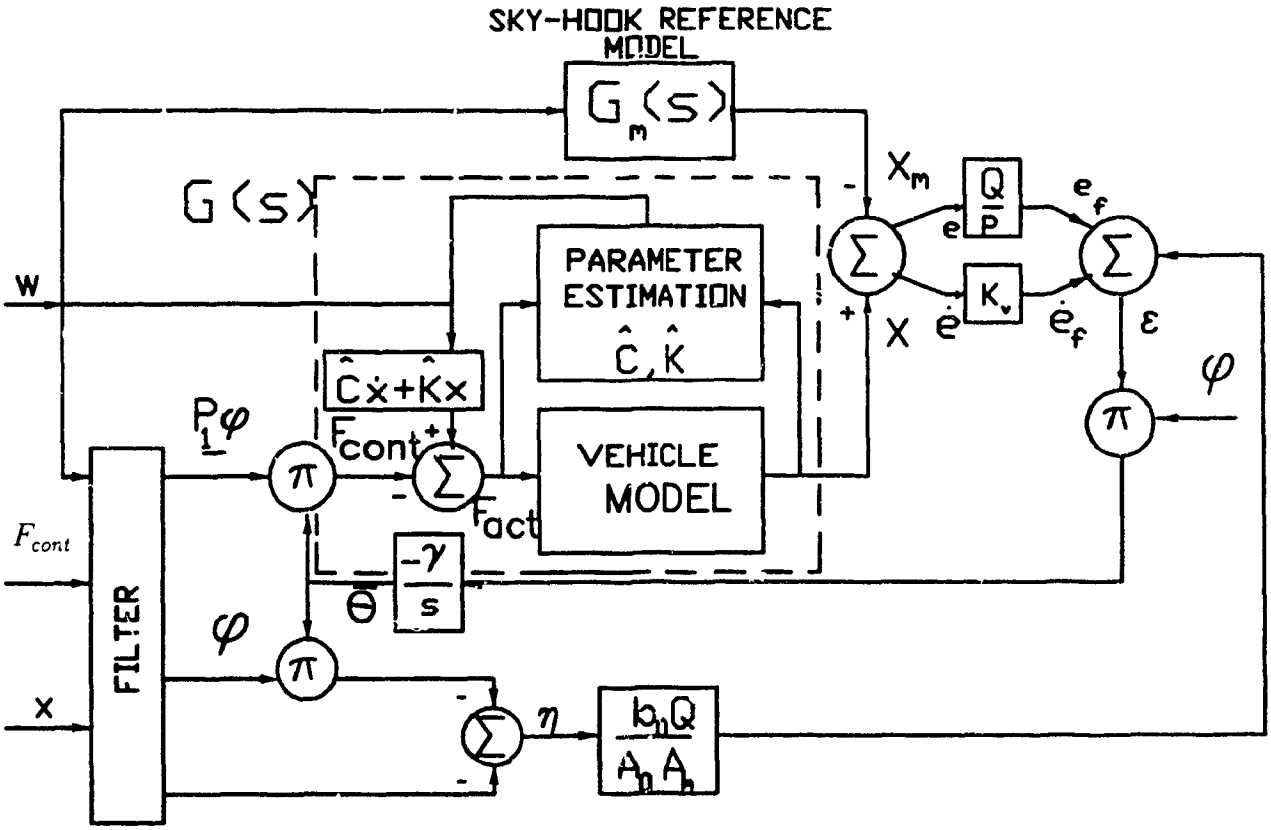


Fig.3.5: Single degree of freedom continuous time adaptive controller block diagram

## 3.4 Simulation Results

As shown in Fig 3.1 the controller developed is implemented for SDOF model. Comparative study of the adaptive active suspension with that of a passive suspension is made throughout the presentation. The nominal values of the suspension parameters for a SDOF model are taken as follows. The sprung mass $M(t)$ is considered to vary about nominal value ($M^*$) taken as 250 kg. The nominal values of stiffness ($K^*$) and damping ($C^*$) are taken as 5000 $\frac{N}{m}$ and 250 $\frac{Ns}{m}$ respectively. The reference model is chosen to have $M_m = 250\ kg$, $K_m = 5000\ \frac{N}{m}$, and $D_m = 6000\ \frac{Ns}{m}$

The objective of implementing an adaptive controller to an active suspension is to achieve the required dynamic performance as specified by the reference model in Fig.3.3 even under large and unknown variations of system parameters. The controller should be able to take care of these parameter variations without any a priori knowledge. Two types of dynamic parameter variations as discussed in chapter 2 such as *Parameter variations mode I* and *Parameter variations mode II* are incorporated to test the controller.

The controller designed should show robustness to the different types of parameter variations and at the same time should be able to achieve the optimal performance as required by the reference model. The model parameters described above are needed only for simulation purposes and are not necessary for control design and implementation of the adaptive active suspension.

### 3.4.1 *Excitation mode I* and *Parameter variations mode I*

The adaptive active suspension and passive suspension are subjected to a deterministic input of the form of a combination of sinusoidal functions with frequencies around the natural frequency, as described in *Excitation mode I* in chapter 2. The active and passive suspensions are also assumed to be imposed with the *Parameter variations*

*mode 1* along with the *Excitation mode 1*. Fig.3.6 shows the sprung mass absolute displacement response of the reference model, the adaptive active suspension model and the passive suspension model in the time domain. The reference model response indicates the performance of the skyhook reference model chosen. The adaptive controller response indicates how the vehicle suspension model would achieve the optimal performance by following the reference model. This response is obtained by solving Eq.3.1 with the actuator force $F_{act}(t)$ calculated from Eq.3.6. The controller force $F_{cont}(t)$ is evaluated from Eq.3.29. The controller updates the gains to achieve the stable tracking of the reference model within 10 seconds of operation. After 20 seconds of operation, the passive and failsafe active models are subjected to sprung mass variations as shown in Fig.2.1c. For sprung mass variation as described in *Parameter variation mode 1*, the passive suspension would have a static deflection corresponding to the spring stiffness. The active suspension which has already adapted to the reference model would maintain its initial static level and continues to follow the reference model. When ever there is a variation of the suspended load, the adaptive controlled active suspension would deviate very little from the optimal performance and adapts to the reference model within a few seconds as indicated at the instants 20 and 40 seconds. Fig.3.6 also shows the robustness of adaptive active suspension to the variations in stiffness constant $K(t)$ and damping coefficient $C(t)$ as described in Figs. 2.7 and 2.8. Fig.3.7 shows the acceleration response for the deterministic input. The adaptive active suspension response has a higher amount of acceleration transmitted in the initial pre-adaptation period. But once the adaptation to the reference model takes place, the acceleration is very low when compared to the passive suspension. Fig.3.8 indicates the variation of controller parameters ($\cdot$ ) as indicated in Eq.3.26. The controller gains are updated from their initial values to some required values to achieve proper tracking of the reference model. The displacement and velocity error during the model following is shown in Fig.3.9. The error reduces exponentially during the transient period and after adaptation during parameter variations. The actuator force $F_{act}(t)$ needed for tracking the reference model is shown in Fig.3.10. The actuator force needed when there is no sprung mass variation is less since the

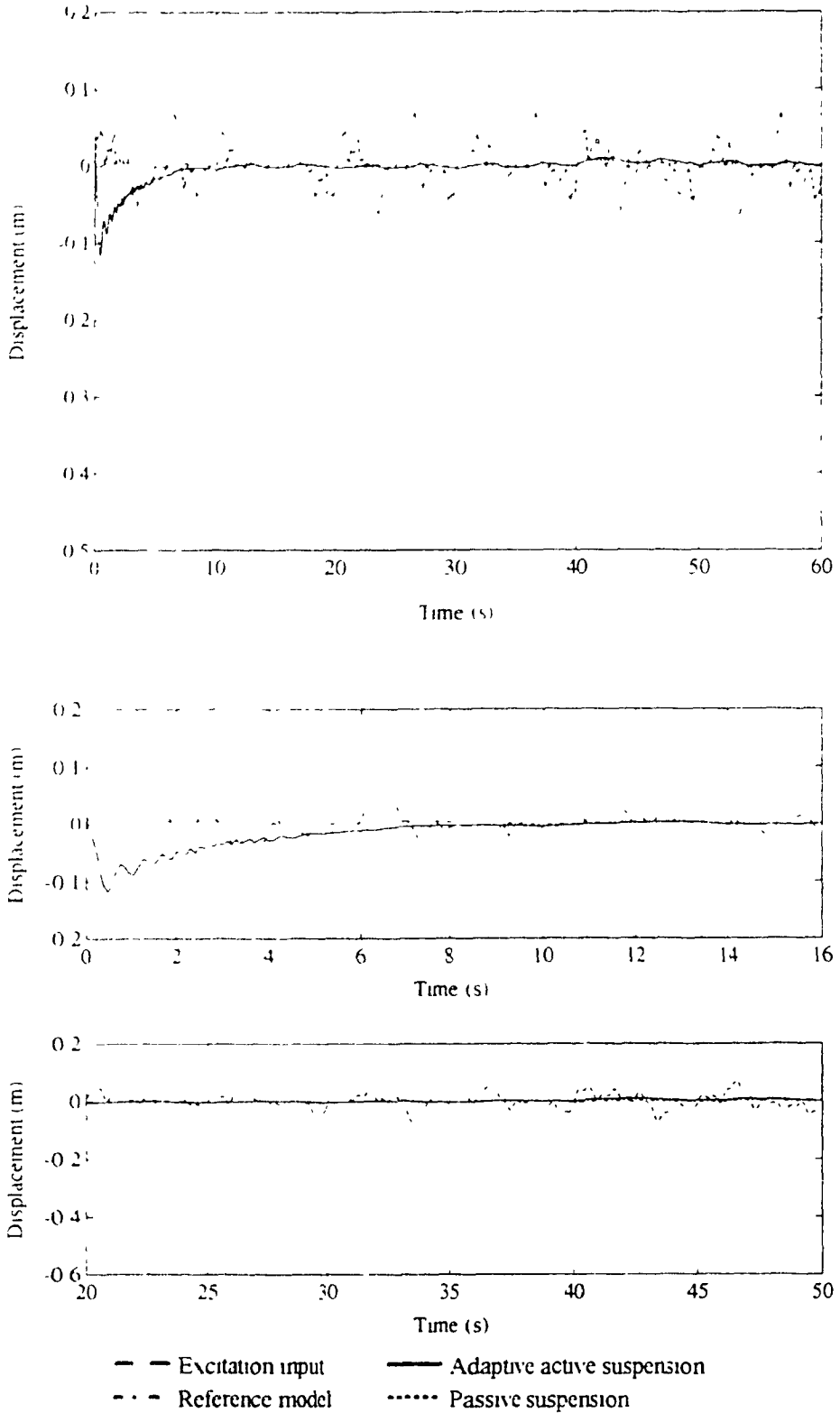


Fig.3.6: Sprung mass absolute displacement response for *Excitation mode I* & *Parametric variations mode I*

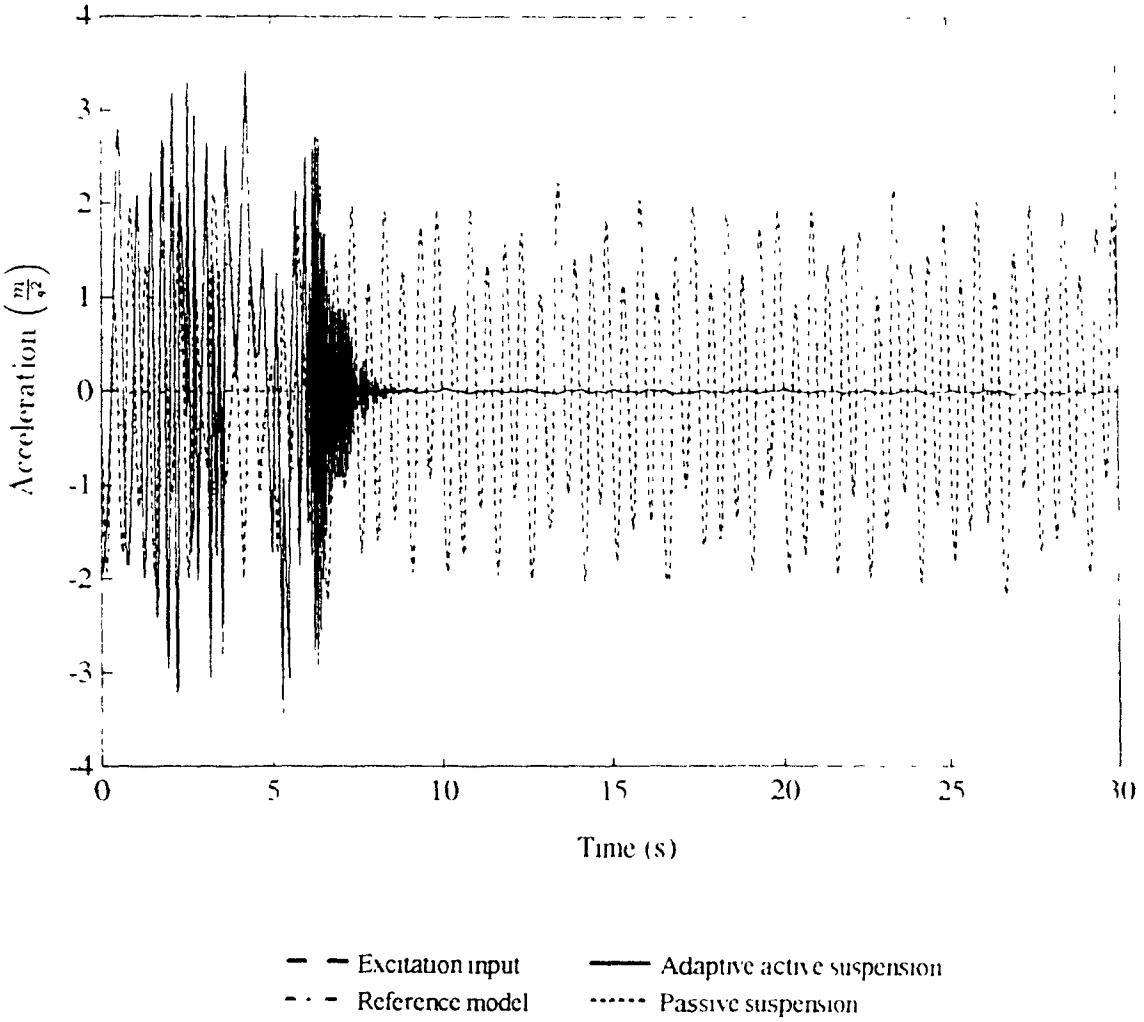


Fig.3.7: Sprung mass absolute acceleration response for *Excitation mode 1* & *Parametric variations mode 1*

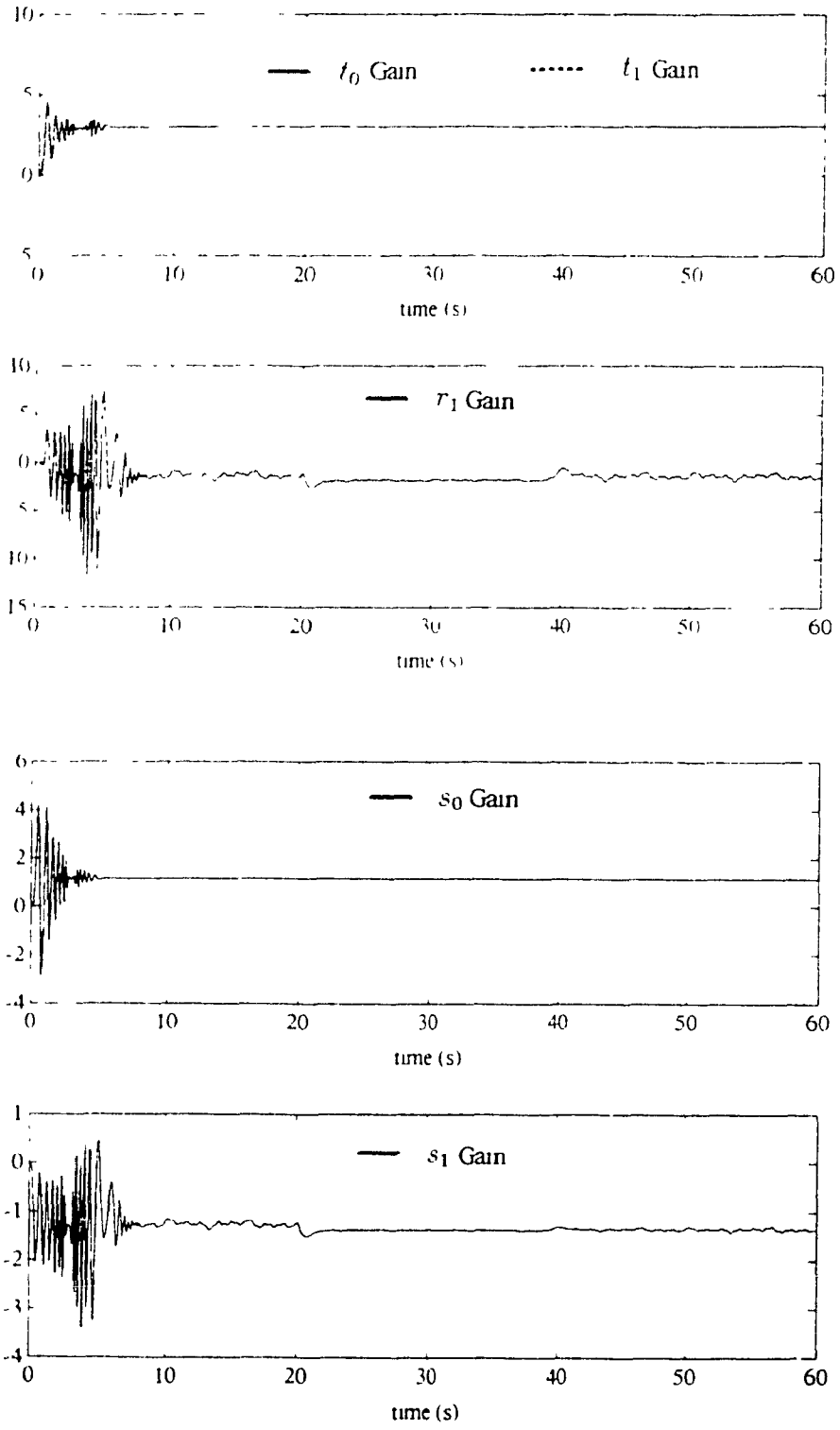


Fig.3.8: Variation of adaptive controller parameters.

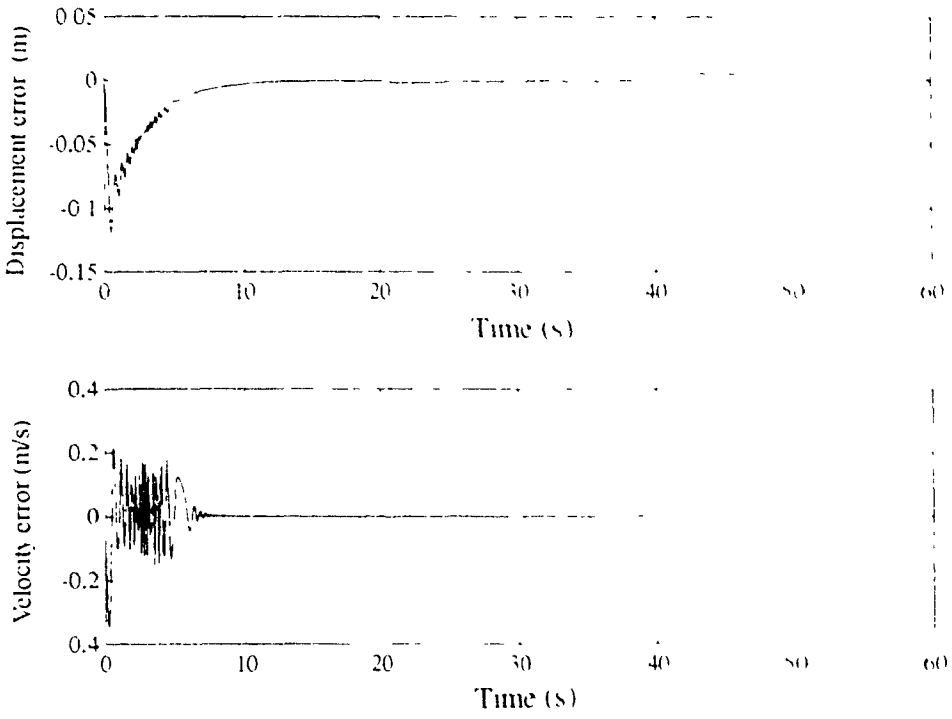


Fig.3.9· Displacement and velocity model following errors

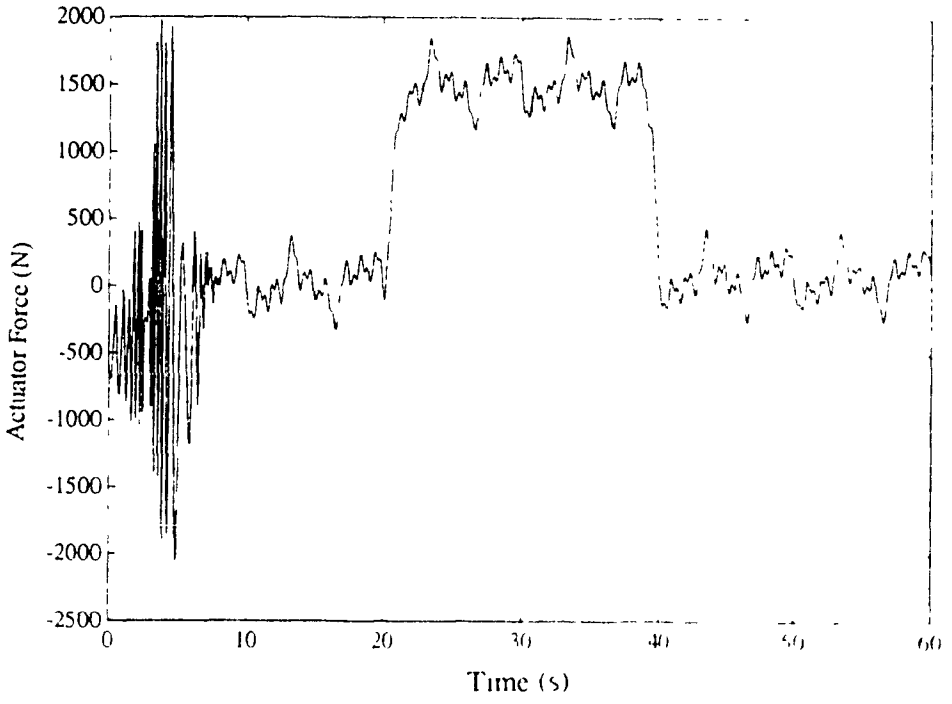


Fig.3.10. Actuator control force

passive elements of failsafe active suspension would share the static load. There is an upward force with a mean value of 1500 N exerted to take care of the static level changes due to the presence of the adaptive active suspension.

### 3.4.2 *Excitation mode II* and *Parametric variations mode II*

The adaptive active suspension and passive suspension are subjected to different random road inputs (asphalt, paved and dirt roads) described as *Excitation mode II* in section 2.2.2. The results obtained for dirt roads which have higher amplitudes are presented in this section. As described under *Parameter variations mode II*, the adaptive active and passive suspension systems are subjected to various parameter variations. Here we assume that the parameters are completely unknown a priori as described in section 2.3.2. Fig.3.11 shows the real time simulation sprung mass absolute displacement response for an adaptive active suspension and a passive suspension. Due to the sprung mass estimation error of 40% and the reduction of the suspension spring stiffness by 10% the passive suspension would result in a static deflection and would continue to have higher amplitude at lower frequencies. But an adaptive active suspension would adapt to the reference model and shows no static deflection. Results obtained in terms of Power spectral density (PSD) for absolute displacement and relative displacement for excitation, reference model, adaptive active suspension and passive suspension are presented in this section. System gain factors which represent the magnitude of the transfer functions of absolute displacement and relative displacement with respect to excitation input are also presented.

Fig.3.12 indicates the PSD of absolute displacements for the reference model, the adaptive active suspension and passive models when excited by a dirt road with PSD as shown in Fig.2.1. A passive suspension would have a static deflection as shown in Fig.3.11 which is shown as a large amplitude at lower frequencies and would shift the PSD curve to higher magnitude. The reference model PSD shows a well damped displacement response both at natural and higher frequencies. The adaptive

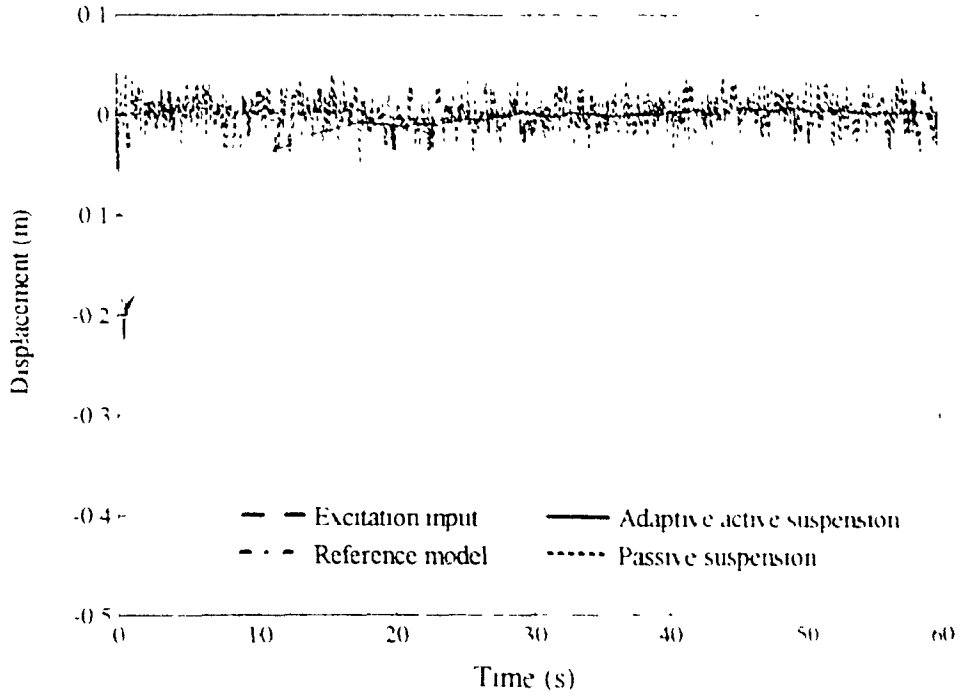


Fig.3.11: Sprung mass absolute displacement response for *Excitation mode II* & *Parametric variations mode II*

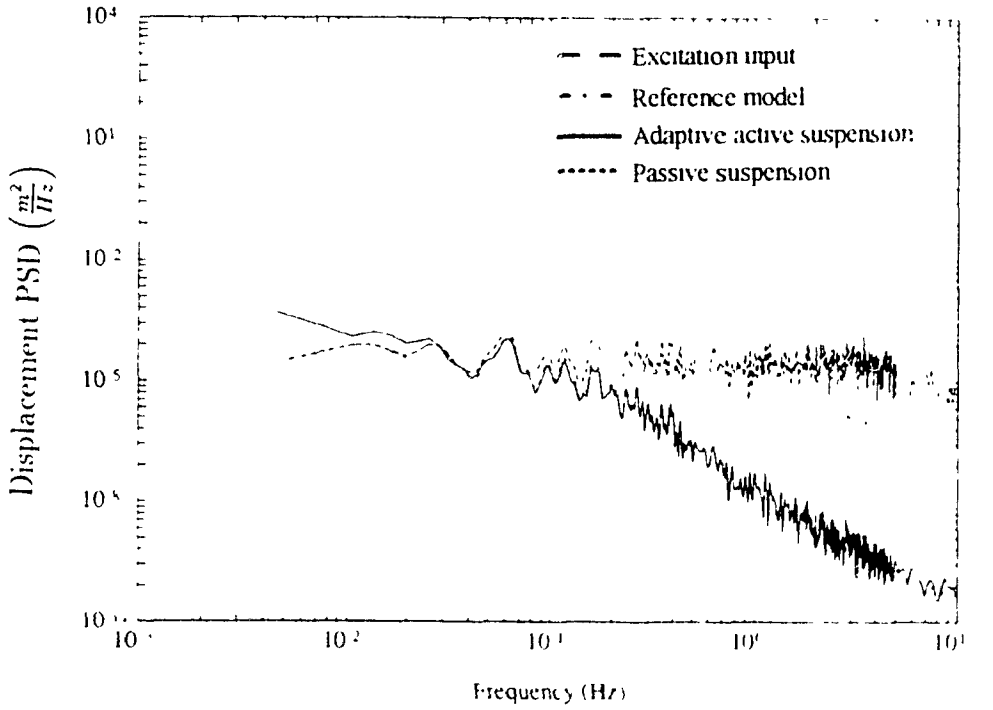


Fig.3.12: Sprung mass absolute displacement power spectral density (PSD) response for *Excitation mode II* & *Parametric variations mode II*.

active suspension would follow the reference model very closely at most of the frequency range. Fig.3.13 shows the system gain factor between absolute displacement of various models and excitation input. Fig.3.13 also shows that an adaptive active suspension adapts to the reference model and hence maintains the static equilibrium level. But a passive suspension shows magnitude shift due to change in the static level under suspended load variation. The adaptive active suspension response shows good isolation properties throughout the frequency range but deviates at very low frequency because of initial adaptation to the reference model. Fig.3.14 shows the relative displacement PSD curves for the reference, adaptive active and passive suspension models. The constant static deflection due to suspended load variation which results in a constant relative displacement for passive suspension shows at low frequencies. The adaptive active suspension shows deviation from the reference model only at low frequencies because of initial adaptation. Figures 3.11, 3.12, 3.13 and 3.14 indicate the effect of *Parameter variations mode II* where, the initial unknown parameters of the model exist and the adaptive controller adapts to the reference model maintaining static equilibrium and optimal suspension characteristics. The reference model and adaptive active suspension relative displacement response indicates a lower magnitude at all the frequencies due to maintenance of static equilibrium and achieves the required active suspension characteristics.

When the vehicle is operating at the nominal parametric conditions and is not subjected to any parametric variations, then the passive suspension would exhibit no static deflection. Results obtained under these conditions are presented in figures 3.15 and 3.16. These figures indicate the system gain factor between the absolute and relative displacements with respect to the excitation input. When compared to a passive suspension system, Fig.3.15 shows good isolation properties at the natural frequency and at higher frequencies. The adaptive active suspension adapts to the reference model throughout the range. Fig.3.16 shows the relative displacement characteristics with respect to the excitation input in terms of the system gain factor. The reference and the adaptive active suspension performance indicates good reduction of rattle

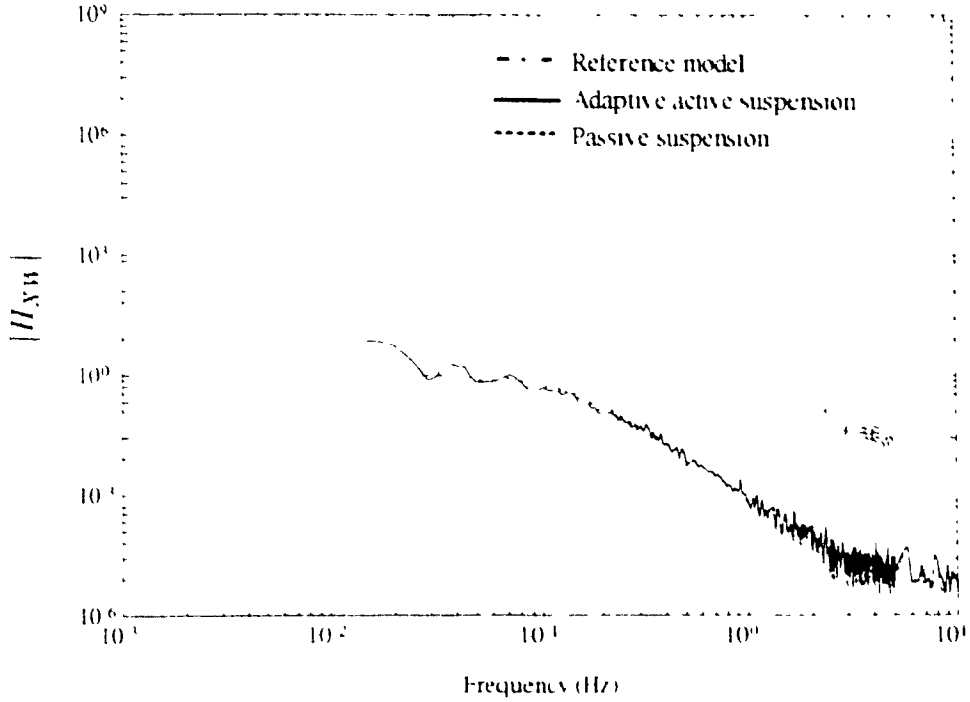


Fig.3.13. System gain factor of sprung mass absolute displacement with respect to excitation input.

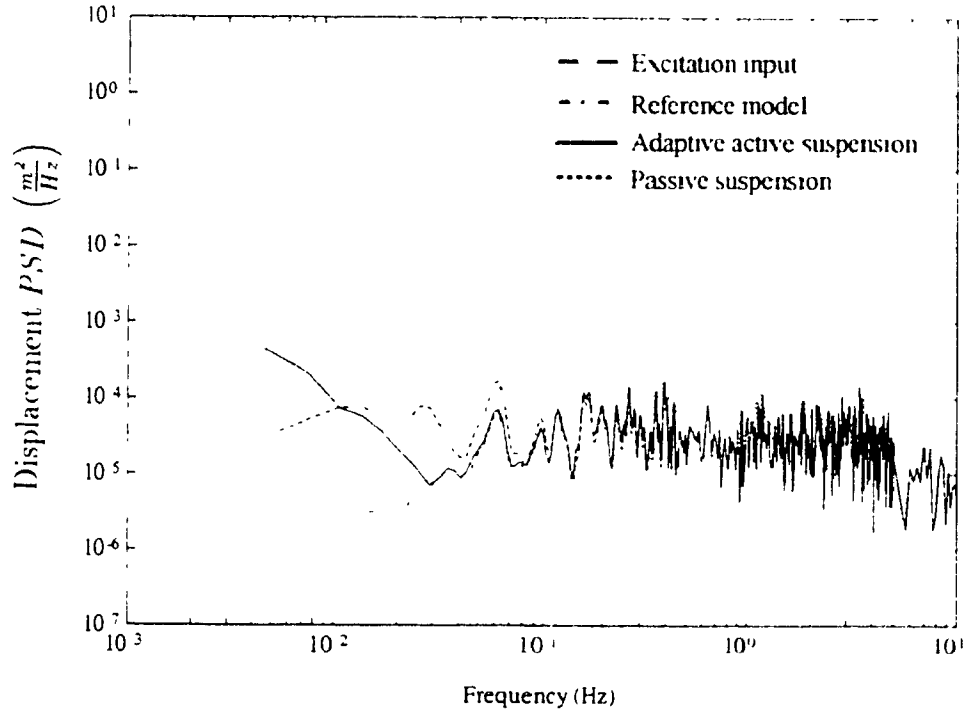


Fig.3.14: Relative displacement power spectral density (PSD) response for *Parametric variations mode II.*

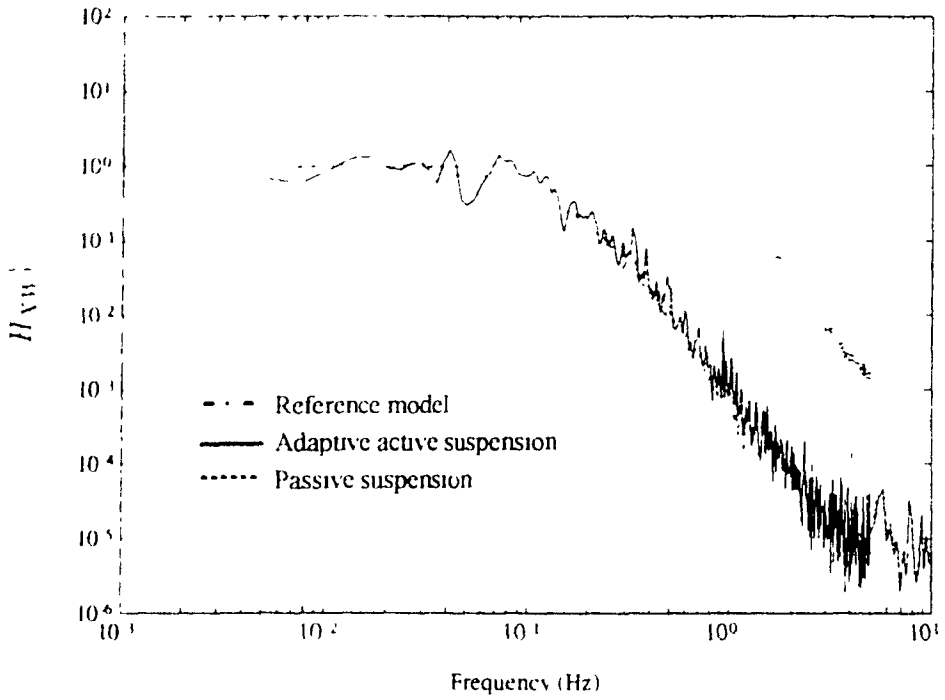


Fig.3.15 System gain factor of sprung mass absolute displacement with respect to excitation input without static deflection.

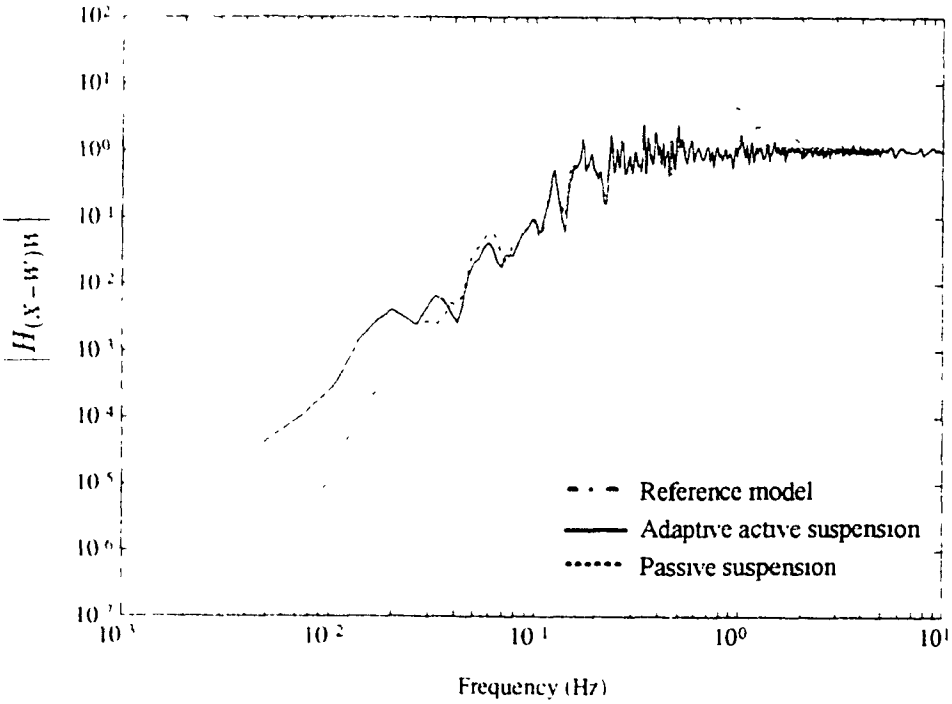


Fig 3.16: System gain factor of relative displacement with respect to excitation input without static deflection.

space at the natural frequency. Figures 3.15 and 3.16 indicate better performance by an adaptive active suspension both in terms of absolute and relative displacements for the nominal design parameters of the vehicle model. The results presented so far for the stochastic input indicates that an adaptive controlled active suspension would give an optimal performance by reducing both absolute and relative displacements at the same time without any static deflection even under gross operational parameter variations.

## 3.5 Discussion

Simulation results for a basic failsafe suspension system have been presented to initially demonstrate the concept of an adaptive active suspension system. The results for *Excitation mode I & II* and *Parameter variations mode I & II* indicate good adaptation to the reference model. The results also indicate that the objectives set forward in Chapter 1 subjected to some of the assumptions in Chapter 2 are achievable. The simulation results obtained for deterministic input and stochastic input are based on the sampling interval of 0.01 seconds. Since the sampling frequency is not very high, the hardware necessary for practical implementation need not be sophisticated. This would also increase the reliability and ruggedness of the hardware which in turn would reduce the installation and maintenance costs. A lesser sampling interval would improve the tracking performance further due to faster computer control. The initial controller parameters $(\cdot\cdot)$ can be chosen to be of any arbitrary values. Better transient response in the reference model following could be achieved by having some knowledge about the initial values of the gains. The reference model need not be physically realizable and its parameters are coded in the controller. As described in Eq.3.8, the active suspension performance required could be specified by varying the damping and natural frequency parameters of the reference model in the controller. Fig.3.11 shows the results for *Excitation mode II* and *Parameter variation mode II* which indicate good initial adaptation even with uncertainty in the gross

nominal values. More detailed designs involving nonlinearities and MDOF models are discussed in the following chapters.

## 3.6 Summary

An adaptive control approach for an active suspension in the continuous time domain for a single degree of freedom nonlinear time varying model that deals with time varying parameters has been discussed. The adaptive control approach has been analyzed for the maintenance of static equilibrium levels for the first time. A continuous time model reference adaptive control with velocity error term added has been designed to enhance the tracking of the reference model. Simulation results for the real time control with *Excitation mode I & Parameter variation mode I* and *Excitation mode II & Parameter variation mode II* are presented. A block diagram representation of the adaptive controller that was designed was also presented. Simulation results indicate very good performance of adaptive active suspension in adapting to the reference model thereby obtaining optimal performance and maintaining static equilibrium level under large dynamic load variations.

# Chapter 4

# Discrete Adaptive Controller for Single Degree of Freedom Nonlinear Time Varying Active Suspension

## 4.1 General

Implementation of advanced control algorithms generally involves digital computers and micro-electronics. The ease of implementation of micro-processor based computer controlled systems for on line control problems is well known. Discrete domain analysis is very instrumental in dealing with digital controllers in general and with complicated situations involving large time delays in particular. In this chapter the single degree of freedom nonlinear time varying (SDOF-NTV) suspension model is analyzed in the discrete domain incorporating various time delays normally encountered in practical implementation for the first time. Variation in the static equilibrium position of any suspension due to static or dynamic load changes like payload variations and load variations due to acceleration or deceleration as discussed in chapter 2 is also incorporated. Deterministic auto-regressive moving average (DARMA) models of the linearized suspension model and linear time invariant (LTI) and reference model

are derived. A discrete model reference adaptive control (MRAC) approach with recursive least square (RLS) estimation is used to form the controller. The analytical results obtained in this chapter are experimentally validated in chapter 8.

## 4.2 Dynamic Equations for Single Input Single Output Model

### 4.2.1 Nonlinear Failsafe Active Suspension Model

A nonlinear SDOF suspension model as shown in Fig.4.1 is considered for analysis. The suspension model is considered to have Coulomb friction damping, an elastic spring supporting the mass, viscous damper with velocity squared viscous damping

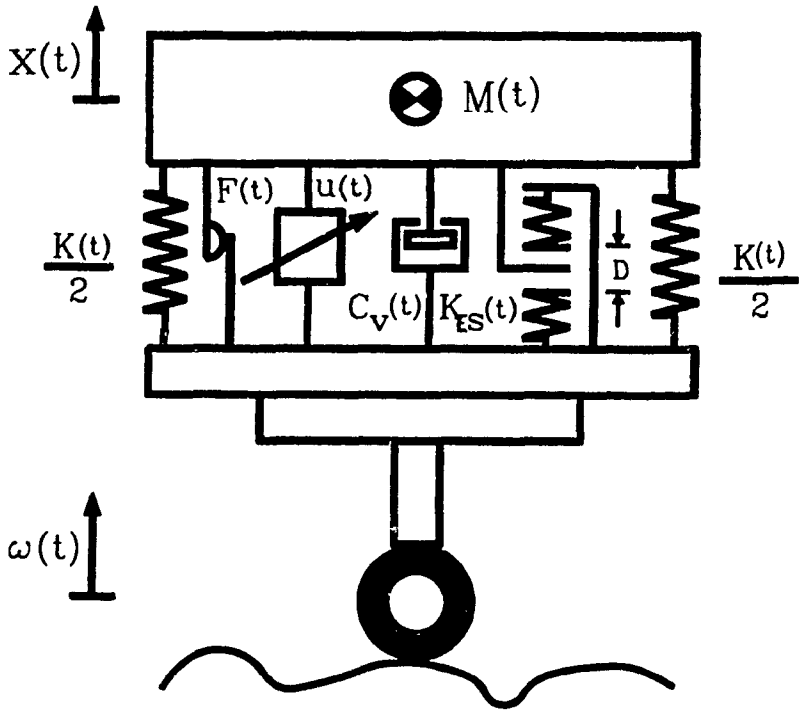


Fig.4.1: Nonlinear single degree of freedom failsafe active suspension model.

and elastic motion limit stops as discussed in section 2.4. Taking into consideration various nonlinear time varying terms and static deflection due to inertial mass variation, the equations of motion in terms of the relative displacement ($z = x - w$) can be written as

$$M(t)\ddot{z} + \mathcal{F}(z,\dot{z},t) = u(t) - M(t)\ddot{w}(t) + K(t)\delta_{st} - M(t)g \tag{4.1}$$

$$M^*g = K^*\delta_{st} \tag{4.2}$$

where, $M(t)$, $K(t)$ and $u(t)$ denote the time varying spring mass suspended, coil spring stiffness and actuator force exerted on the mass. The term $\delta_{st}$ in Eq.4.2 denotes the static deflection of the nominal mass $M^*$ when suspended by the nominal stiffness $K^*$. At the static condition the second equation is satisfied at the nominal operating conditions. The NTV term $\mathcal{F}(z,\dot{z},t)$ represents the cumulative force exerted due to elastic limit stops, velocity squared viscous damping, Coulomb friction damping and suspension spring force as discussed in section 2.4 [141]

$$\mathcal{F}(z,\dot{z},t) = F_s(z,t) + F_d(\dot{z},t) + F_c(\dot{z},t) + F_k(z,t) \tag{4.3}$$

*where,*

$$F_s(z,t) = K_{es}(t)S^*\left[z - \tfrac{D}{2}sgn(z)\right]$$

$$S^* = \begin{cases} 0 & \text{if } |z| \le \frac{D}{2} \\ 1 & \text{otherwise} \end{cases}$$

$$F_d(\dot{z},t) = C_v(t)\,|\dot{z}|\,(\dot{z})$$

$$F_c(\dot{z},t) = F(t)sgn(\dot{z})$$

$$F_k(z,t) = K(t)z$$

### 4.2.2 Reference Model

A skyhook damper linear time invariant (LTI) model as shown in Fig.4.2 is chosen as the reference model which describes the performance needed by the suspension.

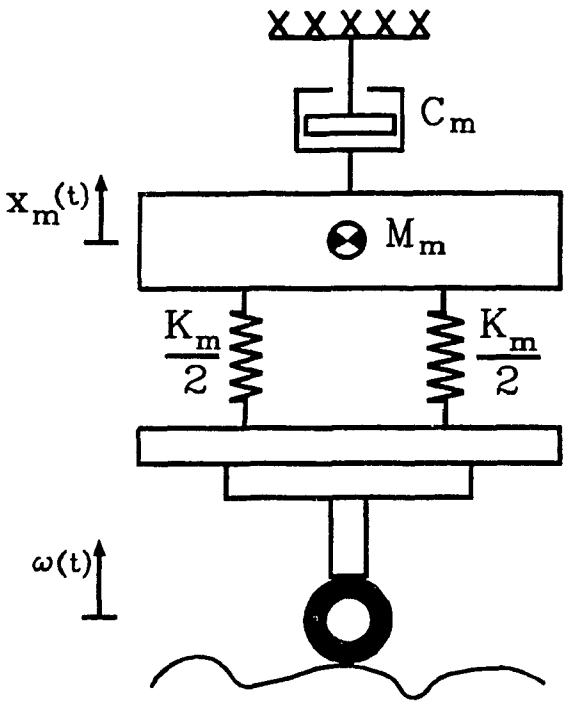


Fig.4.2: Linear time invariant reference model.

It is established in the literature that a skyhook suspension whose damping force is proportional to the absolute velocity, would give an optimal performance between the acceleration transmitted and the suspension travel. The reference model is needed theoretically and it is not needed to be physically realizable for practical implementation of the adaptive controller. The equation of motion of the model in terms of relative displacement ($z_m = x_m - w$) is given as

$$M_m \ddot{z}_m + C_m \dot{z}_m + K_m z_m = -M_m \ddot{w} - C_m \dot{w} \tag{4.4}$$

where, $M_m, C_m, K_m$ denote the mass, damping coefficient and stiffness constant of the model.

### 4.2.3 Linearization of Suspension Model

The nonlinear discontinuous model described in Eqs.4.1, 4.2 and 4.3 are transformed to nonlinear and analytic equations using the Fourier integrals. By using the results derived in section 2.4 of chapter 2, the nonlinear discontinuous terms in Eq.4.3 could be modified as

$$\begin{aligned} F_s(z,t) &= K_{es}(t)S^* \left[z - \tfrac{D}{2}sgn(z)\right] \\ S^* &= 1 - \tfrac{2}{\pi}\int_0^{\aleph}\left[\tfrac{\sin(\frac{\omega D}{2})\cos(\omega z)}{\omega}\right] d\omega \\ sgn(z) &= \tfrac{2}{\pi}\int_0^{\aleph}\left[\tfrac{(1-\cos(\omega D))}{\omega}\sin(\omega z)\right] d\omega \qquad (4.5) \\ F_c(\dot{z},t) &= F(t)sgn(\dot{z}) \\ sgn(\dot{z}) &= \tfrac{2}{\pi}\int_0^{\aleph}\left[\tfrac{(1-\cos(\omega D))}{\omega}\sin(\omega \dot{z})\right] d\omega \end{aligned}$$

Now the analytic functions are linearized about an operating point $\mathcal{OP}(t_0, z_0, u_0, w_0)$. If $(\triangle t, \triangle z, \triangle u, \triangle w)$ are the variation of the parameters $(t, z, u, w)$ about the operating point $\mathcal{OP}$, then

$$\begin{aligned} t &= t_0 + \triangle t \\ z &= z_0 + \triangle z \\ u &= u_0 + \triangle u \\ w &= w_0 + \triangle w \qquad (4.6) \end{aligned}$$

At the operating point from Eqs.4.1, 4.2 and 4.3 the dynamic equation of motion can be written as

$$\begin{aligned} M(t_0)\ddot{z}_0 + F_s(z_0,t_0) + F_d(\dot{z}_0,t_0) + F_c(\dot{z}_0,t_0) + F_k(z_0,t_0) = u(t_0) - \\ M(t_0)\ddot{w}(t_0) + K(t_0)\delta_{st} - M(t_0)g \qquad (4.7) \end{aligned}$$

The nonlinear and time varying terms in Eq.4.5 which are analytic at every point can be expanded by the Taylor series about the operating point (taking into consideration

the first order terms only) as

$$\begin{aligned}
F_s(z,t) &= F_s(z_0,t_0) + \left.\frac{\partial F_s}{\partial z}\right|_{\mathcal{OP}} \triangle z + \left.\frac{\partial F_s}{\partial t}\right|_{\mathcal{OP}} \triangle t + \cdots \\
F_d(\dot{z},t) &= F_d(\dot{z}_0,t_0) + \left.\frac{\partial F_d}{\partial \dot{z}}\right|_{\mathcal{OP}} \triangle \dot{z} + \left.\frac{\partial F_d}{\partial t}\right|_{\mathcal{OP}} \triangle t + \cdots \\
F_c(\dot{z},t) &= F_c(\dot{z}_0,t_0) + \left.\frac{\partial F_c}{\partial \dot{z}}\right|_{\mathcal{OP}} \triangle \dot{z} + \left.\frac{\partial F_c}{\partial t}\right|_{\mathcal{OP}} \triangle t + \cdots \\
F_k(z,t) &= F_k(z_0,t_0) + \left.\frac{\partial F_k}{\partial z}\right|_{\mathcal{OP}} \triangle z + \left.\frac{\partial F_k}{\partial t}\right|_{\mathcal{OP}} \triangle t + \cdots \\
M(t) &= M(t_0) + \left.\frac{\partial M}{\partial t}\right|_{\mathcal{OP}} \triangle t + \cdots \\
K(t) &= K(t_0) + \left.\frac{\partial K}{\partial t}\right|_{\mathcal{OP}} \triangle t + \cdots
\end{aligned} \tag{4.8}$$

For the evaluation of partial derivatives in the above terms which in turn involves definite integrals, the following theorem based on derivative of an integral is used.

The derivative of the integral of the form $\int_p^q f(x,a)\,dx$ is given as [147]

$$\frac{d}{da}\left[\int_p^q f(x,a)\,dx\right] = \int_p^q \frac{\partial}{\partial a}[f(x,a)]\,dx + f(q,a)\frac{dq}{da} - f(p,a)\frac{dp}{da} \tag{4.9}$$

**Example:**

For the evaluation of the term $\left.\frac{\partial F_s}{\partial z}\right|_{\mathcal{OP}} \triangle z$ where,

$$F_s(z,t) = K_{es}(t)S^*\left[z - \frac{D}{2}sgn(z)\right] \tag{4.10}$$

*where,*

$$S^* = 1 - \frac{2}{\pi}\int_0^{\aleph}\left[\frac{\sin\left(\frac{\omega D}{2}\right)\cos(\omega z)}{\omega}\right]d\omega$$

$$sgn(z) = \frac{2}{\pi}\int_0^{\aleph}\left[\frac{\left(1-\cos(\omega D)\right)}{\omega}\sin(\omega z)\right]d\omega$$

But

$$\begin{aligned}
\frac{\partial F_s(z,t)}{\partial z} &= K_{es}(t)\frac{d}{dz}\left[S^*\left(z - \frac{D}{2}sgn(z)\right)\right] \\
&= K_{es}(t)\left[\frac{d}{dz}[S^*z] - \frac{D}{2}\frac{d}{dz}[S^*sgn(z)]\right] \\
&= K_{es}(t)\left[S^* + z\frac{d}{dz}[s^*] - \frac{D}{2}S^*\frac{d}{dz}[sgn(z)] - \frac{D}{2}sgn(z)\frac{d}{dz}[S^*]\right]
\end{aligned} \tag{4.11}$$

On applying the theorem in Eq.4.9 to evaluate various terms in the above equation, we obtain

$$\begin{aligned}\frac{d}{dz}[s^*] &= \frac{d}{dz}\left[1 - \frac{2}{\pi}\int_0^{\aleph}\left[\frac{\sin\left(\frac{\omega D}{2}\right)\cos(\omega z)}{\omega}\right]d\omega\right] \\ &= -\frac{2}{\pi}\int_0^{\aleph}\frac{\partial}{\partial z}\left[\frac{\sin\left(\frac{\omega D}{2}\right)\cos(\omega z)}{\omega}\right]d\omega \qquad (4.12) \\ &= \frac{2}{\pi}\int_0^{\aleph}\left[sin\left(\frac{\omega D}{2}\right)sin\left(\omega z\right)\right]d\omega\end{aligned}$$

Since the limits are constant, the contributions due to the terms involving the limits of integration in Eq.4.9 are zeros. Similarly

$$\begin{aligned}\frac{d}{dz}[sgn(z)] &= \frac{d}{dz}\left[\frac{2}{\pi}\int_0^{\aleph}\left[\frac{1-cos\omega\acute{D}}{\omega}sin\left(\omega z\right)d\omega\right]\right] \\ &= \frac{2}{\pi}\int_0^{\aleph}\left[\left(1-cos\omega\acute{D}\right)cos\left(\omega z\right)\right]d\omega \qquad (4.13)\end{aligned}$$

Now equation 4.11 could be written in terms of the derivatives in Eq.4.12 and Eq.4.13 as

$$\left.\frac{\partial F_s}{\partial z}\right|_{\mathcal{OP}} = K_{es}(t)\left[\varpi_1 + z_0\varpi_2 - \frac{D}{2}\varpi_1\varpi_4 - \frac{D}{2}\varpi_3\varpi_2\right] \qquad (4.14)$$

where,

$$\varpi_1 = 1 - \frac{2}{\pi}\int_0^{\aleph}\left[\frac{\sin\left(\frac{\omega D}{2}\right)\cos(\omega z_0)}{\omega}\right]d\omega$$

$$\varpi_2 = \frac{2}{\pi}\int_0^{\aleph}\left[sin\left(\frac{\omega D}{2}\right)sin\left(\omega z_0\right)\right]d\omega$$

$$\varpi_3 = \frac{2}{\pi}\int_0^{\aleph}\left[\frac{\left(1-cos\left(\omega\acute{D}\right)\right)}{\omega}sin\left(\omega z_0\right)\right]d\omega$$

$$\varpi_4 = \frac{2}{\pi}\int_0^{\aleph}\left[\left(1-cos\left(\omega\acute{D}\right)\right)cos\left(\omega z_0\right)\right]d\omega$$

The partial derivative $\left.\frac{\partial F_s}{\partial t}\right|_{\mathcal{OP}}$ could be derived to be of the form

$$\begin{aligned}\left.\frac{\partial F_s}{\partial t}\right|_{\mathcal{OP}} &= \dot{K}_{es}(t_0)S^*\left[z_0 - \tfrac{D}{2}sgn(z_0)\right] \\ &= \dot{K}_{es}(t_0)\varpi_1\left[z_0 - \tfrac{D}{2}sgn(z_0)\right] \qquad (4.15)\end{aligned}$$

The linearized term of the viscous damping could be written as

$$\begin{aligned} F_d(\dot{z},t) &= F_d(\dot{z}_0,t_0) + \left.\frac{\partial F_d}{\partial \dot{z}}\right|_{\mathcal{OP}} \Delta\dot{z} + \left.\frac{\partial F_d}{\partial t}\right|_{\mathcal{OP}} \Delta t + \cdots \\ &= F_d(\dot{z}_0,t_0) + C_v(t_0)\left[2\dot{z}_0\right]\Delta\dot{z} + \dot{C}_v(t_0)\left|\dot{z}_0\right|\dot{z}_0\Delta t \end{aligned} \tag{4.16}$$

where, $\Delta\dot{z}$ represents the deviation of the actual point from the operating point and takes a positive or negative value. Applying the partial derivatives theorem discussed above to the Coulomb friction term we obtain

$$\begin{aligned} F_c(\dot{z},t) &= F_c(\dot{z}_0,t_0) + \left.\frac{\partial F_c}{\partial \dot{z}}\right|_{\mathcal{OP}} \Delta\dot{z} + \left.\frac{\partial F_c}{\partial t}\right|_{\mathcal{OP}} \Delta t + \cdots \\ &= F_c(\dot{z}_0,t_0) + F(t_0)\frac{d}{d\dot{z}}\left[sgn(\dot{z})\right]\Delta\dot{z} + sgn(\dot{z}_0)\dot{F}(t_0)\Delta t + \cdots \\ &= F_c(\dot{z}_0,t_0) + F(t_0)\varpi_5\Delta\dot{z} + sgn(\dot{z}_0)\dot{F}(t_0)\Delta t \end{aligned} \tag{4.17}$$

*where,*

$$\varpi_5 = \frac{d}{d\dot{z}}\left(sgn(\dot{z})\right) = \frac{2}{\pi}\int_0^{\aleph}\left[\left(1 - cos\left(\omega\dot{D}\right)\right)cos\left(\omega\dot{z}_0\right)\right]\, d\omega$$

The spring force, load and stiffness terms could also be written as

$$\begin{aligned} F_k(z,t) &= F_k(z_0,t_0) + \left.\frac{\partial F_k}{\partial z}\right|_{\mathcal{OP}} \Delta z + \left.\frac{\partial F_k}{\partial t}\right|_{\mathcal{OP}} \Delta t + \cdots \\ &= F_k(z_0,t_0) + K(t_0)\Delta z + \dot{K}(t_0)z_0\Delta t \\ M(t) &= M(t_0) + \left.\frac{\partial M}{\partial t}\right|_{\mathcal{OP}} \Delta t + \cdots \\ &= M(t_0) + \dot{M}(t_0)\Delta t \\ K(t) &= K(t_0) + \left.\frac{\partial K}{\partial t}\right|_{\mathcal{OP}} \Delta t + \cdots \\ &= K(t_0) + \dot{K}(t_0)\Delta t \end{aligned} \tag{4.18}$$

For simplification of the linearized equations the following assumptions are made. Linearization is assumed to be performed about a small operating region which implies $\Delta t$ is very small. The variation of vehicle parameters at a slow rate along with close operating points would result in very small values of $\dot{M}(t_0), \dot{K}(t_0), \dot{C}_v(t_0), \dot{F}(t_0)$and $\dot{K}_{es}(t_0)$. Neglecting the product of $\Delta t$ and rate of vehicle parameters, Eqs.4.14...4.18 can be

simplified as

$$\begin{aligned}
F_s(z,t) &= F_s(z_0,t_0) + K_{es}(t_0)\left[\varpi_1 + z_0\varpi_2 - \tfrac{D}{2}\varpi_1\varpi_4 - \tfrac{D}{2}\varpi_3\varpi_2\right]\Delta z \\
F_d(\dot{z},t) &= F_d(\dot{z},t_0) + C_v(t_0)\left[2\dot{z}_0\right]\Delta\dot{z} \\
F_c(\dot{z},t) &= F_c(\dot{z}_0,t_0) + F(t_0)\varpi_5\Delta\dot{z} \\
F_k(z,t) &= F_k(z_0,t_0) + K(t_0)\Delta z \\
M(t) &= M(t_0) \\
K(t) &= K(t_0)
\end{aligned} \tag{4.19}$$

The above equations are substituted along with Eq.4.3 in Eq.4.1 to obtain a linearized form as

$$\begin{aligned}
M(t_0)\left[\ddot{z}_0 + \Delta\ddot{z}\right] + F_s(z_0,t_0) + K_{es}(t_0)\left[\varpi_1 + z_0\varpi_2 - \frac{D}{2}\varpi_1\varpi_4 - \frac{D}{2}\varpi_3\varpi_2\right]\Delta z \\
+F_d(\dot{z}_0,t_0) + C_v(t_0)\left[\dot{z}_0\right]\Delta\dot{z} + F_c\left(\dot{z}_0,t_0\right) + F(t_0)\varpi_5\Delta\dot{z} + F_k\left(z_0,t_0\right) \\
+K(t_0)\Delta z = u_0 + \Delta u - M(t_0)\left[\ddot{w} + \Delta\ddot{w}\right] + K(t_0)\delta_{st} - M(t_0)g
\end{aligned} \tag{4.20}$$

Now subtracting the nonlinear equation at the operating point i.e. Eq.4.7 from Eq.4.20 we obtain

$$\begin{aligned}
M(t_0)\Delta\ddot{z} + \left[C_v(t_0)\left[\dot{z}_0\right] + F(t_0)\varpi_5\Delta\dot{z}\right]\Delta\dot{z} \\
+\left[K_s(t_0)\left[\varpi_1 + z_0\varpi_2 - \frac{D}{2}\varpi_1\varpi_4 - \frac{D}{2}\varpi_3\varpi_2\right] + K(t_0)\right]\Delta z = \Delta u - M(t_0)\Delta\ddot{w}
\end{aligned} \tag{4.21}$$

Eq.4.21 forms a Linear Time Invariant (LTI) equation in the operating region. This equation can be written as

$$M_0\Delta\ddot{z} + C_0\Delta\dot{z} + K_0\Delta z = \Delta u - M_0\Delta\ddot{w} \tag{4.22}$$

*where* $M_0 = M(t_0)$

$$C_0 = C_v(t_0)\left[2\dot{z}_0\right] + F(t_0)\varpi_5$$

$$K_0 = K_s(t_0)\left[\varpi_1 + z_0\varpi_2 - \tfrac{D}{2}\varpi_1\varpi_4 - \tfrac{D}{2}\varpi_3\varpi_2\right] + K(t_0)$$

where, $M_0, C_0$ and $K_0$ are considered to be constant about some operating region. The above linearized equation is transferred into the state space form by letting $x_1 = \triangle z$ and $x_2 = \triangle \dot{z}$ as

$$\begin{aligned} \dot{X} &= \mathcal{A}X + \mathcal{B}U \\ Y &= \mathcal{C}X \end{aligned} \tag{4.23}$$

*where*,

$$\mathcal{A} = \begin{bmatrix} 0 & 1 \\ \frac{-K_0}{M_0} & \frac{-C_0}{M_0} \end{bmatrix}; \quad \mathcal{B} = \begin{bmatrix} 0 & 0 \\ \frac{1}{M_0} & -1 \end{bmatrix}; \quad \mathcal{C} = \begin{Bmatrix} 1 & 0 \end{Bmatrix}$$

*and* $$X = \begin{Bmatrix} x_1 \\ x_2 \end{Bmatrix}; \qquad U = \begin{Bmatrix} \triangle u \\ \triangle \ddot{w} \end{Bmatrix}$$

### 4.2.4 Derivation of Discrete Auto-Regressive Moving Average Model for Linearized Suspension Model

Taking laplace transform of the state space equation 4.23, we can write the state transition matrix as

$$(sI - \mathcal{A})^{-1} = \frac{1}{s^2 + \frac{C_0}{M_0}s + \frac{K_0}{M_0}} \begin{bmatrix} s + \frac{C_0}{M_0} & 1 \\ \frac{-K_0}{M_0} & s \end{bmatrix} \tag{4.24}$$

The matrix $(sI - \mathcal{A})$ is non-singular since the coefficients $K_0$ and $C_0$ are always positive as described by the following inequalities.

$$K_0 = K(t_0) + K_s(t_0)\left[\varpi_1 + z_0\varpi_2 - \frac{D}{2}\varpi_1\varpi_4 - \frac{D}{2}\varpi_3\varpi_2\right] > 0 \tag{4.25}$$

$$C_0 = C_v\left[|\dot{z}_0| + \dot{z}_0\right] + F(t_0)\varpi_5 \geq 0 \qquad \text{for all real values of } \dot{z}_0$$

The state space equation in Eq.4.23 can represented in the discrete system form as

$$\begin{aligned} X\left[k\check{h} + \check{h}\right] &= \mathcal{Q}X[k\check{h}] + \mathcal{F}U[k\check{h}] \\ Y[k\check{h}] &= \mathcal{C}X[k\check{h}] \end{aligned} \tag{4.26}$$

*where*,

$$\mathcal{Q}(\check{h}) = e^{\mathcal{A}\check{h}}$$
$$\mathcal{F}(\check{h}) = \int_0^{\check{h}} e^{\mathcal{A}s} ds\, \mathcal{B}$$

where, $\check{h}$ denotes the sampling interval. The inverse laplace transform of state transition matrix method is used to derive the discrete state equations. Let us assume $\varrho = \frac{C_0}{2M_0}$ and $\varphi = \sqrt{\left(\frac{C_0}{2M_0}\right)^2 - \frac{K_0}{M_0}}$. The response of the linearized system depends on the radical under the root in $\varphi$. Depending on the following relation if $\left(\frac{C_0}{2M_0}\right)^2 - \frac{K_0}{M_0}$, then the system is overdamped, critically damped and underdamped respectively Then $\mathcal{Q}(\check{h})$ and $\mathcal{F}(\check{h})$ are evaluated as

$$\mathcal{Q}(\check{h}) = \begin{bmatrix} \left(\frac{\varrho+\varphi}{2\varphi}e^{-(\varrho-\varphi)\check{h}} + \frac{\varphi-\varrho}{2\varrho}e^{-(\varphi+\varrho)\check{h}}\right) & \frac{1}{2\varphi}\left[e^{-(\varrho-\varphi)\check{h}} - e^{-(\varphi+\varrho)\check{h}}\right] \\ \frac{-K_0}{2\varphi M_0}\left[e^{-(\varrho-\varphi)\check{h}} - e^{-(\varphi+\varrho)\check{h}}\right] & \left(\frac{\varrho+\varphi}{2\varphi}e^{-(\varrho+\varphi)\check{h}} + \frac{\varphi-\varrho}{2\varrho}e^{-(\varphi-\varrho)\check{h}}\right) \end{bmatrix}$$

$$\mathcal{F}(\check{h}) = \begin{bmatrix} \frac{1}{2\varphi M_0}\left[\frac{e^{-(\varrho-\varphi)\check{h}}-1}{(\varphi-\varrho)} + \frac{e^{-(\varrho+\varphi)\check{h}}-1}{(\varphi+\varrho)}\right] & \frac{-1}{2\varphi}\left[\frac{e^{-(\varrho-\varphi)\check{h}}-1}{(\varphi-\varrho)} + \frac{e^{-(\varrho+\varphi)\check{h}}-1}{(\varphi+\varrho)}\right] \\ \frac{1}{2\varphi M_0}\left[e^{-(\varrho-\varphi)\check{h}} - e^{-(\varrho+\varphi)\check{h}}\right] & \frac{-1}{2\varphi}\left[e^{-(\varrho-\varphi)\check{h}} - e^{-(\varrho+\varphi)\check{h}}\right] \end{bmatrix} \quad (4.27)$$

The transfer function between the input vector $U[k]$ and output $Y[k]$ in Eq.4.26 can be written as

$$Y[k] = C\left[qI - \mathcal{Q}(\check{h})\right]^{-1}\mathcal{F}(\check{h})U[k] \quad (4.28)$$

where, $q$ denotes the forward shift operator which performs as $qY[k] = Y[k+1]$. On simplification the transfer function vector can be derived as

$$Y[k] = \left[\frac{-1}{2K_0}\frac{\dot{B}(q^{-1})}{A(q^{-1})} \quad , \quad \frac{M_0}{2K_0}\frac{\dot{B}(q^{-1})}{A(q^{-1})}\right]U[k] \quad (4.29)$$

Eq.4.26 can be put in special form as a SISO transfer function with the modification of the input as

$$\triangle U_T[k] = \frac{-1}{2K_0}\triangle u[k] + \frac{M_0}{2K_0}\triangle\ddot{w}[k] \quad (4.30)$$

Eq.4.26 can be represented as a transfer function in the left difference operator $(q^{-1})$

$$Y[k] = \frac{\dot{B}(q^{-1})}{A(q^{-1})}\triangle U_T[k] \quad (4.31)$$

where, $\dot{B}(q^{-1})$ and $A(q^{-1})$ denote the polynomials in the backward shift operator $(q^{-1})$ which performs $q^{-1}Y[k] = Y[k-1]$. The polynomials are represented in the form

$$A\left(q^{-1}\right) = 1 + q^{-1}\left[-e^{-(\varrho-\varphi)\check{h}} - e^{-(\varrho+\varphi)\check{h}}\right] + q^{-2}e^{-2\varrho\check{h}}$$

$$\dot{B}\left(q^{-1}\right) = q^{-1}\left[(\varrho+\varphi)\epsilon^{-(\varrho-\varphi)\check{h}} + (\varphi-\varrho)\epsilon^{-(\varrho+\varphi)\check{h}} - 2\varphi\right] + q^{-2}\left[(\varphi-\varrho)\epsilon^{-(\varrho-\varphi)\check{h}} + (\varphi+\varrho)\epsilon^{-(\varrho+\varphi)\check{h}} - 2\varphi\epsilon^{-2\varrho\check{h}}\right] \quad (4.32)$$

but in the underdamped case if $\left(\frac{C_0}{2M_0}\right)^2 < \frac{K_0}{M_0}$ the value of $\varphi$ is imaginary and can be written as $\varphi = \iota\dot{\varphi}$ where, $\iota$ denotes the complex number $\left(\sqrt{-1}\right)$ and $\dot{\varphi} = \sqrt{\frac{K_0}{M_0} - \left(\frac{C_0}{2M_0}\right)^2}$. On substituting these into the coefficients of polynomials in Eq.4.32 we can derive that

$$A\left(q^{-1}\right) = 1 - q^{-1}2cos\left(\dot{\varphi}\check{h}\right)\epsilon^{-\varrho\check{h}} + q^{-2}\epsilon^{-2\varrho\check{h}}$$

$$\dot{B}\left(q^{-1}\right) = q^{-1}2\left[\epsilon^{-\varrho\check{h}}cos\left(\dot{\varphi}\check{h}\right) + \frac{\varrho}{\dot{\varphi}}\epsilon^{-\varrho\check{h}}sin\left(\dot{\varphi}\check{h}\right) - 1\right] + q^{-2}2\left[\epsilon^{-\varrho\check{h}}cos\left(\dot{\varphi}\check{h}\right) - \frac{\varrho}{\dot{\varphi}}\epsilon^{-\varrho\check{h}}sin\left(\dot{\varphi}\check{h}\right) - \epsilon^{-2\varrho\check{h}}\right] \quad (4.33)$$

Introducing a time delay ($\ddot{d}$) between the input signal $\triangle U_T[k]$ and the output $Y[k]$ we can write Eq.4.31 as

$$A\left(q^{-1}\right)Y[k] = q^{-\ddot{d}}\dot{B}\left(q^{-1}\right)\triangle U_T[k] \quad (4.34)$$

This equation is modified to yield a transfer function in the form of a DARMA model in terms of a new time delay $d$ as

$$A\left(q^{-1}\right)Y[k] = q^{-d}B\left(q^{-1}\right)\triangle U_T[k] \quad (4.35)$$

The polynomials $A(q^{-1})$ and $B(q^{-1})$ are of the order $n = 2$ and $\ell = 1$ respectively and in the form

$$\begin{aligned} A(q^{-1}) &= 1 + a_1q^{-1} + a_2q^{-2} \\ B(q^{-1}) &= b_0 + b_1q^{-1} \end{aligned} \quad (4.36)$$

### 4.2.5 Derivation of Discrete Auto-Regressive Moving Average Model for Reference Model.

The reference model described in Eq.4.4 can be represented in the state space form as

$$\dot{X}_m = \mathcal{A}_m X_m + \mathcal{B}_m U_m$$

$$Y_m = \quad C_m X_m \tag{4.37}$$

*where,*

$$\mathcal{A}_m = \begin{bmatrix} 0 & 1 \\ \frac{-K_m}{M_m} & \frac{-C_m}{M_m} \end{bmatrix} \; ; \; \mathcal{B}_m = \begin{bmatrix} 0 & 0 \\ \frac{-C_m}{M_m} & -1 \end{bmatrix} \; , \; C_m = \begin{bmatrix} 1 & 0 \end{bmatrix}$$

$$X_m = \begin{Bmatrix} z_m \\ \dot{z}_m \end{Bmatrix} \; \& \; U_m = \begin{Bmatrix} w \\ \dot{w} \end{Bmatrix}$$

Taking Laplace transform of Eq.4.37 we can describe the state transition matrix as

$$(sI - \mathcal{A}_m)^{-1} = \frac{1}{s^2 + \frac{C_m}{M_m}s + \frac{K_m}{M_m}} \begin{bmatrix} s + \frac{C_m}{M_m} & 1 \\ -\frac{K_m}{M_m} & s \end{bmatrix} \tag{4.38}$$

The model parameters are chosen such that the matrix $(sI \quad \mathcal{A}_m)$ is non singular The state space equation (4.37) is transferred to the discrete domain state space form as

$$X_m[k\check{h} + \check{h}] = Q_m X_m[k\check{h}] + \mathcal{F}_m U_m[k\check{h}]$$

$$Y_m[k\check{h}] = C_m X_m[k\check{h}] \tag{4.39}$$

*where,*

$$Q_m(\check{h}) = e^{\mathcal{A}_m \check{h}}$$

$$\mathcal{F}_m(\check{h}) = \int_0^{\check{h}} e^{\mathcal{A}_m s} ds \, \mathcal{B}_m$$

Generally the reference model is chosen to be critical or overdamped, hence it satisfies the condition $\left(\frac{C_m}{2M_m}\right)^2 \geq \frac{K_m}{M_m}$. Similar to the plant model let us assume that $\varrho_m \quad \frac{C_m}{2M_m}$ and $\varphi_m = \sqrt{\left(\frac{C_m}{2M_m}\right)^2 - \frac{K_m}{M_m}}$. The matrices in the discrete domain state space equation are derived from Eq.4.39 as

$$Q_m(\check{h}) = \begin{bmatrix} \left(\frac{\varrho_m + \varphi_m}{2\varphi_m} e^{-(\varrho_m - \varphi_m)\check{h}} + \frac{\varphi_m - \varrho_m}{2\varphi_m} e^{-(\varphi_m + \varrho_m)\check{h}}\right) & \frac{1}{2\varphi_m}\left[e^{-(\varrho_m \; \varphi_m)\check{h}} \; - e^{-(\varrho_m + \varphi_m)\check{h}}\right] \\ \frac{-K_m}{2\varphi_m M_m}\left[e^{-(\varrho_m - \varphi_m)\check{h}} - e^{-(\varrho_m + \varphi_m)\check{h}}\right] & \left(\frac{\varrho_m + \varphi_m}{2\varphi_m} e^{-(\varrho_m + \varphi_m)\check{h}} + \frac{\varphi_m - \varrho_m}{2\varphi_m} e^{(\varrho_m \; \varphi_m)\check{h}}\right) \end{bmatrix}$$

$$\mathcal{F}_m(\check{h}) = \begin{bmatrix} \frac{-C_m}{2\varphi_m M_m}\left[\frac{e^{-(\varrho_m - \varphi_m)\check{h}} - 1}{(\varphi_m - \varrho_m)} + \frac{e^{-(\varrho_m + \varphi_m)\check{h}} - 1}{(\varphi_m + \varrho_m)}\right] & \frac{-1}{2\varphi_m}\left[\frac{e^{-(\varrho_m - \varphi_m)\check{h}} - 1}{(\varphi_m - \varrho_m)} + \frac{e^{-(\varrho_m + \varphi_m)\check{h}} - 1}{(\varphi_m + \varrho_m)}\right] \\ \frac{-C_m}{2\varphi_m M_m}\left[e^{-(\varrho_m - \varphi_m)\check{h}} - e^{-(\varrho_m + \varphi_m)\check{h}}\right] & \frac{-1}{2\varphi_m}\left[e^{-(\varrho_m \; \varphi_m)\check{h}} \; - e^{(\varrho_m + \varphi_m)\check{h}}\right] \end{bmatrix}$$

(4.40)

On simplifying similar to the plant, the discrete auto-regressive moving average (DARMA) model of the reference model is derived in terms of the backward shift operator as

$$A_m\left(q^{-1}\right) Y_m[k] = \psi B_m\left(q^{-1}\right) w_m[k] \tag{4.41}$$

*where,*

$$\psi = -\frac{M_m}{2K_m}$$

$$A_m\left(q^{-1}\right) = 1 + \left[-e^{-(\varrho_m-\varphi_m)h} - e^{-(\varrho_m+\varphi_m)h}\right] q^{-1} + e^{-2\varrho_m h} q^{-2}$$

$$B_m\left(q^{-1}\right) = 1 + q^{-1}\left[\frac{(\varphi_m-\varrho_m)e^{-(\varrho_m-\varphi_m)h} + (\varrho_m+\varphi_m)e^{-(\varrho_m+\varphi_m)h} - 2\varphi_m e^{-2\varrho_m h}}{(\varrho_m+\varphi_m)e^{-(\varrho_m-\varphi_m)h} + (\varrho_m-\varphi_m)e^{-(\varrho_m+\varphi_m)h} - 2\varphi_m}\right]$$

The input to the model ($w_m[k]$) is defined to be the sum of velocity and acceleration of the road profile multiplied by constants $\psi_1$ and $\psi_2$ as

$$w_m[k] = \psi_1 \dot{w}[k] + \psi_2 \ddot{w}[k] \tag{4.42}$$

$$\textit{where,}\quad \psi_1 = -\frac{C_m}{M_m}\left[\left(1 + \frac{\varrho_m}{\varphi_m}\right) e^{-(\varrho_m-\varphi_m)h} + \left(1 - \frac{\varrho_m}{\varphi_m}\right) e^{-(\varrho_m+\varphi_m)h} - 2\right]$$

$$\psi_2 = -1\left[\left(1 + \frac{\varrho_m}{\varphi_m}\right) e^{-(\varrho_m-\varphi_m)h} + \left(1 - \frac{\varrho_m}{\varphi_m}\right) e^{-(\varrho_m+\varphi_m)h} - 2\right]$$

$\acute{d}$ denotes the time delay between the input signal ($w_m[k]$) and the output ($Y_m[k]$) of the model as represented in Eq.4.41. Since the model is LTI the values of $\psi_1$ and $\psi_2$ are dependent only on the sampling interval. For the fixed sampler, these quantities remain constant and the input $w_m[k]$ to the model can be evaluated from Eq.4.42. The equation of the reference model can be written in the DARMA model form as

$$A_m\left(q^{-1}\right) Y_m[k] = q^{-\acute{d}} \psi B_m\left(q^{-1}\right) w_m[k] \tag{4.43}$$

*where,*

$$\psi = -\frac{M_m}{2K_m}$$

The polynomials $A_m\left(q^{-1}\right)$, and $B_m\left(q^{-1}\right)$ are of the order $n = 2$ and $\ell = 1$ respectively and are in the form

$$\begin{aligned} A_m\left(q^{-1}\right) &= 1 + a_{m_1} q^{-1} + a_{m_2} q^{-2} \\ B_m\left(q^{-1}\right) &= 1 + b_m q^{-1} \end{aligned} \tag{4.44}$$

## 4.3 Discrete Adaptive Control Problem Formulation

The linearized vehicle plant and reference models as described in sections 4.2.4 and 4.2.5 in Eqs.4.4 and 4.22 have been represented in the DARMA model in terms of left difference operator as follows

Vehicle plant model:

$$A(q^{-1})Y[k] = q^{-d}B(q^{-1})\triangle U_T[k] \tag{4.45}$$

where,

"d" denotes the time delay in the system.

$A(q^{-1})$ is a polynomial of order (n) 2 in the form $(1 + a_1q^{-1} + a_2q^{-2})$.

$B(q^{-1})$ is a polynomial of order $(\ell)$ 1 in the form $(b_0 + b_1q^{-1})$.

Reference Model:

$$A_m(q^{-1})Y_m[k] = q^{-d}\psi B_m(q^{-1})w_m[k] \tag{4.46}$$

where,

"$d$" denotes the time delay in the reference model.

$A_m(q^{-1})$ is a polynomial of order (n) 2 in the form $(1 + a_{m_1}q^{-1} + a_{m_2}q^{-2})$.

$B(q^{-1})$ is a polynomial of order $(\ell)$ 1 in the form $(1 + b_mq^{-1})$.

$A_m(q^{-1})$ sh ld be chosen to be a stable polynomial such that all the zeros of $A_m(q^{-1})$ lie within the unit circle. The adaptive control problem can be formulated as to design a controller which adapts the actual SDOF-NTV model to the reference model with various input and parametric variations. The controller design is based on the linearized model described by Eq.4.45 and the reference model given in Eq.4.46. The variations in the parameters are neither necessary to be known a priori nor to

be sensed on line. The control input sequence is evaluated on line with the controlled gains being updated to achieve the desired reference performance.

### 4.3.1 Discrete Model Reference Adaptive Control

Assume that the delay induced in the plant and the model in Eqs.4.45 and 4.46 is the same ($= d$). Let us assume two polynomials $F(q^{-1})$ and $G(q^{-1})$. Multiplying Eq.4.45 by $F(q^{-1})q^d$ and by adding $G(q^{-1})Y[k]$ on both sides, we obtain

$$\left(F(q^{-1})A(q^{-1}) + q^{-d}G(q^{-1})\right) Y[k+d] = G(q^{-1})Y[k] + F(q^{-1})B(q^{-1})\triangle U_T[k] \quad (4.47)$$

The output of the system in Eq.4.45 can be expressed as the output of a d-step ahead predictor of the form as described in [146].

$$A_m\left(q^{-1}\right) Y\left(k+d\right) = \alpha(q^{-1})Y[k] + \beta\left(q^{-1}\right) \triangle U_T[k] \quad (4.48)$$

*where,*

$$\alpha\left(q^{-1}\right) = \alpha_0 + \alpha_1 q^{-1} + \cdots \alpha_{(n-1)} q^{-(n-1)}$$

$$\beta\left(q^{-1}\right) = \beta_0 + \beta_1 q^{-1} + \cdots \beta_{(\ell+d-1)} q^{-(\ell+d-1)}$$

The polynomials can be simplified for $n = 2$ and $\ell = 1$ and for time delay $d = 1$ as

$$\alpha\left(q^{-1}\right) = \alpha_0 + \alpha_1 q^{-1}$$
$$\beta\left(q^{-1}\right) = \beta_0 + \beta_1 q^{-1}$$

Comparing Eq.4.47 and 4.48, we can form the following equations

$$\begin{aligned} F\left(q^{-1}\right) A\left(q^{-1}\right) + q^{-d} G\left(q^{-1}\right) &= A_m\left(q^{-1}\right) \\ \alpha\left(q^{-1}\right) &= G\left(q^{-1}\right) \\ \beta\left(q^{-1}\right) &= F\left(q^{-1}\right) B\left(q^{-1}\right) \end{aligned} \quad (4.49)$$

If the dynamics of the model are completely known, then from Eq.4.49, we can solve for the polynomials $\alpha(q^{-1})$ and $\beta(q^{-1})$. Comparing Eqs.4.46 and 4.48 with the condition of perfect model following, i.e $Y[k+d] = Y_m[k+d]$ we have

$$\alpha\left(q^{-1}\right) Y[k] + \beta\left(q^{-1}\right) \triangle U_T[k] = \psi B_m\left(q^{-1}\right) w_m[k] \quad (4.50)$$

The incremental control input $\Delta U_T'[k]$ denotes the control input needed for good tracking of the model. The control input $\Delta U_T'[k]$ can be evaluated from Eq.4.50, only with the complete knowledge of the polynomials $\alpha(q^{-1})$ and $\beta(q^{-1})$ which in turn needs the information about the dynamics of the system. But in the adaptive controller design, the knowledge of plant dynamics is neither necessary nor available a priori.

An one step ahead controller in the linear form appended with an estimator is used to obtain the adaptive version of the controller in Eq.4.50. The predictor in Eq.4.48 is transformed into a linear form by dividing with $\beta_0$ to obtain

$$\frac{1}{\beta_0}A_m\left(q^{-1}\right)Y[k+d] = \frac{1}{\beta_0}\alpha\left(q^{-1}\right)Y[k] + \frac{1}{\beta_0}\beta\left(q^{-1}\right)\Delta U_T[k]$$

$$\frac{1}{\beta_0}A_m\left(q^{-1}\right)Y[k+d] = \acute{\alpha}\left(q^{-1}\right)Y[k] + \left(\acute{\beta}\left(q^{-1}\right)+1\right)\Delta U_T[k] \qquad (4.51)$$

*where,*

$$\acute{\alpha}(q^{-1}) = \tfrac{\alpha_0}{\beta_0} + \tfrac{\alpha_1}{\beta_0}q^{-1} = \acute{\alpha_0} + \acute{\alpha_1}q^{-1}$$

$$\acute{\beta}(q^{-1}) = \acute{\beta_1}q^{-1}$$

The control input $\Delta U_T[k]$ from Eq.4.51 can be written in the form as

$$\Delta U_T[k] = \frac{1}{\beta_0}A_m\left(q^{-1}\right)Y[k+d] - \acute{\alpha_0}Y[k] - \acute{\alpha_1}Y[k-1] - \acute{\beta_1}\Delta U_T[k-1] \qquad (4.52)$$

which can be represented in the vector form as

$$\Delta U_T[k] = \tilde{\varphi}[k]^T\varphi \qquad (4.53)$$

*where,*

$$\varphi^T = \left[\acute{\alpha_0}, \acute{\alpha_1}, \acute{\beta_1}, \tfrac{1}{\beta_0}\right]$$

$$\tilde{\varphi}[k]^T = \left[-Y[k], -Y[k-1], -\Delta U_T[k-1], Y[k+d]\right]$$

$$\bar{Y}[k+d] = A_m\left(q^{-1}\right)Y[k+d]$$

Let's assume that an exact controller parameter vector $(\hat{\Theta})$ can be found. This would achieve $Y[k+d] = Y_m[k+d]$ then

$$\begin{aligned} A_m(q^{-1})Y[k+d] &= A_m(q^{-1})Y_m[k+d] \\ &= \psi B_m(q^{-1})w_m[k] \end{aligned} \qquad (4.54)$$

Then the control law in Eq.4.53 can be written as

$$\Delta U_T^*[k] = \hat{\varphi}[k]^T \hat{\Theta} \tag{4.55}$$

*where,*

$$\hat{\varphi}[k]^T = [-Y[k], -Y[k-1], -\Delta U_T[k-1], Y_E[k]]$$

$$Y_E[k] = \psi B_m\left(q^{-1}\right) w_m[k]$$

The one step-ahead adaptive controller in the linear control form can be extended to model reference adaptive control by on-line estimation of controller parameter vector ($\hat{\Theta}$) which satisfies Eq.4.54. The controller parameters can be estimated by the recursive least square (RLS) estimation technique which has fast convergence compared to other methods. But for the time varying problem the estimation has to be performed on-line which could be achieved by a covariance modification as proposed by Vogel and Edgar in [148].

The estimates of the controller parameters by the RLS can be updated by

$$\hat{\Theta}[k] = \hat{\Theta}[k-1] + \frac{\mathcal{P}[k-2]\tilde{\varphi}[k-1]}{1+\tilde{\varphi}[k-1]^T\mathcal{P}[k-2]\varphi[k-1]}\left[\Delta U_T^*[k-1] - \tilde{\varphi}[k-1]^T\hat{\Theta}[k-1]\right] \tag{4.56}$$

*where,*

$$\tilde{\mathcal{P}}[k-1] = \mathcal{P}[k-2] - \frac{\mathcal{P}[k-2]\tilde{\varphi}[k-1]\tilde{\varphi}[k-1]^T\mathcal{P}[k-2]}{1+\tilde{\varphi}[k-1]^T\mathcal{P}[k-2]\tilde{\varphi}[k-1]}$$

$$\mathcal{P}[k-1] = \tilde{\mathcal{P}}[k-1] + Q[k-1] \qquad 0 \leq Q[k-1] < \infty$$

A modification is needed to be made when the $\lambda_{max}[\mathcal{P}[k-1]]$ exceeds beyond a limit. This can be made by monitoring the trace of $\mathcal{P}[k-1]$ and by initializing $\mathcal{P}[k-1] = \tilde{\mathcal{P}}[k-1]$ if $tr[(\mathcal{P}[k-1]] \geq$ *preset upper bound.* The convergence of this algorithm is discussed in Ref.[146].

A schematic diagram of the controller is shown in the Fig.4.3. Nonlinear vehicle plant represents the actual suspension model involving nonlinearities, time dependent factors and time delays as described earlier. Figure 4.3 also shows the computer controlled system involving the sampler (S) and zero order hold (ZOH).

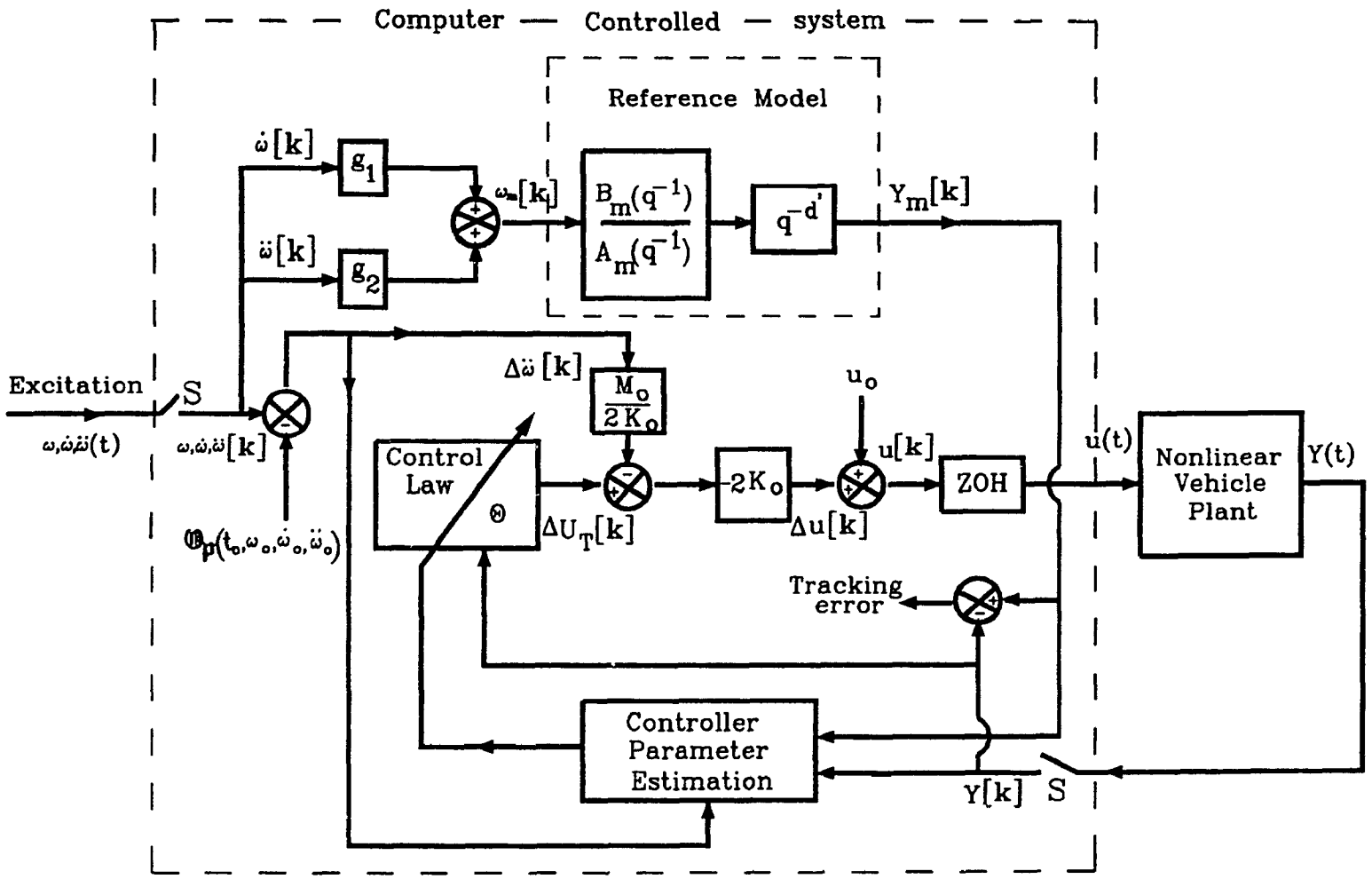


Fig.4.3: Schematic diagram of discrete domain adaptive controller.

## 4.4 Simulation Results

The digital controller developed is implemented for SDOF NTV model as shown in Fig.4.1 and the dynamic equations are described in Eq.4.1. Comparative study of the adaptive active suspension with that of a passive suspension is made throughout the presentation in this chapter. To better appreciate the capabilities of adaptive active suspension, both for maintenance of static equilibrium in time domain and for minimization of absolute displacement and rattle space at the natural frequency, a proportionately reduced model is considered. A higher sprung mass is taken to reduce the natural frequency for better demonstration of results. The nominal values of the suspension parameters typical of a quarter car model are considered as follows: the sprung mass $M(t)$ is considered to vary about nominal value ($M^*$) taken as 250 kg.; the stiffness of spring $K(t)$ is taken as 5000 $\frac{N}{m}$; the various other nominal values are taken as $C_v = 250\frac{Ns}{m}$, $K_{es} = 40\frac{kN}{m}$, $F = 1000N$ and maximum suspension deflection allowed ($D$) is 25 cms..

The DMRAC controller designed is implemented on a computer and is subjected to realistic conditions as *Parametric variations mode I* with *Excitation mode I* and *Parametric variations mode II* with *Excitation mode II*. The controller designed should be robust to this type of parameter variations and at the same time should be able to achieve the optimal performance as required by the reference model as illustrated by the continuous time controller designed in chapter 3. The controller should also adapt to the changing conditions like maintenance of static equilibrium levels under parametric variations described in mode I and II.

### 4.4.1 *Excitation mode I* and *Parametric variations mode I*

As described in *Excitation mode I*, the input to the suspension model is chosen as a combination of various sinusoidal inputs of different frequencies in the range of the

natural frequency of the system. The dynamics are made to vary as described in *Parametric variations mode I*, where the load changes are transformed over to a single axle to evaluate the performance in the time domain. Fig.4.4 compares the displacement response of the reference model, the adaptive active suspension model and the passive suspension model. This figure also shows the input excitation displacement to which the reference model, adaptive active suspension and passive suspension models are subjected. The reference model response indicates the performance of the skyhook model as described by the difference equation 4.46. The adaptive active displacement response shows how the adaptive controller estimates the gains on line so that active suspension would follow the reference model response. Fig.4.4 also shows that the model following is achieved within 1.5 seconds of operation due to initial high covariance matrix ($\mathcal{P}[k-2]$) in the recursive estimation equation 4.56. As indicated in Fig.2.4, after 20 seconds, the actual nonlinear suspension models for both adaptive and passive systems are subjected to sprung mass load variation. For sprung mass increase of 150 Kg, the passive suspension would have a static deflection subjected to the maximum deflection ($D$), spring and elastic stops stiffnesses. The passive suspension would respond with usual high amplitudes along with a static deflection of approximately 15 cms. and would rebound to initial level as mass drops back to the nominal value. Fig.4.4 shows how the adaptive active suspension maintains the static level and tries to follow the reference model even under a sudden change of 75% in the model parameters caused by various dynamic manoeuvres of the vehicle. Fig.4.4 shows the robustness of adaptive active suspension to the spring stiffness $K(t)$ and damping coefficient $C_v(t)$ variation as shown in Figs.2.7 and 2.8.

The covariance modification introduced in RLS estimator in Eq.4.56 would keep the covariance matrix to a high value so that the adaptation is faster whenever there are changes in the vehicle operational conditions Ref.[148].

Fig.4.5 shows the acceleration response. The reference model and adaptive active suspension has smaller values compared to that of the passive suspension. The

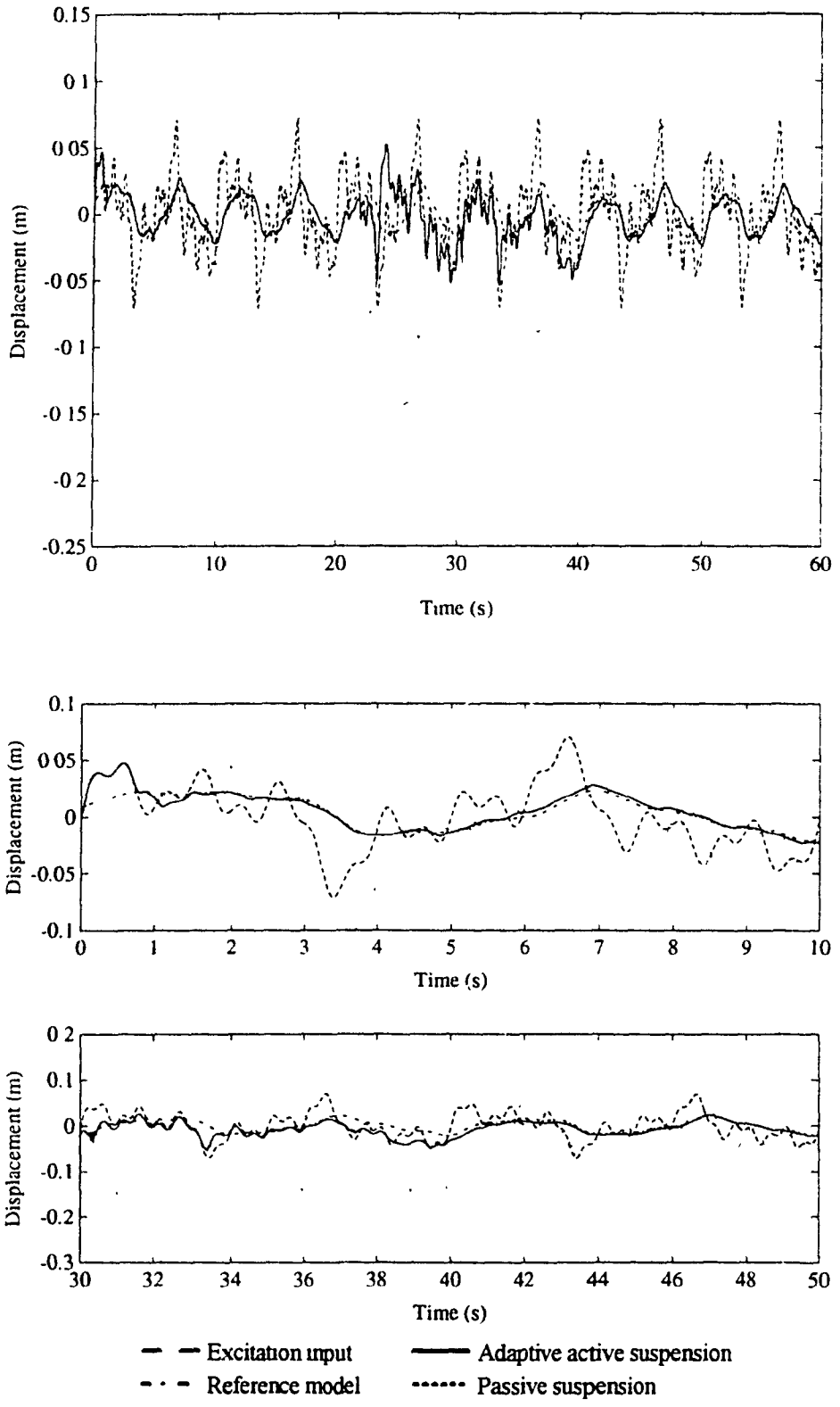


Fig.4.4: Sprung mass absolute displacement response for *Excitation mode I & Parametric variations mode I.*

adaptive active suspension produces high frequency signals of low magnitude during reference model following. Fig.4.6 indicates the variation of estimated controller parameters ($\hat{\Theta}$) in Eq.4.56. The estimated controller parameters converge very fast from initial values and vary depending on the parametric changes caused during various vehicle operational conditions. The error in the model following ($Y_m(t) - Y(t)$) which would also drive the estimator in Eq.4.26, varies as shown in Fig.4.7. The error comes to zero in less than 1.5 seconds initially, but when large parametric changes occur after 20 seconds the error would oscillate about zero with exponentially decreasing magnitude. Fig.4.8 shows the control force needed by the actuator to achieve the required reference model performance. The actuator forces necessary when there is no sprung mass variation are less, the reason being that the passive elements of the failsafe active suspension would share the static load. Fig.4.8 shows an upward force with a mean value of 1500 N exerted to take care of the static level changes that would have occurred if not for the active suspension.

### 4.4.2 *Excitation mode II* and *Parametric variations mode II*

The adaptive active suspension that is being controlled by a DMRAC controller is subjected to different random road inputs (asphalt, paved and dirt roads) as described in *Excitation mode II* in chapter 2. The results obtained for dirt road excitation which has higher magnitudes are presented in this section. Fig.4.9 shows the absolute displacement response obtained for the reference model, the adaptive active suspension and passive suspension systems in time domain. The adaptive active suspension would adapt to the reference model very closely within the first 12 seconds of operation. From this figure, the response for a passive suspension can be compared with the response for an adaptive active suspension. The time domain system responses for *Excitation mode II* of various models have been represented as magnitude squared transfer functions for absolute and relative displacements with respect to excitation input. Fig. 4.10 shows the system gain factor of absolute displacement of various

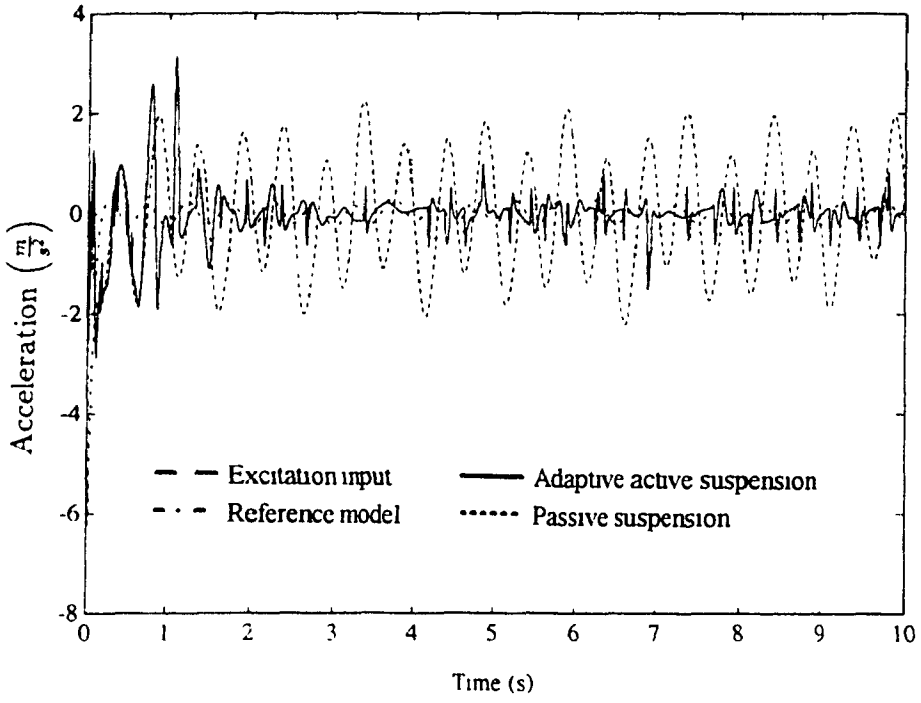


Fig.4.5: Sprung mass absolute acceleration response for *Excitation mode I & Parametric variations mode I.*

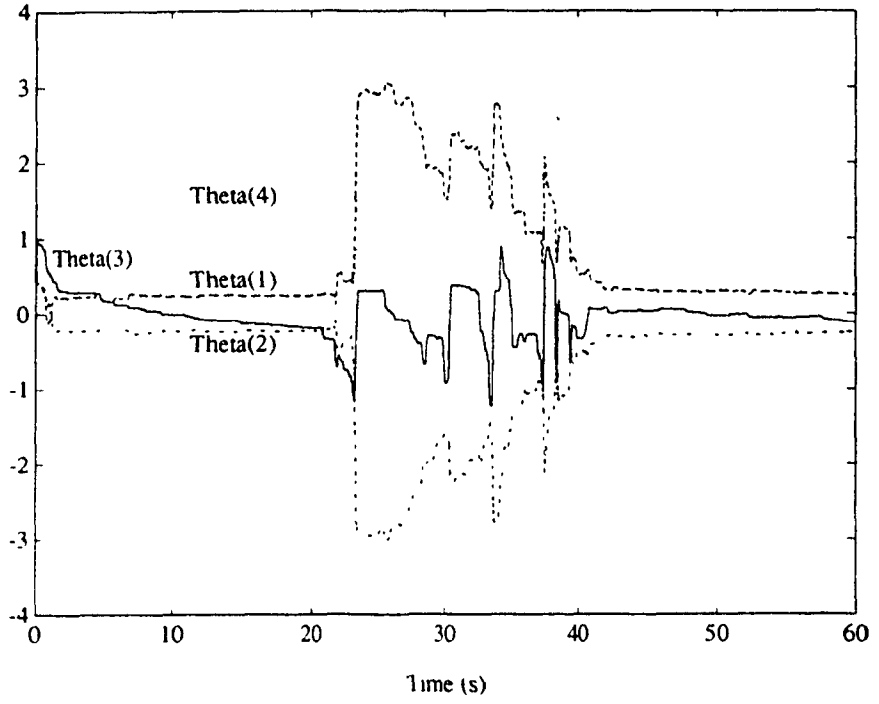


Fig.4.6: Discrete adaptive controller parameters estimated.

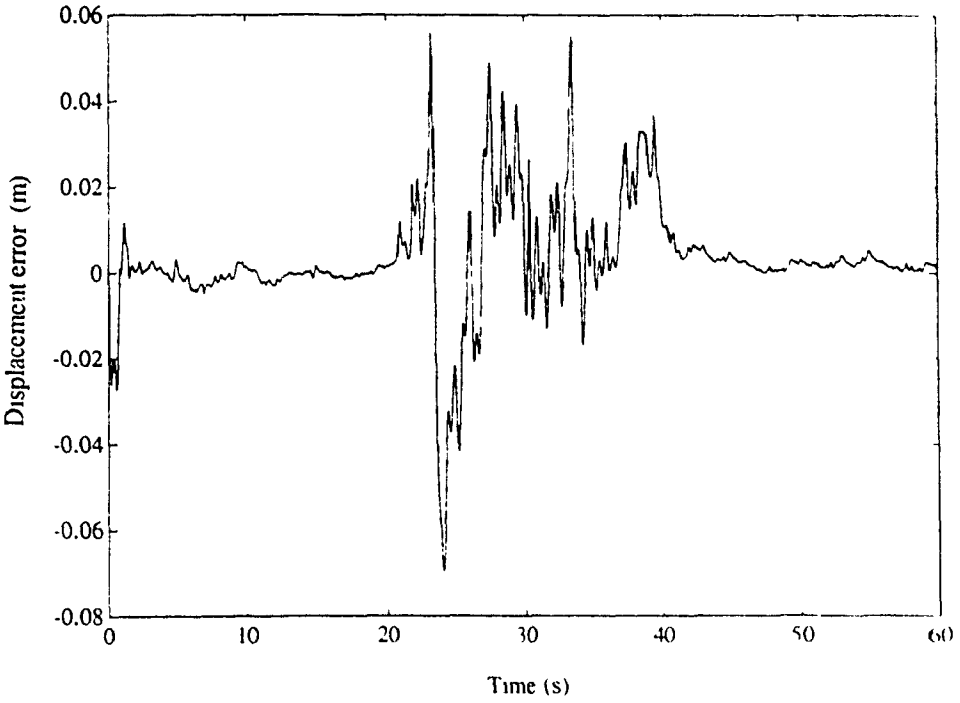


Fig.4.7: Displacement error in model following.

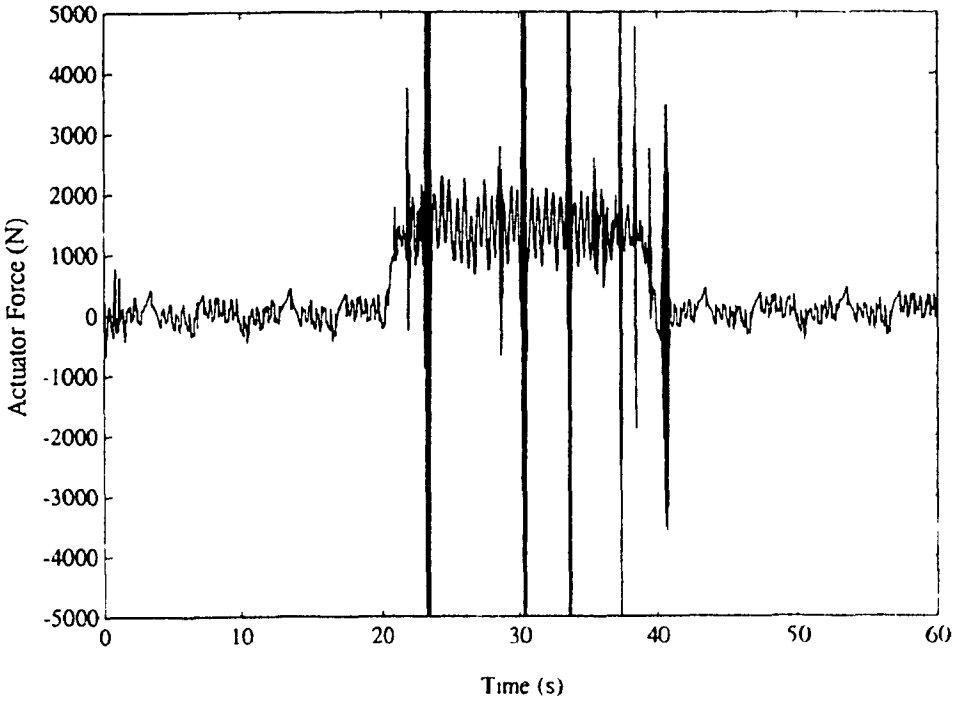


Fig.4.8: Actuator control force.

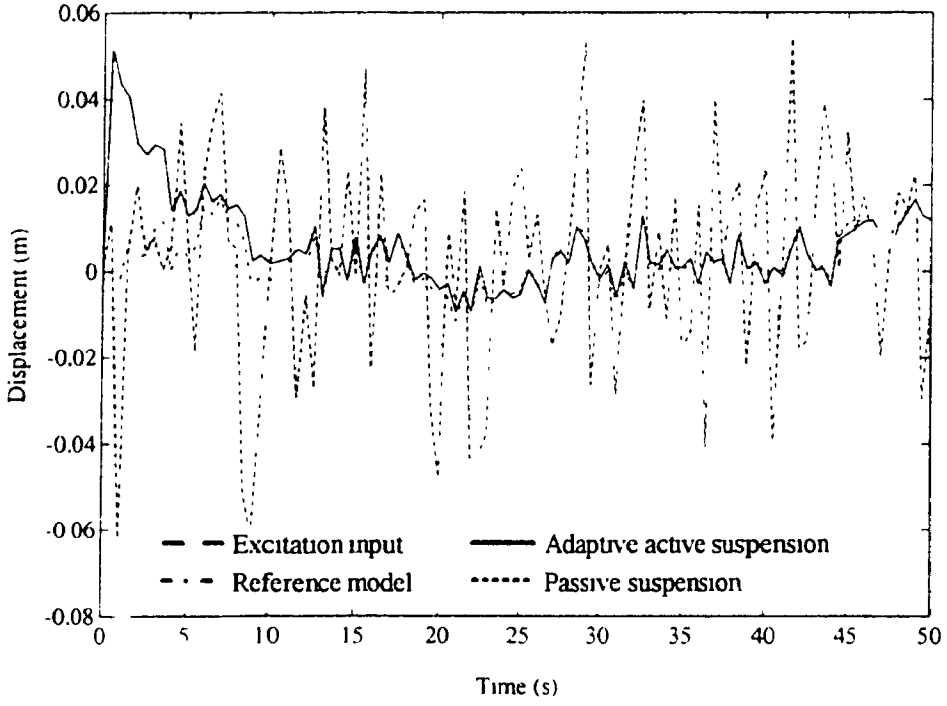


Fig.4.9: Sprung mass absolute displacement response for *Excitation mode II.*

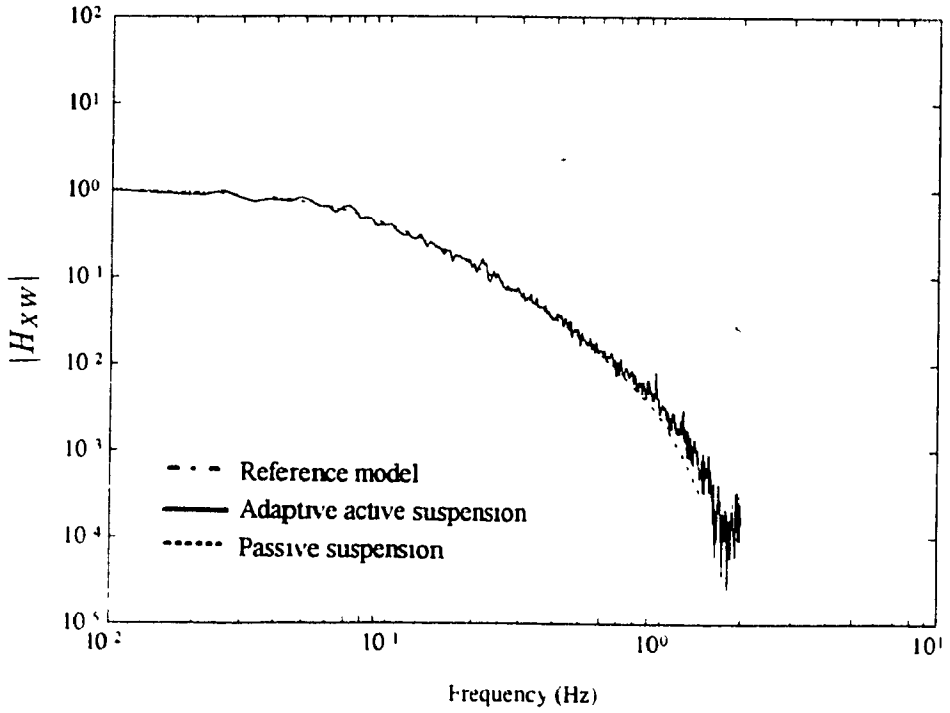


Fig.4.10: System gain factor of sprung mass absolute displacement with respect to excitation input.

models with respect to the excitation input. The adaptive active suspension closely follows the reference model at most of the frequency range, but it deviates slightly at the higher frequencies. The system gain factor for the absolute acceleration response of the sprung mass to the excitation acceleration which gives the magnitude of the transfer function is shown in Fig.4.11. The deviation of adaptive active suspension from the reference model at higher frequencies is higher in acceleration compared to that in the displacement response. Both absolute displacement and absolute acceleration responses of adaptive active suspension indicate good isolation properties at natural frequency and higher frequencies. Fig.4.12 shows the system gain factor of the suspension travel to the excitation input for reference model, adaptive active suspension and passive suspension models. The relative displacement of the passive suspension model is lower than the reference model at lower frequencies but is greater at the natural frequency and at higher frequencies. Comparison of Figs.4.10, 4.11 and 4.12 indicate that the chosen reference model and hence the adaptive active suspension model would give an optimal performance by reducing both absolute and relative displacements(suspension travel) at the same time. An adaptive active suspension would give this optimal performance irrespective of any dynamic parameter variations caused due to various vehicle manoeuvres which are not known a priori.

## 4.5 Discussion

In this chapter digital adaptive controller results based on discrete time analysis for SDOF active suspension have been presented. The simulation results obtained for *Excitation mode I* and *Excitation mode II* are based on the sampling interval ($\acute{h}$) of 0.01 and 0.005 seconds respectively. Since the sampling frequency is not very high, the hardware which is required for practical implementation need not be sophisticated. The results also incorporate the time delay which is normally encountered during the hardware implementation. A time delay of 0.05 secs. ($5 \times \acute{h}$) in terms of sampling interval has been specified and used for these simulation results. The results were

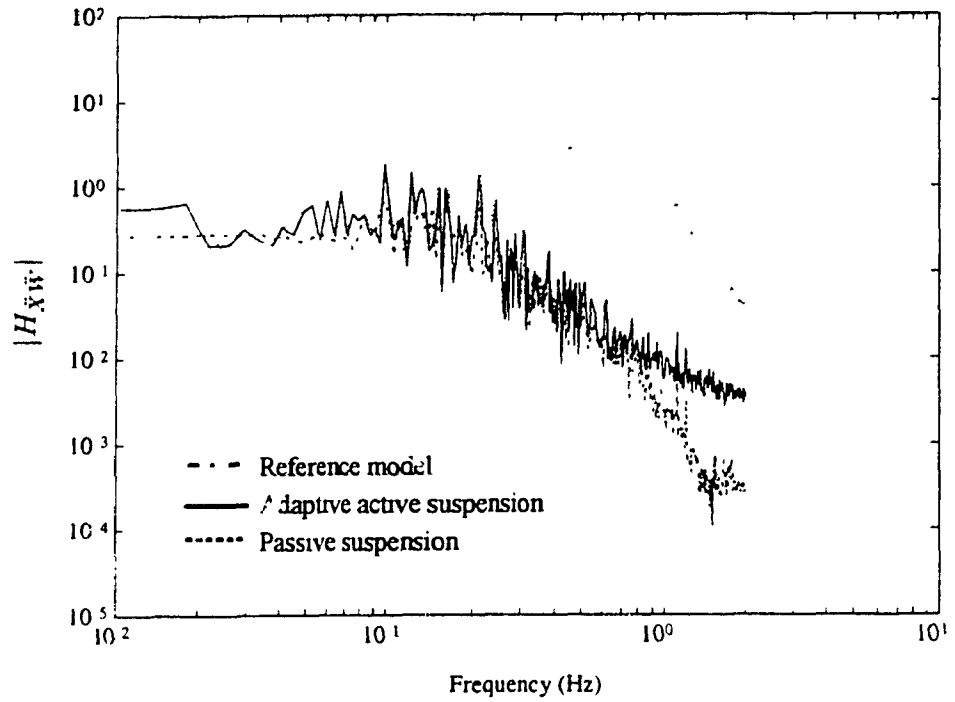


Fig.4.11: System gain factor of sprung mass absolute acceleration with respect to excitation input..

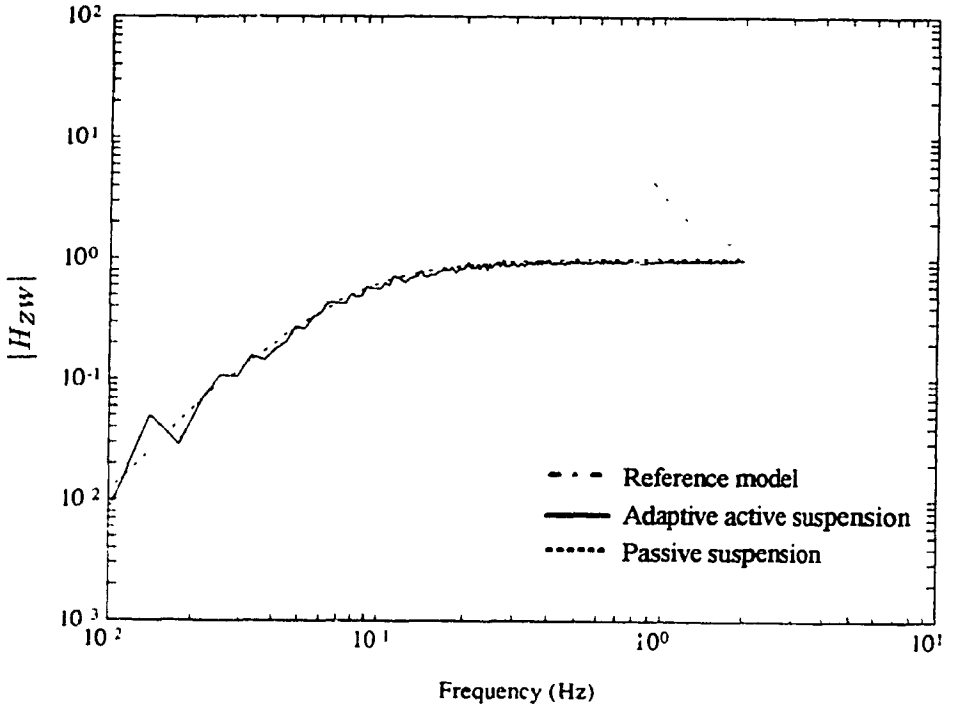


Fig.4.12: System gain factor of relative displacement with respect to excitation input.

found to be very satisfactory for a wide range of time delay values. The computational time in the controller parameter evaluation is found to be very low mainly due to the structure of estimator and adaptation equations. But caution is recommended for larger models involving more DOF's and complex format of NTV dynamic equations. The later chapters indicate the complexity of the controller structure for more generous applications.

The adaptive controller was found to give the optimal performance in the case of time varying parameters, unmodelled nonlinear dynamics and for different velocities and road profiles as indicated by the results in this chapter.

## 4.6 Summary

Single degree of freedom failsafe active suspension model is considered. This model incorporates various nonlinearities as in a real suspension model. Discrete model representations of the linearized suspension model and the reference model are derived. An adaptive controller based on discrete model reference adaptive control has been used to obtain the required reference model following. Recursive least squares estimation along with covariance modification is used for evaluation of the controller gains. The controller is subjected to *Excitation mode I* and *Excitation mode II* for the excitation input along with some unknown changes as indicated in *Parametric variations mode I* and *Parametric variations mode II*. Simulation results indicate good optimal performance of the adaptive active suspension even under a large percentage of vehicle parameter variations. Changes in the static equilibrium level due to squat and nose diving during vehicle longitudinal manoeuvres and time delay in the hardware implementation circuit were also taken care of by the approach discussed in this chapter.

# Chapter 5

# Real Time Adaptive Control Compared With Stochastic Optimal Control of Active Suspension

## 5.1 General

A real time adaptive control scheme for a Single Degree Of Freedom (SDOF) vehicle model with active suspension has been discussed as a continuous time model in chapter 3 and as a discrete model in chapter 4. Some of the references as referred to in section 1.4.2 of chapter 1, have discussed the concept of adaptive control in which the gains are calculated off-line for different Linear Time Invariant (LTI) models. The gains which are tabulated in a look-up table could be used for on line system performance. These gains could be evaluated by various control optimization schemes as discussed in [63] and [128].

Optimization of passive and active suspension systems using spectral techniques has been a popular technique. The stochastic optimal control for evaluation of optimal gains optimized with respect to parameters such as ride comfort, road

holding, working space and control force is a popular design. This method requires predetermination of the structure and assumes the model to be a LTI over the period of evaluation. The significance of the adaptive control designed in the previous chapter could be well appreciated when it is compared with the contemporary state of the art design schemes. In this chapter the stochastic optimal controller is compared with the adaptive controlled active suspension results for a SDOF vehicle suspension model.

## 5.2 Single Degree of Freedom Dynamic System Model

A stochastic dynamic model which assumes that the model parameters remain constant but the excitation is stochastic in nature representing asphalt, paved or dirt road inputs is derived for SDOF systems. A complete stochastic dynamic model using the stochastic input model and a SISO dynamic model independently, is discussed in sections 5.2.1 and 5.2.2 respectively. Then in section 5.2.3, the combined dynamic model that involves the stochastic input is analyzed for the development of the stochastic optimal controller.

### 5.2.1 Stochastic Input Model Describing Road Unevenness

As described in sections 2.2.2 of chapter 2, under *Excitation mode II* it is assumed that the PSD of the road/terrain roughness is reconstructed from the accelerometer measurements at the axle and modelled as a rational function described in Eq.2.1. As described in Eq.2.3, the excitation input is extracted as the output of a third order linear filter with white noise as input as given below.

$$\vartheta_0 \dddot{w} + \vartheta_1 \ddot{w} + \vartheta_2 \dot{w} + \vartheta_3 w = \vartheta_4 \dot{\xi} + \vartheta_5 \dot{\xi} + \vartheta_6 \xi \tag{5.1}$$

As described in Eq.2.5, the coefficients of the filter equation are derived in terms of the characteristic constants representing the type of road/terrain, velocity and PSD of the white noise. Now the linear filter equation shown in Eq.5.1 is represented in a state space form which is appended to the dynamic model as described in Eq.5.2. Assuming the states defined in the following form

$$\begin{aligned} w_1 &= w \\ w_2 &= \dot{w}_1 - \chi_1 \xi \\ w_3 &= \dot{w}_2 - \chi_2 \xi = \ddot{w}_1 - \chi_1 \dot{\xi} - \chi_2 \xi \end{aligned} \tag{5.2}$$

the filter equation 5.1 could be represented as a state space equation of the form

$$\dot{W} = \mathcal{M}_d W + \mathcal{D}_d \xi \tag{5.3}$$

*where,*

$$W = \begin{Bmatrix} w_1 \\ w_2 \\ w_3 \end{Bmatrix}$$

The matrices $\mathcal{M}_d$ and $\mathcal{D}_d$ should be deduced from the filter equation represented in Eq.5.1. On substituting Eq.5.2 in the left hand side of Eq.5.1 we obtain

$$\begin{aligned} \dot{w}_1 &= w_2 + \chi_1 \xi \\ \dot{w}_2 &= w_3 + \chi_2 \xi \\ \dot{w}_3 &= \ddot{w}_1 - \chi_1 \dot{\xi} - \chi_2 \dot{\xi} \end{aligned} \tag{5.4}$$

Substituting the first equation of Eq.5.2 in Eq.5.1 we obtain

$$\vartheta_0 \dddot{w}_1 + \vartheta_1 \ddot{w}_1 + \vartheta_2 \dot{w}_1 + \vartheta_3 w_1 = \vartheta_4 \ddot{\xi} + \vartheta_5 \dot{\xi} + \vartheta_6 \xi \tag{5.5}$$

By substituting Eq.5.5, the third equation of Eq.5.4 could be simplified as

$$\begin{aligned} \dot{w}_3 &= \vartheta_4 \ddot{\xi} + \vartheta_5 \dot{\xi} + \vartheta_6 \xi - \vartheta_1 \ddot{w}_1 - \vartheta_2 \dot{w}_1 - \vartheta_3 w_1 - \chi_1 \ddot{\xi} - \chi_2 \dot{\xi} \\ &= (\vartheta_4 - \chi_1) \ddot{\xi} + (\vartheta_5 - \chi_2) \dot{\xi} + \vartheta_6 \xi - \vartheta_1 \left( w_3 + \chi_1 \dot{\xi} + \chi_2 \xi \right) - \vartheta_2 \left( w_2 + \chi_1 \xi \right) - \vartheta_3 w_1 \\ &= (\vartheta_4 - \chi_1) \ddot{\xi} + (\vartheta_5 - \chi_2 - \vartheta_1 \chi_1) \dot{\xi} + (\vartheta_6 - \vartheta_1 \chi_2 - \vartheta_2 \chi_1) \xi - \vartheta_1 w_3 - \vartheta_2 w_2 - \vartheta_3 w_1 \end{aligned} \tag{5.6}$$

To represent Eq.5.6 as the third row of the matrix equation 5.3, we have to satisfy the equalities of the form

$$\begin{aligned} \chi_1 &= \vartheta_4 \\ \chi_2 &= \vartheta_5 - \vartheta_1 \chi_1 \\ \chi_3 &= \vartheta_6 - \vartheta_1 \chi_2 - \vartheta_2 \chi_1 \end{aligned} \tag{5.7}$$

Substituting Eq.5.4 and Eq.5.7 in Eq.5.3, we obtain the elements of the matrices $\mathcal{M}_d$ and $\mathcal{D}_d$ as

$$\mathcal{M}_d = \begin{bmatrix} 0 & 1 & 0 \\ 0 & 0 & 1 \\ -\vartheta_3 & -\vartheta_2 & -\vartheta_1 \end{bmatrix} \; ; \; \mathcal{D}_d = \begin{Bmatrix} \backslash 1 \\ \backslash 2 \\ \backslash 3 \end{Bmatrix} \tag{5.8}$$

Knowing the characteristic constants of different types of road/terrain inputs, the state vector $W$ could be solved from Eq.5.3 and could be used in Eq.5.2 to obtain different required derivatives of the terrain input.

### 5.2.2 Single Degree of Freedom Continuous Time Dynamic Model

The SDOF failsafe active suspension model as described in chapter 3 is considered for the development of the stochastic optimal controller for comparison. Since the stochastic optimal controller requires a priori knowledge of the model parameters and the model to be Linear Time Invariant (LTI), the parameters in the model are considered to be independent of operation time. Fig.3.1 shows the vehicle suspension model whose continuous time dynamic equation could be written as

$$M^*\ddot{x} + K^*(x - w) + C^*(\dot{x} - \dot{w}) - F_{act} = 0 \tag{5.9}$$

The corresponding state space equation could be written in the form

$$\begin{aligned} \dot{X}_p &= \mathcal{M}_p X_p + \mathcal{P}_p F_{act} + \mathcal{D}_p W_p \\ x &= \mathcal{C}_p X_p \end{aligned} \tag{5.10}$$

*where,*

$$X_p = \begin{Bmatrix} x \\ \dot{x} \end{Bmatrix}; \; W_p = \begin{Bmatrix} w \\ \dot{w} \end{Bmatrix}; \; \mathcal{M}_p = \begin{bmatrix} 0 & 1 \\ -\frac{K^*}{M^*} & -\frac{C^*}{M^*} \end{bmatrix};$$

$$\mathcal{P}_p = \begin{Bmatrix} 0 \\ \frac{1}{M^*} \end{Bmatrix}; \; \mathcal{D}_p = \begin{bmatrix} 0 & 0 \\ \frac{K^*}{M^*} & \frac{C^*}{M^*} \end{bmatrix}; \mathcal{C}_p = \begin{Bmatrix} 1 & 0 \end{Bmatrix}$$

where, $x$ denotes the absolute displacement of sprung mass and $w$ is the excitation input.

**Controllability:**

Consider the transition matrix $\mathcal{M}_p$ and contribution due to the input ($\mathcal{P}_p$), then the point wise state controllability matrix could be written as

$$\begin{aligned} \phi_c &= \left[\mathcal{P}_p, \mathcal{M}_p\mathcal{P}_p, {\mathcal{M}_p}^2\mathcal{P}_p, \cdots {\mathcal{M}_p}^{n-1}\mathcal{P}_p\right] \quad \text{where } n = 2 \\ \phi_c &= \begin{bmatrix} 0 & \frac{1}{M^*} \\ \frac{1}{M^*} & \frac{-C^*}{M^{*2}} \end{bmatrix} \text{ and } det\,|\phi_c| = \frac{-1}{M^{*2}} \end{aligned} \tag{5.11}$$

This matrix is of full rank as the determinant is never equal to zero. Hence the system is completely controllable.

**Observability:**

The point wise observability matrix from Eq.5.10 could be written in the form

$$\begin{aligned} \phi_o &= \left[{\mathcal{C}_p}^T, {\mathcal{M}_p}^T{\mathcal{C}_p}^T, \left({\mathcal{M}_p}^T\right)^2{\mathcal{C}_p}^T, \cdots \left({\mathcal{M}_p}^T\right)^{n-1}{\mathcal{C}_p}^T\right] \quad \text{where } n = 2 \\ \phi_o &= \begin{bmatrix} 1 & 0 & 0 & \frac{-K^*}{M^*} \\ 0 & 1 & 1 & \frac{-C^*}{M^*} \end{bmatrix} \end{aligned} \tag{5.12}$$

So for any values of $C^*$, $K^*$, or $M^*$ we have a sub-matrix whose $det \neq 0$ and hence the matrix $\phi_0$ is of full rank. Therefore, the model in Eq.5.10 is completely observable.

### 5.2.3 Combined Dynamic Model

The state space dynamic model in Eq.5.10 could be combined with the stochastic input state space model as described in Eq.5.3 to obtain a complete combined dynamic model in state space as follows

$$\dot{X} = \mathcal{M}X + \mathcal{P}F_{act} + \mathcal{D}\xi \tag{5.13}$$

*where,*

$$X = \begin{Bmatrix} X_p \\ W_p \end{Bmatrix}; \mathcal{P} = \begin{Bmatrix} \mathcal{P}_p \\ 0 \end{Bmatrix} = \begin{Bmatrix} 0 \\ \frac{1}{M} \\ 0 \\ 0 \\ 0 \end{Bmatrix}; \mathcal{D} = \begin{Bmatrix} 0 \\ \mathcal{D}_d \end{Bmatrix} = \begin{Bmatrix} 0 \\ 0 \\ \gamma_1 \\ \gamma_2 \\ \gamma_3 \end{Bmatrix};$$

$$\mathcal{M} = \begin{bmatrix} \mathcal{M}_p & \mathcal{D}_p \\ 0 & \mathcal{M}_d \end{bmatrix} = \begin{bmatrix} 0 & 1 & 0 & 0 & 0 \\ -\frac{K^*}{M^*} & -\frac{C^*}{M^*} & \frac{K^*}{M^*} & \frac{C^*}{M^*} & 0 \\ 0 & 0 & 0 & 1 & 0 \\ 0 & 0 & 0 & 0 & 1 \\ 0 & 0 & -\vartheta_3 & -\vartheta_2 & -\vartheta_1 \end{bmatrix}$$

## 5.3 Stochastic Optimal Control

In this section, a SISO vehicle model with active suspension is optimized with respect to ride comfort, working space and active control force. The solution is obtained by application of modern stochastic optimal linear control theory.

### 5.3.1 Performance Index

The primary goal of optimization is to minimize the mean square of the vertical acceleration $\mathcal{E}\left[(\ddot{x})^2\right]$ of the mass, secondly to minimize the mean square value of the relative displacement $\mathcal{E}\left[(x - w)^2\right]$ between the sprung and unsprung masses and finally to minimize the mean square value of the suspension force required $\mathcal{E}\left[{F_{act}}^2\right]$. The total Performance Index $\mathcal{PI}$ is taken as the sum of these components multiplied by the weighting constants $\rho_1$ *and* $\rho_2$.

$$\mathcal{PI} = \mathcal{E}\left[(\ddot{x})^2 + \rho_1 (x - w)^2 + \rho_2 (F_{act})^2\right] \tag{5.14}$$

Substituting the value of the acceleration $\ddot{x}$ from Eq.5.9 in Eq.5.14, we obtain

$$\mathcal{PI} = \mathcal{E}\left[\left(\frac{F_{act}}{M^*} - \frac{K^*}{M^*}(x - w) - \frac{C^*}{M^*}(\dot{x} - \dot{w})\right)^2 + \rho_1 (x - w)^2 + \rho_2 {F_{act}}^2\right] \tag{5.15}$$

The quadratic term in Eq.5.15 can be expressed in the form of matrix notation as

$$\mathcal{PI} = \mathcal{E}\left[\{X\ F_{act}\}^T [\mathcal{H}] \left\{ \begin{array}{c} X \\ F_{act} \end{array} \right\}\right] \tag{5.16}$$

where $\mathcal{H}$ is the Hessain matrix of the quadratic function. Taking the second partial derivatives with respect to the vector $\{X\ F_{act}\}$ we obtain

$$\mathcal{H} = \frac{1}{2}\begin{bmatrix} \frac{2K^{*2}}{M^{*2}} + 2\rho_1 & \frac{2K^*C^*}{M^{*2}} & \frac{-2K^{*2}}{M^{*2}} - 2\rho_1 & \frac{-2K^*C^*}{M^{*2}} & 0 & \frac{-2K^*}{M^{*2}} \\ \frac{2K^*C^*}{M^{*2}} & \frac{2C^{*2}}{M^{*2}} & \frac{-2K^*C^*}{M^{*2}} & \frac{-2C^{*2}}{M^{*2}} & 0 & \frac{-2C^*}{M^{*2}} \\ \frac{-2K^{*2}}{M^{*2}} - 2\rho_1 & \frac{-2K^*C^*}{M^{*2}} & \frac{2K^{*2}}{M^{*2}} + 2\rho_1 & \frac{2K^*C^*}{M^{*2}} & 0 & \frac{2K^*}{M^{*2}} \\ \frac{-2K^*C^*}{M^{*2}} & \frac{-2C^{*2}}{M^{*2}} & \frac{2K^*C^*}{M^{*2}} & \frac{2C^{*2}}{M^{*2}} & 0 & \frac{2C^*}{M^{*2}} \\ 0 & 0 & 0 & 0 & 0 & 0 \\ \frac{-2K^*}{M^{*2}} & \frac{-2C^*}{M^{*2}} & \frac{2K^*}{M^{*2}} & \frac{2C^*}{M^{*2}} & 0 & \frac{2}{M^{*2}} + 2\rho_2 \end{bmatrix} \tag{5.17}$$

From which we can express Eq.5.16 as

$$\mathcal{PI} = \mathcal{E}\left[\{X\ F_{act}\}^T \begin{bmatrix} \mathcal{L} & \mathcal{T} \\ \mathcal{T}^T & \mathcal{G} \end{bmatrix} \left\{ \begin{array}{c} Y \\ u \end{array} \right\}\right] \tag{5.18}$$

*where,*

$$\mathcal{L} = \frac{1}{2}\begin{bmatrix} \frac{2K^{*2}}{M^{*2}} + 2\rho_1 & \frac{2K^*C^*}{M^{*2}} & \frac{-2K^{*2}}{M^{*2}} - 2\rho_1 & \frac{-2K^*C^*}{M^{*2}} & 0 \\ \frac{2K^*C^*}{M^{*2}} & \frac{2C^{*2}}{M^{*2}} & \frac{-2K^*C^*}{M^{*2}} & \frac{-2C^{*2}}{M^{*2}} & 0 \\ \frac{-2K^{*2}}{M^{*2}} - 2\rho_1 & \frac{-2K^*C^*}{M^{*2}} & \frac{2K^{*2}}{M^{*2}} + 2\rho_1 & \frac{2K^*C^*}{M^{*2}} & 0 \\ \frac{-2K^*C^*}{M^{*2}} & \frac{-2C^{*2}}{M^{*2}} & \frac{2K^*C^*}{M^{*2}} & \frac{2C^{*2}}{M^{*2}} & 0 \\ 0 & 0 & 0 & 0 & 0 \end{bmatrix}$$

$$\mathcal{T} = \frac{1}{2}\left\{\frac{-2K^*}{M^{*2}}, \frac{-2C^*}{M^{*2}}, \frac{2K^*}{M^{*2}}, \frac{2C^*}{M^{*2}}, 0\right\}^T ; \mathcal{G} = \frac{1}{2}\left(\frac{2}{M^{*2}} + 2\rho_2\right)$$

The scalar value $\mathcal{G}$ is positive definite, hence it satisfies the requirement of optimal control theory.

### 5.3.2 Optimal Control

The optimal control problem can be stated to find the control force $F_{act}(t)$ for the dynamic system represented by Eq.5.9 by minimizing the performance index given by Eq.5.14. The control force $F_{act}(t)$ can be determined by the stochastic optimal control as

$$F_{act}(t) = -\mathcal{C}X(t) \tag{5.19}$$

where the control gain matrix is given as

$$\mathcal{C} = \mathcal{G}^{-1}\left(\mathcal{T}^T + \mathcal{P}^T\mathcal{R}\right) \tag{5.20}$$

where $\mathcal{R}$ is a symmetric positive-definite solution of the Matrix Ricatti equation of the form

$$-\mathcal{R}\left(\mathcal{M} - \mathcal{P}\mathcal{G}^{-1}\mathcal{T}^T\right) - \left(\mathcal{M} - \mathcal{P}\mathcal{G}^{-1}\mathcal{T}^T\right)^T\mathcal{R} + \mathcal{R}\mathcal{P}\mathcal{G}^{-1}\mathcal{P}^T\mathcal{R} - \left(\mathcal{L} - \mathcal{T}\mathcal{G}^{-1}\mathcal{T}^T\right) = 0 \tag{5.21}$$

In general, for stochastic control problems, the excitation in the system equation is white noise. But in this case, the equation which describes the random excitation is added, hence it deviates from the white noise assumption. Various algorithms used for solving the Matrix Ricatti equation require the complete controllability, i.e. variances of all the state vectors can be reduced by introducing the appropriate control input. But in the case of the stochastic system discussed here the last state vector component is the disturbance input which cannot be controlled. This lack of complete controllability of Eq.5.13 can be taken care of by means of additional necessary conditions of controllability for a stationary system. This problem can be avoided by decomposing the matrices as described in [120]. The terms in the Eq.5.21 can be broken as

$$\mathcal{L} = \begin{bmatrix} (\mathcal{L}_{11})_{2\times2} & (\mathcal{L}_{12})_{2\times3} \\ (\mathcal{L}_{21})_{3\times2} & (\mathcal{L}_{22})_{3\times3} \end{bmatrix}; \mathcal{R} = \begin{bmatrix} (\mathcal{R}_{11})_{2\times2} & (\mathcal{R}_{12})_{2\times3} \\ (\mathcal{R}_{21})_{3\times2} & (\mathcal{R}_{22})_{3\times3} \end{bmatrix}; \mathcal{T} = \begin{Bmatrix} (\mathcal{T}_1)_{2\times1} \\ (\mathcal{T}_2)_{3\times1} \end{Bmatrix} \tag{5.22}$$

Substituting the matrices in Eq.5.22 and Eq.5.13 into Eq.5.21, and on simplification through matrix operations, we obtain the following equations

$$-\mathcal{R}_{11}\left[\mathcal{M}_p - \mathcal{P}_p\mathcal{G}^{-1}\mathcal{T}_1^T\right] - \left[\mathcal{M}_p - \mathcal{P}_p\mathcal{G}^{-1}\mathcal{T}_1^T\right]^T\mathcal{R}_{11} + \mathcal{R}_{11}\mathcal{P}_p\mathcal{G}^{-1}\mathcal{P}_p{}^T\mathcal{R}_{11} - \left[\mathcal{L}_{11} - \mathcal{T}_1\mathcal{G}^{-1}\mathcal{T}_1^T\right] = 0 \tag{5.23}$$

$$-\mathcal{R}_{12}\mathcal{M}_d - \left[\left(\mathcal{M}_p - \mathcal{P}_p\mathcal{G}^{-1}\mathcal{T}_1^T\right)^T - \mathcal{R}_{11}\mathcal{P}_p\mathcal{G}^{-1}\mathcal{P}_p{}^T\right]\mathcal{R}_{12} - \mathcal{R}_{11}\left[\mathcal{D}_p - \mathcal{P}_p\mathcal{G}^{-1}\mathcal{T}_2^T\right] - \mathcal{L}_{12} + \mathcal{T}_1\mathcal{G}^{-1}\mathcal{T}_2^T = 0 \tag{5.24}$$

$$-\mathcal{M}_d{}^T\mathcal{R}_{21} - \mathcal{R}_{21}\left[\left(\mathcal{M}_p - \mathcal{P}_p\mathcal{G}^{-1}\mathcal{T}_1^T\right) - \mathcal{P}_p\mathcal{G}^{-1}\mathcal{P}_p{}^T\mathcal{R}_{11}\right] -$$

$$\left[\mathcal{D}_p - \mathcal{P}_p\mathcal{G}^{-1}\mathcal{T}_2{}^T\right]^T \mathcal{R}_{11} - \mathcal{L}_{21} + \mathcal{T}_2\mathcal{G}^{-1}\mathcal{T}_1{}^T = 0 \quad (5.25)$$

$$-\mathcal{R}_{22}\mathcal{M}_d - \mathcal{M}_d{}^T\mathcal{R}_{22} - \mathcal{R}_{21}\mathcal{D}_p - D_p{}^T\mathcal{R}_{12} - \mathcal{L}_{22} + \mathcal{R}_{21}\mathcal{P}_p\mathcal{G}^{-1}\mathcal{P}_p{}^T\mathcal{R}_{12} + \left[\mathcal{P}_p\mathcal{G}^{-1}\mathcal{T}_2{}^T\right]^T \mathcal{R}_{12} + \mathcal{R}_{21}\mathcal{P}_p\mathcal{G}^{-1}\mathcal{T}_2{}^T + \mathcal{T}_2\mathcal{G}^{-1}\mathcal{T}_2{}^T = 0 \quad (5.26)$$

Then the control gain matrix from Eq.5.20 can be derived on substituting matrices from Eq.5.13 and Eq.5.22 as

$$\mathcal{C} = \mathcal{G}^{-1}\left[\left(\mathcal{T}_1{}^T + \mathcal{P}_p{}^T\mathcal{R}_{11}\right), \left(\mathcal{T}_2{}^T + \mathcal{P}_p{}^T\mathcal{R}_{12}\right)\right]_{(1\times 5)} \quad (5.27)$$

Eqs.5.23 to 5.26 could be solved for the evaluation of matrix $\mathcal{R}$. Eq.5.23 is the Matrix Ricatti equation, while Eqs.5.24 and 5.25 are the linear equations and the final one Eq.5.26 is a Lyapunov equation.

**Solution of Matrix Ricatti Equation**

The matrix Ricatti equation in Eq.5.23 can be written as

$$\mathcal{R}_{11}\mathcal{S}_{E1} + \mathcal{S}_{E1}{}^T\mathcal{R}_{11} - \mathcal{R}_{11}\mathcal{P}_p\mathcal{G}^T\mathcal{P}_p{}^T\mathcal{R}_{11} + \mathcal{S}_{E2} = 0 \quad (5.28)$$

$$where, \quad \mathcal{S}_{E1} = \mathcal{M}_p - \mathcal{P}_p\mathcal{G}^{-1}\mathcal{T}_1$$

$$\mathcal{S}_{E2} = \mathcal{L}_{11} - \mathcal{T}_1\mathcal{G}^{-1}\mathcal{T}_1{}^T$$

This is of the general form as

$$\mathcal{S}\mathcal{A} + \mathcal{A}^T\mathcal{S} - \mathcal{S}\mathcal{B}\mathcal{R}^{-1}\mathcal{B}^T\mathcal{S} + \mathcal{Q} = 0 \quad (5.29)$$

The equivalent Hamiltonian matrix of Eq.5.29 is of the form

$$\mathcal{N} = \begin{bmatrix} \mathcal{A} & -\mathcal{B}\mathcal{R}^{-1}\mathcal{B}^T \\ \mathcal{Q} & -\mathcal{A}^T \end{bmatrix} \quad (5.30)$$

For a unique positive definite solution $\mathcal{S}$ in Eq.5.29, the pair $(\mathcal{A},\mathcal{B})$ is controllable and $(\mathcal{A},\mathcal{C})$ is observable. Where $\mathcal{C}$ is solved from the following relation

$$\mathcal{Q} = \mathcal{C}\mathcal{C}^T \quad (5.31)$$

Equating the equivalent terms in equations Eq.5.28 and Eq.5.29 we obtain the matrix $\mathcal{A}$ as $\mathcal{M}_p - \mathcal{P}_p\mathcal{G}^{-1}\mathcal{T}_1$ and $\mathcal{B}$ as $\mathcal{P}_p$. On simplifying the terms we obtain the matrices as

$$\mathcal{A} = \begin{bmatrix} 0 & 1 \\ \frac{-K^*M^*\rho_2}{1+M^{*2}\rho_2} & \frac{-C^*M^*\rho_2}{1+M^{*2}\rho_2} \end{bmatrix}; \quad \mathcal{B} = \begin{Bmatrix} 1 \\ \frac{1}{M^*} \end{Bmatrix} \tag{5.32}$$

But $\mathcal{Q}$ which is $\mathcal{S}_{E2} = \mathcal{L}_{11} - \mathcal{T}_1\mathcal{G}^{-1}\mathcal{T}_1{}^T$ could be resolved into the form $\mathcal{C}\mathcal{C}^T$, where, $\mathcal{C}$ is an upper triangle form. On simplification $\mathcal{Q}$ could be derived to be of the form

$$\mathcal{Q} = \begin{bmatrix} \frac{K^{*2}\rho_2}{1+M^{*2}\rho_2} + \rho_1 & \frac{K^*C^*\rho_2}{1+M^{*2}\rho_2} \\ \frac{K^*C^*\rho_2}{1+M^{*2}\rho_2} & \frac{C^2\rho_2}{1+M^{*2}\rho_2} \end{bmatrix} \tag{5.33}$$

Substituting in Eqs.5.31, 5.33 and assuming $\mathcal{C}$ to be of the form $\begin{bmatrix} \alpha & \beta \\ 0 & \gamma \end{bmatrix}$, we could solve for various elements to obtain

$$\mathcal{C} = \begin{bmatrix} \frac{\pm c^*}{\hat{c}} & \frac{\pm K^* c \rho_2}{\hat{c} c^*} \\ 0 & \frac{\pm c\sqrt{\rho_2\rho_1}}{c^*} \end{bmatrix} \tag{5.34}$$

$$where,\ c^* = \sqrt{K^{*2}\rho_2 + \rho_1\left(1+\rho_2 M^{*2}\right)}\ and\ \hat{c} = \sqrt{1+\rho_2 M^{*2}}$$

The pairs $(\mathcal{A},\mathcal{B})$ and $(\mathcal{A},\mathcal{C})$ in Eqs.5.32 and 5.34 could be checked if they are controllable and observable respectively.

The Controllability matrix is found to be of the form

$$\phi_c = [\mathcal{B}, \mathcal{A}\mathcal{B}, \mathcal{A}^2\mathcal{B}, \cdots \mathcal{A}^{n-1}\mathcal{B}] \quad \text{where, } n = 2$$

$$\phi_c = \begin{bmatrix} 1 & \frac{1}{M^*} \\ \frac{1}{M^*} & \left[\frac{-K^*M^*\rho_2}{1+M^{*2}\rho_2} - \frac{C^*\rho_2}{1+M^{*2}\rho_2}\right] \end{bmatrix} \tag{5.35}$$

The $det[\phi_c] = \frac{-K^*M^*\rho_2}{1+M^{*2}\rho_2} - \frac{C^*\rho_2}{1+M^{*2}\rho_2} - \frac{1}{M^{*2}}$ which indicates that the $det[\phi_c] \neq 0$ and the matrix $\phi_c$ is of full rank.

The pair $(\mathcal{A},\mathcal{C})$ is checked for the observability by forming the Observability matrix of the form

$$\phi_o = \left[\mathcal{C}^T, \mathcal{A}^T\mathcal{C}^T, \left(\mathcal{A}^T\right)^2\mathcal{C}^T, \cdots \left(\mathcal{A}^T\right)^{n-1}\mathcal{C}^T\right] \quad \text{where, } n = 2 \tag{5.36}$$

On considering the first submatrix $C^T$ we could see that $det[C]^T \neq 0$ unless $\rho_1$ and/or $\rho_2$ are equal to zero. Since $\rho_1$ and/or $\rho_2$ are not equal to zero, it violates the basic assumptions made in the performance index. Hence the matrix $\phi_o$ is of full rank and the pair $(\mathcal{A}, \mathcal{C})$ is completely observable. This indicates that a solution to the matrix Ricatti equation is possible.

The Ricatti equation is solved using McFarlane and Potter [159] method in which eigen values and eigen vectors are used to obtain the matrix $\mathcal{R}_{11}$. The solution is evaluated by a computer program and forms as a part of the simulation program.

The second equation 5.24 could be solved for the matrix $\mathcal{R}_{12}$ as a solution of linear equations. This equation involves the solution of the Ricatti equation as described above, and hence contains the elements of the matrix $\mathcal{R}_{11}$. Eq.5.24 can be simplified by substituting various matrices and assuming that the solution of Ricatti equation and the matrix $\mathcal{R}_{12}$ has the form

$$\begin{aligned} \mathcal{R}_{11} &= \begin{bmatrix} \mathcal{R}_{11_a} & \mathcal{R}_{11_b} \\ \mathcal{R}_{11_c} & \mathcal{R}_{11_d} \end{bmatrix} \\ \mathcal{R}_{12} &= \begin{bmatrix} \mathcal{R}_{12_a} & \mathcal{R}_{12_b} & \mathcal{R}_{12_c} \\ \mathcal{R}_{12_d} & \mathcal{R}_{12_e} & \mathcal{R}_{12_f} \end{bmatrix} \end{aligned} \tag{5.37}$$

On simplification Eq.5.24 could be arranged to be solved as a system of linear equations of the form

$$[\mathcal{U}]_{6\times 6} \left\{ \vec{\mathcal{R}}_{12} \right\}_{6\times 1} = \{\mathcal{V}\}_{6\times 1} \tag{5.38}$$

where,

$$\mathcal{U} = \begin{bmatrix} 0 & 0 & -\vartheta_3 & 1 - \frac{\mathcal{R}_{11_b}}{1+M^{*2}\rho_2} & 0 & 0 \\ 1 & 0 & -\vartheta_2 & 0 & 1 - \frac{\mathcal{R}_{11_b}}{1+M^{*2}\rho_2} & 0 \\ 0 & 1 & -\vartheta_1 & 0 & 0 & 1 - \frac{\mathcal{R}_{11_b}}{1+M^{*2}\rho_2} \\ \frac{-K^*M^*\rho_2}{1+M^{*2}\rho_2} & 0 & 0 & \frac{-\left(C^*M^*\rho_2+\mathcal{R}_{11_d}\right)}{1+M^{*2}\rho_2} & 0 & -\vartheta_3 \\ 0 & \frac{-K^*M^*\rho_2}{1+M^{*2}\rho_2} & 0 & 1 & \frac{-\left(C^*M^*\rho_2+\mathcal{R}_{11_d}\right)}{1+M^{*2}\rho_2} & -\vartheta_2 \\ 0 & 0 & \frac{-K^*M^*\rho_2}{1+M^{*2}\rho_2} & 0 & 1 & -\vartheta_1 - \frac{\left(C^*M^*\rho_2+\mathcal{R}_{11_d}\right)}{1+M^{*2}\rho_2} \end{bmatrix}$$

$$\vec{\mathcal{R}}_{12} = \left\{ \mathcal{R}_{12_a} \quad \mathcal{R}_{12_b} \quad \mathcal{R}_{12_c} \quad \mathcal{R}_{12_d} \quad \mathcal{R}_{12_e} \quad \mathcal{R}_{12_f} \right\}^T$$

$$\mathcal{V} = \left\{ \begin{array}{c} \rho_1 + \frac{K^{*2}\rho_2}{1+M^{*2}\rho_2} - \frac{K^*M^*\rho_2\mathcal{R}_{11_b}}{1+M^{*2}\rho_2} \\ \frac{K^*C^*\rho_2}{1+M^{*2}\rho_2} - \frac{C^*M^*\rho_2\mathcal{R}_{11_b}}{1+M^{*2}\rho_2} \\ 0 \\ \frac{K^*C^*\rho_2}{1+M^{*2}\rho_2} - \frac{K^*M^*\rho_2\mathcal{R}_{11_d}}{1+M^{*2}\rho_2} \\ \frac{C^{*2}\rho_2}{1+M^{*2}\rho_2} - \frac{C^*M^*\rho_2\mathcal{R}_{11_b}}{1+M^{*2}\rho_2} \\ 0 \end{array} \right\}$$

The solution of Eq.5.25 in the form $\mathcal{F}_{21}$ is the transpose of $\mathcal{R}_{12}$ which was already solved above. The solution of Equation 5.26 which would yield $\mathcal{R}_{22}$ is not needed in the control gain matrix as indicated in Eq.5.27. The control gain matrix can be simplified in terms of $\mathcal{R}_{11}$ and $\mathcal{R}_{12}$ as

$$\mathcal{C} = \left\{ \frac{-K^*+M^*\mathcal{R}_{11_c}}{1+\rho_2 M^{*2}} \quad \frac{-C^*+M^*\mathcal{R}_{11_d}}{1+\rho_2 M^{*2}} \quad \frac{K^*+M^*\mathcal{R}_{12_d}}{1+\rho_2 M^{*2}} \quad \frac{C^*+M^*\mathcal{R}_{12_e}}{1+\rho_2 M^{*2}} \quad \frac{M^*\mathcal{R}_{12_f}}{1+\rho_2 M^{*2}} \right\} \qquad (5.39)$$

## 5.4 Simulation Results

A comparative study has been performed for the stochastic optimal controller (SOC) developed in the previous sections and also for an adaptive controller developed in chapter 3. Simulation results for the nominal values of the vehicle model parameters (Mass($M^*$) = $250Kg$, Stiffness ($K^*$) = $5\text{x}10^3\frac{N}{m}$, damping constant of proportionality ($C^*$) = $250\frac{Ns}{m}$) are presented. The stochastic excitation input of the form as *Excitation mode II* (as described in chapter 2) is considered. The study involves relative performance of both controllers under constant vehicle parameters and robustness of the controllers for *Parametric variations mode II.*

### 5.4.1 Constant Vehicle Parameters

In this section, the performance difference of the adaptive controller developed in chapter 3 and the stochastic optimal controller (SOC) developed earlier are discussed by presenting the simulation results for vehicle models with known vehicle parameters.

Fig.5.1 indicates the adaptive controlled suspension system's absolute displacement which is derived in Eq.3.28 and is compared with the reference and passive suspension models. Fig.5.2 describes the absolute sprung mass displacement response for the same model with a SOC actuator force as derived in Eq.5.19. Fig.5.1 shows that the adaptive controller follows the reference model and indicates that the response is better at the higher frequencies whereas the SOC is better at lower frequencies. SOC controller gives an optimized performance for these nominal vehicle parameters. Figs.5.3 and 5.4 show the frequency domain power spectral density (PSD) of the sprung mass absolute displacement responses of the adaptive controlled and SOC models. The system gain factors of absolute sprung mass displacement with respect to the excitation input for the adaptive control and the SOC are represented in Figs. 5.5 and 5.6 respectively. The adaptive control shows a better performance than SOC at both the natural frequency ($0.71 Hz$) and at higher frequencies which could also be seen from the Figs.5.1 and 5.2. As shown in Fig.2.1, the second peak at 2 Hz. is due to the excitation input. Figures 5.7 and 5.8 show the comparison of PSD's of relative displacement or the rattle space and work done by the actuators for the adaptive controller and the SOC. The Figs. 5.2 and 5.4 indicate that the SOC has a better absolute displacement response at low frequency but higher relative displacement and work done by the actuators.

### 5.4.2 Vehicle Parameter Variations

To study the robustness of the controllers the vehicle models are subjected to parametric variations such as operational load on the SDOF suspension and stiffness variations with respect to time. The results indicate that the adaptive controller performs as the reference model described in previous chapters and as shown in Figs.5.1, 5.3 and 5.5. The results indicate the adaptive nature of the controller where, the gains are adapted and the adaptation is at the expense of controller force needed. But a SOC which was performing well for the LTI model is not robust enough to

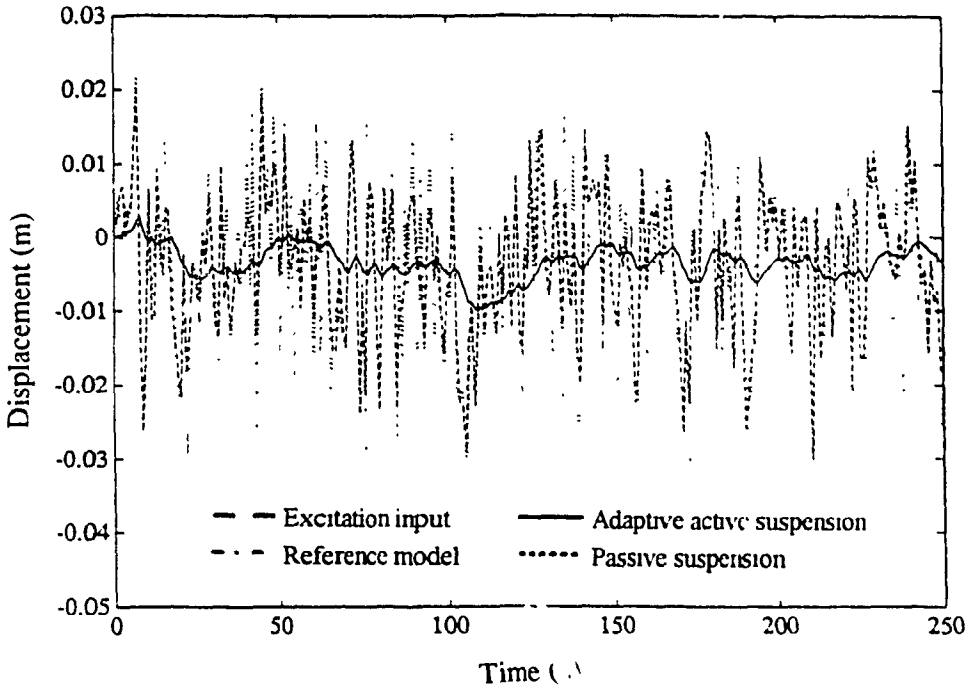


Fig.5.1: Sprung mass absolute displacement response for model reference adaptive control.

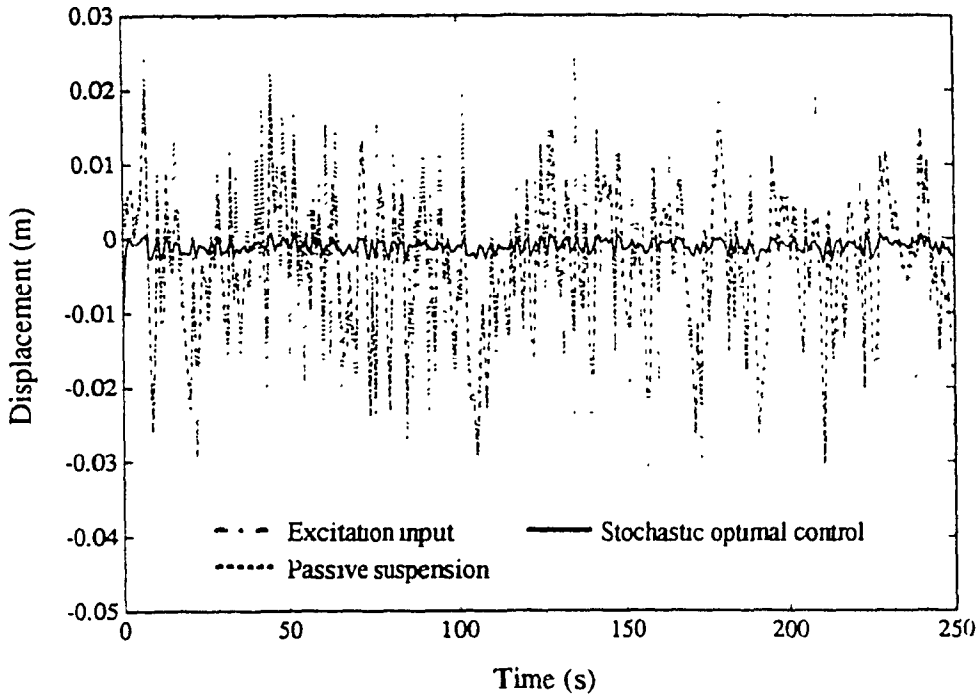


Fig.5.2: Sprung mass absolute displacement response for stochastic optimal control.

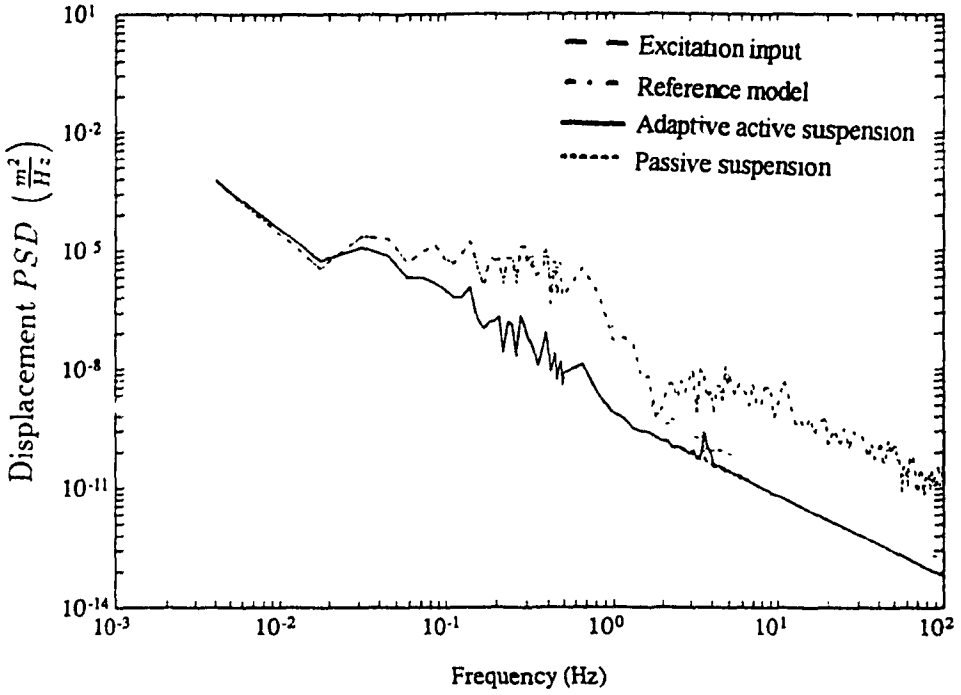


Fig.5.3: Power spectral density (PSD) of sprung mass absolute displacement response using model reference adaptive control.

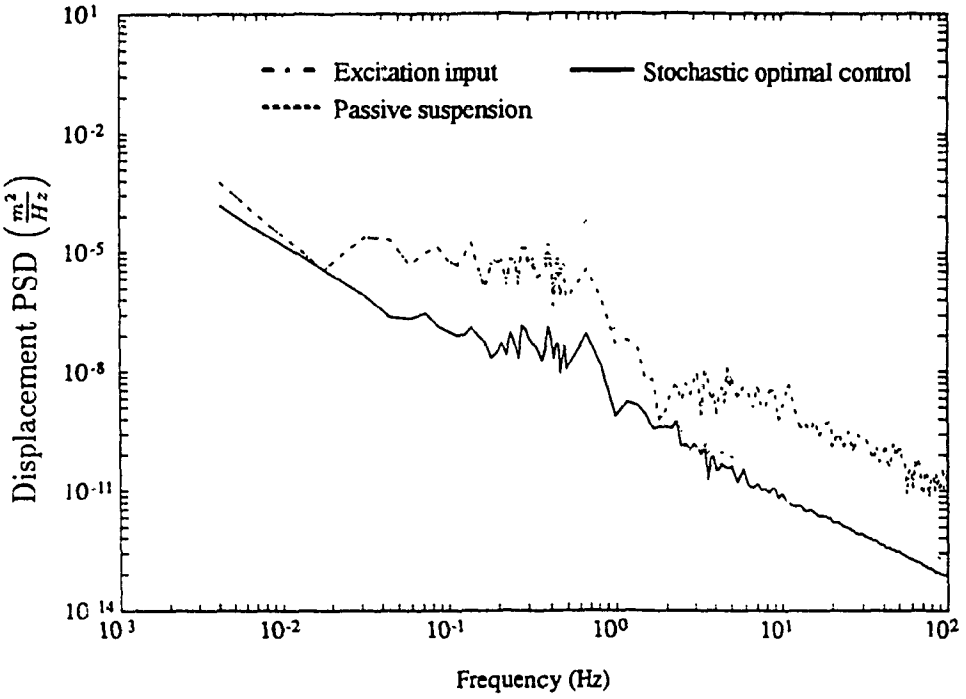


Fig.5.4: Power spectral density (PSD) of sprung mass absolute displacement response using stochastic optimal control.

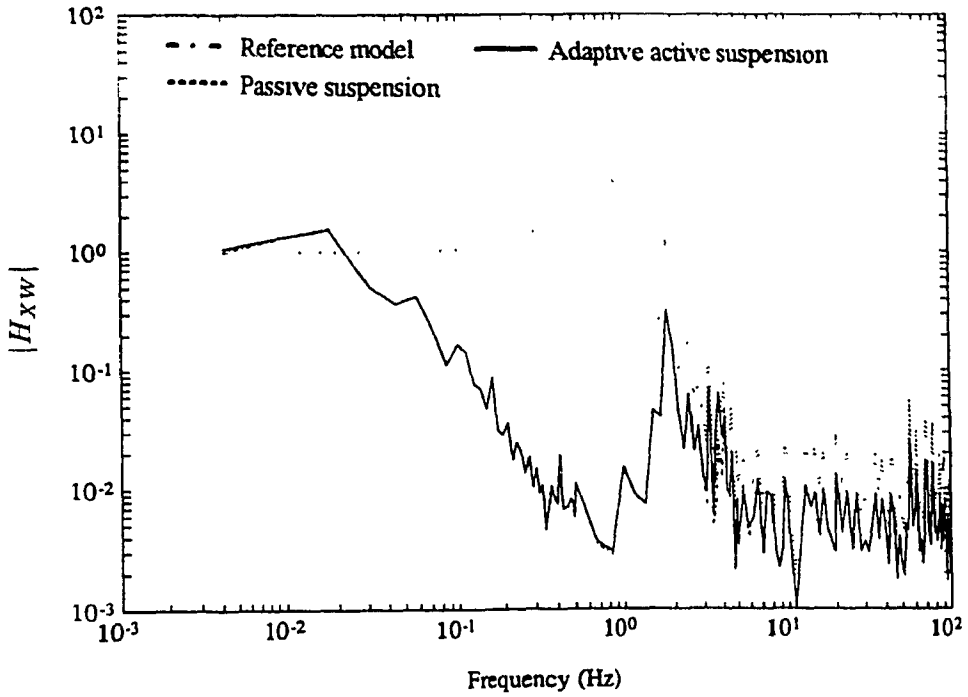


Fig.5.5: System gain factor of absolute displacement with respect to excitation input for a model reference adaptive control system.

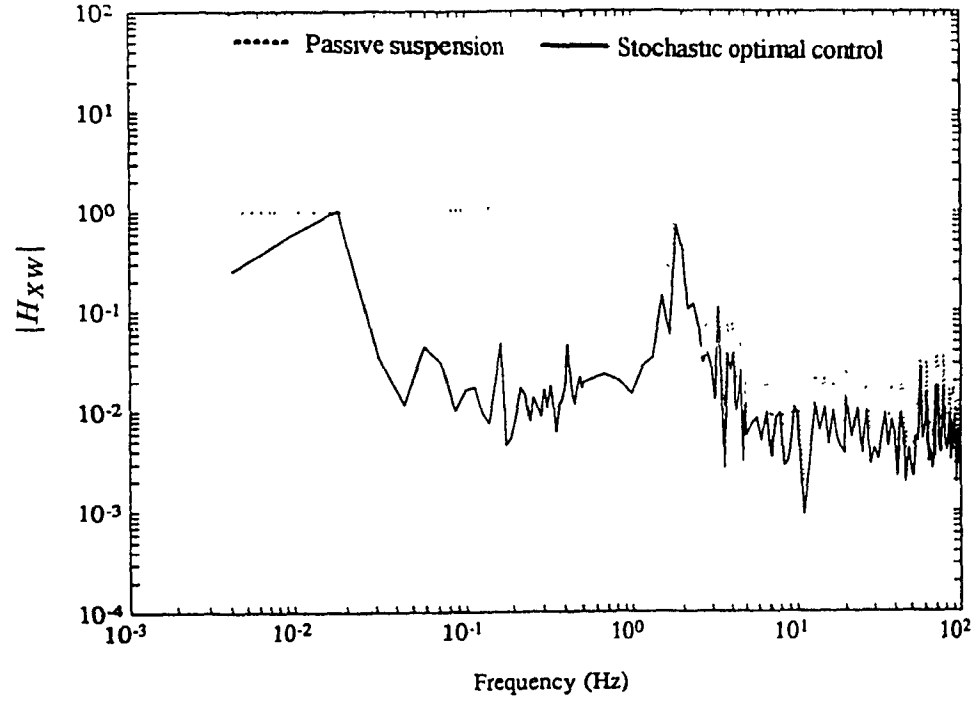


Fig.5.6: System gain factor of absolute displacement with respect to excitation input for a stochastic optimal control system.

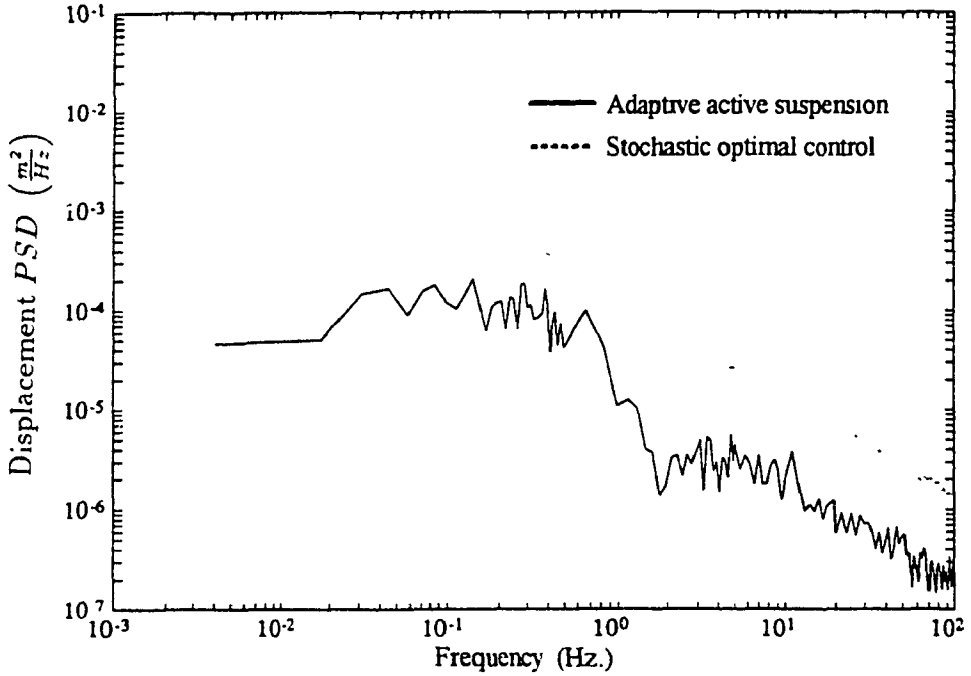


Fig.5.7: Comparison of relative displacements (Rattle Space) power spectral density (PSD) response.

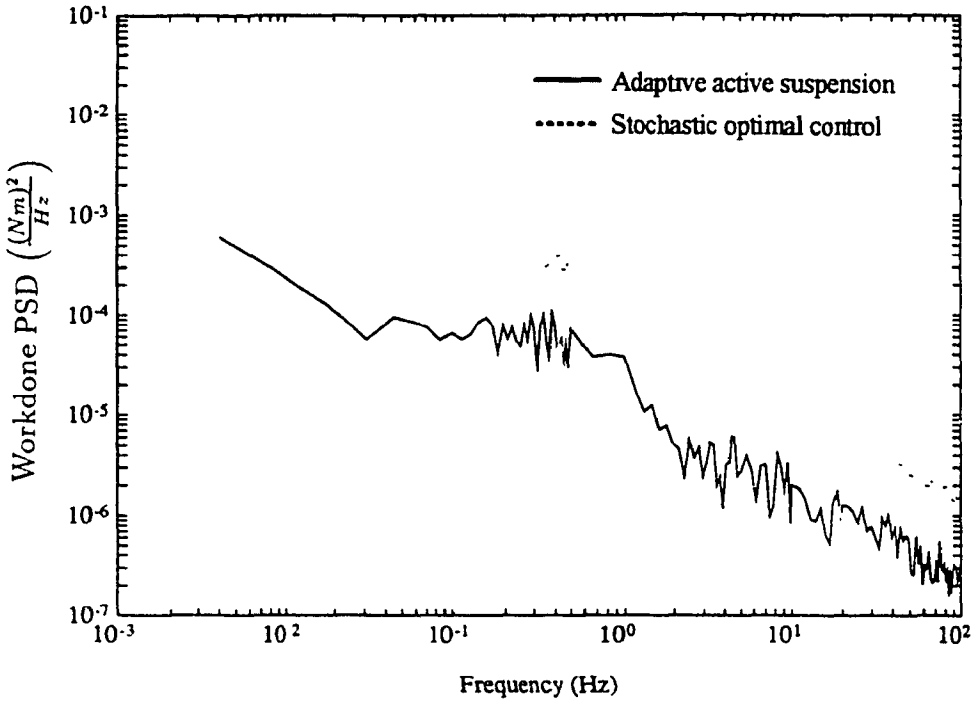


Fig.5.8: Comparison of workdone by actuators as power spectral density (PSD) response.

take care of the time dependent parameter variations. Figs.5.9, 5.10 and 5.11 show the time domain response for the gains being not updated and updating every 10 and 5 seconds respectively. Fig.5.9 shows the instability that would occur for the SOC by the use of the same controller gains even for parametric variations. Figures 5.10 and 5.11 show how the performance from Fig.5.9 could be enhanced by updating the online stochastic optimal control gains. However, this is not robust enough for various parametric variations. When the gains are updated using an online SOC with the assumption that the parametric variations are known a priori, then the response becomes stable. This has been shown in Figs.5.10 and 5.11. Even with the online variation of SOC gains, the response is not robust enough for the parametric variations. The results are found to be analogous to the mass and stiffness variations. An adaptive controlled active suspension would maintain its adaptation to the reference model even under wide range of parametric variations. Hence the system response remains as described in Fig.5.5. But in order to maintain any robustness to the system parameter variations, as described in Figs.5.10 and 5.11, the stochastic optimal controller has to be subjected to an online calculation of the gains.

## 5.5 Discussion

The results presented in the previous section indicate the relative performance of the adaptive controller and the stochastic optimal controller. The frequency domain responses are converted from the time domain simulation results by using fast Fourier transform (FFT) Cooley-Tukey procedure. The results show that even under nominal conditions, the implemented SOC could be robust to some extent but could not achieve the required skyhook reference model performance. For large parametric variations the adaptive controller shows the robustness at the expense of more control input and on line controller hardware. The conventional SOC designed for piece wise linear time invariant model cannot be robust for large parametric variations. Even if the implemented SOC gains are updated at a faster rate with the assumption of

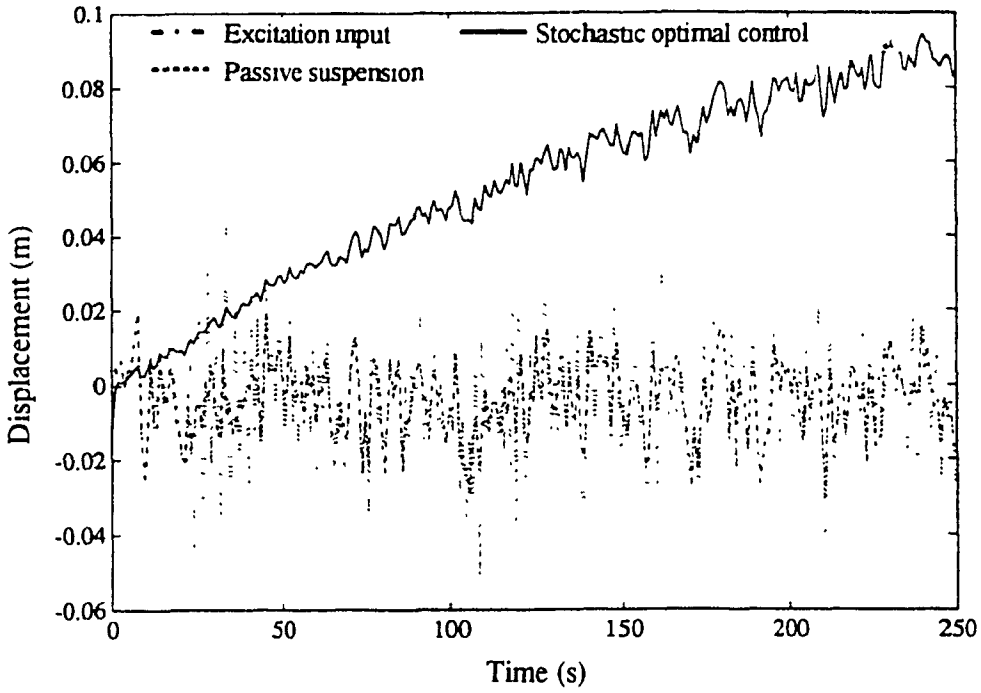


Fig.5.9: Sprung mass absolute displacement response with gains not updated using stochastic optimal control.

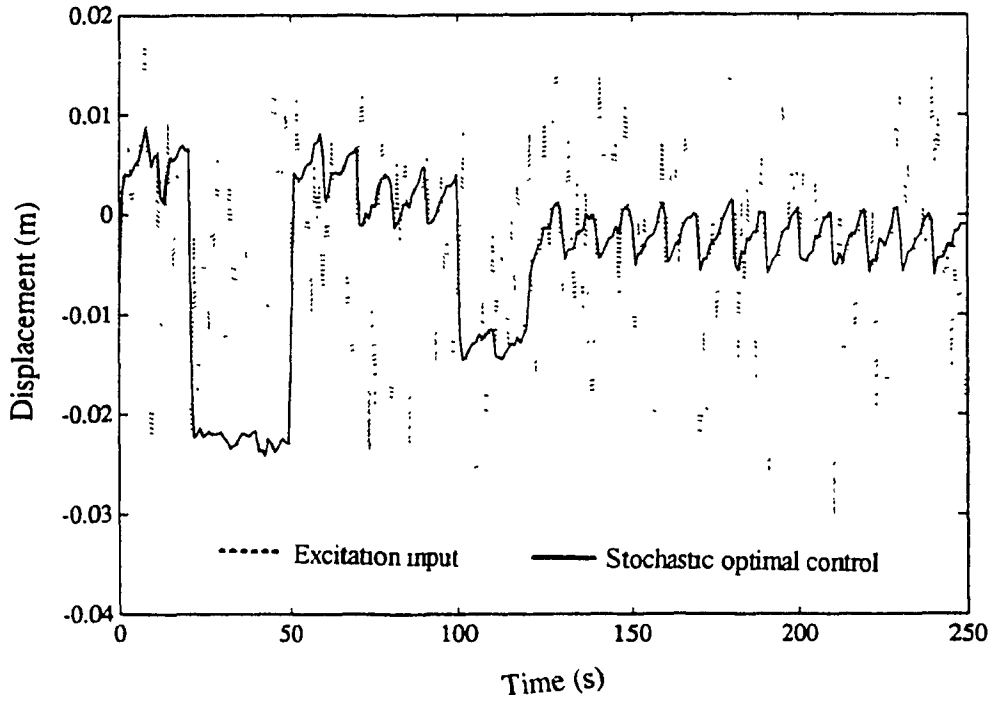


Fig.5.10: Sprung mass absolute displacement response with gains updated every 10 seconds using stochastic optimal control.

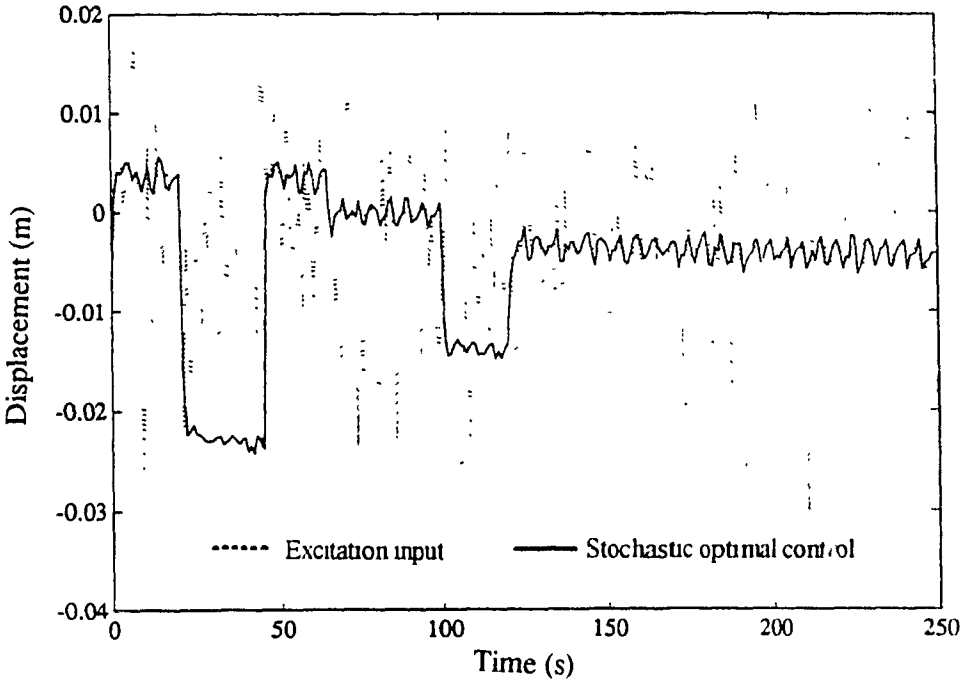


Fig.5.11: Sprung mass absolute displacement response with gains updated every 5 seconds using stochastic optimal control.

the knowledge of parametric variations, the performance of an adaptive controller is found to be superior. But the optimal controller could be designed to be robust towards parameter variations, modelling errors and time delays by designing bounds on the perturbations. An estimate of the bounds for the nonlinear time varying perturbations has to be made and then they have to be used up in the quadratic $\mathcal{PI}$ [123]. Bounds had to be laid on various perturbations involving plant parameters, forward velocity and different inputs. Actually it would be more appropriate to compare the adaptive controller with the robust stochastic optimal controller which remains an open problem for research on suspension. But in any case an adaptive controller does not need any knowledge of the perturbations and by adapting the gains we could attain less rattle space and expend less amount of actuator work. This has been shown in Figs.5.7 and 5.8.

## 5.6 Summary

A comparison of robustness of a stochastic optimal controller and the adaptive nature of an adaptive controller was discussed in this chapter. In the earlier publications using optimal control, the control gain vector is calculated off-line for various velocities, inputs and parametric variations. In these cases the plant models are assumed to be piece wise linear time invariant and the variation in the operating conditions is known a priori by means of preview sensors. This approach gives an optimal performance at various discrete operating points. But the stochastic optimal controller derived in this chapter was subjected to variation in parameters and was found not to be robust enough for large parametric variations which are discussed in chapter 2. The stochastic optimal controller results were compared with an adaptive active suspension controller performance. An adaptive controller was found to be robust by updating the gains for different dynamic parameter variations without any a priori knowledge of the changes. The comparison study indicates that a stochastic optimal controller is less robust than an adaptive controller when subjected to parametric

variations due to various vehicle operating conditions.

# Chapter 6

# Continuous Time Adaptive Control For Multi-Degree of Freedom Model

## 6.1 General

Chapters 3 and 4 discussed earlier involve the study of a single degree of freedom vehicle suspension system in continuous time and discrete time domains. In contrast to this, chapters 6 and 7 involve the study of multi-degree of freedom (MDOF) systems. Due to the richness of control theory in continuous time domain, this chapter extends the adaptive active suspension concept in the continuous time domain to the MDOF system. A general nonlinear time varying model has been used which could be analyzed for various applications by imposing appropriate special conditions. The performance of a general nonlinear passive model selected has been analyzed by using the discrete harmonic linearization technique (DHLEM) [141], to compare it with the reference model. The basic idea involves obtaining optimal performance of any nonlinear time varying (NTV) suspension model by adaptively following a predefined reference model. Optimal performance is achieved by an adaptive control law which involves feedforward, feedback and auxiliary control inputs by evaluating various feed-

back parameters. Model reference adaptive control approach used in this chapter, has been adapted from the method described by Seraji [154]. The controller designed has been implemented for a two DOF bounce NTV model. Simulation results for *Excitation mode I, Parametric variations mode I* and *Excitation mode II, Parametric variations mode II* have been presented.

## 6.2 General Nonlinear Time Varying Model Formulation

The controller discussed in this chapter incorporates a general "n" DOF NTV model. Specific constraints could be imposed which would formulate the problem for various applications. Initially, a two DOF nonlinear bounce suspension model has been used to form the nonlinear matrix equations and is then extended to a general formulation. Figure 6.1 shows a two DOF NTV bounce suspension model. This figure shows a

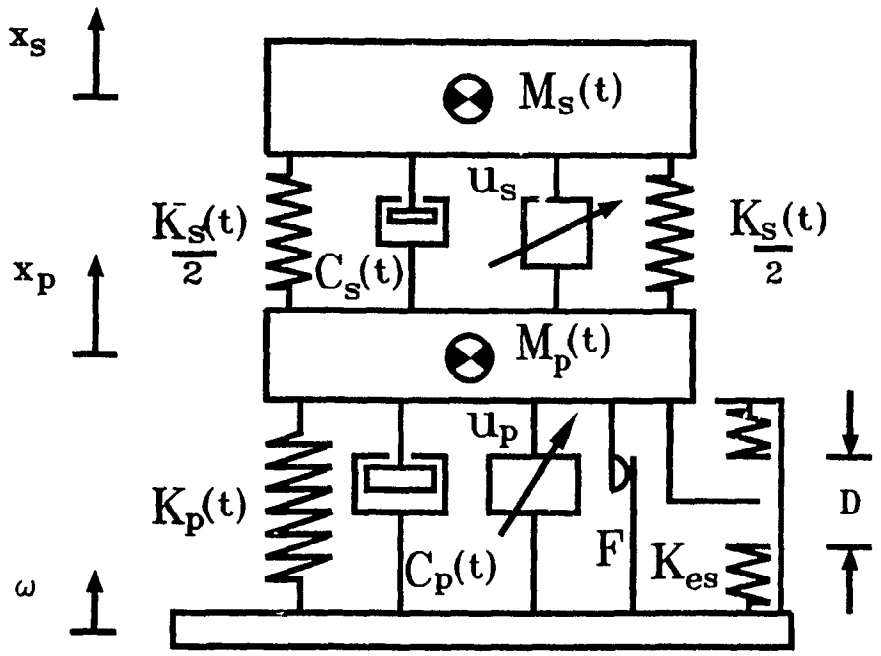


Fig.6.1: 2-degree of freedom nonlinear time varying active suspension model.

secondary suspension mass $M_s(t)$ and a primary suspension mass $M_p(t)$ suspended by various nonlinear components and also subjected to excitation at the base. The general two DOF model described in this section could be applied for various suspension examples such as primary and secondary suspension in the rail vehicles, cab suspension for trucks, etc.. For achieving optimal isolation of the secondary mass $M_s$, two actuators are used for the control forces $u_s$ and $u_p$ at the secondary and primary suspension levels respectively.

As explained in section 2.4 of chapter 2, the general model incorporates various NTV properties such as Coulomb friction, velocity squared viscous damping and elastic limit stops. The dynamic equations involving the secondary and primary bounce DOF's $(x_s)$ and $(x_p)$ are derived as follows. For the sake of simplicity, the secondary damping is considered to possess linear viscous damping characteristics. The NTV discontinuous equations of motion in terms of the suspension deflections at the primary and secondary level as $z_s = (x_s - x_p)$ and $z_p = (x_s - w)$ could be written as

$$M_s(t)\left(\ddot{z}_s + \ddot{z}_p\right) + C_s(t)\dot{z}_s + K_s(t)z_s = -M_s(t)\ddot{w} + u_s \tag{6.1}$$

$$M_p(t)\ddot{z}_p - K_s(t)z_s - C_s(t)\dot{z}_s + K_p(t)z_p + F_c + F_d + F_s = -M_p(t)\ddot{w} + u_p - u_s$$

where,

$$\begin{aligned} F_c(t, \dot{z}_p) &= F(t)\, sgn\,(\dot{z}_p) \\ F_d(\dot{z}_p, t) &= C_p\,|\dot{z}_p|\,(\dot{z}_p) \\ F_s(z_p, t) &= K_{es}S^*\left(z_p - \tfrac{D}{2}sgn\,(z_p)\right) \\ S^* &= \begin{cases} 0 & \text{if } |z_p| \le \frac{D}{2} \\ 1 & \text{otherwise} \end{cases} \end{aligned}$$

The time varying terms $M_s(t)$, $M_p(t)$, $C_s(t)$, $C_p(t)$, $K_s(t)$ and $K_p(t)$ denote the mass, damping constant of proportionality and stiffness that varies with time. To simplify the model, the secondary suspension damping is assumed to be linear

damping and $C_s(t)$ as the damping coefficient. The forcing components $F_c$, $F_d$, $F_e$ represent Coulomb, velocity squared viscous damping and elastic limit stop forces that are nonlinear. These forcing components contain coefficients $F$, $K_{es}$, $C_p$ whose actual values are not known and vary with time. $\ddot{w}$ denotes the excitation acceleration. Eq.6.2 can be represented in the matrix form as

$$\begin{bmatrix} M_s(t) & M_p(t) \\ 0 & M_p(t) \end{bmatrix} \begin{Bmatrix} \ddot{z}_s \\ \ddot{z}_p \end{Bmatrix} + \begin{bmatrix} C_s(t) & 0 \\ -C_s(t) & C_p(t)\,|\dot{z}_p| \end{bmatrix} \begin{Bmatrix} \dot{z}_s \\ \dot{z}_p \end{Bmatrix} +$$

$$\begin{bmatrix} K_s(t) & 0 \\ -K_s(t) & K_p(t) + K_{es}s^* \end{bmatrix} \begin{Bmatrix} z_s \\ z_p \end{Bmatrix} + \begin{Bmatrix} 0 \\ F\,sgn\,(\dot{z}_p) \end{Bmatrix} +$$

$$\begin{Bmatrix} 0 \\ -K_{es}s^* \frac{D}{2}\,sgn\,(z_p) \end{Bmatrix} = - \begin{Bmatrix} M_s(t) \\ M_p(t) \end{Bmatrix} \ddot{w} + \begin{bmatrix} 1 & 0 \\ -1 & 1 \end{bmatrix} \begin{Bmatrix} u_s \\ u_p \end{Bmatrix} \tag{6.2}$$

It follows from Eq.6.2 that a general equation for n degrees of freedom model can be written as

$$\mathcal{M}(t)|_{n\times n}\,\ddot{Z} + \mathcal{C}\left(t, Z, \dot{Z}\right)\Big|_{n\times n} + \mathcal{K}\left(t, Z\right)|_{n\times 1} + \mathcal{L}\left(t, \dot{Z}\right)\Big|_{n\times 1} = -\,\mathcal{D}(t)|_{n\times 1}\,\ddot{w} + \mathcal{P}|_{n\times n}\,U \tag{6.3}$$

where,

$$\mathcal{M}(t) = \begin{bmatrix} M_s(t) & M_p(t) \\ 0 & M_p(t) \end{bmatrix}$$

$$\mathcal{C}\left(t, Z, \dot{Z}\right) = \begin{Bmatrix} C_s(t)\dot{z}_s + K_s(t)z_s \\ -C_s(t)\dot{z}_s + C_p(t)\,|\dot{z}_s|\,\dot{z}_p - K_s(t)z_s + (K_p(t) + K_{es}S^*)\,z_p \end{Bmatrix}$$

$$\mathcal{K}(t, z) = \begin{Bmatrix} 0 \\ -K_{es}S^*\frac{D}{2}sgn(z_p) \end{Bmatrix}$$

$$\mathcal{L}\left(t, \dot{z}\right) = \begin{Bmatrix} 0 \\ F sgn\,(\dot{z}_p) \end{Bmatrix}$$

$$\mathcal{D}(t) = \begin{Bmatrix} M_s(t) \\ M_p(t) \end{Bmatrix}$$

$$\mathcal{P} = \begin{bmatrix} 1 & 0 \\ -1 & 1 \end{bmatrix}$$

$$Z = \begin{Bmatrix} z_s \\ z_p \end{Bmatrix}$$

$$U = \begin{Bmatrix} u_s \\ u_p \end{Bmatrix}$$

The matrix $\mathcal{P}$ always consists of constant elements and hence is independent of nonlinear and time varying terms. The matrices $\mathcal{M}$ and $\mathcal{P}$ are positive definite (eg. $\mathcal{M}$ and $\mathcal{P}$ in Eq.6.3 are nonsingular positive definite matrices).

A skyhook linear time invariant (LTI) reference model of the form shown in Fig.6.2 is chosen for the development of controller purpose only. The presence of the reference model is needed only for theoretical purposes. It is not needed to be physically realizable for practical implementation of the adaptive controller. The equation of motion of the model in terms of relative displacements is given as

$$M_{m_s}\left(\ddot{z}_{m_s} + \ddot{z}_{m_p}\right) + D_{m_s}\left(\dot{z}_{m_s} + \dot{z}_{m_p}\right) + K_{m_s} z_{m_s} = -M_{m_s}\ddot{w} - D_{m_s}\dot{w}$$

$$M_{m_p}\ddot{z}_{m_p} - K_{m_s} z_{m_s} + D_{m_p}\dot{z}_{m_p} + K_{m_p} z_{m_p} = -M_{m_p}\ddot{w} - D_{m_p}\dot{w} \qquad (6.4)$$

Where $M_{m_s}$,$M_{m_p}$,$D_{m_s}$,$D_{m_p}$,$K_{m_s}$ and $K_{m_p}$ are mass, damping constant of proportionalities and stiffness constant of the model. The terms $z_{m_s}$ and $z_{m_p}$ represent the model relative displacements $\left(x_{m_s} - x_{m_p}\right)$ and $\left(x_{m_p} - w\right)$ respectively. The model parameters are time invariant and can be chosen to be of any value as per the required suspension performance.

Various system gain factors in the form of acceleration transmissibility and relative displacement transmissibility for the LTI reference model (shown in Fig.6.2) and nonlinear passive bounce isolator (shown in Fig.6.1) are formed from the above equations. The transfer functions are studied to show the reference model performance and the effect of damping values. This study is used in choosing the reference

model parameters. These results on comparison with the passive model facilitates in validating the simulation results obtained by using the adaptive control approach.

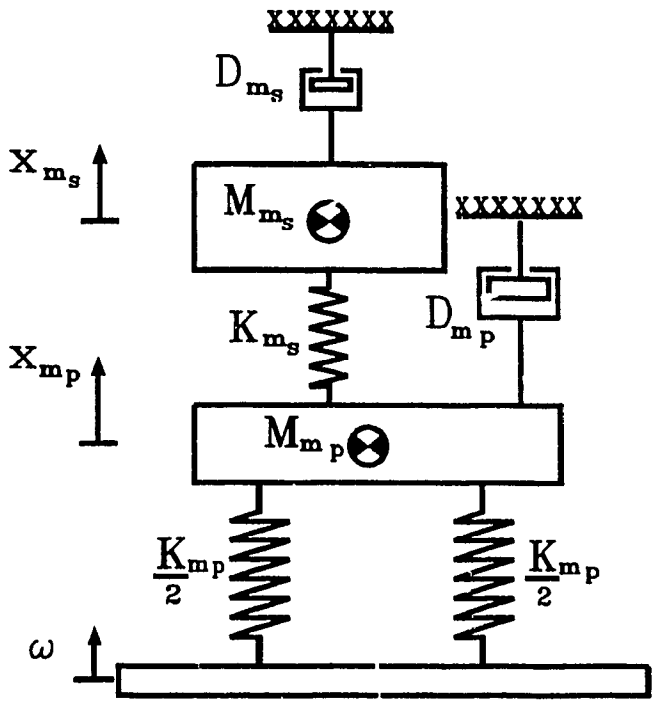


Fig.6.2: 2-degree of freedom dual skyhook reference model.

An equivalent viscous damping coefficient for a nonlinear passive system at different frequencies is calculated on the basis of energy equalization principle for dry friction and orifice damping. The DHLEM [141] based on energy equalization is used in this approach. Figures 6.3 and 6.4 describe the secondary and primary suspension mass acceleration system gain factor with respect to the excitation input. These figures also indicate the response characteristics for various damping coefficients. The system gain factors of relative displacements at the secondary and primary suspension with respect to excitation input are shown in Figs. 6.5 and 6.6 respectively. A comparative study for various primary and secondary skyhook damping coefficients $D_{m_p}$ and $D_{m_s}$ has been conducted. The study of above figures indicate that increasing the damping

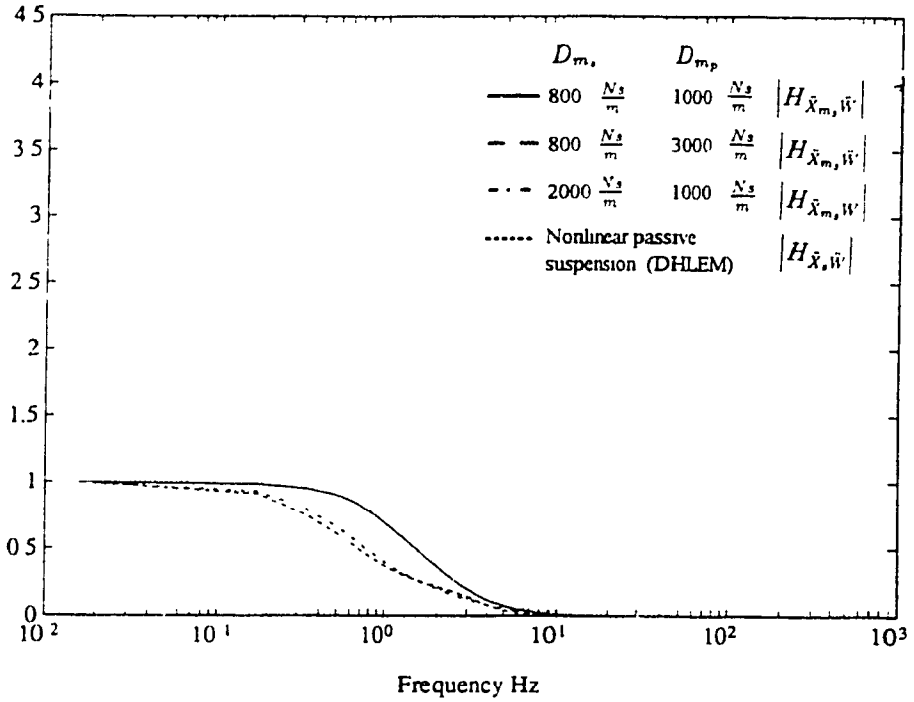


Fig.6.3: System gain factor of secondary suspension mass absolute acceleration with respect to excitation input.

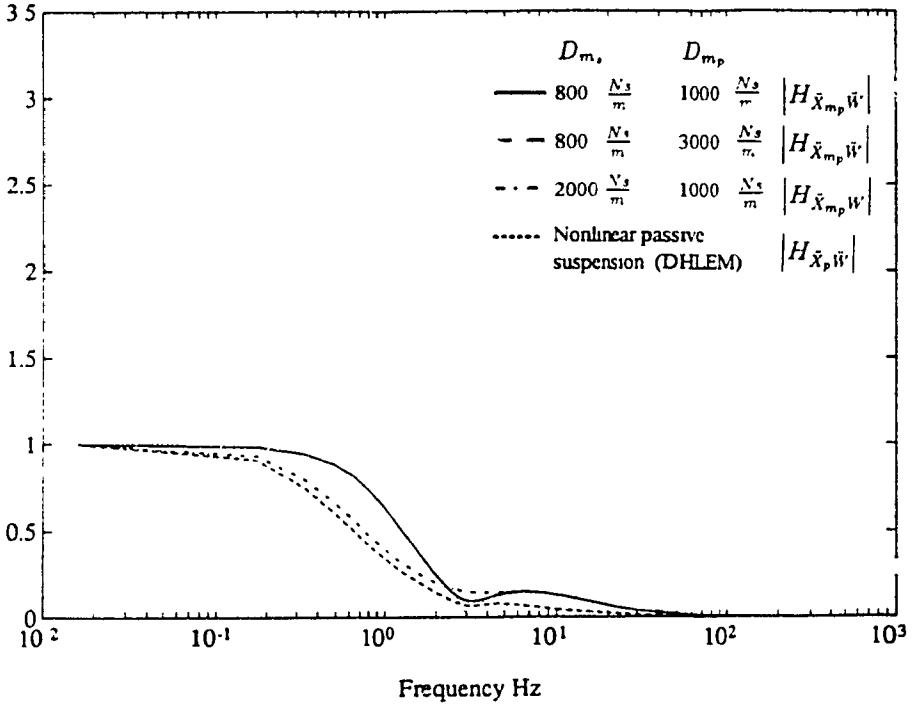


Fig.6.4: System gain factor of primary suspension mass absolue acceleration with respect to excitation input .

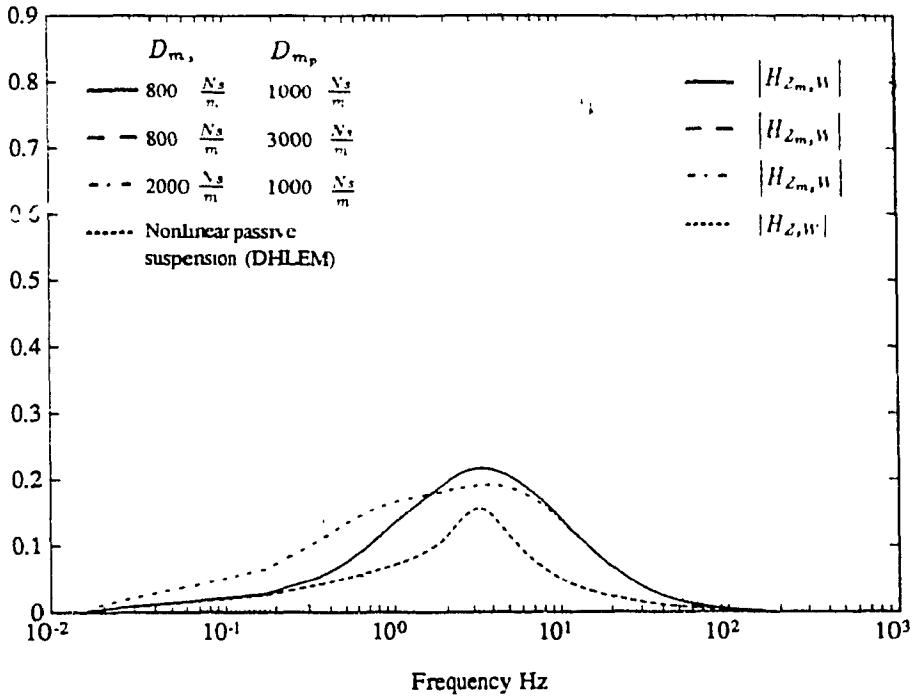


Fig.6.5: System gain factor of secondary suspension relative displacement with respect to excitation input.

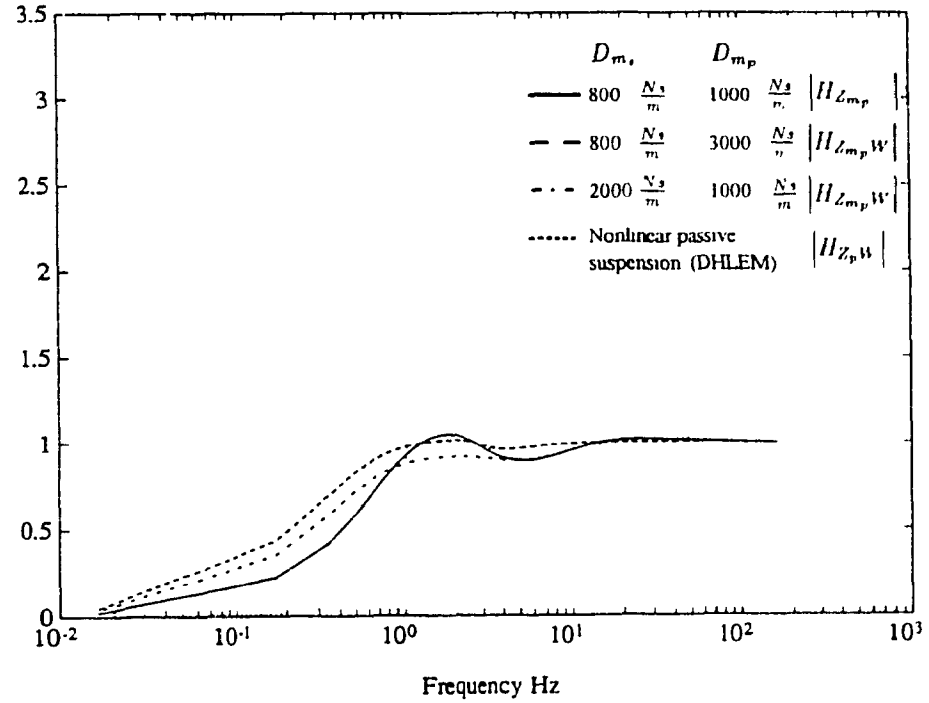


Fig.6.6: System gain factor of primary suspension relative displacement with respect to excitation input.

coefficient $D_{m_s}$ would increase the primary and secondary rattle space, but increase in the coefficient $D_{m_p}$ would reduce secondary rattle space and increase the primary rattle space. The reference model leaves a great scope of choice for its parameters depending on the application chosen for analysis and implementation.

The general adaptive controller problem can be stated as to force the general NTV MDOF bounce model (defined in Eq.6.3) with its actual parameters not known a priori, and also to achieve the optimal suspension performance (defined by Eq.6.4) by adaptively varying the controller gains.

## 6.3 Controller Structure

The controller structure in this approach is divided into three different aspects: feed forward controller, feedback controller and auxiliary signal. An extension of this concept as studied in Ref.[154] with modifications for a general MDOF suspension model has been described in the following sections. Let P(s) denote a black box transfer function of the NTV suspension model which is physically present and is being controlled by the adaptive controller. The actual unknown dynamics of this model could be closely represented by the non-linear time varying equations given in Eq.6.3. M(s) refers to the reference model transfer function which specifies the required suspension performance in various degrees of freedom (DOF). It is defined as a LTI optimal suspension model in the form of skyhook damping suspension model which is defined in Eq.6.4 and is shown in Fig.6.2.

### 6.3.1 Feedforward Controller

Let W(s) denote the linearized model about the operating point of the actual vehicle model P(s). Let us assume there exists a dynamical inverse of W(s) represented by Q(s) [154]. If the plant model P(s) is LTI and perfectly known, then Q(s) will

also be LTI and known. Let $\ddot{w}$ denote the road or track/guide way irregularities to the suspension. The output of the decentralized optimal reference model M(s) will be $Z_m(t)$ which denotes the desired performance of the suspension in various degrees of freedom. By the concept of *"Inverse systems"*, if the plant P(s) is preceded by its inverse Q(s) and the inverse is driven by the desired signal $Z_m(t)$, then the inverse will generate control action. This ensures that the plant output $Z(t)$ will be the same as $Z_m(t)$ [154]. But in real sense P(s) is a NTV model and is not perfectly known at every instant. Hence Q(s) is chosen as a linearized model about the operating conditions and its parameters are updated depending on the error occurred. The adaptive feedforward controller takes care of the slow time varying properties of the actual plant and achieves fast response. The term $Q_I(s)$ represents the feedforward term that is dependent on the road/terrain disturbance input $\ddot{w}$ called input feedforward controller.

### 6.3.2 Feedback Controller

The role of the feedback controller is to provide a stable closed loop system. Inadequate knowledge of actual plant P(s) and its linearized inverse model Q(s) which is updated at slower rate requires the feedback controller V(s) to adapt its gains so as to attain perfect model following.

An auxiliary signal is used to represent the operating point about which the feedforward controller operates. Fig.6.7 shows the schematic representation of the controller modules that operate on various signals to calculate a stable control input to the actual hardware system. The block diagram indicates that the final signal to the suspension model is addition of feedforward, feedback and auxiliary signals.

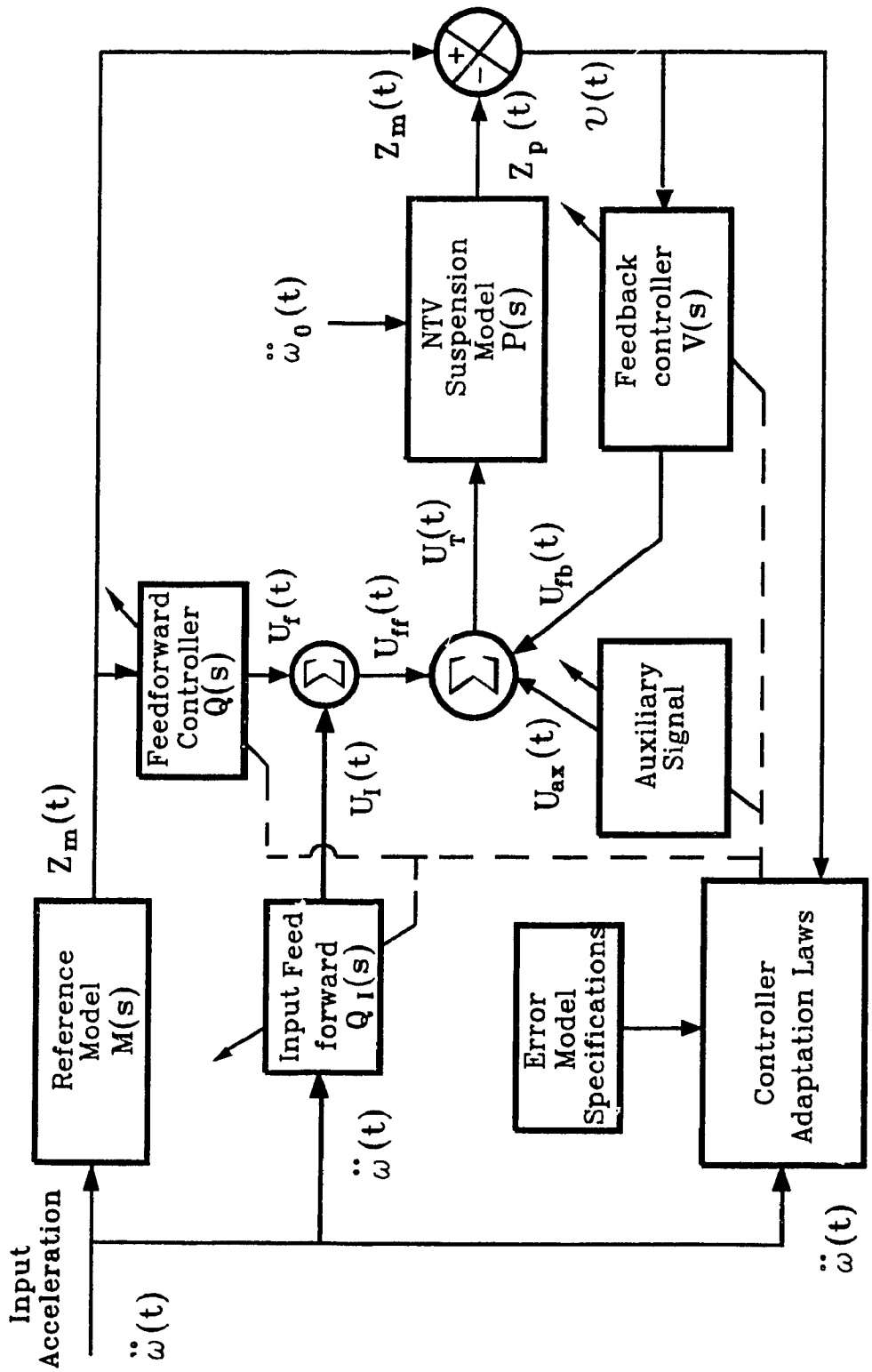


Fig.6.7: Block diagram representation of the adaptive controller for the general model.

## 6.4 Linearization of Suspension Model

The general nonlinear system of equations represented by Eq.6.3 is a function of position, velocity, and acceleration $(Z, \dot{Z}, \ddot{Z})$. Eq.6.3 can be linearized about an operating point by using Taylor series expansion as discussed below. Let the nominal values of the operating point be represented by $\mathcal{OP}\left(t_0, Z_0, \dot{Z}_0, \ddot{Z}_0, \ddot{w}_0 \text{ and } U_0\right)$. If $\left(\Delta t, \Delta Z, \Delta \dot{Z}, \Delta \ddot{Z}, \Delta \ddot{w} \text{ and } \Delta U\right)$ are the variations of the respective parameters about the operating point $\mathcal{OP}$, then

$$\begin{array}{rcl} t & = & t_0 + \Delta t \\ Z & = & Z_0 + \Delta Z \\ \dot{Z} & = & \dot{Z}_0 + \Delta \dot{Z} \\ \ddot{Z} & = & \ddot{Z}_0 + \Delta \ddot{Z} \\ \ddot{w} & = & \ddot{w}_0 + \Delta \ddot{w} \\ U & = & U_0 + \Delta U \end{array} \tag{6.5}$$

The general nonlinear and discontinuous equation (Eq.6.3) could be represented as a nonlinear continuous equation whose terms are analytic at all points so that the Taylor series expansion could be applied. The analytic form of the generalized equation 6.3 could be written as

$$\mathcal{M}(t)\ddot{Z} + \mathcal{C}\left(t, Z, \dot{Z}\right) + \mathcal{K}\left(t, Z\right) + \mathcal{L}\left(t, \dot{Z}\right) = -\mathcal{D}(t)\ddot{w} + \mathcal{P}U \tag{6.6}$$

The nonlinear terms in $\mathcal{C}\left(t, Z, \dot{Z}\right), \mathcal{K}\left(t, Z\right)$ and $\mathcal{L}\left(t, \dot{Z}\right)$ could be replaced by analytic continuous approximation expressions such as

$$\begin{array}{rcl} S^*\left(Z_p\right) & = & 1 - \frac{2}{\pi}\int_0^{\aleph} \frac{\sin\left(\omega\frac{D}{2}\right)\cos\left(\omega Z_p\right)}{\omega} d\omega \\ sgn\left(Z_p\right) & = & \frac{2}{\pi}\int_0^{\aleph} \left(\frac{1-\cos\left(\omega \acute{D}\right)}{\omega}\right) \sin\left(\omega Z_p\right) d\omega \\ sgn\left(\dot{Z}_p\right) & = & \frac{2}{\pi}\int_0^{\aleph} \left(\frac{1-\cos\left(\omega \grave{D}\right)}{\omega}\right) \sin\left(\omega \dot{Z}_p\right) d\omega \end{array} \tag{6.7}$$

where, $\acute{D}$ and $\grave{D}$ are some large numbers much greater than $D$.

On substituting the operating point $\mathcal{OP}$ the dynamic equation could be written as

$$\mathcal{M}(t_0)\ddot{Z}_0 + \mathcal{C}\left(t_0, Z_0, \dot{Z}_0\right) + \mathcal{K}\left(t_0, Z_0\right) + \mathcal{L}\left(t_0, \dot{Z}_0\right) = -\mathcal{D}(t_0)\ddot{w}_0 + \mathcal{P}U_0 \tag{6.8}$$

Using the Taylor series, the nonlinear and time varying terms in Eq.6.6 which are analytic at every point could be expanded about the operating point as

$$\begin{aligned} \mathcal{M}(t) &= \mathcal{M}(t_o) + \left.\frac{\partial \mathcal{M}}{\partial t}\right|_{\mathcal{OP}} \Delta t + \cdots \\ &= \mathcal{M}(t_o) + \dot{\mathcal{M}}(t_o)\Delta t + \cdots \\ \mathcal{D}(t) &= \mathcal{D}(t_o) + \left.\frac{\partial \mathcal{D}}{\partial t}\right|_{\mathcal{OP}} \Delta t + \cdots \\ &= \mathcal{D}(t_o) + \dot{\mathcal{D}}(t_o)\Delta t + \cdots \end{aligned} \tag{6.9}$$

The discontinuous terms which have been transformed into the continuous functions are linearized as follows.

$$\begin{aligned} \mathcal{C}\left(t, Z, \dot{Z}\right) &= \mathcal{C}\left(t_0, Z_0, \dot{Z}_0\right) + \left.\frac{\partial \mathcal{C}}{\partial t}\right|_{\mathcal{OP}} \Delta t + \left.\frac{\partial \mathcal{C}}{\partial Z}\right|_{\mathcal{OP}} \Delta Z + \left.\frac{\partial \mathcal{C}}{\partial \dot{Z}}\right|_{\mathcal{OP}} \Delta \dot{Z} + \cdots \\ \mathcal{K}\left(t, Z\right) &= \mathcal{K}\left(t_0, Z_0\right) + \left.\frac{\partial \mathcal{K}}{\partial t}\right|_{\mathcal{OP}} \Delta t + \left.\frac{\partial \mathcal{K}}{\partial Z}\right|_{\mathcal{OP}} \Delta Z + \cdots \\ \mathcal{L}\left(t, \dot{Z}\right) &= \mathcal{L}\left(t_0, \dot{Z}_0\right) + \left.\frac{\partial \mathcal{L}}{\partial t}\right|_{\mathcal{OP}} \Delta t + \left.\frac{\partial \mathcal{L}}{\partial \dot{Z}}\right|_{\mathcal{OP}} \Delta \dot{Z} + \cdots \end{aligned} \tag{6.10}$$

On assuming the variation of vehicle parameters at a slow rate along with close operating points, the second order derivatives of the parameter variations are also assumed to be very small. Hence we could further simplify the Taylor series terms to be of the form

$$\begin{aligned} \mathcal{M}(t) &= \mathcal{M}(t_o) \\ \mathcal{C}\left(t, Z, \dot{Z}\right) &= \mathcal{C}\left(t_0, Z_0, \dot{Z}_0\right) + \left.\frac{\partial \mathcal{C}}{\partial Z}\right|_{\mathcal{OP}} \Delta Z + \left.\frac{\partial \mathcal{C}}{\partial \dot{Z}}\right|_{\mathcal{OP}} \Delta \dot{Z} \\ \mathcal{K}\left(t, Z\right) &= \mathcal{K}\left(t_0, Z_0\right) + \left.\frac{\partial \mathcal{K}}{\partial Z}\right|_{\mathcal{OP}} \Delta Z \\ \mathcal{L}\left(t, \dot{Z}\right) &= \mathcal{L}\left(t_0, \dot{Z}_0\right) + \left.\frac{\partial \mathcal{L}}{\partial \dot{Z}}\right|_{\mathcal{OP}} \Delta \dot{Z} \\ \mathcal{D}(t) &= \mathcal{D}(t_o) \end{aligned} \tag{6.11}$$

On substituting Eq.6.11 and terms of Eq.6.5 in Eq.6.6 and subtracting the operating point condition from Eq.6.8 we obtain

$$\mathcal{M}(t_0)\Delta\ddot{Z} + \left[\left.\frac{\partial \mathcal{C}}{\partial \dot{Z}}\right|_{\mathcal{OP}} + \left.\frac{\partial \mathcal{L}}{\partial \dot{Z}}\right|_{\mathcal{OP}}\right]\Delta\dot{Z} + \left[\left.\frac{\partial \mathcal{C}}{\partial Z}\right|_{\mathcal{OP}} + \left.\frac{\partial \mathcal{L}}{\partial Z}\right|_{\mathcal{OP}}\right]\Delta Z = -\mathcal{D}(t_0)\Delta\ddot{w} + \mathcal{P}\Delta U \tag{6.12}$$

This equation forms a linear time invariant (LTI) equation in the operating region and could be written as

$$\mathcal{M}_0\Delta\ddot{Z} + \mathcal{C}_0\Delta\dot{Z} + \mathcal{K}_0\Delta Z = -\mathcal{D}_0\Delta\ddot{w} + \mathcal{P}\Delta U \tag{6.13}$$

The linearized equation 6.13 could be represented in the state space form as

$$\begin{aligned} \dot{X} &= \mathcal{A}X + \mathcal{B}\Delta U + \mathcal{D}\Delta\ddot{w} \\ Y &= \mathcal{C}X \end{aligned} \tag{6.14}$$

where,

$$X = \begin{Bmatrix} \Delta Z \\ \Delta\dot{Z} \end{Bmatrix} \quad Y = \begin{Bmatrix} \Delta z_s \\ \Delta z_p \end{Bmatrix}$$

$$\mathcal{A} = \begin{bmatrix} 0 & \mathcal{I}_4 \\ -\frac{\mathcal{K}_o}{\mathcal{M}_o} & -\frac{\mathcal{C}_o}{\mathcal{M}_o} \end{bmatrix} \mathcal{B} = \begin{bmatrix} 0 \\ \frac{\mathcal{P}}{\mathcal{M}_o} \end{bmatrix} \mathcal{D} = \begin{bmatrix} 0 \\ \frac{-\mathcal{D}_o}{\mathcal{M}_o} \end{bmatrix} \mathcal{C} = \begin{bmatrix} \mathcal{I}_2 & 0 \end{bmatrix}$$

The state space form in Eq.6.14 is checked for controllability and observability.

For a 2 DOF bounce model, the controllability matrix of the form

$$\begin{aligned} \phi_c &= \begin{bmatrix} \mathcal{B} & \mathcal{A}\mathcal{B} & \mathcal{A}^2\mathcal{B} & \cdots \end{bmatrix} \\ &= \begin{bmatrix} 0 & \mathcal{M}_0^{-1}\mathcal{P} & \cdots \\ \mathcal{M}_0^{-1}\mathcal{P} & -\mathcal{M}_0^{-1}\mathcal{C}\mathcal{M}_0^{-1}\mathcal{P} & \cdots \end{bmatrix} \end{aligned} \tag{6.15}$$

can be simplified to the form

$$\phi_c = \begin{bmatrix} 0 & \mathcal{M}_0^{-1}\mathcal{P} & \cdots \\ \frac{1}{M_s M_p}\begin{bmatrix} M_s + M_p & -M_s \\ -M_s & M_s \end{bmatrix} & -\mathcal{M}_0^{-1}\mathcal{C}\mathcal{M}_0^{-1}\mathcal{P} & \cdots \end{bmatrix} \tag{6.16}$$

On observing the first column, the rank is at least equal to 2. On simplification the second column cannot be deduced as a linear combination of the first column. Hence the system is controllable.

Similarly the observability matrix can be formed as

$$\begin{aligned}\phi_o &= \begin{bmatrix} C^T & A^T C^T & \cdots \end{bmatrix} \\ &= \begin{bmatrix} \mathcal{I} & \begin{bmatrix} 0 & \mathcal{I} \\ -\mathcal{M}_0^{-1}\mathcal{K}_0 & -\mathcal{M}_0^{-1}\mathcal{C} \end{bmatrix} \begin{Bmatrix} \mathcal{I} \\ 0 \end{Bmatrix} \cdots \end{bmatrix} \\ &= \begin{bmatrix} \mathcal{I} & 0 & \cdots \\ 0 & \mathcal{I} & \cdots \end{bmatrix}\end{aligned} \tag{6.17}$$

The first two columns are linearly independent and hence the rank is at least 2n. Therefore, the state space system is observable. From equations 6.16 and 6.17, for a general linearized model about an operating point, it could be generalized as observable and controllable.

## 6.5 Error Model for Linear Time Invariant Suspension Model

Let us assume that the actual vehicle suspension model is LTI and is perfectly known at the operating point to be of the form in Eq.6.13. Let $(\Delta z_p, \Delta \dot{z}_p, \Delta \ddot{z}_p)$ represent the actual response of the suspension model in this idealized situation. Then Eq.6.13 can be written in the form

$$\mathcal{P}^{-1}\mathcal{M}_0\Delta\ddot{z}_p + \mathcal{P}^{-1}\mathcal{C}_0\Delta\dot{z}_p + \mathcal{P}^{-1}\mathcal{K}_0\Delta z_p + \mathcal{P}^{-1}\mathcal{D}_0\Delta\ddot{w} = \Delta U \tag{6.18}$$

Let the total control input which is divided into feedforward and feedback controller as discussed in section 6.3, could be written as

$$\Delta U = \Delta U_{ff} + \Delta U_{fb} \tag{6.19}$$

Let the output of the reference model about the operating point be denoted by $\left(\Delta Z_m, \Delta \dot{Z}_m, \Delta \ddot{Z}_m\right)$. Since it is assumed that the model parameters are all known the LTI matrices $(\mathcal{M}_0, \mathcal{C}_0, \mathcal{K}_0, \mathcal{D}_0)$ are assumed to be known, the feedforward control law could be written to be of the form

$$\Delta U_{ff} = \mathcal{P}^{-1}\mathcal{M}_0\Delta\ddot{z}_m + \mathcal{P}^{-1}\mathcal{C}_0\Delta\dot{z}_m + \mathcal{P}^{-1}\mathcal{K}_0\Delta z_m + \mathcal{P}^{-1}\mathcal{D}_0\Delta\ddot{w} \tag{6.20}$$

Assuming the feedback control to be function of the model following error in displacement and velocity with the respective gains as

$$\Delta U_{fb} = \mathcal{P}^{-1}K_p e + \mathcal{P}^{-1}K_v\dot{e} \tag{6.21}$$

$$\textit{where,} \quad e = (\Delta Z_m - \Delta Z_p) \textit{ and } \dot{e} = \left(\Delta \dot{Z}_m - \Delta \dot{Z}_p\right)$$

On substituting Eqs.6.19, 6.20 and 6.21 into the Eq.6.18 we obtain

$$\begin{aligned}\mathcal{P}^{-1}\mathcal{M}_0\Delta\ddot{z}_p + \mathcal{P}^{-1}\mathcal{C}_0\Delta\dot{z}_p + \mathcal{P}^{-1}\mathcal{K}_0\Delta z_p + \mathcal{P}^{-1}\mathcal{D}_0\Delta\ddot{w} = \mathcal{P}^{-1}\mathcal{M}_0\Delta\ddot{z}_m + \\ \mathcal{P}^{-1}\mathcal{C}_0\Delta\dot{z}_m + \mathcal{P}^{-1}\mathcal{K}_0\Delta z_m + \mathcal{P}^{-1}\mathcal{D}_0\Delta\ddot{w} + \mathcal{P}^{-1}K_p e + \mathcal{P}^{-1}K_v\dot{e}\end{aligned} \tag{6.22}$$

Post multiplying by matrix $\mathcal{P}$ on either side and simplifying we obtain

$$\mathcal{M}_0\ddot{e} + (\mathcal{C}_0 + K_v)\dot{e} + (\mathcal{K}_0 + K_p)e = 0 \tag{6.23}$$

If the suspension model is LTI, perfectly known and the control input is chosen as in Eq.6.19, 6.20 and 6.21 then $K_p$ and $K_v$ can be chosen such that $e \to 0$ as $t \to \infty$. $K_p$ and $K_v$ can be chosen by pole placement technique to obtain the asymptotic stability. There is no forcing function on the right side of error equation in Eq.6.23. Hence the response of the error would depend on what damping is introduced into Eq.6.23 by the gains $K_p$ and $K_v$. The solution of Eq.6.23 is given as

$$e(t) = \left[\sum_{i=1}^{2n}\lambda_i e^{(\gamma_i t)}\right]e(0) + \left[\sum_{i=1}^{2n}\chi_i e^{(\gamma_i t)}\right]\dot{e}(0) \tag{6.24}$$

where $\lambda_i$ and $\chi_i$ denotes some constant matrices and $\gamma_i$ are roots of the $2n^{th}$ order error characteristic equation. The gains $K_p$ and $K_v$ can be designed by the pole

placement based on the following error equation.

$$\ddot{e} + \cap_2 \dot{e} + \cap_1 e = 0 \tag{6.25}$$

$$where, \quad \cap_1 = diag.[\omega_i{}^2] \; and \; \cap_2 = diag.[2\zeta_i\omega_i]$$

This leads to a decoupled equation of the form

$$\ddot{e} + 2\zeta_i\omega_i\dot{e} + \omega_i{}^2 e = 0$$

## 6.6 Error Model for General Nonlinear Time Varying Suspension Model

The error model equations derived so far for the LTI model about the operating point for the incremental values $\left(\triangle Z_p, \triangle \dot{Z}_p, \triangle \ddot{Z}_p\right)$ are extended to the general NTV model equations. The actual real time quantities could be obtained as

$$\begin{aligned} Z_m(t) &= Z_{m_0}(t_i) + \triangle Z_m(t) \\ Z_p(t) &= Z_{p_0}(t_i) + \triangle Z_p(t) \\ \ddot{w}(t) &= \ddot{w}_0(t_i) + \triangle \ddot{w}(t) \end{aligned} \tag{6.26}$$

where, the values at $t_i$ denote the $i^{th}$ operating point. Let $U_i$ be the force that is necessary for the nominal positions of the suspension, then the total control law is written as

$$U_T(t) = \mathcal{P}^{-1}U_i(t) + \triangle U(t) \tag{6.27}$$

From Eqs.6.19, 6.20 and 6.21 we obtain

$$\begin{aligned} U_T(t) = \mathcal{P}^{-1}U_i(t) + \mathcal{P}^{-1}\mathcal{M}_0\triangle\ddot{Z}_m(t) + \mathcal{P}^{-1}\mathcal{C}_0\triangle\dot{Z}_m(t) + \mathcal{P}^{-1}\mathcal{K}_0\triangle Z_m(t) + \\ \mathcal{P}^{-1}\mathcal{D}_0\triangle\ddot{w}_0(t) + \mathcal{P}^{-1}K_p\left(\triangle Z_m(t) - \triangle Z_p(t)\right) + \\ \mathcal{P}^{-1}K_v\left(\triangle\dot{Z}_m(t) - \triangle\dot{Z}_p(t)\right) \end{aligned} \tag{6.28}$$

But from Eq.6.26 we obtain

$$U_T(t) = \mathcal{P}^{-1}U_i(t) + \mathcal{P}^{-1}\mathcal{M}_0\left(\ddot{Z}_m(t) - \ddot{Z}_{m_0}(t_i)\right) + \mathcal{P}^{-1}\mathcal{C}_0\left(\dot{Z}_m(t) - \dot{Z}_{m_0}(t_i)\right) +$$

$$\mathcal{P}^{-1}\mathcal{K}_0\left(Z_m(t) - Z_{m_0}(t_i)\right) + \mathcal{P}^{-1}\mathcal{D}_0\left(\ddot{Y}_0(t) - \ddot{w}_0(t_i)\right) + \mathcal{P}^{-1}K_p\left(Z_m(t) - Z_{m_0}(t_i) - Z_p(t) + Z_{m_0}(t_i)\right) + \mathcal{P}^{-1}K_v\left(\dot{Z}_m(t) - \dot{Z}_{m_0}(t_i) - \dot{Z}_p(t) + \dot{Z}_{m_0}(t_i)\right) \tag{6.29}$$

Let the global error be represented as $E = Z_m(t) - Z_p(t)$, then

$$U_T(t) = \mathcal{P}^{-1}\left(U_i(t) - \mathcal{M}_0\ddot{Z}_{m_0}(t_i) - \mathcal{C}_0\dot{Z}_{m_0}(t_i) - \mathcal{K}_0 Z_{m_0}(t_i) - \mathcal{D}_0\ddot{w}_0(t_i)\right) + \mathcal{P}^{-1}\left(\mathcal{M}_0\ddot{Z}_m(t) + \mathcal{C}_0\dot{Z}_m(t) + \mathcal{K}_0 Z_m(t) + \mathcal{D}_0\ddot{w}_0(t)\right) + \mathcal{P}^{-1}K_p E + \mathcal{P}^{-1}K_v\dot{E} \tag{6.30}$$

On observing Eq.6.30, the total input can be subgrouped as a function of various terms representing different functionalities. The first term represents the influence of operating point and it can be represented by $U_{ax}(t)$, then

$$U_{ax}(t) = U_i(t) - \mathcal{M}_0\ddot{Z}_{m_0}(t_i) - \mathcal{C}_0\dot{Z}_{m_0}(t_i) - \mathcal{K}_0 Z_{m_0}(t_i) - \mathcal{D}_0\ddot{w}_0(t_i) \tag{6.31}$$

Then from Eq.6.30 we obtain

$$U_T(t) = \mathcal{P}^{-1}U_{ax}(t) + \mathcal{P}^{-1}\mathcal{M}_0\ddot{Z}_m(t) + \mathcal{P}^{-1}\mathcal{C}_0\dot{Z}_m(t) + \mathcal{P}^{-1}\mathcal{K}_0 Z_m(t) + \mathcal{P}^{-1}\mathcal{D}_0\ddot{w}_0(t) + \mathcal{P}^{-1}K_p E + \mathcal{P}^{-1}K_v\dot{E} \tag{6.32}$$

This equation represents the total control input that incorporates the auxiliary signal, feedforward controller depending on both feedforward gains and input gain and feedback controller. Hence the total control input can be derived as

$$U_T(t) = U_{ax}(t) + U_{ff}(t) + U_{fb}(t) \tag{6.33}$$

The general nonlinear suspension model in Eq.6.3 involving the actual output states $\left(Z_p, \dot{Z}_p \text{ and } \ddot{Z}_p\right)$ can be rewritten in a more general form.

$$\mathcal{M}^*(t)|_{n\times n}\ddot{Z}_p + \mathcal{C}^*\left(t, Z, \dot{Z}_p\right)\Big|_{n\times n} + \mathcal{K}^*(t, Z_p)|_{n\times 1} + \mathcal{N}^*(t, Z_p)|_{n\times 1} + \mathcal{L}^*\left(t, \dot{Z}_p\right)\Big|_{n\times 1} = -\mathcal{D}^*(t)|_{n\times 1}\ddot{w} + \mathcal{P}|_{n\times n}U_I \tag{6.34}$$

Where $\mathcal{M}^*, \mathcal{C}^*, \mathcal{K}^*, \mathcal{N}^*, \mathcal{L}^*, \mathcal{D}^*$ denote the nonlinear terms which include the viscous and Coulomb friction components. The total control law in Eq.6.32 is added to the terms $\mathcal{N}_0$ and $\mathcal{L}_0$ of order $(n \times 1)$ containing varying gains to match for the terms $\mathcal{N}^*$ and $\mathcal{L}^*$. This type of arrangement would facilitate to take care of any sort of nonlinearities without any assumptions in gravity, Coulomb and viscous friction terms. The total control law is now written as

$$U_T(t) = \mathcal{P}^{-1}U_{ax}(t) + \mathcal{P}^{-1}\mathcal{M}_0\ddot{Z}_m(t) + \mathcal{P}^{-1}\mathcal{C}_0\dot{Z}_m(t) + \mathcal{P}^{-1}\mathcal{K}_0 Z_m(t) + \mathcal{P}^{-1}\mathcal{N}_0(t) + \mathcal{P}^{-1}\mathcal{L}_0(t) + \mathcal{P}^{-1}\mathcal{D}_0\ddot{w}(t) + \mathcal{P}^{-1}K_pE + \mathcal{P}^{-1}K_v\dot{E} \quad (6.35)$$

Substituting Eq.6.35 into Eq.6.34, we derive a closed loop equation of the form

$$\mathcal{M}^*\ddot{Z}_p + \mathcal{C}^*\dot{Z}_p + \mathcal{K}^*Z_p + \mathcal{N}^* + \mathcal{L}^* = -\mathcal{D}^*\ddot{w} + U_{ax}(t) + \mathcal{M}_0\ddot{Z}_m + \mathcal{C}_0\dot{Z}_m + \mathcal{K}_0Z_m + \mathcal{N}_0 + \mathcal{L}_0 + \mathcal{D}_0\ddot{w} + K_pE + K_v\dot{E} \quad (6.36)$$

Simplifying the above equation in terms of the error, we obtain

$$\mathcal{M}^*\ddot{E} + (\mathcal{C}^* + K_v)\dot{E} + (\mathcal{K}^* + K_p)E = -U_{ax}(t) + (\mathcal{M}^* - \mathcal{M}_0)\ddot{Z}_m + (\mathcal{C}^* - \mathcal{C}_0)\dot{Z}_m + (\mathcal{K}^* - \mathcal{K}_0)Z_m + (\mathcal{N}^* - \mathcal{N}_0) + (\mathcal{L}^* - \mathcal{L}_0) + (\mathcal{D}^* - \mathcal{D}_0)\ddot{w} \quad (6.37)$$

The matrix differences $(\mathcal{M}^* - \mathcal{M}_0), (\mathcal{C}^* - \mathcal{C}_0), (\mathcal{K}^* - \mathcal{K}_0), (\mathcal{N}^* - \mathcal{N}_0), (\mathcal{L}^* - \mathcal{L}_0), (D^* - D_0)$ show the error in the controller gains from the actual matrices. Hence these act as forcing functions of the error equation. Therefore $U_{ax}, \mathcal{M}_0, \mathcal{C}_0, \mathcal{K}_0, \mathcal{N}_0, \mathcal{L}_0$ *and* $\mathcal{D}_0$ should be updated such that the right hand side of Eq.6.37 would be zero so that the error model coincides with that in Eq.6.23. The gains $K_p$ and $K_v$ could be adjusted by pole placement so that error dynamics could be modified to make the error go to zero asymptotically as $t \rightarrow \infty$. Let us define an error vector with position and velocity errors as

$$\vartheta(t) = \begin{Bmatrix} E(t) \\ \dot{E}(t) \end{Bmatrix}_{2n \times 1} \quad (6.38)$$

Using Eq.6.38 we can represent Eq.6.37 in the state space form as

$$\dot{\vartheta} = \begin{bmatrix} 0 & I \\ -\mathcal{M}^{*-1}(\mathcal{K}^* + K_p) & -\mathcal{M}^{*-1}(\mathcal{C}^* + K_v) \end{bmatrix} \left\{ \vartheta \right\} +$$

$$\left\{ \begin{matrix} 0 \\ -\mathcal{M}^{*-1} U_{ax}(\cdot) \end{matrix} \right\} + \left\{ \begin{matrix} 0 \\ \mathcal{M}^{*-1}(\mathcal{M}^* - \mathcal{M}_0)\ddot{Z}_m \end{matrix} \right\} +$$

$$\left\{ \begin{matrix} 0 \\ \mathcal{M}^{*-1}(\mathcal{C}^* - \mathcal{C}_0)\dot{Z}_m \end{matrix} \right\} + \left\{ \begin{matrix} 0 \\ \mathcal{M}^{*-1}(\mathcal{K}^* - \mathcal{K}_0) Z_m \end{matrix} \right\} +$$

$$\left\{ \begin{matrix} 0 \\ \mathcal{M}^{*-1}(\mathcal{N}^* - \mathcal{N}_0) \end{matrix} \right\} + \left\{ \begin{matrix} 0 \\ \mathcal{M}^{*-1}(\mathcal{L}^* - \mathcal{L}_0) \end{matrix} \right\} + \left\{ \begin{matrix} 0 \\ \mathcal{M}^{*-1}(\mathcal{D}^* - \mathcal{D}_0)\ddot{w} \end{matrix} \right\} \tag{6.39}$$

Eq.6.39 forms the adjustable system in the state space form. Tracking error ($E$) can be made to follow a reference error model which would achieve the desired performance. The desired performance of the tracking error can be defined in terms of a decoupled second order homogeneous differential equation. Let the desired error of $i^{th}$ DOF be $E_i(t) = Z_{m_i}(t) - Z_{p_i}(t)$. The desired error vector may be defined in the form

$$\vartheta_m(t) = \left\{ \begin{matrix} E_i(t) \\ \dot{E}_i(t) \end{matrix} \right\}_{2n\times 1} \tag{6.40}$$

The desired error reference model in terms of differential equation as described in Eq.6.25 could be written in state space form as

$$\begin{aligned} \left[\dot{\vartheta}_m(t)\right]_{2n\times 1} &= \begin{bmatrix} 0 & \mathcal{I}_n \\ -\cap_1 & -\cap_2 \end{bmatrix}_{2n\times 2n} [\vartheta_m(t)]_{2n\times 1} \\ &= \cap \vartheta_m(t) \end{aligned} \tag{6.41}$$

Where $\cap_1 = diag.(\omega_i^2)$ and $\cap_2 = diag.(2\zeta_i\omega_i)$ are constant diagonal matrices. From Eq.6.41 if $\cap$ is chosen as a stable matrix, then it should satisfy the Lyapunov equation of the form

$$\mathcal{R}\cap + \cap^T\mathcal{R} = -\mathcal{Q}^+ \quad where, \quad \mathcal{R} = \begin{bmatrix} [\mathcal{R}_1]_{n\times n} & [\mathcal{R}_2]_{n\times n} \\ [\mathcal{R}_2]_{n\times n} & [\mathcal{R}_3]_{n\times n} \end{bmatrix}_{2n\times 2n} \tag{6.42}$$

For any $\mathcal{Q}^+$, a positive definite matrix, there exists a positive definite matrix $\mathcal{R}$ as solution of Eq.6.42 such that $\vartheta_m(t) \to 0$ as $t \to \infty$.

## 6.7 Controller Parameter Adaptation Laws

The controller adaptation laws for the feed forward, feed back and auxiliary parameters as used in the total control law in Eq.6.35 are derived as described in Appendix A. A Lyapunov function in terms of the actual error and reference error model has been used for deriving the control laws. Parameter adaptation laws as derived in Eq.A.24 of Appendix A could be expressed as first order trapezoidal integral equation of the form as

$$
\begin{aligned}
K_p(t) &= K_p(0) + \alpha_1 \int_0^t \ominus(t) E^T(t) dt + \beta_1 \ominus(t) E^T(t) \\
K_v(t) &= K_v(0) + \alpha_2 \int_0^t \ominus(t) \dot{E}^T(t) dt + \beta_2 \ominus(t) \dot{E}^T(t) \\
U_{ax}(t) &= U_{ax}(0) + \alpha_3 \int_0^t \ominus(t) dt + \beta_3 \ominus(t) \\
\mathcal{M}_0(t) &= \mathcal{M}_0(0) + \alpha_4 \int_0^t \ominus(t) \ddot{Z}_m^T dt + \beta_4 \ominus(t) \ddot{Z}_m^T \\
\mathcal{C}_0(t) &= \mathcal{C}_0(0) + \alpha_5 \int_0^t \ominus(t) \dot{Z}_m^T dt + \beta_5 \ominus(t) \dot{Z}_m^T \\
\mathcal{K}_0(t) &= \mathcal{K}_0(0) + \alpha_6 \int_0^t \ominus(t) {Z_m}^T dt + \beta_6 \ominus(t) {Z_m}^T \\
\mathcal{N}_0(t) &= \mathcal{N}_0(0) + \alpha_7 \int_0^t \ominus(t) dt + \beta_7 \ominus(t) \\
\mathcal{L}_0(t) &= \mathcal{L}_{0_\backslash} + \alpha_8 \int_0^t \ominus(t) dt + \beta_8 \ominus(t) \\
\mathcal{D}_0(t) &= \mathcal{D}_0(0) + \alpha_9 \int_0^t \ominus(t) \ddot{w}(t) dt + \beta_9 \ominus(t) \ddot{w}(t)
\end{aligned}
\tag{6.43}
$$

where $\ominus = \mathcal{R}_2 E + \mathcal{R}_3 \dot{E}$. The constants $\alpha_i$ and $\beta_i$ for $i = 1,9$ in the controller laws can be used to specify the steady state and transient behavior of the model following

error.

## 6.8 Simulation Results

The continuous time domain controller for a MDOF generalized suspension which was developed in the previous section was implemented on computer simulation. A two degrees of freedom NTV model as discussed in section 6.2 was used as an example. Fig.6.1 shows the selected 2 DOF bounce suspension model with primary and secondary suspended masses. Fig.6.2 indicates the skyhook reference model that is used for the adaptive model following. The nominal values of the suspension model in Fig.6.1 are taken as $M_s = 85\,Kg, M_p = 4.5\,Kg$, $K_s = 31.5\,\frac{kN}{m}, K_p = 8.7\,\frac{kN}{m}, F = 100N$, $C_s = 100\,\frac{Ns}{m}, C_p = 200\,\frac{Ns^2}{m^2}$ and $K_{cs} = 7\,\frac{KN}{m}$ [141]. The actual model parameters are unknown and are assumed to vary with the operating conditions and the period of operation. The parameters of the reference model are time invariant and could be chosen depending on a particular suspension application as described in earlier sections. The model parameters are chosen as $M_{m_s} = 85\,Kg, M_{m_p} = 4.5\,Kg$, $K_{m_s} = 31.5\,\frac{kN}{m}, K_{m_p} = 8.7\,\frac{kN}{m}$, $D_{m_s} = 800\,\frac{Ns}{m}$ and $D_{m_p} = 2000\,\frac{Ns}{m}$. As discussed earlier, Figs.6.3, 6.4, 6.5 and 6.6 indicate the required performance of the reference model in terms of the absolute and relative displacement for the primary and secondary suspension.

The tuning of adaptation gains $\alpha_i$ and $\beta_i$ for $i = 1,9$ in Eq.6.67 has to be performed to attain the required performance. The time varying parameter $\phi(t)$ is evaluated on the basis of global tracking error ($E$) and its derivative ($\dot{E}$). The matrices $\mathcal{R}_2$ and $\mathcal{R}_3$ are solved by the Lyapunov equation in Eq.6.42 for a positive definite matrix $\mathcal{Q}^+$. The values of $\omega_i$ and $\zeta_i$ for $i = 1,2$ are chosen to achieve the required reference model tracking performance.

To check the adaptation capabilities in terms of the adaptation laws and to

bustness of the controller to achieve the reference model performance, the suspension parameters are subjected to *Parametric variation mode I* and *Parametric variation mode II*. As discussed earlier, these two modes are used for simulating the realistic combination of various parameter variations. A priori knowledge of the dynamic parameter variations of the model are used for simulating the model response and to test the capability of the controller to adapt to the reference model irrespective of changes in the operating conditions.

Time domain results for *Excitation mode I* in which the models are excited by a combination of sine functions are presented in the following figures. Fig.6.8 shows the secondary suspension mass absolute displacement response for the reference model, the adaptive active suspension and passive suspension models. The reference model indicates that the response characteristics achieve better isolation at natural frequency and at higher frequencies. On evaluating the controller gains using the adaptation laws, the adaptive controlled suspension model adapts to the reference model. The controller gains are used to calculate the controller input to the model so that the NTV model deviates from the passive response and adapts to the reference model response. As shown in Fig.6.8 the adaptation is very quick owing to the larger number of controller gains adapted and the model itself being a second order system. The performance indicates that the controller could be effectively used for a more general and complicated models involving larger number of DOF's. Fig.6.9 shows the comparative responses of primary suspension mass absolute displacement for various models. Fig.6.10 shows the velocity response of the secondary suspension for various reference, adaptive active and passive suspension models. As the time of adaptation increases, the adaptive controlled system follows the reference model more closely. The oscillatory responses of the active suspension are damped out and the system adapts to the reference model. Hence the error in the reference model following changes from an initial oscillatory ur damped type to critically or overdamped system. Fig.6.11 shows the secondary suspension relative displacement response and adaptation of the active suspension to the reference model. Based on

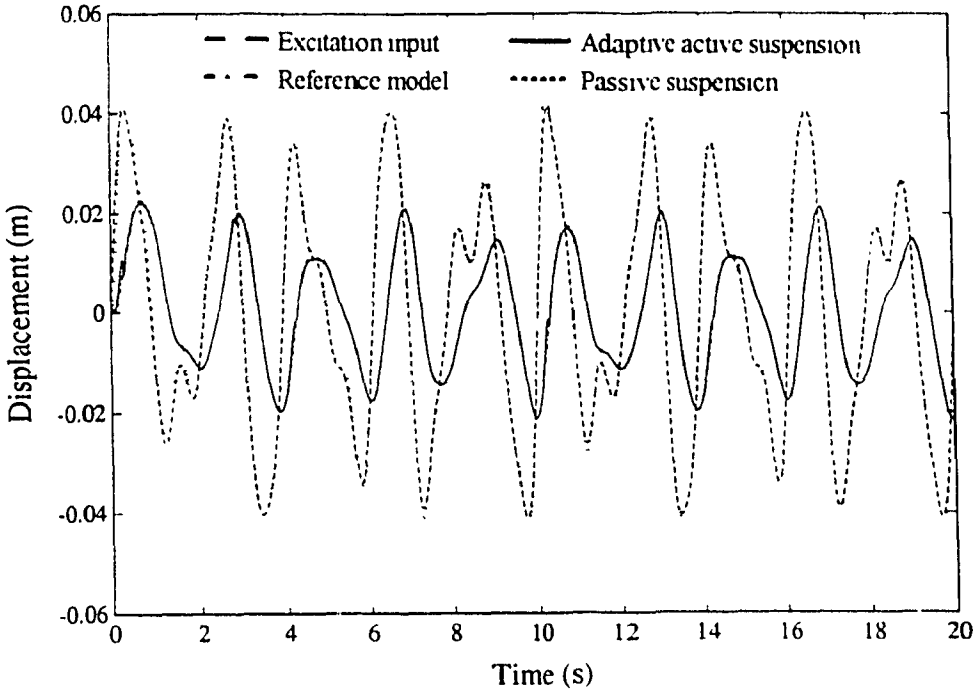


Fig.6.8: Secondary suspension mass absolute displacement response.

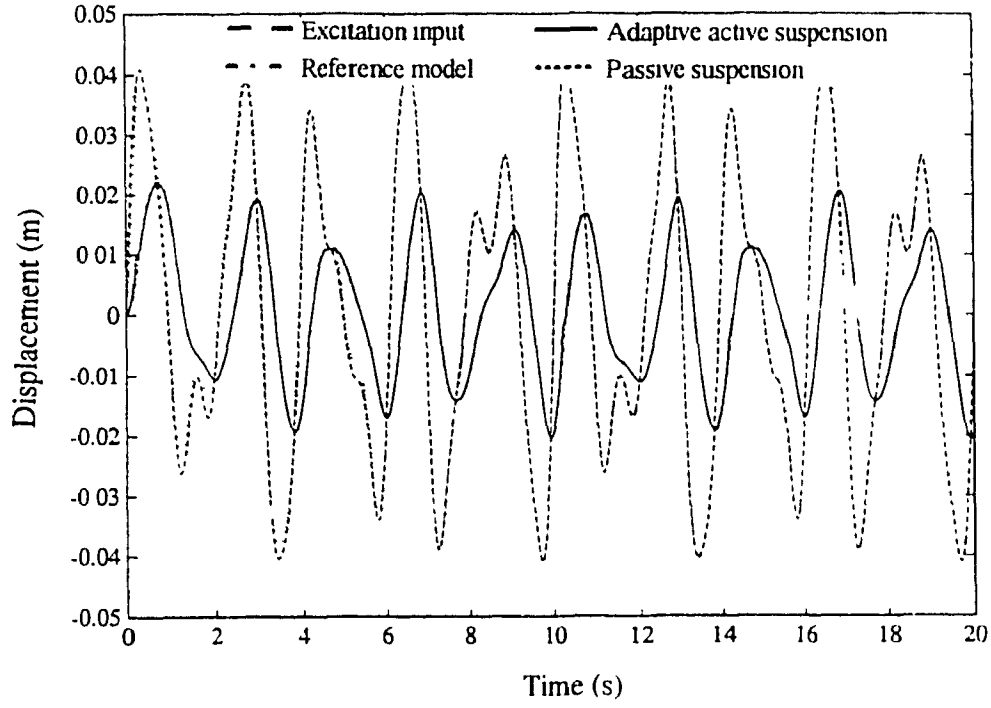


Fig.6.9: Primary suspension mass absolute displacement response.

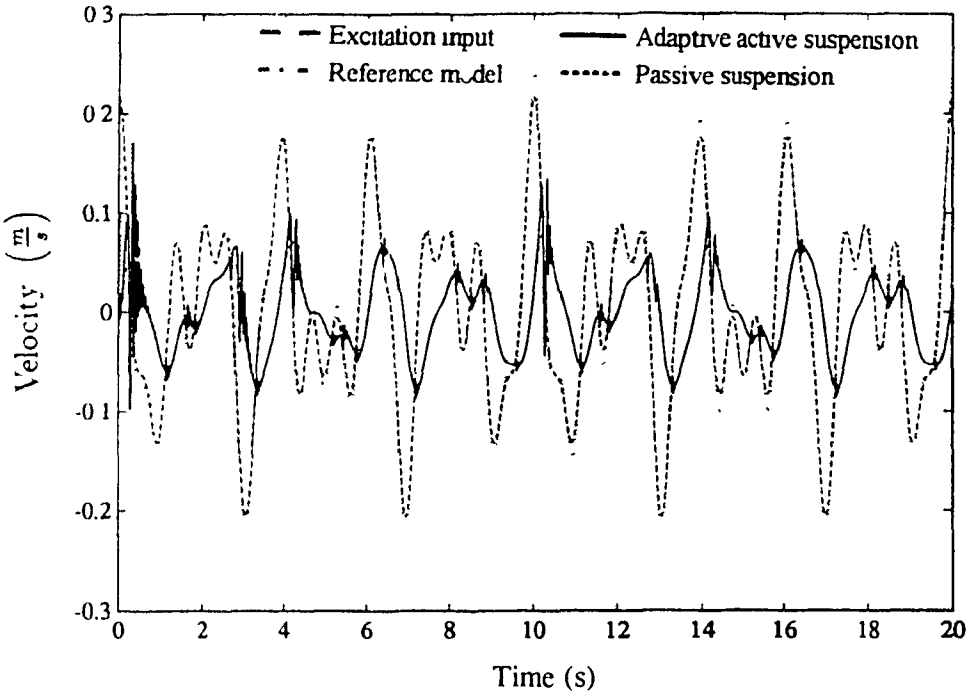


Fig.6.10: Secondary suspension mass absolute velocity response.

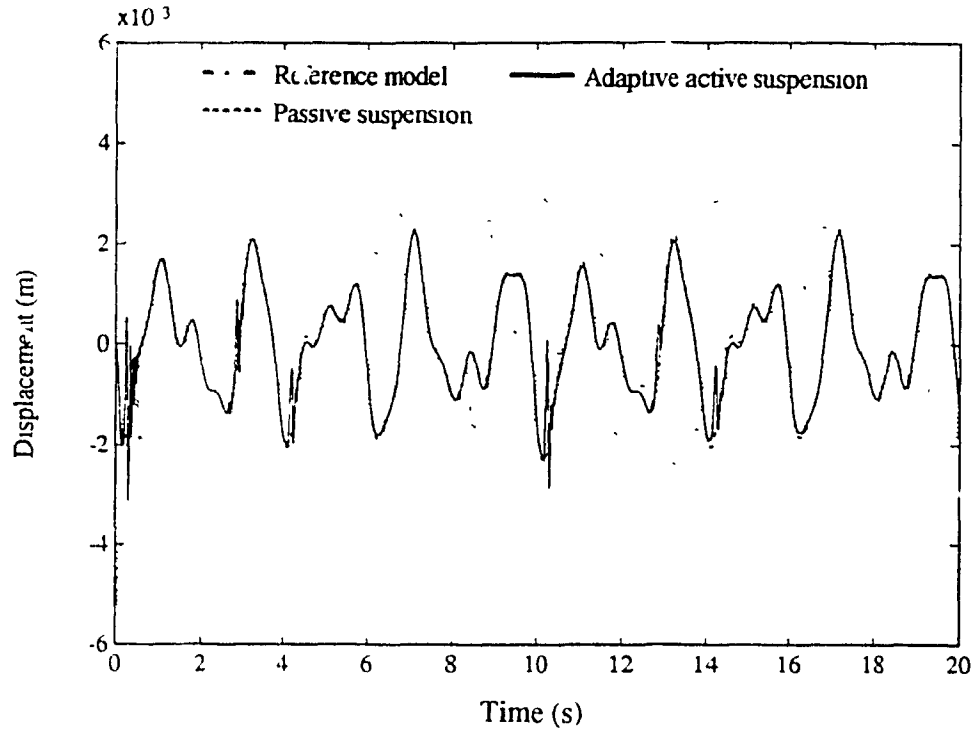


Fig.6.11: Secondary suspension relative displacement response.

the control law and by adapting the gains, the actuator forces needed in the primary and secondary suspension are calculated as shown in Fig.6.12. The results indicate a higher primary actuator force which contributes mainly to the isolation from the input and the high frequency low amplitude secondary actuator forces would adapt the active suspension model to the reference model response.

Time domain results for a deterministic Half-sine (bump) input with time dependent *Parametric variations mode I* are presented in Fig.6.13 The model displacement response is the skyhook reference model secondary mass ($M_s$) response for the bump input. This behaves as a forced motion with lower magnitude and damped nature. The controller adapts the gains which would make the active suspension model to follow the reference model by applying the control inputs to the primary and secondary masses as indicated in Fig.6.14. The secondary force $u_s(t)$ needed in the secondary suspension is low in magnitude but has higher frequency components. The primary force $u_p(t)$ is larger in magnitude but less oscillatory in nature. The overall actuator forces needed for adaptation to the reference model are found to be less for the size of the suspended masses. The sharing of the loads between the two actuators would enhance the accuracy of adaptation and also reduce the capacity of hardware necessary for practical implementation.

The frequency domain study has been conducted by exciting the base of the general model by a random input. The results from the time domain are converted to the frequency domain by using the fast Fourier transformations. The adaptive active suspension model was found to closely follow the reference model at most of the frequency ranges as shown in the following figures. Figures 6.15 and 6.16 show the system gain factor of the primary and secondary suspension mass absolute acceleration with respect to the excitation input acceleration. Figures 6.17 and 6.18 represent the system gain factors of the primary and secondary relative displacement with respect to the excitation input. These figures indicate that the adaptive active suspension system closely follows the reference model and exhibits good isolation at

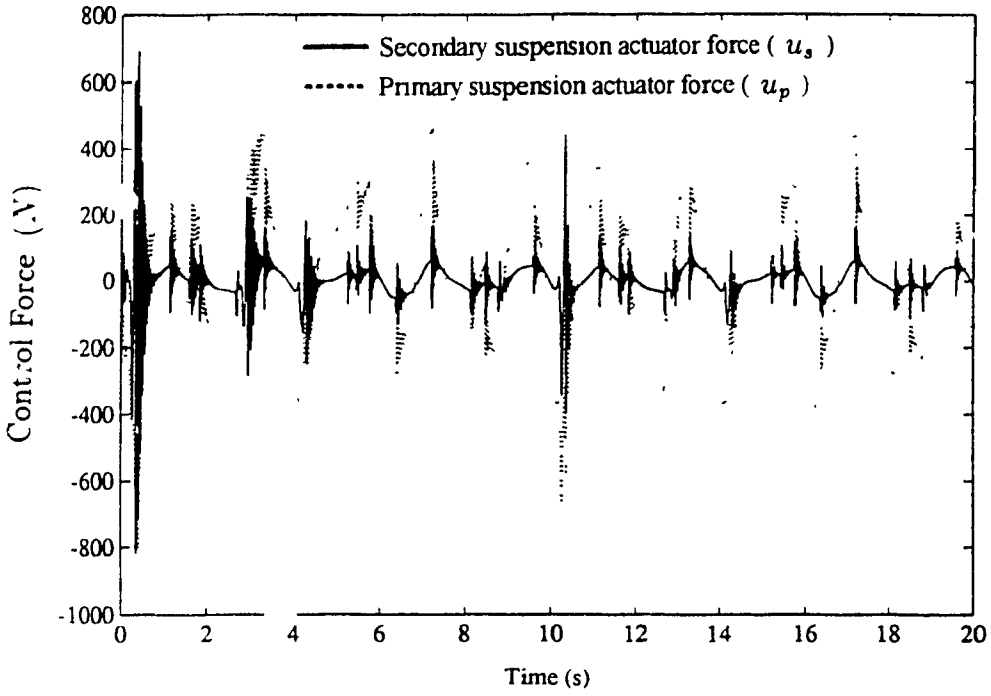


Fig.6.12: Secondary and primary suspension actuator control force variations.

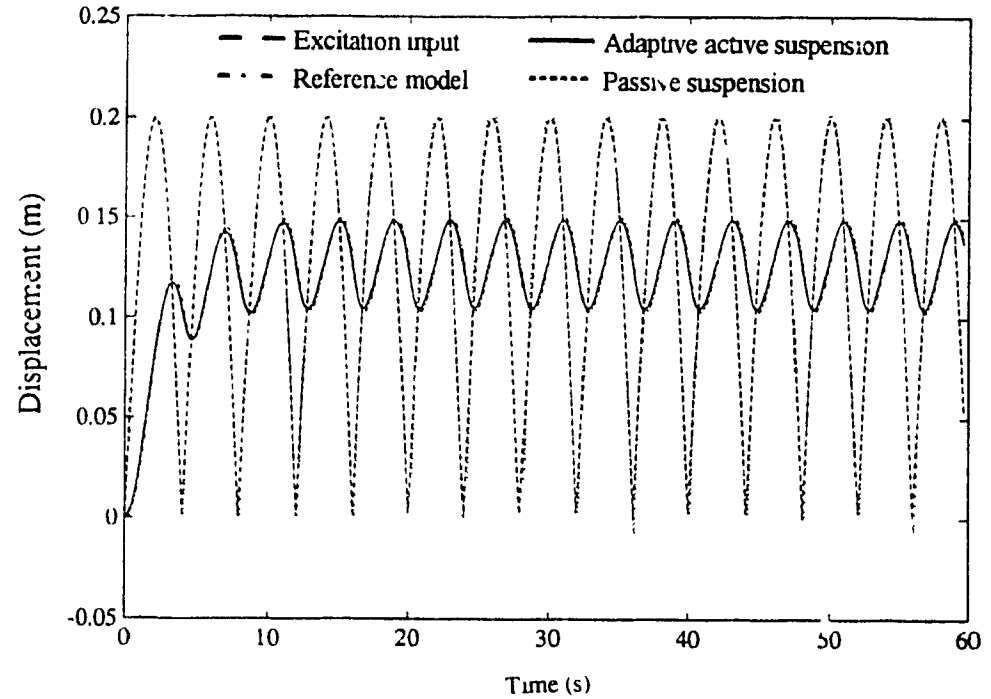


Fig.6.13: Secondary suspension mass absolute displacement response for half-sine (Bump) input.

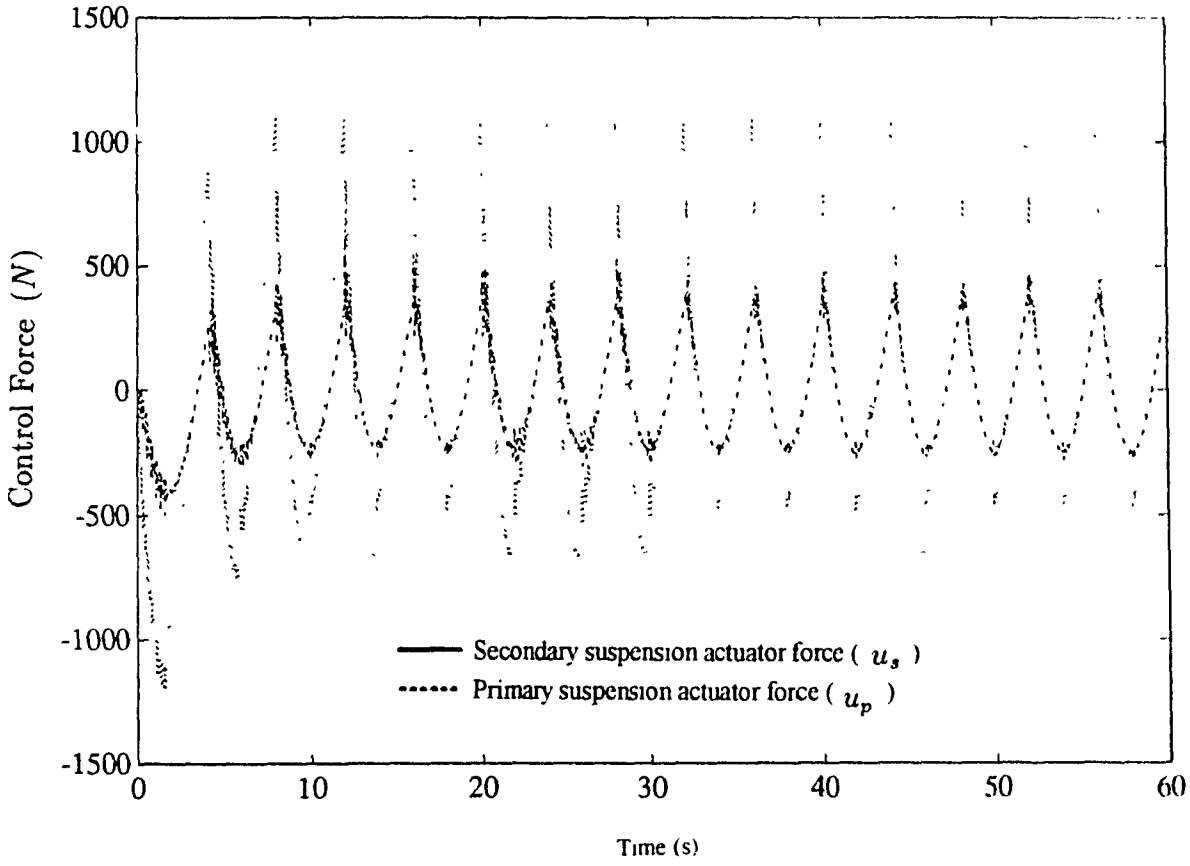


Fig.6.14: Secondary and primary suspension actuator control forces for bump input.

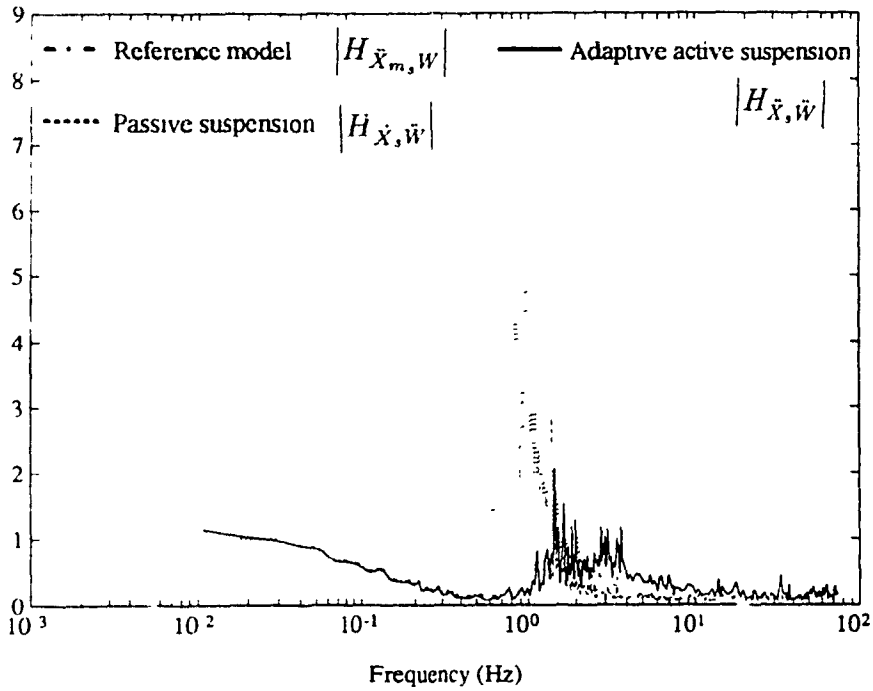


Fig.6.15: System gain factor of secondary suspension mass absolute acceleration with respect to excitation input acceleration.

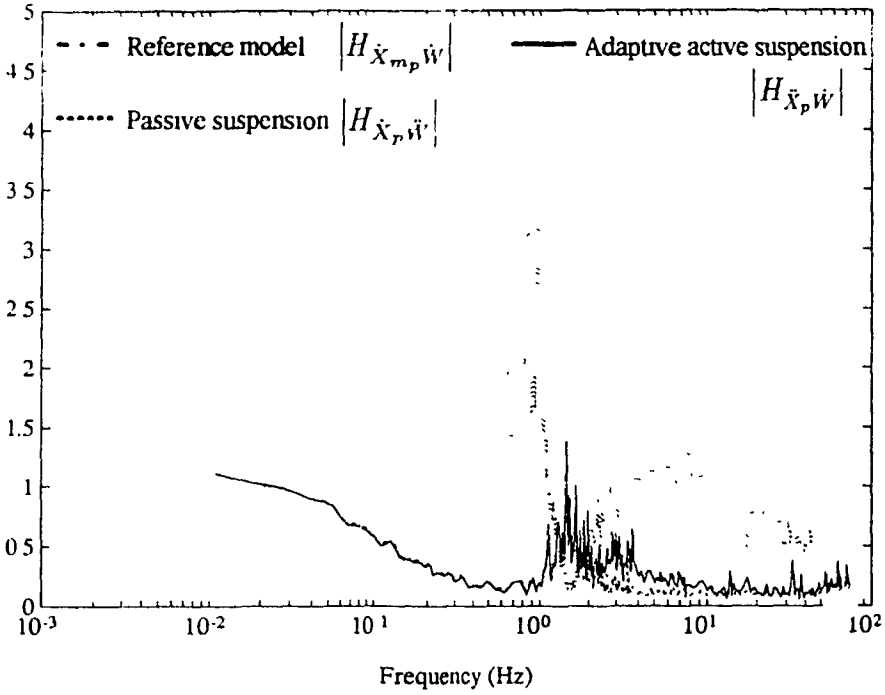


Fig.6.16: System gain factor of primary suspension mass absolute acceleration with respect to excitation input acceleration.

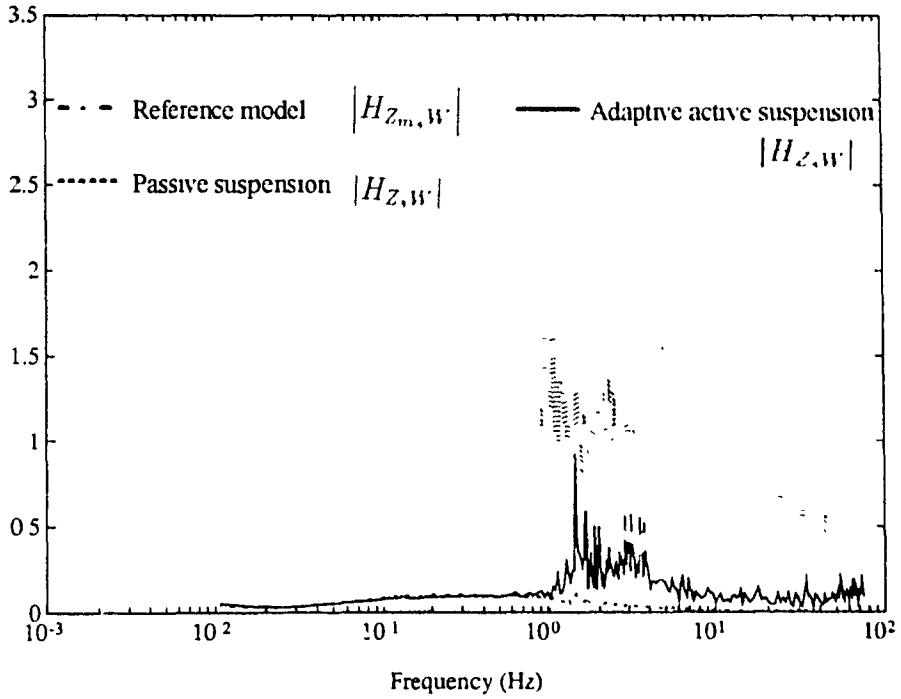


Fig.6.17: System gain factor of secondary suspension relative displacement with respect to excitation input displacement.

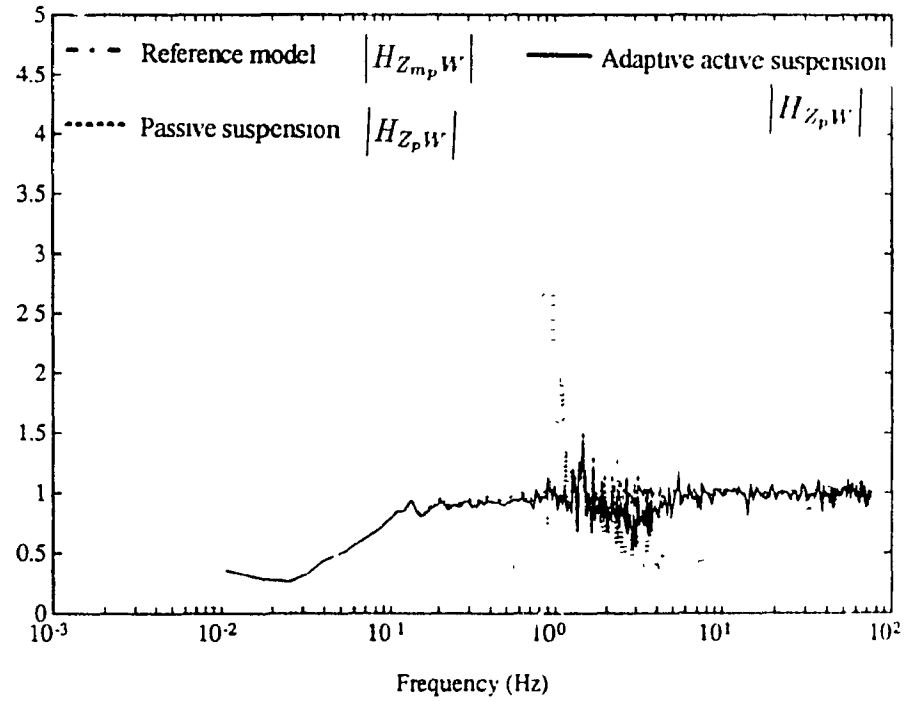


Fig.6.18: System gain factor of primary suspension relative displacement with respect to excitation input displacement.

most of the frequency ranges for both primary and secondary suspension masses. The adaptive controlled responses are compared with the transfer functions derived and implemented using DHLEM as shown in Figs.6.3, 6.4, 6.5 and 6.6. Both sets of plots indicate the closeness of the trend of results and the benefits of using the adaptive controller in terms of reducing the absolute and relative displacements for primary and secondary suspensions at the expense of the actuator forces. The reference model chosen would isolate the secondary mass as a highly damped system but at the same time would behave as a passive system at higher frequencies. The responses also show large isolation properties of the entire system compared to a passive suspension system. The relative displacement responses in figures 6.17 and 6.18 indicate the responses as predicted in Figs. 6.5 and 6.6. These responses also show a significant reduction in the relative displacement at natural frequencies of the adaptive controlled suspension system.

The above figures indicate that the concept of adaptive active suspension would facilitate the achievement of an optimal performance which would reduce the absolute displacement and relative displacement mainly at natural frequencies and also over a wider range of frequencies. The active suspension behaves as a soft primary suspension and a hard secondary suspension simultaneously. The above described acceleration and relative displacement results indicate that an adaptive active suspension can achieve reduced acceleration and relative displacements simultaneously. Comparison of adaptive active suspension results in time domain indicate that the reference model response can be achieved irrespective of parametric variations.

## 6.9 Discussion

The results presented in the previous section for a MDOF NTV general suspension with various nonlinearities indicate how effectively the large dynamic variations and uncertainties in the suspension model parameters could be taken care of and at the

same time achieve an optimal performance at all operating conditions.

The controller adaptation laws are first order definite integrals and the gains could be evaluated at a faster rate by simple trapezoidal integration. Since the computational time of these equations is very short, the controller can be implemented on line without much time delay in the signals to the actuators, hence it could be conveniently implemented for many DOF's. The practical limitations such as actuator saturation can be taken care of by the controller.

The presence of feed forward controller and an auxiliary signal that depend on the input acceleration and operating conditions would improve the tracking performance of the controller. Since the control input feedforward signal is proportional to the excitation input acceleration, the performance of the overall controller is enhanced. The tuning of the controller can be very effectively performed due to the presence of many adaptation gains. These gains could be adjusted to attain fast and better tracking of the reference model and also to make the system robust to hardware limitations.

Stable asymptotic tracking is guaranteed as the adaptation laws are derived from the derivative of Lyapunov function which involves reference model tracking and controller parameter errors. The convergence of the adaptive scheme is independent of the initial values in the adaptation laws in Eq.6.43. Hence they need not be preset to any values but need to be tuned based on the application of the controller.

A decentralized adaptive controller can be derived from this study which would independently control each DOF for a MDOF system as discussed by Malek and Hedrick [40]. The decentralized approach could be very effectively applied by assigning a different micro-processor for each DOF which makes the whole system computationally fast.

## 6.10 Summary

This chapter studied the extension of the concept of adaptive active suspension for a general suspension model. The generalized model is developed to include most of the nonlinearities encountered in the suspension studies. A 2 degree of freedom (DOF) bounce model has been derived as a subcase and a double skyhook reference model has been developed.

Frequency domain transfer functions for the 2 DOF bounce model including non-linear time varying terms using discrete harmonic linearization technique have been evaluated. A comparison with the reference model for various damping values has been made to choose the proper reference model required for the adaptive control. An adaptive control approach including feed forward, feedback and auxiliary input approach has been extended for the generalized suspension model. The controller parameters which are evaluated based on first order trapezoidal integration and termed as adaptation laws are used for control input evaluation. The controller does not need any a priori knowledge of the suspension parameters, hence it could be implemented to any model.

This concept has been implemented for a two DOF bounce model and the results are presented in terms of time and frequency domain. The time domain results indicate good adaptation to the reference model. The results of the adaptive controlled system presented in the frequency domain indicate the characteristics as evaluated by the transfer functions. An optimal performance with good isolation and reduction in relative displacements have been obtained even under large variations of the model parameters. The generalized model could be used for any sort of suspension configurations with feasibility for a large number of DOF's. Various models such as, multi-DOF automotive suspension, bounce DOF rail vehicle suspension, seat suspension model for off road vehicles etc. could be conveniently realized by the generalized model.

# Chapter 7

# Discrete Time Adaptive Active Suspension For Multi-Degree of Freedom Half-car Model

## 7.1 General

The discrete adaptive control concepts developed in chapter 4 for a single degree of freedom (SDOF) model are extended for a multi-degree of freedom (MDOF) half-car model. In this chapter a half-car model incorporating the pitch and heave of the carbody and bounce degree of freedom (DOF) of the front and rear unsprung masses is developed. As explained in chapter 2, a half-car model incorporating the pitch DOF would strengthen the idea of adaptation during the longitudinal manoeuvres and would reduce the effect of squat and nose dive of the vehicle. Most studies dealing with active suspensions utilize a heave only or 2 degrees of freedom models which are very useful for understanding the concepts and designing the control strategies. If such simple models are used individually for heave, pitch, roll and warp DOF's while designing for a complete vehicle, it would not reflect the coupling between the modes. But coupling is an important tool while tuning the ride characteristics of the vehicle in the case of heave and pitch and the handling characteristics in the case of roll and

warp. Another major shortcoming of simple SDOF models is their inability to reflect the effect of the control strategy on the tire normal load distribution between the four corners. This is one of the factors which determine the handling characteristics such as understeer and oversteer capabilities of the vehicle. A seven DOF vehicle model incorporating heave, roll and pitch of the sprung mass and four independent unsprung mass bounce DOF's was analyzed for the coupling and decoupling effect on a full car active suspension system by Malek and Hedrick [10]. It was concluded that decoupling the heave and pitch body modes improves both body isolation and reduces fore-aft tire load transfers. An optimal control of active suspension for a MDOF track/vehicle system has been designed by Yoshimura et al. [13]. Here a secondary active suspension for a four DOF model incorporating track uneveness as input has been designed.

In the design presented in this chapter, the road excitation to the rear wheels is considered as a time delayed front wheel input. This concept has been used in the past by various researchers in which preview sensors are used for the actual active suspension implementation. The more obvious form involves using a road height sensor which looks ahead of the front wheels, which was studied theoretically in conjunction with a SDOF by Bender [162]. The less obvious form involves recognizing that the inputs to the rear wheels can be realistically considered to be time delayed replicas of the front. The second approach which has more practicality has been investigated by various authors such as Thompson and Pearce [163], Frühauf et al. in [65] and Louam et al. [66] with different control approaches. Sasaki et al. considered the vehicle body to have pitch and bounce degrees of freedom but supported on a passive front suspension and ideal force producing active rear suspension involving a front preview sensor. The optimal controller properties were found to be dependent on the correlation of the front and rear input and the vehicle speed. Thompson and Pearce came out with contradictory results indicating the independence of the optimal control on the correlation of the front and rear inputs. Frühauf et al. included both forms of preview and derived control laws for a full vehicle system involving

pade approximations for the time delays between front and rear inputs. Louam et al. discussed an optimal control law for a half-car system using a discrete linear quadratic regulator frame work involving the time delay between the front and rear wheel inputs which could not be dealt using continuous linear quadratic regulator (LQR) theory. A suboptimal control does not incorporate front wheel road information and hence neglecting the time delay in the disturbances was compared with an optimal control

A reference model incorporating two levels of skyhook damping has been designed and analyzed. The reference model performance was found to achieve an optimal performance in terms of sprung mass isolation and suspension travel. The continuous time domain nonlinear time varying (NTV) equations for the reference model have been written. The NTV equations are linearized about the operating point by first expressing discontinuous terms as analytic functions using the Fourier transforms. Then a linear time invariant (LTI) model in the continuous time domain about the operating point is formed. The continuous time piecewise LTI model is transformed to a discrete auto regressive moving average (DARMA) model. Discrete model reference adaptive control (DMRAC) is used for the formation of adaptation laws in terms of the error in model following. A modified version of Least Squares Estimation (LSE) in which the controller parameters are updated as a matrix rather than as a vector [146] has been derived. The convergence properties of LSE and global convergence properties of the complete system with the parameters being updated as a matrix have been proved. Finally the system response for *Parameter variations mode I* under the *Excitation modes I and II* has been presented in the simulation results.

## 7.2 Dynamic System Model

Figure 2.9 in chapter 2 shows a passively suspended in-plane half-car model, typically called as bicycle model. As explained in section 2.4 the model incorporates various

NTV properties such as Coulomb friction, stiffness, velocity squared viscous damping and elastic limit stops. The equations involving sprung mass bounce ($x_s$), in plane pitch ($\theta$) at the C.G. of the carbody, leading and trailing unsprung mass bounce degrees of freedom ($x_{t_1}$ and $x_{t_2}$) are derived as follows. The NTV discontinuous equations of motion taking into consideration of the static deflection due to inertial loads can be written as

$$
\begin{aligned}
M_s(t)\ddot{x}_s &= u_l + u_t - F_{c_l} - F_{c_t} - F_{k_l} - F_{k_t} - F_{d_l} - F_{d_t} - F_{s_l} - F_{s_t} + K_l(t)\delta_{st_l} + \\
&\quad K_l(t)\delta_{st_l} - M_s(t)\tfrac{d_1}{L}g - M_s(t)\tfrac{f_r}{l}q + M_s(t)\tfrac{h}{l}a \qquad M_s(t)\tfrac{h}{l}a \\
I_{MI}(t)\ddot{\theta} &= F_{c_t}d_2 + F_{k_t}d_2 + F_{d_t}d_2 + F_{s_t}d_1 + M_s(t)\tfrac{ih}{L}d_2 - K_t(t)\delta_{st_t}d_2 \qquad u_t d_2 \\
&\quad F_{c_l}d_1 - F_{k_l}d_1 - F_{d_l}d_1 - F_{s_l}d_1 + M_s(t)\tfrac{ih}{l}d_1 + K_l(t)\delta_{st_l}d_1 + u_l d_1 \\
M_{u_l}(t)\ddot{x}_{t_1} &= F_{c_l} + F_{k_l} - u_l + F_{d_l} + F_{s_l} - K_l(t)\delta_{st_l} - K_{tire}(t)(x_{t_1} - w(t)) + K_{tire}(t)\delta_{t_l} \\
M_{u_t}(t)\ddot{x}_{t_1} &= F_{c_t} + F_{k_t} - u_t + F_{d_t} + F_{s_t} - K_t(t)\delta_{st_t} - K_{tire}(t)(x_{t_1} - w(t-\tau)) + K_{tire}(t)\delta_{t_t}
\end{aligned}
$$

*where,*

$$
\begin{aligned}
F_{c_t} &= F_t(t)sgn(\dot{x}_{t_2} - \dot{x}_{t_1}) \qquad & F_{k_t} &= K_t(t)(x_{t_2} - x_{t_1}) \\
F_{d_t} &= C_t(t)|\dot{x}_{t_2} - \dot{x}_{t_1}|(\dot{x}_{t_2} - \dot{x}_{t_1}) \qquad & F_{s_t} &= K_{es_t}(t)S^*\left[x_{t_2} - x_{t_1} - \tfrac{D}{2}sgn(x_{t_2} - x_{t_1})\right] \\
S^* &= \begin{cases} 0 & if\ |x_{t_2} - x_{t_1}| \le \frac{D}{2} \\ 1 & otherwise \end{cases} \qquad & & t\ varies\ as\ l\ and\ t
\end{aligned}
\tag{7.1}
$$

The terms $M_s(t)$, $I_{MI}(t)$, $M_{u_l}(t)$ and $M_{u_t}(t)$ represent the carbody sprung mass, polar moment of inertia about the pitch axis through c.g. and unsprung masses at the leading and trailing ends. The forcing components $F_{c_l}$, $F_{c_t}$, $F_{k_l}$, $F_{k_t}$, $F_{d_l}$, $F_{d_t}$, $F_{s_l}$ *and* $F_{s_t}$ represent the Coulomb friction, stiffness, velocity squared viscous damping and elastic limit stop forces that are nonlinear and contain coefficients $F_l$, $F_t$, $K_l$, $K_t$, $C_l$, $C_t$, $K_{es_l}$ and $K_{es_t}$ whose actual values are not known and could be varying with time of operation. '$D$' denotes the maximum displacement limit imposed on the suspension travel by the elastic stops. Above equations could be simplified and represented in

matrix form in terms of $x_b, \theta, x_{l_1}$ and $x_{t_1}$ degrees of freedom by using the following transformation equations

$$x_{l_2} = x_b + d_1\theta$$
$$x_{t_2} = x_b - d_2\theta \tag{7.2}$$

The dynamic equations could be written as a NTV second order differential equations in the matrix form as

$$\mathcal{M}(t)\dot{Z} + \mathcal{F}(Z, \dot{Z}, t) = \mathcal{G}U(t) + \mathcal{H}(t)W(t) + \mathcal{S}(t) \tag{7.3}$$

*where*,

$$Z = \begin{Bmatrix} x_b \\ \theta \\ x_{l_1} \\ x_{t_1} \end{Bmatrix} \qquad \mathcal{M}(t) = \begin{bmatrix} M_s(t) & 0 & 0 & 0 \\ 0 & I_{MI}(t) & 0 & 0 \\ 0 & 0 & M_{u_l}(t) & 0 \\ 0 & 0 & 0 & M_{u_t}(t) \end{bmatrix}$$

$$\mathcal{G} = \begin{bmatrix} 1 & 1 \\ d_1 & -d_2 \\ -1 & 0 \\ 0 & -1 \end{bmatrix} \quad \mathcal{H}(t) = \begin{bmatrix} 0 & 0 \\ 0 & 0 \\ K_{tire}(t) & 0 \\ 0 & K_{tire}(t) \end{bmatrix}$$

The forcing term in Eq.7.3 is resolved into two types of inputs, namely the control input induced onto the suspension and the disturbance input due to the road excitation. The NTV term $\mathcal{F}(Z, \dot{Z}, t)$ represents the cumulative force exerted due to elastic limit stops, velocity squared viscous damping, Coulomb friction damping and suspension spring force. The combined force can be represented as follows

$$\mathcal{F}(Z, \dot{Z}, t) = F_s(z, t) + F_d(\dot{Z}, t) + F_c(\dot{Z}, t) + F_h(Z, t) \tag{7.4}$$

where,

$$F_c(Z,t) = \begin{Bmatrix} K_{es_l}(t)S_l^*\left[x_b + d_1\theta - x_{l_1} - \frac{D}{2}sgn\left[x_b + d_1\theta - x_{l_1}\right]\right] + K_{es_t}(t) \\ \qquad S_t^*\left[x_b - d_2\theta - x_{t_1} - \frac{D}{2}sgn\left[x_b - d_2\theta - x_{t_1}\right]\right] \\ K_{es_l}(t)S_l^*\left[x_b + d_1\theta - x_{l_1} - \frac{D}{2}sgn\left[x_b + d_1\theta - x_{l_1}\right]\right]d_1 - K_{es_t}(t) \\ \qquad S_t^*\left[x_b - d_2\theta - x_{t_1} - \frac{D}{2}sgn\left[x_b - d_2\theta - x_{t_1}\right]\right]d_2 \\ -K_{es_l}(t)S_l^*\left[x_b + d_1\theta - x_{l_1} - \frac{D}{2}sgn\left[x_b + d_1\theta - x_{l_1}\right]\right] \\ -K_{es_t}(t)S_t^*\left[x_b - d_2\theta - x_{t_1} - \frac{D}{2}sgn\left[x_b - d_2\theta - x_{t_1}\right]\right] \end{Bmatrix}$$

where,

$$S_1^* = \begin{cases} 0 & if\ |x_b + d_1\theta \quad x_{t_1} \cdot \quad \frac{l}{2} \\ 1 & otherwise \end{cases}$$

$$S_2^* = \begin{cases} 0 & if\ |x_b - d_2\theta \quad x_{t_1} \cdot \quad \frac{l}{2} \\ 1 & otherwise \end{cases}$$

$$sgn\left(x_b + d_1\theta - x_{t_1}\right) = \begin{cases} -1 & if\ (x_b + d_1\theta - x_{t_1}) < 0 \\ 1 & otherwise \end{cases}$$

$$sgn\left(x_b - d_2\theta - x_{t_1}\right) = \begin{cases} -1 & if\ (x_b - d_2\theta - x_{t_1}) < 0 \\ 1 & otherwise \end{cases}$$

$$F_d\left(\dot{Z}, t\right) = \left\{ \begin{array}{l} C_t(t)\left|\dot{x}_b + d_1\dot{\theta} - \dot{x}_{t_1}\right|\left(x_b + d_1\theta - x_{t_1}\right) + \\ \quad C_t(t)\left|x_b - d_2\dot{\theta} - x_{t_1}\right|\left(\dot{x}_b - d_2\theta - \dot{x}_{t_1}\right) \\ \\ C_t(t)\left|\dot{x}_b + d_1\dot{\theta} - x_{t_1}\right|\left(x_b + d_1\theta - \dot{x}_{t_1}\right) d_1 \\ \quad C_t(t)\left|\dot{x}_b - d_2\dot{\theta} - \dot{x}_{t_1}\right|\left(\dot{x}_b - d_2\dot{\theta} - x_{t_1}\right) d_2 \\ \\ -C_t(t)\left|x_b + d_1\dot{\theta} - \dot{x}_{t_1}\right|\left(\dot{x}_b + d_1\theta - x_{t_1}\right) \\ \\ -C_t(t)\left|\dot{x}_b - d_2\theta - x_{t_1}\right|\left(\dot{x}_b - d_2\dot{\theta} - x_{t_1}\right) \end{array} \right\}$$

$$F_c\left(\dot{Z}, t\right) = \left\{ \begin{array}{l} F_l(t)sgn\left(\dot{x}_b + d_1\dot{\theta} - \dot{x}_{t_1}\right) + F_t(t)sgn\left(\dot{x}_b - d_2\dot{\theta} - \dot{x}_{t_1}\right) \\ \\ F_l(t)sgn\left(\dot{x}_b + d_1\dot{\theta} - \dot{x}_{t_1}\right) d_1 - F_t(t)sgn\left(\dot{x}_b - d_2\theta \quad \dot{x}_{t_1}\right) d_2 \\ \\ -F_l(t)sgn\left(\dot{x}_b + d_1\dot{\theta} - \dot{x}_{t_1}\right) \\ \\ -F_t(t)sgn\left(\dot{x}_b - d_2\dot{\theta} - \dot{x}_{t_1}\right) \end{array} \right\}$$

$$sgn\left(\dot{x}_b + d_1\dot{\theta} - \dot{x}_{t_1}\right) = \begin{cases} -1 & if\ \left(\dot{x}_b + d_1\dot{\theta} - x_{t_1}\right) < 0 \\ 1 & otherwise \end{cases}$$

$$sgn\left(\dot{x}_b - d_2\dot{\theta} - \dot{x}_{t_1}\right) = \begin{cases} -1 & if\ \left(\dot{x}_b - d_2\dot{\theta} - \dot{x}_{t_1}\right) < 0 \\ 1 & otherwise \end{cases}$$

$$F_k(Z,t) = \begin{Bmatrix} K_l(t)(x_s + d_1\theta - x_{t_1}) + K_t(t)(x_s - d_2\theta - x_{t_2}) \\ K_l(t)(x_s + d_1\theta - x_{t_1})d_1 - K_t(t)(x_s - d_2\theta - x_{t_2})d_2 \\ -K_l(t)(x_s - d_1\theta - x_{t_1}) + K_{tire}(t)x_{t_1} \\ -K_t(t)(x_s - d_2\theta - x_{t_2}) + K_{tire}(t)x_{t_2} \end{Bmatrix}$$

The terms $F_s(Z,t)$, $F_d(\dot{Z},t)$, $F_c(\dot{Z},t)$ and $F_k(Z,t)$ represent the nonlinearities due to elastic stops, velocity squared viscous damping, Coulomb friction and suspension stiffness forces. The active control input and disturbance vectors denoted as $U(t)$ and $W(t)$ respectively are represented as

$$U(t) = \begin{Bmatrix} u_l(t) \\ u_t(t) \end{Bmatrix} \quad W(t) = \begin{Bmatrix} w(t) \\ w(t-\tau) \end{Bmatrix} \tag{7.5}$$

The term $\mathcal{S}(t)$ as shown below indicates the variations with respect to the static equilibrium position

$$\mathcal{S}(t) = \begin{Bmatrix} K_t(t)\delta_{st_t} + K_l(t)\delta_{st_l} - M_s(t)g \\ K_l(t)\delta_{st_l}d_1 - K_t(t)\delta_{st_t}d_2 + M_s(t)ah \\ K_{tire}(t)\delta_{t_l} - K_l(t)\delta_{st_l} \\ K_{tire}(t)\delta_{t_t} - K_t(t)\delta_{st_t} \end{Bmatrix} \tag{7.6}$$

But for the nominal values of the vehicle parameters, when the vehicle travels at a constant or zero velocity the static equilibrium is maintained. Therefore, if $K_t(t) = K_t^*$, $K_l(t) = K_l^*$, $M_s(t) = M_s^*$, $K_{tire}(t) = K_{tire}^*$ and $a = 0$ then we have $\mathcal{S}(t) = 0$ in Eq.7.6. The NTV dynamic equations as described in equations 7.3, 7.4, 7.5 and 7.6 are linearized about the operating point as described in Appendix B. The discontinuous terms in $F_s(Z,t)$and $F_c(\dot{Z},t)$ in the Eq.7.4 are made continuous by adopting the Fourier integrals as discussed in section 2.4. The linearized equations as derived in Eq.B.16 in Appendix B are transformed to the state space form as follows

$$\begin{aligned} \dot{X} &= \mathcal{A}X + \mathcal{B}\triangle U + \mathcal{D}\triangle W \\ Y &= \mathcal{C}X \end{aligned} \tag{7.7}$$

where,

$$X = \begin{Bmatrix} \Delta Z \\ \Delta \dot{Z} \end{Bmatrix} \quad Y = \begin{Bmatrix} x_h \\ \theta \end{Bmatrix}$$

$$\mathcal{A} = \begin{bmatrix} 0 & I_1 \\ -\frac{k_{ss}}{M_s} & -\frac{c_{ss}}{M_s} \end{bmatrix} \mathcal{B} = \begin{bmatrix} 0 \\ \frac{c_{ss}}{M_s} \end{bmatrix} D = \begin{bmatrix} 0 \\ \frac{k_{ss}}{M_s} \end{bmatrix} C \quad \begin{bmatrix} I_2 & 0 \end{bmatrix}$$

The above system is found to be completely controllable and observable

### 7.2.1 Discrete Auto Regressive Moving Average Model

The linearized model described as a continuous time state space Eq 7.7 is transferred to a discrete time state space equation of the form

$$\begin{aligned} X[k\check{h} + \check{h}] &= \mathcal{Q}(\check{h})X[k\check{h}] + \mathcal{F}_1(\check{h})\Delta U[k\check{h}] + \mathcal{F}_2(h)\Delta W[kh] \\ Y[k\check{h}] &= CX[k\check{h}] \end{aligned} \tag{7.8}$$

where,

$$\begin{aligned} \mathcal{Q}(\check{h}) &= \mathcal{R}e^{\mathcal{L}\check{h}}\mathcal{R}^{-1} \\ \mathcal{L} &= \begin{bmatrix} \lambda_1 & 0 & 0 \\ 0 & \ddots & 0 \\ 0 & 0 & \lambda_n \end{bmatrix} \quad e^{\mathcal{L}\check{h}} = \begin{bmatrix} e^{\lambda_1 \check{h}} & 0 & 0 \\ 0 & \cdot & 0 \\ 0 & 0 & e^{\lambda_n \check{h}} \end{bmatrix} \\ \mathcal{F}_1(\check{h}) &= \left[\int_0^{\check{h}} \left[\mathcal{R}e^{\mathcal{L}\nu}\mathcal{R}^{-1}\right] d\nu\right] \mathcal{B} \\ \mathcal{F}_2(\check{h}) &= \left[\int_0^{\check{h}} \left[\mathcal{R}e^{\mathcal{L}\nu}\mathcal{R}^{-1}\right] d\nu\right] D \end{aligned}$$

$\lambda_i$, $i = 1, \cdots n$ are the eigen values of matrix $\mathcal{A}$ and $\mathcal{R}$ is a matrix made of the column vectors containing the co-factors of the same row of the matrix $[sI - \mathcal{A}]$ for different eigen values. These equations could be modified to form the DARMA model by expressing it as a transfer function as described below

$$Y[k] = C\left[qI - \mathcal{Q}(\check{h})\right]^{-1}\mathcal{F}_1(\check{h})\Delta U[k] + C\left[qI - \mathcal{Q}(\check{h})\right]^{-1}\mathcal{F}_2(\check{h})\Delta W[k] \tag{7.9}$$

The matrices $W_1(q,h) = C\left[qI - Q(h)\right]^{-1} F_1(h)\triangle U[k]$ and $W_2(q,h) = C\left[qI - Q(h)\right]^{-1} F_2(h)\triangle W[k]$ represent the transfer function matrices in the discrete domain. The direct method of evaluating $W_1$ and $W_2$ is through the simplification of resolvent matrix $\left[qI - Q(h)\right]^{-1}$ which is cumbersome for the higher order systems and the approach is extremely proven to numerical round off errors. A number of approaches for the computation of transfer function matrices of linear multi-variable systems from the state space equations have been derived in the past. One of the schemes is called the pole-zero approach where the coefficients of the denominator and numerator are evaluated by solving the eigen value problems [158] and generalized eigen value problems [156]. The accuracy of the scheme depends on the accuracy of the eigen values computation and could create problems for ill-conditioned eigen value and generalized eigen value problems. These difficulties are avoided by an efficient method proposed by Misra and Patel [157]. This method involves computing the coefficients directly by using the variant of Hyman's method. The algorithm proposed here performs orthogonal similarity transformations using the householder transformations to find the minimal order subsystem. This subsystem corresponds to each input output pair and uses the same determinant identities to determine the elements of the transfer function matrices. In this approach each separate single input, single output subsystem ( $Q, F_j, C_i$, where $i$ and $j$ indicate the $i^{th}$ output and $j^{th}$ input ) is reduced to the minimal order form by removing the input and/or output decoupling zeros to make the system controllable and observable. In this process the system matrices are transferred to lower and upper Hessenberg matrices by sequential orthogonal transformations. Hence each element of the transfer function matrix corresponds to the controllable and observable subsystems.

Equation 7.9 could be simplified as

$$Y[k] = \left[\frac{B^1(q^{-1})}{A(q^{-1})}\right] \triangle U[k] + \left[\frac{B^2(q^{-1})}{A(q^{-1})}\right] \triangle W[k] \qquad (7.10)$$

which can be written to be of the form

$$Y[k]A(q^{-1}) = B^1(q^{-1})\triangle U[k] + B^2(q^{-1})\triangle W[k] \qquad (7.11)$$

where, various elements of the matrices could be simplified to be of the form

$$A(q^{-1}) = a_0 + a_1 q^{-1} + \quad + a_8 q^{-8}$$
$$B^1_{ij}(q^{-1}) = b^1_{i_0} q^{-1} + \quad + b^1_{i_8} q^{-8}$$
$$B^2_{ij}(q^{-1}) = b^2_{i_0} q^{-1} + \quad + b^2_{i_8} q^{-8}$$
$$\text{where,} \quad i \in \{1,2\} \quad \& \quad j \in \{1,2\}$$

In the multi-variable case the delay structure of the transfer function is a matrix so that the leading coefficients of $B^1(q^{-1})$ and $B^2(q^{-1})$ are made non zeros. This is similar to SISO system where, the delay structure is transparent and scalar in nature. This is of the form $q^d$. Equation 7.11 would satisfy the basic assumptions necessary for the formation of interactor matrix namely, the number of outputs are the same as the number of inputs and the determinant of the transfer function is nonzero for all q. The determinant $\left[\breve{A}(q^{-1} = a_0 + a_1 q^{-1} + \cdots + a_8 q^{-8}\right]$ is non zero because, $a_0$ is a non zero constant for all values of q.

An interactor matrix $\mathcal{U}(q)$ is found from the polynomial matrix $B^1(q^{-1})$ since $\triangle U[k]$ is the actual input that is to be evaluated and $\triangle W[k]$ is the disturbance input that is assumed to be known. So the interactor matrix is evaluated such that $\lim_{Z \to \infty} \mathcal{U}(Z)\breve{A}(Z^{-1})^{-1} B^1(Z^{-1}) = \kappa$. The interactor matrix $\mathcal{U}(q)$ is assumed to be the product of $\mathcal{J}(q)\mathcal{N}(q)$ where,

$$\mathcal{N}(q) = diag\left[q^{f_1} \cdots q^{f_m}\right] \tag{7.12}$$
$$f_i \geq d_i \equiv min \quad d_{ij} \qquad i \leq j \leq m$$

$d_{ij}$ is the delay between $j^{th}$ input of $\triangle U[k]$ and $i^{th}$ output in $Y[k]$ and $m$ ( 2) the order of the transfer function matrix. $\mathcal{J}(q)$ is an unimodular matrix which could be assumed to be an identity matrix ($\mathcal{I}_2$).

## 7.3 Linear Time Invariant Reference Model

To achieve an optimal suspension performance and exhibit robustness to the model parameter variations due to various dynamic manoeuvres a two tier linear time invariant reference model as shown in Fig.7.1 is chosen. The dynamic performance of the two tier skyhook damping reference model at two different levels are constrained to reside in the controller.

Using Lagrange's method for writing dynamic equations, we can derive the reference model equations using the following Kinetic ($E_{KE}$), Potential ($E_{PE}$) and Damping ($E_{DE}$) energy terms

$$\begin{aligned} E_{KE} &= \tfrac{1}{2}M_{m_{ut}}\left(\dot{x}_{m_{t_1}}\right)^2 + \tfrac{1}{2}M_{m_{ul}}\left(\dot{x}_{m_{l_1}}\right)^2 + \tfrac{1}{2}M_{m_s}(\dot{x}_{m_b})^2 + \tfrac{1}{2}I_{m_{MI}}\left(\dot{\theta}_m\right)^2 \\ E_{PE} &= \tfrac{1}{2}K_{m_t}\left(x_{m_{t_2}} - x_{m_{t_1}}\right)^2 + \tfrac{1}{2}K_{m_l}\left(x_{m_{l_2}} - x_{m_{l_1}}\right)^2 + \\ &\quad \tfrac{1}{2}K_{m_{tire}}\left(x_{m_{t_1}} - \omega(t-\tau)\right)^2 + \tfrac{1}{2}K_{m_{tire}}\left(x_{m_{l_1}} - \omega(t)\right)^2 \\ E_{DE} &= \tfrac{1}{2}D_{m_t}\left(\dot{x}_{m_{t_2}}\right)^2 + \tfrac{1}{2}D_{m_l}\left(\dot{x}_{m_{l_2}}\right)^2 + \tfrac{1}{2}C_{m_t}\left(\dot{x}_{m_{t_1}}\right)^2 + \tfrac{1}{2}C_{m_l}\left(\dot{x}_{m_{l_1}}\right)^2 \end{aligned} \tag{7.13}$$

A transformation of displacement DOF's $\left[x_{m_{l_1}}, x_{m_{l_2}}, x_{m_{t_1}}, x_{m_{t_2}}\right]$ to the DOF's involving pitch DOF $\left[x_{m_b}, \theta_m, x_{m_{l_1}}, x_{m_{t_1}}\right]$ is performed using

$$\begin{aligned} x_{m_{l_2}} &= x_{m_b} + d_1\theta_m \\ x_{m_{t_2}} &= x_{m_b} + d_2\theta_m \end{aligned} \tag{7.14}$$

Energy equations are transformed to the Lagrange's form as

$$\begin{aligned} E_{LE} = E_{KE} - E_{PE} &= \tfrac{1}{2}M_{m_{ut}}\left(\dot{x}_{m_{t_1}}\right)^2 + \tfrac{1}{2}M_{m_{ul}}\left(\dot{x}_{m_{l_1}}\right)^2 + \tfrac{1}{2}M_{m_s}(\dot{x}_{m_b})^2 + \tfrac{1}{2}I_{m_{MI}}\left(\dot{\theta}_m\right)^2 \\ &\quad -\tfrac{1}{2}K_{m_t}\left(x_{m_b} - d_2\theta_m - x_{m_{t_1}}\right)^2 - \tfrac{1}{2}K_{m_l}\left(x_{m_b} + d_1\theta_m - x_{m_{l_1}}\right)^2 \\ &\quad -\tfrac{1}{2}K_{m_{tire}}\left(x_{m_{t_1}} - \omega(t-\tau)\right)^2 - \tfrac{1}{2}K_{m_{tire}}\left(x_{m_{l_1}} - \omega(t)\right)^2 \end{aligned} \tag{7.15}$$

$$E_{DF} = \tfrac{1}{2}D_{m_t}\left(\dot{x}_{m_b} - d_2\dot{\theta}_m\right)^2 + \tfrac{1}{2}D_{m_l}\left(\dot{x}_{m_b} + d_1\dot{\theta}_m\right)^2 + \tfrac{1}{2}C_{m_t}\left(\dot{x}_{m_{t_1}}\right)^2 + \tfrac{1}{2}C_{m_l}\left(\dot{x}_{m_{l_1}}\right)^2$$

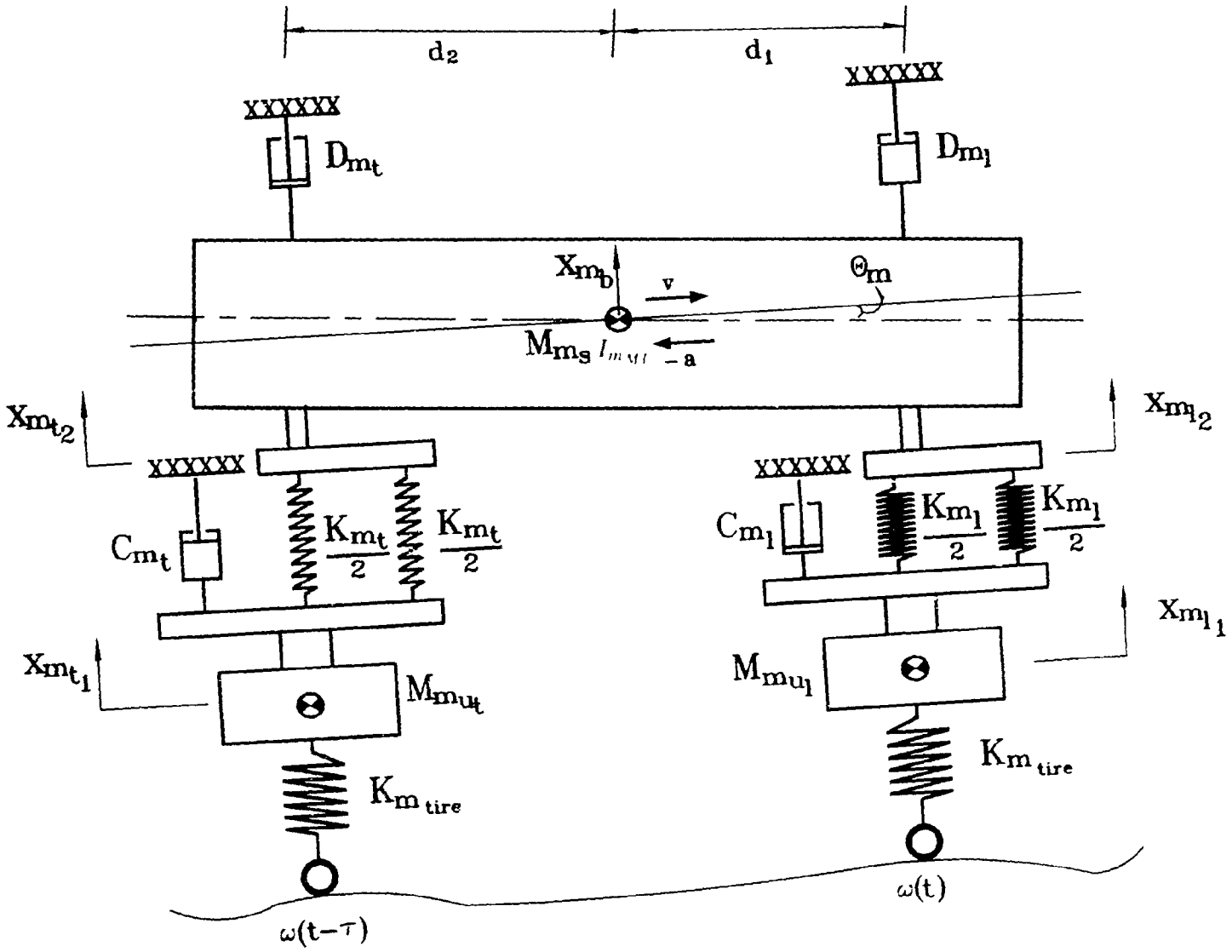


Fig 7.1: Linear time invariant half-car reference model

The above equations are used in the Lagrange's equation to derive the final dynamic equations

$$\frac{d}{dt}\left[\frac{\partial E_{LE}}{\partial q_i}\right] - \frac{\partial E_{LE}}{\partial q_i} + \frac{\partial E_{DE}}{\partial \dot{q}_i} = 0 \tag{7.16}$$

where,

$$q_i = \left[x_{m_b}, \theta_m, x_{m_{i_1}}, x_{m_{t_1}}\right]$$

The final equations which were verified with Newton's form of formulation could be simplified and written in the matrix form as follows

$$\mathcal{M}_m \ddot{Z}_m + \mathcal{C}_m \dot{Z}_m + \mathcal{K}_m Z_m = \mathcal{H}_m W(t) \tag{7.17}$$

where,

$$Z_m = \begin{Bmatrix} x_{m_b} \\ \theta_m \\ x_{m_{i_1}} \\ x_{m_{t_1}} \end{Bmatrix} \qquad W(t) = \begin{Bmatrix} w(t) \\ w(t-\check{h}) \end{Bmatrix}$$

$$\mathcal{M}_m = \begin{bmatrix} M_{m_s} & 0 & 0 & 0 \\ 0 & I_{m_M} & 0 & 0 \\ 0 & 0 & M_{m_{u_l}} & 0 \\ 0 & 0 & 0 & M_{m_{u_t}} \end{bmatrix} \quad \mathcal{H}_{r_i} = \begin{bmatrix} 0 & 0 \\ 0 & 0 \\ K_m & 0 \\ 0 & K_m \end{bmatrix}$$

$$\mathcal{C}_m = \begin{bmatrix} (D_{m_l} + D_{m_t}) & (D_{m_l} d_1 - D_{m_t} d_2) & 0 & 0 \\ (D_{m_l} d_1 - D_{m_t} d_2) & \left(D_{m_l} {d_1}^2 + D_{m_t} {d_2}^2\right) & 0 & 0 \\ 0 & 0 & C_{m_l} & 0 \\ 0 & 0 & 0 & C_{m_t} \end{bmatrix}$$

$$\mathcal{K}_m = \begin{bmatrix} (K_{m_l} + K_{m_t}) & (K_{m_l} d_1 - K_{m_t} d_2) & -K_{m_l} & -K_{m_t} \\ (K_{m_l} d_1 - K_{m_t} d_2) & \left(K_{m_l} {d_1}^2 + K_{m_t} {d_2}^2\right) & -K_{m_l} d_1 & K_{m_t} d_2 \\ -K_{m_l} & -K_{m_l} d_1 & K_{m_l} + K_{m_{tire}} & 0 \\ -K_{m_t} & K_{m_t} d_2 & 0 & K_{m_t} + K_{m_{tire}} \end{bmatrix}$$

To evaluate the transfer function of the reference model, let us assume the leading wheel input $w(t)$ to be of a sinusoidal form represented as

$$w(t) = \cap e^{i\omega t} \tag{7.18}$$

Then the trailing wheel input $w(t-\tau)$ which incorporates the time delay can be written as

$$\begin{aligned} w(t-\tau) &= \cap e^{\iota\omega(t-\tau)} \\ &= \cap e^{\iota\omega t} e^{-\iota\omega\tau} \end{aligned} \tag{7.19}$$

The response of the second order system represented in Eq.7.17 for a forced sinusoidal input of the form represented in Eq.7.18 could be written as $z_m(t) = e^{\lambda t}$ where, $\lambda$ is complex of the form $\alpha + \iota\omega$, then

$$\begin{aligned} Z_m(t) &= e^{(\alpha+\iota\omega)t} = e^{\alpha t} e^{\iota\omega t} = \check{Z}_m e^{\iota\omega t} \\ \dot{Z}_m &= \check{Z}_m \iota\omega e^{\iota\omega t} \\ \ddot{Z}_m &= -\check{Z}_m \omega^2 e^{\iota\omega t} \end{aligned} \tag{7.20}$$

substituting Eqs.7.18, 7.19 and 7.20 in Eq.7.21 we obtain

$$-\mathcal{M}_m \check{Z}_m \omega^2 + \mathcal{C}_m \check{Z}_m \iota\omega + \mathcal{K}_m \check{Z}_m = \mathcal{H}_m \begin{Bmatrix} 1 \\ e^{-\iota\omega\tau} \end{Bmatrix} \cap$$

$$\frac{\check{Z}_m}{\cap}(\omega) = \left[\mathcal{K}_m - \omega^2 \mathcal{M}_m + \iota\omega \mathcal{C}_m\right]^{-1} \mathcal{H}_m \begin{Bmatrix} 1 \\ e^{-\iota\omega\tau} \end{Bmatrix} \tag{7.21}$$

Equation 7.21 represents a transfer function for various DOF's with respect to an input excitation. Figure 7.2 shows the passive and reference model system gain factor between sprung and unsprung masses various DOF's and excitation input. Figure 7.3 shows the system gain factors of relative displacements with respect to the excitation input. The figures indicate how the skyhook reference model isolates and at the same time reduces the rattle space at the natural frequency. The transmissibility characteristics for the isolation indicate that the response is well damped at the natural frequency and at higher frequencies. The MRAC would achieve the performance of this reference model irrespective of large dynamic parameter variations.

The dynamic equations of the reference model described in Eq.7.17 could be written as a continuous time state space equation of the form

$$\begin{aligned} \dot{X}_m(t) &= \mathcal{A}_m X_m(t) + \mathcal{D}_m W(t) \\ Y_m(t) &= \mathcal{C}_m X_m(t) \end{aligned} \tag{7.22}$$

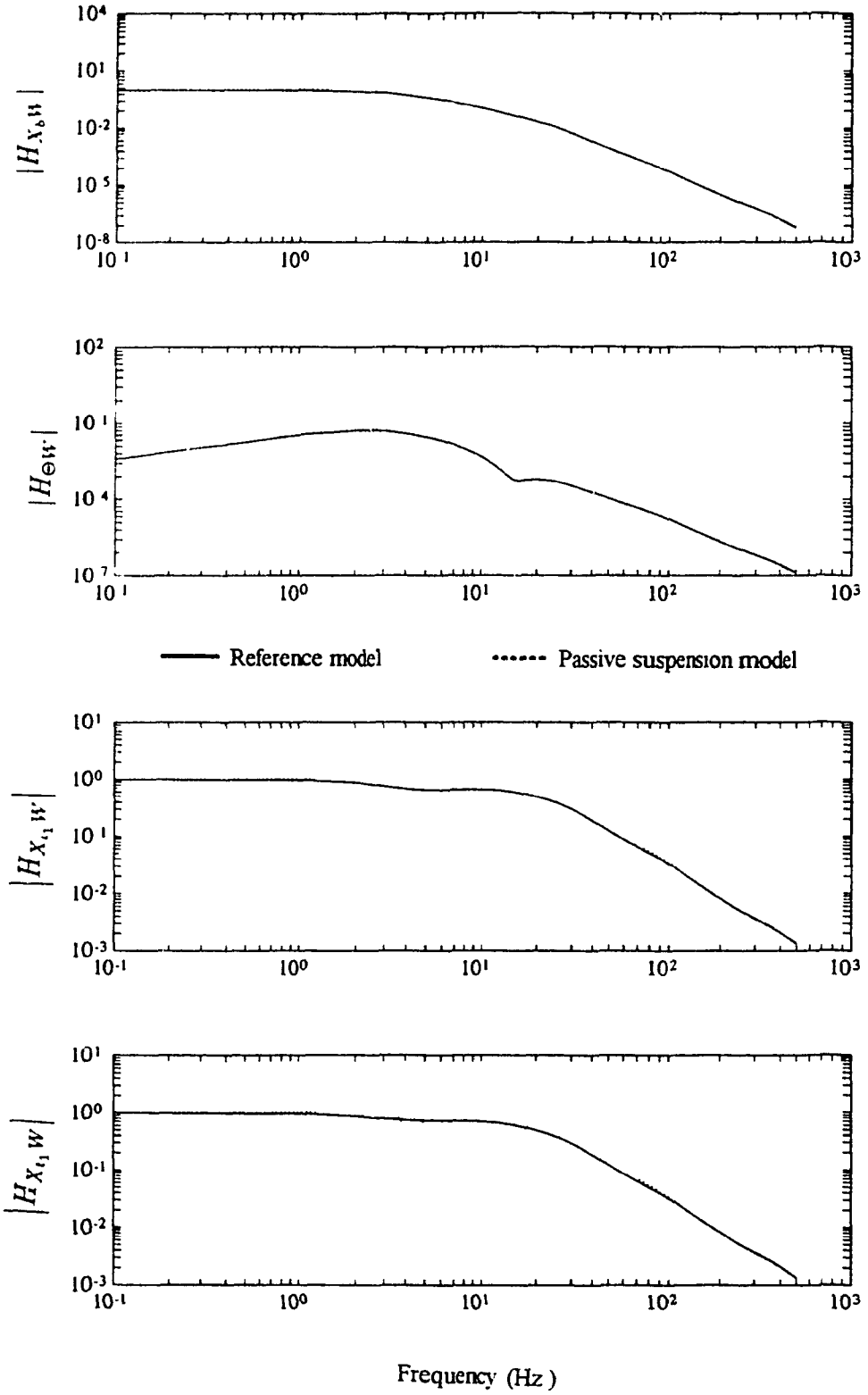


Fig.7.2: Sprung and unsprung mass absolute displacement system gain factors with respect to excitation input.

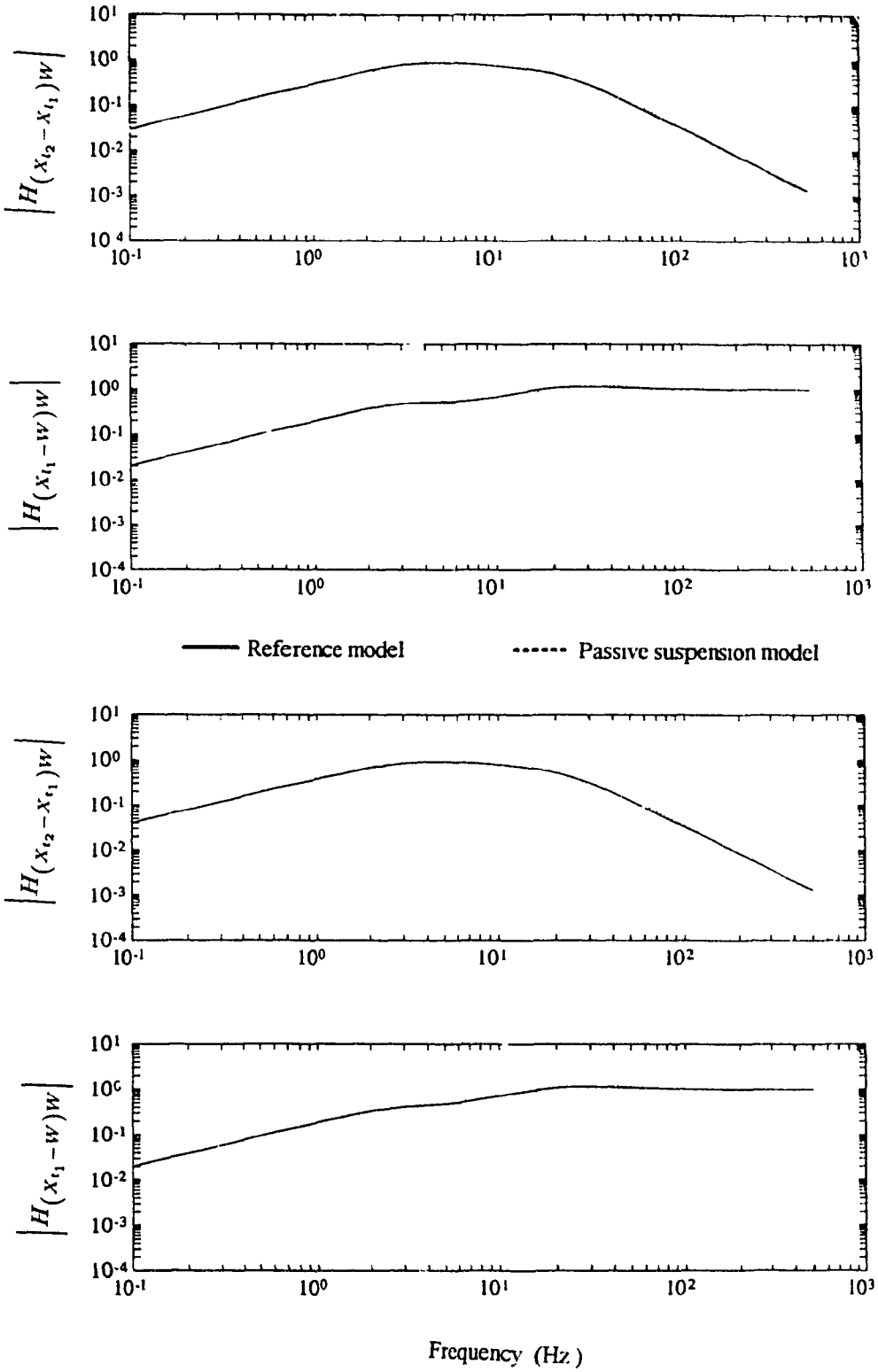


Fig.7.3: Primary and secondary suspension relative displacement system gain factors with respect to excitation input.

where,

$$X_m = \begin{Bmatrix} \triangle Z_m \\ \triangle \dot{Z}_m \end{Bmatrix} \quad Y_m = \begin{Bmatrix} x_{m_b} \\ \theta_m \end{Bmatrix}$$

$$\mathcal{A}_m = \begin{bmatrix} 0 & \mathcal{I}_4 \\ -\frac{K_m}{\mathcal{M}_m} & -\frac{C_m}{\mathcal{M}_m} \end{bmatrix} \mathcal{D}_m = \begin{bmatrix} 0 \\ \frac{\mathcal{H}_m}{\mathcal{M}_m} \end{bmatrix} \mathcal{C}_m = \begin{bmatrix} \mathcal{I}_2 & 0 \end{bmatrix}$$

The continuous time state space equation 7.22 could be transferred to discrete domain model as

$$\begin{aligned} X_m[(k+1)\check{h}] &= \mathcal{Q}_m(\check{h}) X_m[k\check{h}] + \mathcal{F}_m(k\check{h}) W[k\check{h}] \\ Y_m[k\check{h}] &= C_m X_m[k\check{h}] \end{aligned} \tag{7.23}$$

where,

$$\begin{aligned} \mathcal{Q}_m(\check{h}) &= e^{\mathcal{A}_m \check{h}} \\ \mathcal{F}_m(\check{h}) &= \left[\int_0^{\check{h}} e^{\mathcal{A}_m \nu} d\nu\right] \mathcal{D}_m \end{aligned}$$

The above equation could be transferred into a transfer function form as

$$\begin{aligned} Y_m[k] &= \mathcal{C}_m \left[q\mathcal{I} - \mathcal{Q}_m(\check{h})\right]^{-1} \mathcal{F}_m(\check{h}) W[k] \\ Y_m[k] &= \frac{H^*(q^{-1})}{\check{E}(q^{-1})} W[k] \end{aligned} \tag{7.24}$$

Multiplying the above equation by the interactor matrix selected for the vehicle model we could derive

$$\begin{aligned} \mathcal{U}(q) Y_m[k] &= \frac{\mathcal{U}(q) H^*(q^{-1})}{\check{E}(q^{-1})} W[k] \\ \bar{Y}_m[k] \check{E}(q^{-1}) &= H(q^{-1}) W[k] \end{aligned} \tag{7.25}$$

where, $H(q^{-1})$ for the reference model could be evaluated by knowing the order and the coefficients of both $\mathcal{U}(q)$ and $H^*(q^{-1})$.

## 7.4 Discrete Model Reference Adaptive Control Design

A DMRAC is used to achieve the reference model following for the actual vehicle suspension model. Here the controller designed incorporates the reference model

structure and the linearized actual vehicle model as derived in the previous sections Using the interactor matrix as discussed in section 7.2.2, we assume a predictor of the following form for the model reference adaptive control

$$E(q^{-1})\mathcal{U}(q) = F(q)A(q^{-1}) + G(q^{-1}) \tag{7.26}$$

In the above equation $E(q^{-1})$ and $A(q^{-1})$ are assumed as $(2 \times 2)$ matrices derived from the polynomials $\breve{E}(q^1)$ and $\breve{A}(q^{-1})$ which are multiplied by $\mathcal{I}_2$. Knowing the max delay $d_{max}$ in $\mathcal{U}(q)$, we could evaluate the maximum number of terms in the polynomial $F(q)$. Let us assume $F(q)$ to be of the form

$$F(q) = F_o q^{d_{max}} + F_1 q^{d_{max}-1} + \cdots + F_{d_{max}-1} q \tag{7.27}$$

But to know the order of the matrix polynomial $G(q^{-1})$ we should observe the product $E(q^{-1})\mathcal{U}(q)$. In this product knowing the order of the polynomial $E(q^{-1})$ we can observe the minimum order of q in the product $E(q^{-1})\mathcal{U}(q)$ or the most negative of the terms $(d_1 - 8)$ and $(d_2 - 8)$. Then the order of $G(q^{-1})$ would be $d_{min} = max\ |d_i - 8|\ \ for\ i = 1, 2$. The polynomial matrix $G(q^{-1})$ is chosen as

$$G(q^{-1}) = G_0 + G_1 q^{-1} + \cdots + G_{d_{min}} q^{-d_{min}} \tag{7.28}$$

The coefficients of $F(q)$ and $G(q^{-1})$ are $(2 \times 2)$ matrices and the polynomials are modified to suite the predictor equation of the form Eq.7.26. The predictor form in Eq.7.26, the coefficients of the matrices $A(q^{-1})$ and $E(q^{-1})$, the interactor matrix $\mathcal{U}(q)$ along with the values $d_{min}$ and $d_{max}$ are used to solve for the coefficient matrices in polynomials $F(q)$ and $G(q^{-1})$. This is represented in Eqs.7.27 and 7.28. The interactor matrix $\mathcal{U}(q)$ is assumed to be of the form $\begin{bmatrix} q^{d_1} & 0 \\ 0 & q^{d_2} \end{bmatrix}$ where, the values of $d_1$ and $d_2$ are the time delays and the value $d_{max}$ as a maximum of $\{d_1, d_2\}$. Then the

matrix polynomials $E(q^{-1})$, $A(q^{-1})$, $F(q)$ and $G(q^{-1})$ are assumed to be of the form

$$
\begin{aligned}
E(q^{-1}) &= \begin{bmatrix} e_0 + e_1 q^{-1} + \cdots + e_8 q^{-8} & 0 \\ 0 & e_0 + e_1 q^{-1} + \cdots + e_8 q^{-8} \end{bmatrix} \\
A(q^{-1}) &= \begin{bmatrix} a_0 + a_1 q^{-1} + \cdots + a_3 q^{-8} & 0 \\ 0 & a_0 + a_1 q^{-1} + \cdots + a_8 q^{-8} \end{bmatrix} \\
F(q) &= \begin{bmatrix} F_o^1 & F_o^2 \\ F_o^3 & F_o^4 \end{bmatrix} q^{d_{max}} + \begin{bmatrix} F_1^1 & F_1^2 \\ F_1^3 & F_1^4 \end{bmatrix} q^{d_{max}-1} + \cdots + \begin{bmatrix} F^1{}_{d_{max}-1} & F^2{}_{d_{max}-1} \\ F^3{}_{d_{max}-1} & F^4{}_{d_{max}-1} \end{bmatrix} q \\
G(q^{-1}) &= \begin{bmatrix} G_o^1 & G_o^2 \\ G_o^3 & G_o^4 \end{bmatrix} + \begin{bmatrix} G_1^1 & G_1^2 \\ G_1^3 & G_1^4 \end{bmatrix} q^{-1} + \cdots + \begin{bmatrix} G^1{}_{d_{min}} & G^2{}_{d_{min}} \\ G^3{}_{d_{min}} & G^4{}_{d_{min}} \end{bmatrix} q^{-d_{min}}
\end{aligned}
\tag{7.29}
$$

Substituting these in the predictor equation of the form in Eq.7.26, we could solve for various coefficients in the unknown matrices of the polynomials $F(q)$ and $G(q^{-1})$.

---

**Example:** For Solving Matrix Polynomials $F(q)$ and $G(q^{-1})$

Let us consider an example assuming the delay terms in the interactor matrices as $d_1 = 3$ and $d_2 = 1$, which are dictated by the hardware and controller software delays in the actual implementation. This implies $d_{max} = 3$ and $d_{min} = 7$.

Then the interactor matrix $\mathcal{U}(q)$ and $\mathcal{F}(q)$ could be written as

$$
\begin{aligned}
\mathcal{U}(q) &= \begin{bmatrix} q^3 & 0 \\ 0 & q \end{bmatrix} \\
\mathcal{F}(q) &= \mathcal{F}_0 q^3 + \mathcal{F}_1 q^2 + \mathcal{F}_2 q
\end{aligned}
\tag{7.30}
$$

Knowing the matrices $E(q^{-1})$ and $A(q^{-1})$ as represented in Eq.7.29, we could evaluate various individual terms on both left and right hand sides of the predictor equation

7.26 as follows.

$$
\begin{aligned}
E(q^{-1})\mathcal{U}(q) &= \begin{bmatrix} e_0q^3 + e_1q^2 + \cdots + e_8q^{-5} & 0 \\ 0 & e_0q^1 + e_1q^0 + \cdots + e_8q^{-7} \end{bmatrix} \\
F(q)A(q^{-1}) &= \begin{bmatrix} F_0{}^1a_0q^3 + \left(F_0{}^1a_1 + F_1{}^1a_0\right)q^2 + \left(F_0{}^1a_2 + F_1{}^1a_1 + F_2{}^1a_0\right)q + \cdots \\ \cdots + \left(F_0{}^1a_8 + F_1{}^1a_7 + F_2{}^1a_6\right)q^{-5} + \left(F_1{}^1a_8 + F_2{}^1a_7\right)q^{-6} + F_2{}^1a_8q^{-7} \\ F_0{}^3a_0q^3 + \left(F_0{}^3a_1 + F_1{}^3a_0\right)q^2 + \left(F_0{}^3a_2 + F_1{}^3a_1 + F_2{}^3a_0\right)q + \cdots \\ \cdots + \left(F_0{}^3a_8 + F_1{}^3a_7 + F_2{}^3a_6\right)q^{-5} + \left(F_1{}^3a_8 + F_2{}^3a_7\right)q^{-6} + F_2{}^3a_8q^{-7} \end{bmatrix} \\
&\quad \begin{bmatrix} F_0{}^2a_0q^3 + \left(F_0{}^2a_1 + F_1{}^2a_0\right)q^2 + \left(F_0{}^2a_2 + F_1{}^2a_1 + F_2{}^2a_0\right)q + \cdots \\ \cdots + \left(F_0{}^2a_8 + F_1{}^2a_7 + F_2{}^2a_6\right)q^{-5} + \left(F_1{}^2a_8 + F_2{}^2a_7\right)q^{-6} + F_2{}^2a_8q^{-7} \\ F_0{}^4a_0q^3 + \left(F_0{}^4a_1 + F_1{}^4a_0\right)q^2 + \left(F_0{}^4a_2 + F_1{}^4a_1 + F_2{}^4a_0\right)q + \cdots \\ \cdots + \left(F_0{}^4a_8 + F_1{}^4a_7 + F_2{}^4a_6\right)q^{-5} + \left(F_1{}^4a_8 + F_2{}^4a_7\right)q^{-6} + F_2{}^4a_8q^{-7} \end{bmatrix} \\
G(q^{-1}) &= \begin{bmatrix} G_0{}^1 & G_0{}^2 \\ G_0{}^3 & G_0{}^4 \end{bmatrix} + \begin{bmatrix} G_1{}^1 & G_1{}^2 \\ G_1{}^3 & G_1{}^4 \end{bmatrix} q^{-1} + \cdots + \begin{bmatrix} G_7{}^1 & G_7{}^2 \\ G_7{}^3 & G_7{}^4 \end{bmatrix} q^{-7}
\end{aligned}
\tag{7.31}
$$

Observing the left and right hand terms of the predictor equation which are described above we could eliminate some of the unknown coefficients. Since the elements [1,2] and [2,1] on the left hand side are zero and all of the coefficients $a_0, \cdots, a_8$ of the determinant matrix are not equal to zero, we can conclude that $\left(F_0{}^2, F_1{}^2, F_2{}^2\right)$, $\left(F_0{}^3, F_1{}^3, F_2{}^3\right)$, $\left(G_0{}^2, G_1{}^2 \cdots G_7{}^2\right)$ and $\left(G_0{}^3, G_1{}^3 \cdots G_7{}^3\right)$ are all equal to zero.

On simplification of the right hand side of the predictor equation we obtain

$$F(q)A(q^{-1})+G(q^{-1}) = \begin{bmatrix} F_0{}^1a_0q^3+\left(F_0{}^1a_1+F_1{}^1a_0\right)q^2+\left(F_0{}^1a_2+F_1{}^1a_1+F_2{}^1a_0\right)q+\cdots \\ \left(F_0{}^1a_8+F_1{}^1a_7+F_2{}^1a_6\right)q^{-5}+\left(F_1{}^1a_8+F_2{}^1a_7\right)q^{-6}+F_2{}^1a_8q^{-7} \\ \\ 0 \\ \\ 0 \\ \\ F_0{}^1a_0q^3+\left(F_0{}^1a_1+F_1{}^1a_0\right)q^2+\left(F_0{}^1a_2+F_1{}^1a_1+F_2{}^1a_0\right)q+\cdots \\ \left(F_0{}^1a_8+F_1{}^1a_7+F_2{}^1a_6\right)q^{-5}+\left(F_1{}^1a_8+F_2{}^1a_7\right)q^{-6}+F_2{}^1a_8q^{-7} \end{bmatrix} \tag{7.32}$$

On equating the coefficients of various polynomial terms on the left and right hand side we can solve for $\left(F_0{}^1, F_1{}^1, F_2{}^1\right)$ and $\left(F_0{}^4, F_1{}^4, F_2{}^4\right)$ recursively. These could be substituted to solve for various constants of the matrix polynomial $G(q^{-1})$.

---

Writing the determinant $\left(\breve{A}(q^{-1})\right)$ as a matrix, Eq. 7.11 could be written as

$$A(q^{-1})Y[k] = B^1(q^{-1})\triangle U[k] + B^2(q^{-1})\triangle W[k] \tag{7.33}$$

Multiplying the vehicle model in Eq.7.33 with the matrix polynomial $F(q)$ it can be expressed as

$$F(q)A(q^{-1})Y[k] = F(q)B^1(q^{-1})\triangle U[k] + F(q)B^2(q^{-1})\triangle W[k] \tag{7.34}$$

But on postmultiplying the reference model predictor given in Eq.7.26 by $Y[k]$ we have

$$E(q^{-1})\mathcal{U}(q)Y[k] = F(q)A(q^{-1})Y[k] + G(q^{-1})Y[k] \tag{7.35}$$

On substituting Eq.7.34 in Eq.7.35 we obtain

$$E(q^{-1})\mathcal{U}(q)Y[k] = G(q^{-1})Y[k] + F(q)B^1(q^{-1})\triangle U[k] + F(q)B^2(q^{-1})\triangle W[k] \tag{7.36}$$

This equation can be written in the predictor form as

$$E(q^{-1})\mathcal{U}(q)Y[k] = \alpha(q^{-1})Y[k] + \beta^1(q^{-1})\Delta U[k] + \beta^2(q^{-1})\Delta W[k] \qquad (7.37)$$

where,

$$\begin{aligned}
\alpha(q^{-1}) &= G(q^{-1}) \\
&= G_0 + G_1 q^{-1} + \cdots + G_{d_{min}} q^{-d_{min}} \\
&= \alpha_0 + \alpha_1 q^{-1} + \cdots + \alpha_{d_{min}} q^{-d_{min}} \\
\beta^1(q^{-1}) &= F(q)B^1(q^{-1}) \\
&= \beta^1_{[-d_{max}+1]} q^{d_{max}-1} + \cdots + \beta^1_{[-1]} q + \beta^1_0 + \beta^1_1 q^{-1} + \cdots + \beta^1_{d_{min}} q^{-d_{min}} \\
\beta^2(q^{-1}) &= F(q)B^2(q^{-1}) \\
&= \beta^2_{[-d_{max}+1]} q^{d_{max}-1} + \cdots + \beta^2_{[-1]} q + \beta^2_0 + \beta^2_1 q^{-1} + \cdots + \beta^2_{d_{min}} q^{-d_{min}}
\end{aligned}$$

Equation 7.37 could be represented as following transfer functions to apply the condition on the interactor matrix as discussed in Eq.7.12.

$$\begin{aligned}
\frac{Y[k]}{\Delta U[k]} &= \frac{\beta^1(q^{-1})}{[E(q^{-1})\mathcal{U}(q) - \alpha(q^{-1})]} = T_{\Delta U}(q) \\
\frac{Y[k]}{\Delta W[k]} &= \frac{\beta^2(q^{-1})}{[E(q^{-1})\mathcal{U}(q) - \alpha(q^{-1})]} = T_{\Delta W}(q)
\end{aligned} \qquad (7.38)$$

To satisfy the condition $\lim_{q \to \infty} \mathcal{U}(q)T_{\Delta U}(q) = \kappa$, the coefficients of the polynomial $\beta^1(q^{-1})$ should satisfy

$$\beta^1_{[-d_{max}+1]} = \cdots = \beta^1_{[-1]} = 0 \qquad (7.39)$$

This would eliminate the need for construction of an estimator for the control inputs $\Delta U[k + d_{max} - 1] + \cdots + \Delta U[k + 1]$. But the coefficients of $\beta^2(q^{-1})$ which would need a preview estimator of the input could either be estimated or made zero. A preview of the input excitation could be used to evaluate the excitation input values such as $\Delta W[k + d_{max} - 1] + \cdots + \Delta W[k + 1]$. The preview control of this form has been used in the past for the active suspension systems. The adaptive control could

be implemented with the coefficients

$$\mathcal{B}^2_{[-d_{max}+1]} = \cdots = \mathcal{B}^2_{[-1]} = 0 \tag{7.40}$$

Without loss of generality, these coefficients are not made zeros by considering the preview control. The total estimator model can be written as

$$E(q^{-1})\mathcal{U}(q)Y[k] = \alpha(q^{-1})Y[k] + \left[\mathcal{B}^1_0 + \mathcal{B}^1_1 q^{-1} + \cdots + \mathcal{B}^1_{d_{min}} q^{-d_{min}}\right] \triangle U[k] + \left[\mathcal{B}^2_{[-d_{max}+1]} q^{d_{max}-1} + \cdots + \mathcal{B}^2_{[-1]} q + \mathcal{B}^2_0 + \mathcal{B}^2_1 q^{-1} + \cdots + \mathcal{B}^2_{d_{min}} q^{-d_{min}}\right] \triangle W[k] \tag{7.41}$$

The above equation which is in the form of nonlinear model could be converted to a linearized model in terms of the controller output. On substituting $\bar{Y}[k] = \mathcal{U}(q)Y[k]$, we obtain

$$E(q^{-1})Y[k] = \alpha(q^{-1})Y[k] + \left[\mathcal{B}^1_0 + \mathcal{B}^1_1 q^{-1} + \cdots + \mathcal{B}^1_{d_{min}} q^{-d_{min}}\right] \triangle U[k] + \left[\mathcal{B}^2_{[-d_{max}+1]} q^{d_{max}-1} + \cdots + \mathcal{B}^2_{[-1]} q + \mathcal{B}^2_0 + \mathcal{B}^2_1 q^{-1} + \cdots + \mathcal{B}^2_{d_{min}} q^{-d_{min}}\right] \triangle W[k] \tag{7.42}$$

Multiplying both sides by $\left[\mathcal{B}_0{}^1\right]^{-1}$ we have

$$\frac{1}{\mathcal{B}^1_0} E(q^{-1})Y[k] = \alpha^1(q^{-1})Y[k] + \left[\mathcal{I}_2 + \mathcal{B}^{1'}(q^{-1})\right] \triangle U[k] + \left[\mathcal{B}^{2'}(q^{-1})\right] \triangle W[k] \tag{7.43}$$

where,

$$\begin{aligned}
\alpha'(q^{-1}) &= \tfrac{\alpha_0}{\mathcal{B}^1_0} + \tfrac{\alpha_1}{\mathcal{B}^1_0} q^{-1} + \cdots + \tfrac{\alpha_{d_{min}}}{\mathcal{B}^1_0} q^{-d_{min}} \\
&= \alpha'_0 + \alpha'_1 q^{-1} + \cdots + \alpha'_{d_{min}} q^{-d_{min}} \\
\mathcal{B}^{1'}(q^{-1}) &= \tfrac{1}{\mathcal{B}^1_0} \left[\mathcal{B}^1(q^{-1}) - \mathcal{B}^1_0\right] \\
&= \tfrac{1}{\mathcal{B}^1_0} \left[\mathcal{B}^1_1 q^{-1} + \cdots + \mathcal{B}^1_{d_{min}} q^{-d_{min}}\right] \\
&= \mathcal{B}^{1'}_1 q^{-1} + \cdots + \mathcal{B}^{1'}_{d_{min}} q^{-d_{min}} \\
\mathcal{B}^{2'}(q^{-1}) &= \tfrac{1}{\mathcal{B}^1_0} \left[\mathcal{B}^2_{[-d_{max}+1]} q^{d_{max}-1} + \cdots + \mathcal{B}^2_{[-1]} q + \mathcal{B}^2_0 + \mathcal{B}^2_1 q^{-1} + \cdots + \mathcal{B}^2_{d_{min}} q^{-d_{min}}\right] \\
&= \left[\mathcal{B}^{2'}_{[-d_{max}+1]} q^{d_{max}-1} + \cdots + \mathcal{B}^{2'}_{[-1]} q + \mathcal{B}^{2'}_0 + \mathcal{B}^{2'}_1 q^{-1} + \cdots + \mathcal{B}^{2'}_{d_{min}} q^{-d_{min}}\right]
\end{aligned}$$

The equation 7.43 could be rearranged to be represented in the form

$$\Delta U'[k] = \frac{1}{\beta_0^1} E(q^{-1})Y'[k] - \alpha'(q^{-1})Y[k] - \beta^{1'}(q^{-1})\Delta U'[k] - \beta^{2'}(q^{-1})\Delta W'[k] \tag{7.44}$$

The vehicle model in Eq.7.44 can be conveniently represented in the vector form as

$$\Delta U'[k] = \Theta^T \bar{\phi}[k] \tag{7.45}$$

where,

$$\Theta^T = \left[\alpha_0', \alpha_1', \cdots, \alpha_{d_{min}}', \beta_1^{1'}, \cdots, \beta_{d_{min}}^{1'}, \beta_{[-d_{max}+1]}^{2'}, \cdots, \beta_{[-1]}^{2'}, \beta_0^{2'}, \cdots, \beta_{d_{min}}^{2'}, \frac{1}{\beta_0^1}\right]$$

$$\bar{\phi}[k] = \left[-Y[k]^T, -Y[k-1]^T, \cdots, -Y[k-d_{min}]^T, -\Delta U'[k-1]^T, \cdots, -\Delta U'[k-d_{min}]^T, -\Delta W[k+d_{max}]^T, \cdots, -\Delta W[k+1]^T, -\Delta W[k]^T, \cdots, -\Delta W[k-d_{min}]^T, \tilde{Y}[k]^T\right]^T$$

$$\tilde{Y}[k] = E(q^{-1})\mathcal{U}(q)Y[k]$$

The number of control inputs in vector $\Delta U'[k]$ are 2 $(= m)$ and hence, the controller parameters matrix $\left(\Theta^T\right)$ is of the order $2 \times 2\,[d_{max} + 3d_{min} + 2]$ which is of the form $(m \times mn)$. But if the controller parameters $(\Theta^T)$ in the above equation are assumed to be known, then the above model can be converted to a control law with the system output being the desired output of the reference model given by Eq.7.25. Eq.7.25 could be written in the form

$$E(q^{-1})\bar{Y}_m[k] = H(q^{-1})W[k] \tag{7.46}$$

The control law is chosen so that $Y[k] \rightarrow Y_m[k]$ (the output of reference model). To derive the control law we would ideally like to have

$$\begin{aligned} \bar{Y}'[k] &= \mathcal{U}(q)Y[k] = \bar{Y}_m[k] = \mathcal{U}(q)Y_m[k] \\ E(q^{-1})\mathcal{U}(q)Y[k] &= E(q^{-1})\mathcal{U}(q)Y_m[k] \\ \tilde{Y}[k] &= E(q^{-1})\bar{Y}[k] = E(q^{-1})\bar{Y}_m[k] = \tilde{Y}_m[k] \end{aligned} \tag{7.47}$$

On substituting $\tilde{Y}[k]$ from Eq.7.45 in Eq.7.47 and further substituting in Eq.7.46 we obtain

$$\tilde{Y}_m[k] = \tilde{Y}[k] = H(q^{-1})W[k] \tag{7.48}$$

On substituting Eq.7.48 in the Eq.7.45 and by replacing $\tilde{Y}[k]$ we obtain the control law of the form

$$\Delta U^*[k] = \hat{\Theta}^T \phi'[k] \tag{7.49}$$

where,

$$\hat{\Theta}^T = \left[\alpha_0', \alpha_1', \cdots, \alpha_{d_{min}}', \beta_1^{1'}, \cdots, \beta_{d_{min}}^{1'}, \beta_{[-d_{max}+1]}^{2'}, \cdots, \beta_{[-1]}^{2'}, \beta_0^{2'}, \cdots, \beta_{d_{min}}^{2'}, \frac{1}{\beta_0^1}\right]$$

$$\begin{aligned}\phi'[k] = \big[&-Y[k]^T, -Y[k-1]^T, \cdots, Y[k-d_{min}]^T, -\Delta U[k-1]^T, \cdots, -\Delta U[k-d_{min}]^T, \\ &-\Delta W[k+d_{max}]^T, \cdots, -\Delta W[k+1]^T, -\Delta W[k]^T, \cdots, -\Delta W[k-d_{min}]^T, \tilde{Y}_m[k]^T\big]^T\end{aligned}$$

$$\tilde{Y}_m[k]^T = H(q^{-1})W[k]$$

Since the controller parameters are not known exactly, we estimate ($\hat{\Theta}^T$) by using least squares estimation and evaluate the above control law (Eq. 7.49).

### 7.4.1 Controller Parameters Estimation Law

A modified version of the least squares estimation which updates the controller parameters as a matrix rather than as a vector has been derived in this section. Least squares estimation which updates the controller parameters as a vector could be referred to in Ref.[146]. The linearized model in Eq.7.45 could be written in the form where the output ($\Delta U[k]$) at any $k$ is evaluated based on the previous values. Therefore we have

$$\Delta U[k-d] = \hat{\Theta}^T \bar{\phi}[k-d] \tag{7.50}$$

where,

$$\hat{\Theta}^T = \left[\alpha_0', \alpha_1', \cdots, \alpha_{d_{min}}', \beta_1^{1'}, \cdots, \beta_{d_{min}}^{1'}, \beta_{[-d_{max}+1]}^{2'}, \cdots, \beta_{[-1]}^{2'}, \beta_0^{2'}, \cdots, \beta_{d_{min}}^{2'}, \frac{1}{\beta_0^1}\right]$$

$$\begin{aligned}\phi[k-d] = \big[&-Y[k-d]^T, -Y[k-d-1]^T, \cdots, -Y[k-d-d_{min}]^T, -\Delta U[k-d-1]^T, \cdots, \\ &-\Delta U[k-d-d_{min}]^T, -\Delta W[k-d+d_{max}]^T, \cdots, -\Delta W[k-d+1]^T, \cdots, \\ &-\Delta W[k-d]^T, -\Delta W[k-d-d_{min}]^T, \tilde{Y}[k-d]^T\big]^T\end{aligned}$$

$$\tilde{Y}[k-d] = E(q^{-1})\mathcal{U}(q)Y[k-d]$$

In the above equation each DOF could be represented separately as

$$\Delta U_i[k-d]|_{1\times 1} = \theta_i^T|_{1\times mn}\, \phi[k-d]|_{mn\times 1} \qquad (7.51)$$
$$where,\ \ i \in \{1,m\}$$

which could be modified to be of the form

$$\Delta U_i[k-d]|_{1\times 1} = \phi[k-d]^T|_{1\times mn}\, \theta_{i}|_{mn\times 1} \qquad (7.52)$$

For different values of $(i)$ we obtain different equations corresponding to various DOF's. All the equations could be combined to form the following matrix equation

$$\begin{Bmatrix} \Delta U_1(k-d) \\ \Delta U_2(k-d) \\ \vdots \\ \Delta U_m(k-d) \end{Bmatrix}_{m\times 1} = \begin{bmatrix} \phi[k-d]^T & 0 & \cdot & 0 \\ 0 & \phi[k-d]^T & \cdot & 0 \\ \vdots & \vdots & \cdot & \cdot \\ 0 & 0 & \cdot & \phi[k-d]^T \end{bmatrix}_{m\times mn} \begin{Bmatrix} \theta_1 \\ \theta_2 \\ \\ \theta_m \end{Bmatrix}_{mn\times 1} \qquad (7.53)$$

The above equation could be represented as

$$\Delta U[k-d]|_{m\times 1} = \Phi[k-d]^T|_{m\times mn}\, \Theta|_{mn\times 1} \qquad (7.54)$$

The recursive least squares estimation for the multi-output system described in Eq.7.54, where the controller parameters are updated as a vector has been derived by minimizing a performance index ($\mathcal{PI}_N$) of the form

$$\mathcal{PI}_N(\tilde{\Theta}) = \frac{1}{2}\left[\tilde{\Theta} - \tilde{\Theta}_0\right]^T \mathcal{P}^{-1}\left[\tilde{\Theta} - \tilde{\Theta}_0\right] + \frac{1}{2}\sum_{k=1}^{N}\left[\Delta U^T[k-d] - \phi^T[k-d]\tilde{\Theta}\right]^T R^{-1}\left[\Delta U^T[k-d] - \phi^T[k-d]\tilde{\Theta}\right] \qquad (7.55)$$

where, N denotes a big index of data vector and $\tilde{\Theta}$ denotes the unknown true values

of the controller parameter matrix. The weighting matrices $\mathcal{P}$ and $\mathcal{R}$ are of the form

$$\mathcal{P} = \begin{bmatrix} \mathcal{P}^{(1)} & 0 & \cdots & 0 \\ 0 & \mathcal{P}^{(2)} & \cdots & 0 \\ \vdots & \ddots & \mathcal{P}^{(i)} & \vdots \\ 0 & \cdots & \cdots & \mathcal{P}^{(m)} \end{bmatrix}_{mmn \times mmn}$$

$$\mathcal{R} = \begin{bmatrix} r_{11} & 0 & \cdots & 0 \\ 0 & r_{21} & \cdots & 0 \\ \vdots & \ddots & r_{ii} & \vdots \\ 0 & \cdots & \cdots & r_{mm} \end{bmatrix}_{m \times m}$$

*where,* $i \in \{1, m\}$
$r_{ii}$ *are set of scalar quantities*

On further matrix manipulations, evaluating the minimum of the $\mathcal{PI}_N(\widetilde{\Theta})$ by equating $\frac{\partial(\mathcal{PI}_N(\widetilde{\Theta}))}{\partial\widetilde{\Theta}} = 0$ and using various Lemmas as in Ref.[146], we could derive the multi-output least squares algorithm of the form

$$\hat{\widetilde{\Theta}}[k] = \hat{\widetilde{\Theta}}[k-1] + \frac{\mathcal{P}[k-d-1]\bar{\mathcal{O}}[k-d]\left[\Delta U[k-d] - \bar{\mathcal{O}}[k-d]^T\hat{\widetilde{\Theta}}[k-1]\right]}{\mathcal{R} + \bar{\mathcal{O}}[k-d]^T\mathcal{P}[k-d-1]\bar{\mathcal{O}}[k-d]}$$

$$\mathcal{P}[k-d] = \mathcal{P}[k-d-1] - \frac{\mathcal{P}[k-d-1]\bar{\mathcal{O}}[k-d]\bar{\mathcal{O}}[k-d]^T\mathcal{P}[k-d-1]}{\mathcal{R} + \bar{\mathcal{O}}[k-d]^T\mathcal{P}[k-d-1]\bar{\mathcal{O}}[k-d]} \tag{7.56}$$

where, $\hat{\widetilde{\Theta}}[k]$ and $\hat{\widetilde{\Theta}}[k-1]$ indicate estimated values of the controller parameters at any instant $[k]$ which are based on the previous instant $[k-1]$.

In the above Least Square Algorithm (LSA) estimation equations the controller parameters are updated as a vector of order $(mmn \times 1)$ and the Projection Operator Matrix $\mathcal{P}[k-d]$ is updated as a $(mmn \times mmn)$ matrix. Updating such a higher order matrix for large number of DOF's and small sampling times would require higher computational efforts. Hence a modification of the above described algorithm is derived. This updates the controller parameters as a matrix of order $(m \times mn)$ and the projection operator matrix as $(mn \times mn)$ matrix. To achieve this, the above equation is expanded to be represented as matrix update equations using special properties of the constituent matrices. Since the matrices are diagonal in nature it is

possible to write Eq.7.56 as

$$\begin{aligned}
\hat{\bar{\Theta}}_1[k] &= \hat{\bar{\Theta}}_1[k-1] + \mathcal{P}^{(1)}[k-d-1]\bar{\phi}[k-d]\left[r_{11} + \bar{\phi}[k-d]^T\mathcal{P}^{(1)}[k-d-1]\phi[k-d]\right]^{-1} \\
&\qquad \left[\Delta U_1[k-d] - \bar{\phi}[k-d]^T\hat{\bar{\Theta}}_1[k-1]\right] \\
&\vdots \qquad\qquad \vdots \qquad\qquad \vdots \\
\hat{\bar{\Theta}}_i[k] &= \hat{\bar{\Theta}}_i[k-1] + \mathcal{P}^{(i)}[k-d-1]\bar{\phi}[k-d]\left[r_{ii} + \bar{\phi}[k-d]^T\mathcal{P}^{(i)}[k-d-1]\phi[k-d]\right]^{-1} \\
&\qquad \left[\Delta U_i[k-d] - \bar{\phi}[k-d]^T\hat{\bar{\Theta}}_i[k-1]\right] \\
&\vdots \qquad\qquad \vdots \qquad\qquad \vdots \\
\hat{\bar{\Theta}}_m[k] &= \hat{\bar{\Theta}}_m[k-1] + \mathcal{P}^{(m)}[k-d-1]\bar{\phi}[k-d]\left[r_{mm} + \bar{\phi}[k-d]^T\mathcal{P}^{(m)}[k-d-1]\bar{\phi}[k-d]\right]^{-1} \\
&\qquad \left[\Delta U_m[k-d] - \bar{\phi}[k-d]^T\hat{\bar{\Theta}}_m[k-1]\right]
\end{aligned}$$

And the projection operator terms as

$$\begin{aligned}
\mathcal{P}^{(1)}[k-d] &= \mathcal{P}^{(1)}[k-d-1] - \mathcal{P}^{(1)}[k-d-1]\bar{\phi}[k-d]\left[r_{11} + \phi[k-d]^T\mathcal{P}^{(1)}[k-d-1]\right. \\
&\qquad \left.\bar{\phi}[k-d]\right]^{-1}\bar{\phi}[k-d]^T\mathcal{P}^{(1)}[k-d-1] \\
&\vdots \qquad\qquad \vdots \qquad\qquad \vdots \\
\mathcal{P}^{(i)}[k-d] &= \mathcal{P}^{(i)}[k-d-1] - \mathcal{P}^{(i)}[k-d-1]\bar{\phi}[k-d]\left[r_{11} + \bar{\phi}[k-d]^T\mathcal{P}^{(i)}[k-d-1]\right. \\
&\qquad \left.\bar{\phi}[k-d]\right]^{-1}\bar{\phi}[k-d]^T\mathcal{P}^{(i)}[k-d-1] \\
&\vdots \qquad\qquad \vdots \qquad\qquad \vdots \\
\mathcal{P}^{(m)}[k-d] &= \mathcal{P}^{(m)}[k-d-1] - \mathcal{P}^{(m)}[k-d-1]\bar{\phi}[k-d]\left[r_{11} + \bar{\phi}[k-d]^T\mathcal{P}^{(m)}[k-d-1]\right. \\
&\qquad \left.\bar{\phi}[k-d]\right]^{-1}\bar{\phi}[k-d]^T\mathcal{P}^{(m)}[k-d-1]
\end{aligned}$$

$where,\ i \in \{1,\cdots,m\}$

(7.57)

In these equations each of the submatrix ($\mathcal{P}^{(i)}[k-d]$) of the projection operator matrix $\mathcal{P}$ is of the order ($mn \times mn$) and $\bar{\phi}[k-d]$ and $r_{ii}$ are of the orders ($mn \times 1$) and ($1 \times 1$) respectively. An assumption that the initial conditions on the submatrices of projection operator matrix are all equal and are assumed to be matrices of the following form is made.

$$\begin{aligned}
\mathcal{P}^{(i)}[j] &= \mathcal{P}_0^* \\
\mathcal{P}^{(1)}[0] &= \cdots = \mathcal{P}^{(i)}[0] = \cdots = \mathcal{P}^{(m)}[0] = \mathcal{P}_0^* \\
where, &\quad i \in \{1,\cdots,m\} \\
&\quad j \in \{-d,\cdots,0\}
\end{aligned} \tag{7.58}$$

From Eq.7.57 it can be observed that the Projection operator submatrices are updated on the basis of the previous terms $\bar{\phi}[k-d]$ and $r_{ii}$, hence

$$\mathcal{P}^{(i)}[k-d] = Fn.\left(\mathcal{P}^{(i)}[k-d-1], \bar{\phi}[k-d], r_{ii}\right) \tag{7.59}$$

Let us assume the gain matrix to be of the form

$$\begin{aligned} &\mathcal{R} = r\mathcal{I}_m \\ &\Rightarrow r_{11} = \cdots = r_{ii} = \cdots = r_{mm} = r \end{aligned} \tag{7.60}$$

Eq.7.57 could be simplified by using Eqs. 7.58, 7.59 and 7.60 and applying the process of Mathematical Induction as follows

**Step 1:** At the initial conditions ($k = 0$) the Projection operator submatrices are all equal and are equal to ($\mathcal{P}_0^*$).

**Step 2:** Let us assume that the Submatrices ($\mathcal{P}^{(i)}$) are equal for all values of $i \in \{1, \cdots, m\}$ at some $[k-d-1]$

**Step 3:** From Eqs. 7.58 and 7.59 it could be deduced that the Submatrices ($\mathcal{P}^{(i)}$) are equal for all values of $i \in \{1, \cdots, m\}$ at $[k-d]$

**Step 4:** Hence the Submatrices of Projection operator matrices are the same for all $i \in \{1, \cdots, m\}$ as $k \to \infty$.

The simplified form of Eq.7.57 for any $i$ could be written as

$$\begin{aligned} \hat{\bar{\Theta}}_i[k] &= \hat{\bar{\Theta}}_i[k-1] + \frac{\mathcal{P}^*[k-d-1]\bar{\phi}[k-d]\left[\Delta U_i[k-d] - \bar{\phi}[k-d]^T\hat{\bar{\Theta}}_i[k-1]\right]}{\left[r + \bar{\phi}[k-d]^T\mathcal{P}^*[k-d-1]\bar{\phi}[k-d]\right]} \\ \mathcal{P}^*[k-d] &= \mathcal{P}^*[k-d-1] - \frac{\mathcal{P}^*[k-d-1]\bar{\phi}[k-d]\bar{\phi}[k-d]^T\mathcal{P}^*[k-d-1]}{\left[r + \bar{\phi}[k-d]^T\mathcal{P}^*[k-d-1]\bar{\phi}[k-d]\right]} \end{aligned} \tag{7.61}$$

where, the matrices $\mathcal{P}^*[k-d-1]$ and $\mathcal{P}^*[k-d]$ represent the submatrices of the Projection operator matrix $\mathcal{P}$. Above equation could be expressed in the form

$$\begin{aligned} \left[\hat{\bar{\Theta}}_i[k] - \hat{\bar{\Theta}}_i[k-1]\right] = \frac{\mathcal{P}^*[k-d-1]\bar{\phi}[k-d]}{\left[r + \bar{\phi}[k-d]^T\mathcal{P}^*[k-d-1]\bar{\phi}[k-d]\right]} [\Delta U_i[k-d] - \\ \bar{\phi}[k-d]^T\hat{\bar{\Theta}}_i[k-1]\Big] \end{aligned} \tag{7.62}$$

The above equation represents that every set of controller parameters $\left(\hat{\bar{\Theta}}_i[k]\right)$ of order $(mn \times 1)$ differ from the previous values $\left(\hat{\bar{\Theta}}_i[k-1]\right)$ by a constant times the error. Equation 7.61 could be transformed to a row matrix by a transpose operation to the following form

$$\hat{\bar{\Theta}}_i[k]^T = \hat{\bar{\Theta}}_i[k-1]^T + \frac{\left[\Delta U_i[k-d] - \hat{\bar{\Theta}}_i[k-1]^T \phi[k-d]\right] \phi[k-d]^T \mathcal{P}^*[k-d-1]^T}{\left[r + \phi[k-d]^T \mathcal{P}^*[k-d-1]^T \phi[k-d]\right]} \tag{7.63}$$

Equation 7.63 for different values of $i \in \{1, \cdots, m\}$ could be used to form an array of matrix updating equations of the form

$$\hat{\bar{\Theta}}[k]^T = \hat{\bar{\Theta}}[k-1]^T + \frac{\left[\Delta U[k-d] - \hat{\bar{\Theta}}[k-1]^T \bar{\phi}[k-d]\right] \bar{\phi}[k-d]^T \mathcal{P}^*[k-d-1]^T}{\left[r + \bar{\phi}[k-d]^T \mathcal{P}^*[k-d-1]^T \bar{\phi}[k-d]\right]}$$

$$\mathcal{P}^*[k-d] = \mathcal{P}^*[k-d-1] - \frac{\mathcal{P}^*[k-d-1]\phi[k-d]\bar{\phi}[k-d]^T \mathcal{P}^*[k-d-1]}{\left[r + \bar{\phi}[k-d]^T \mathcal{P}^*[k-d-1]^T \phi[k-d]\right]} \tag{7.64}$$

$$where, \quad \hat{\bar{\Theta}}[k]^T = \begin{Bmatrix} \hat{\bar{\Theta}}_1[k]^T \\ \vdots \\ \hat{\bar{\Theta}}_i[k]^T \\ \vdots \\ \hat{\bar{\Theta}}_m[k]^T \end{Bmatrix}$$

The Control law in Eq.7.49 could be modified by using the controller parameters estimation law derived in Eq.7.63 as

$$\Delta U^*[k] = \hat{\bar{\Theta}}[k]^T \phi'[k] \tag{7.65}$$

The basic convergence properties of the least squares estimator with the parameters being updated as a matrix are derived as described in Appendix C. These are based on the properties of a least square estimator, where the control parameter is in the form of a vector [146]. The global convergence properties of the multi-input multi-output DMRAC system with the above control law applied along with the least squares estimation are proved as described in Appendix C. The algorithm as derived in Appendix C shows strong global convergence for a highly nonlinear time varying

problem along with the presence of least square parameter estimator. The design's convergence is enhanced by the judicious application of basic convergence properties of the parameter estimator. The controller hence shows a closed loop stability and the output tracking error asymptotically goes to zero giving perfect model tracking.

## 7.5 Simulation Results

The discrete adaptive controller developed is implemented on a multi-degree of freedom NTV half-car model as shown in Fig.2.9. The adaptive active suspension results are compared with that of a passive suspension and the reference model throughout the presentation.

For simulation purposes the following nominal parameter values for half-car model are assumed.

$M_s^* = 500\,Kg$, $K_l^* = K_t^* = 17\ \frac{kN}{m}$, $C_l^* = C_t^* = 2500\ \frac{Ns}{m}$, $I = 500 * (1.5)^2\ kgm^2$, $K_{tire}^* = 100\ \frac{kN}{m}$, $K_{es_l} = K_{es_t} = 80\ \frac{kN}{m}$, $D = 0.25\ m$, $d_1 = d_2 = 1.5\ m$.

The reference model parameters are chosen as follows.

$M_{m_s} = 500\,Kg$, $K_{m_l} = K_{m_t} = 17\ \frac{kN}{m}$, $C_{m_l} = C_{m_t} = 9\ \frac{kNs}{m}$, $D_{m_l} = D_{m_t} = 9\ \frac{kNs}{m}$, $I_m = 500 * (1.5)^2\ kgm^2$, $K_{m_{tire}} = 100\ \frac{kN}{m}$.

The DMRAC controller designed is implemented on a computer and the vehicle model is subjected to various excitations and operating conditions as assumed in chapter 2, under *Parametric variations mode I* with *Excitation mode I* and *Excitation mode II*. The controller designed should be robust to this type of parameter variations and at the same time should be able to achieve the optimal performance as required by the reference model shown in Figs. 7.2 and 7.3. The controller should also maintain static equilibrium levels under Parametric variations as described in *mode I* and is robust to the operating conditions.

### 7.5.1 Time Domain Results for *Excitation mode I* and *Parametric variations mode I*

The half-car NTV active suspension model as shown in Fig.2.9 has been subjected to the adaptive control actuator forces calculated from Eq.7.65. The time domain results are obtained by solving the dynamic equations 7.1 subjected to the parameter variations as described by *Parametric variations mode I*. The passive suspension response indicates the output by solving the NTV model. The reference model response indicates the dynamic performance of reference model shown in Fig.7.1 and is obtained by solving equation 7.17 subjected to *Excitation mode I*. Fig.7.1 shows the carbody bounce DOF absolute displacement response in the time domain for the reference, active and passive models. The adaptive active suspension adapts to the reference model within first 4 secs., but deviates slightly at the $20^{th}$ sec. when subjected to acceleration manoeuvre. But the vehicle active suspension model adapts to the reference model within the next 5 secs. and remains robust for any further variations. The response is very robust in the bounce DOF at the $40^{th}$ sec., when the vehicle under goes rapid deceleration manoeuvre. Fig.7.5 shows the pitch DOF angular displacement response for reference model, adaptive active suspension and passive suspension models. This figure indicates that the adaptive active system adapts to the reference model within 4 secs., but the controller provides the actuator forces necessary at the $20^{th}$ and $40^{th}$ secs. for elimination of squat and nose dive respectively. Fig.7.5 shows the comparison of passive suspension with respect to active suspension and also indicates elimination of $6^{\circ}$ of nose dive during braking manoeuvre due to adaptation capabilities of active suspension. This figure shows the positive benefits that could be achieved by incorporating adaptive control techniques in the active suspension implementation.

Fig.7.6 shows the leading and trailing actuator forces that are evaluated and applied by the adaptive active suspension. This figure also shows that the leading actuator applies a compressive force whereas the trailing actuator applies a tensile force

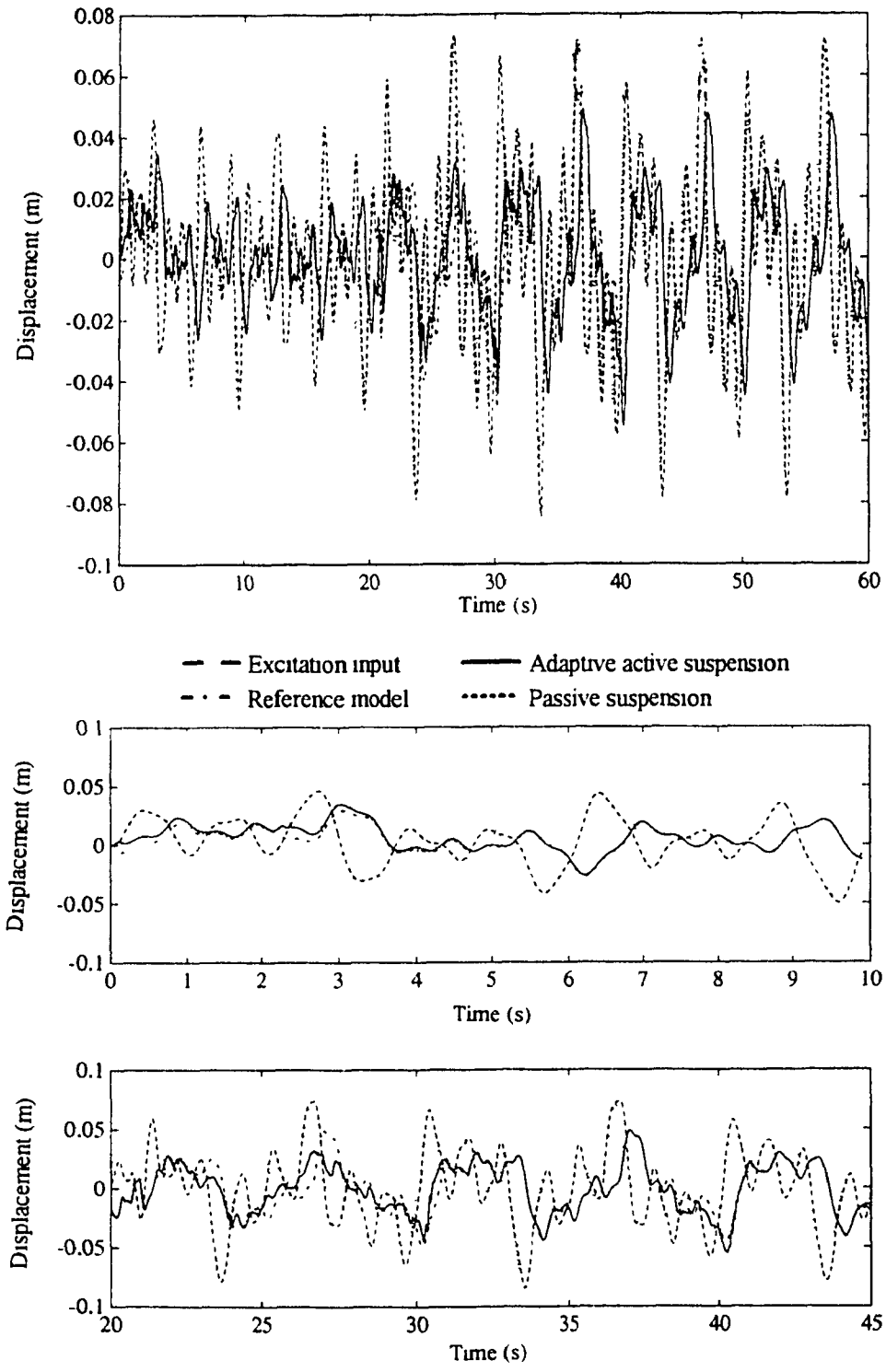


Fig.7.4 : Carbody bounce degree of freedom displacement response for *Excitation mode I & Parametric variations mode I.*

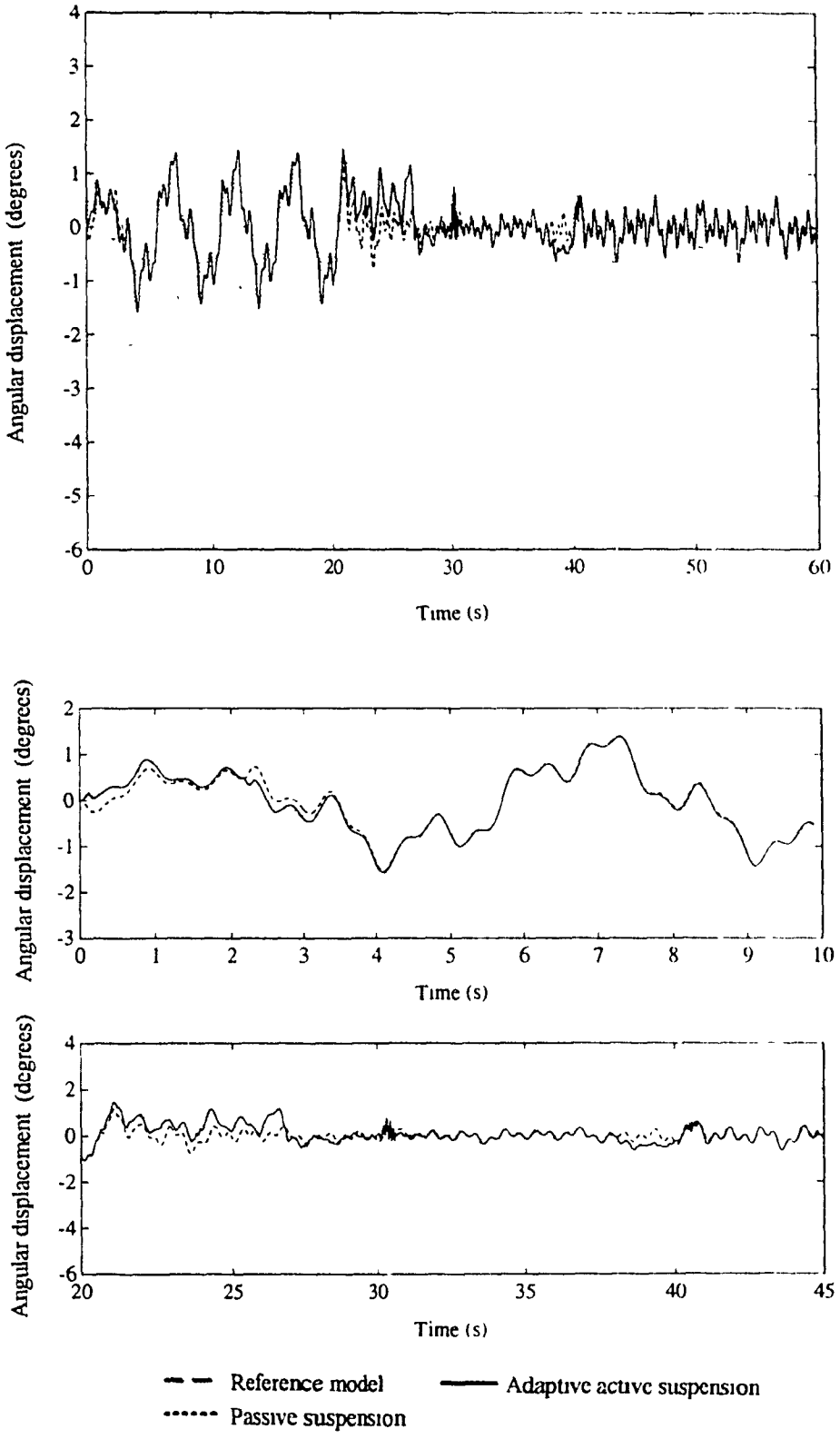


Fig.7.5: Carbody pitch degree of freedom angular displacement response for *Excitation mode I* and *Parametric variations mode I.*

at 20-30 secs. range, to compensate for the squat phenomenon due to acceleration of the vehicle. But during the deceleration at $40^{th}$ sec., the polarities are reversed and the leading actuator applies a higher tensile force to reduce the nose dive phenomenon. The actuator requirement as seen in the figure needs to be studied for the type of actuators needed for implementation. Figures show reasonably lower values of the forces required for the adaptation and maintenance of model following phenomenon due to the failsafe configuration. The average value of the actuator force needed at acceleration and deceleration conditions indicate the load shifts during manoeuvres. Fig.7.7 shows the error in the model following between the active suspension and the reference model in the carbody pitch DOF. This figure also indicates that the error behaves as an undamped system when excited by a disturbance but has a negative exponential window function that reduces the amplitude to zero at an exponential rate. The error function for other DOF's shows similar performance.

### 7.5.2 Time and Frequency Domain Results for Excitation Mode II

The models described earlier are subjected to the dirt road random excitation input as described by *Excitation mode II*. Figs.7.8 and 7.9 show the time domain bounce and pitch DOF responses for the reference, active and passive suspensions. These figures indicate that the active suspension system adapts to the reference model within the first 4 secs., and remains robust during the period of operation. The active suspension follows the reference model response very closely through out the simulation period. The reference model responses in the frequency domain have been presented in Figures 7.2 and 7.3. They indicate good vibration isolation and reduction of the suspension travel at the same time. The adaptive active suspension time domain results which indicate good adaptation to the reference model extends similar responses in the frequency domain. Hence an adaptive active suspension achieves an optimal performance by reducing the vibration isolation and suspension travel, but

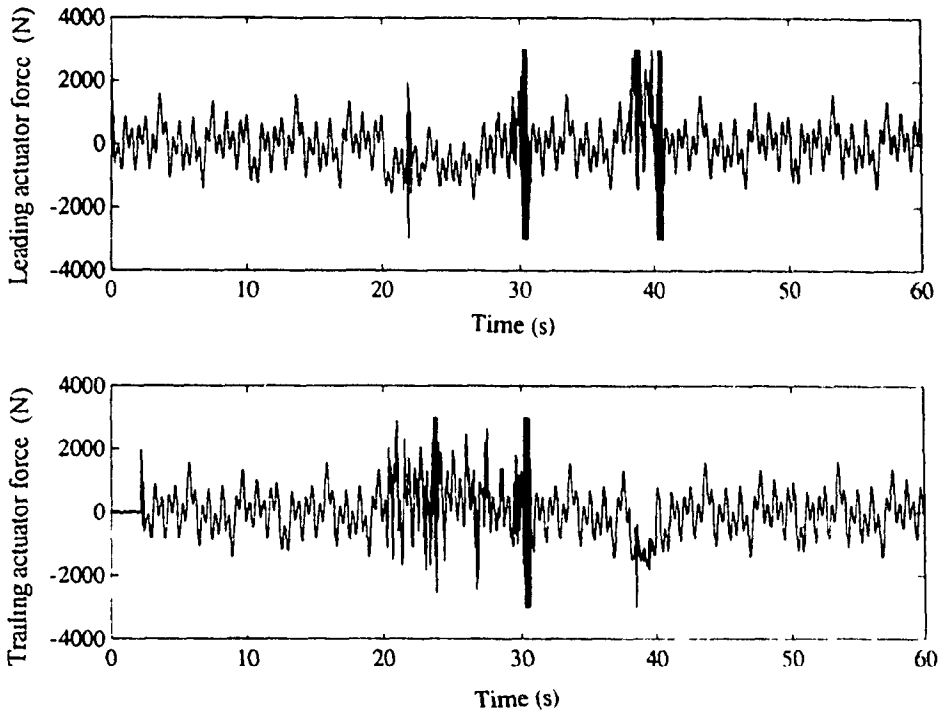


Fig.7.6: Leading and trailing actuators adaptive control forces.

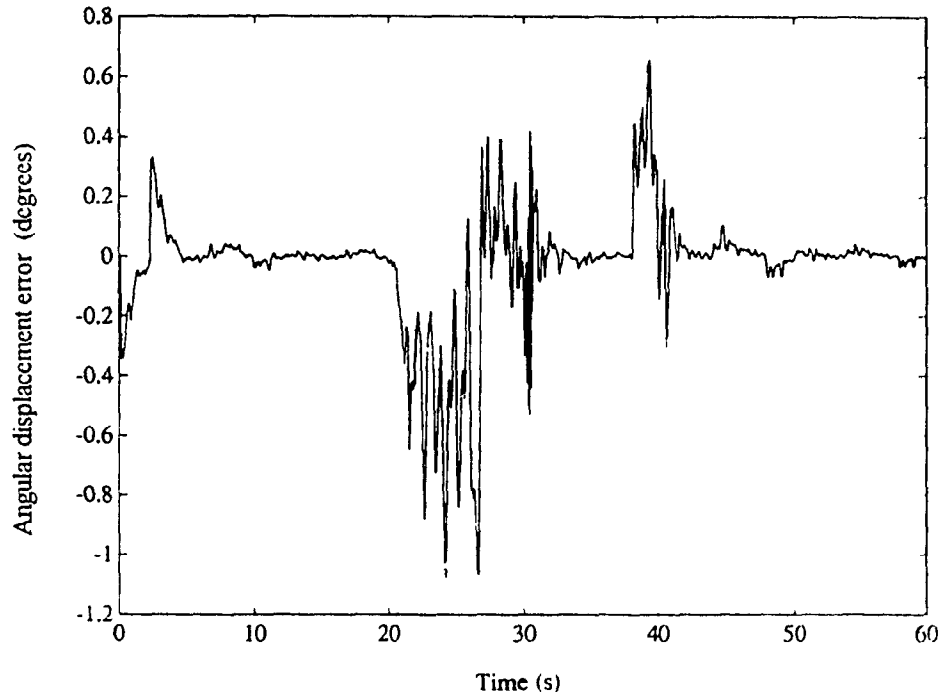


Fig.7.7: The adaptive active suspension pitch degree of freedom model following error.

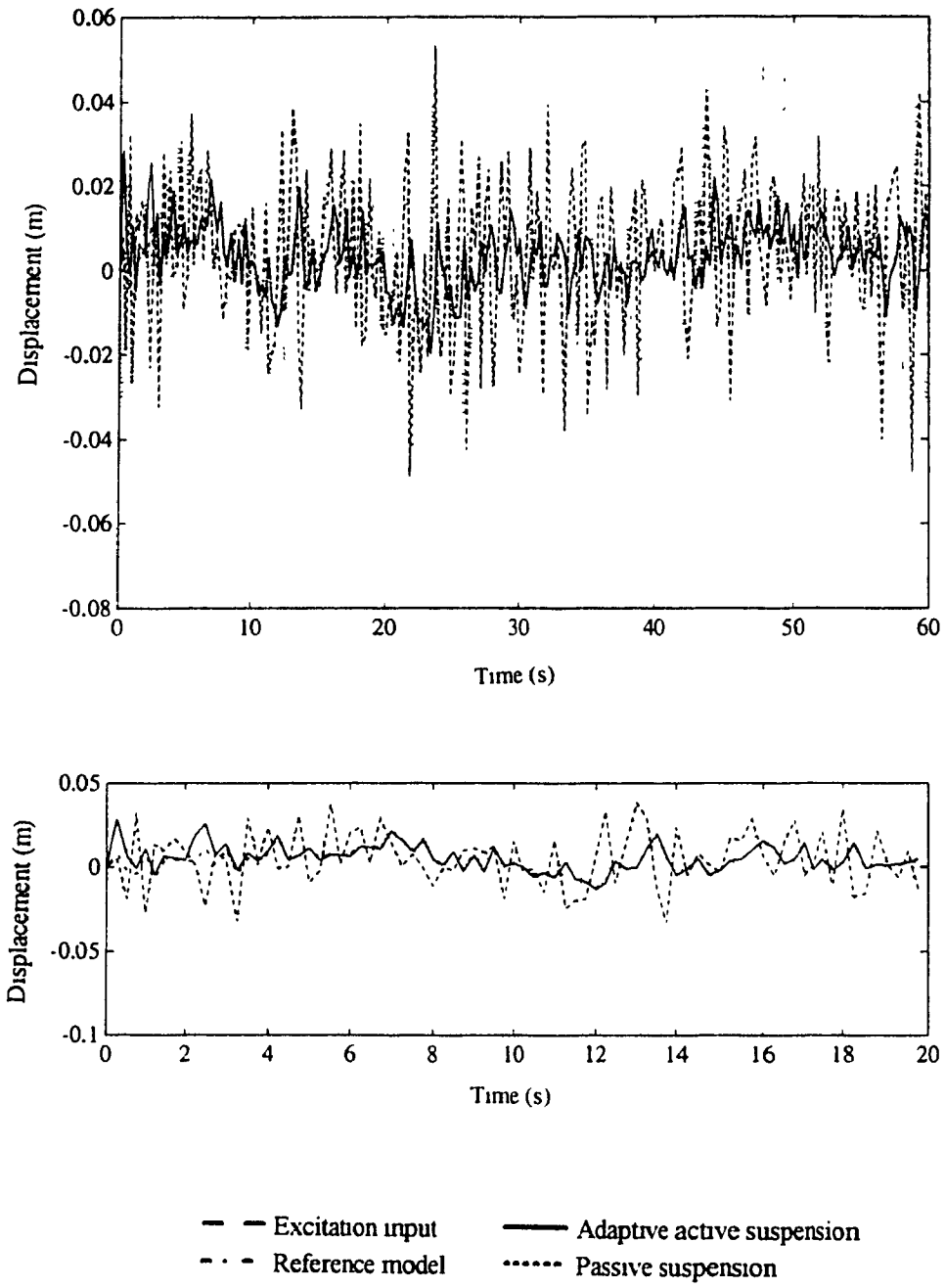


Fig.7.8: Carbody bounce degree of freedom displacement response for *Excitation mode II.*

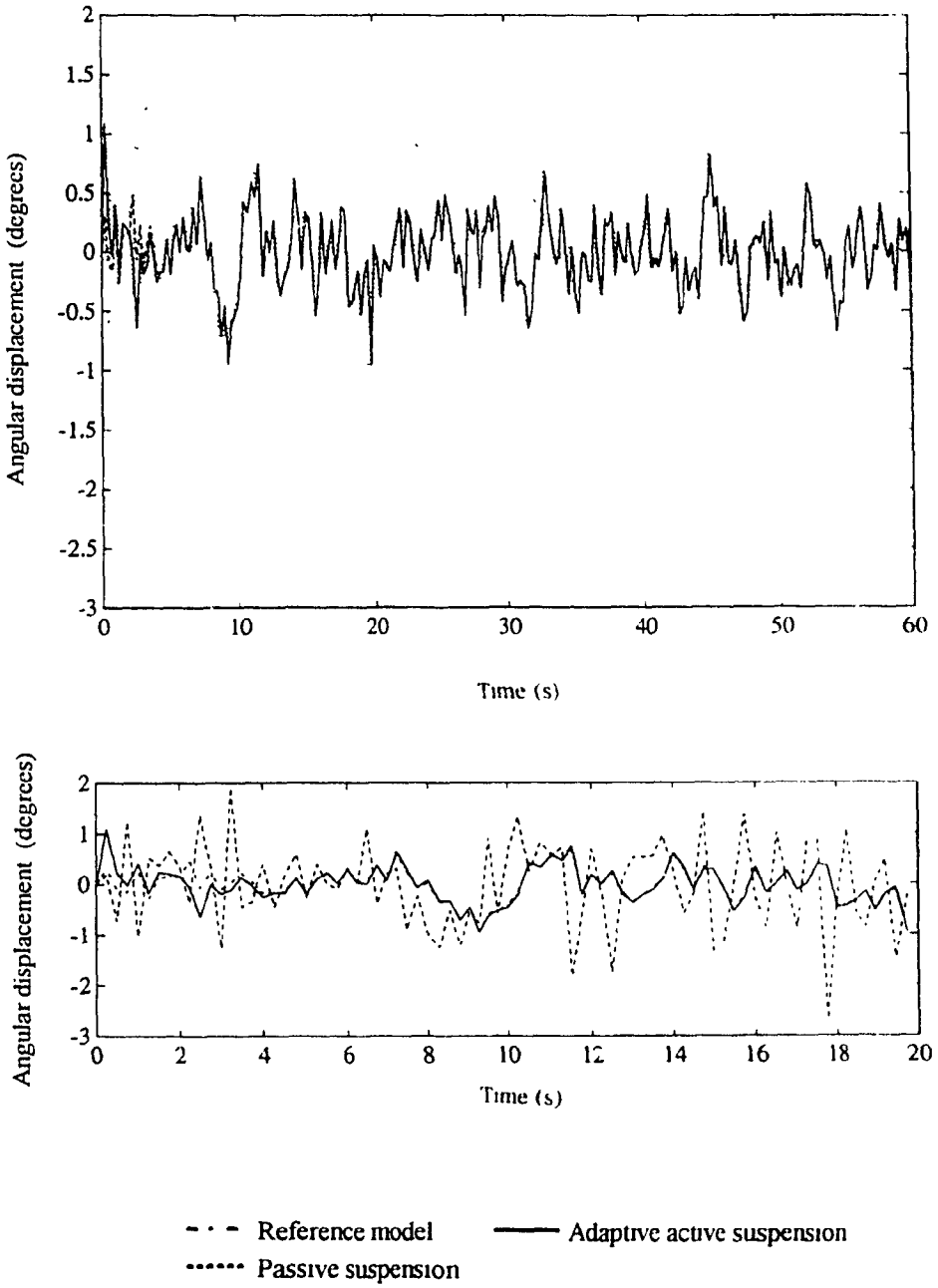


Fig.7.9: Carbody pitch degree of freedom displacement response for *Excitation mode II*

at the same time satisfying the adaptive active suspension requirements. Some of the results indicating the system response for *Excitation mode II* are presented in this section. Fig.7.10 shows the system gain factor of leading unsprung mass bounce displacement degree of freedom with respect to the leading excitation input. This figure shows the adaptive active suspension response to coincide with the reference model response over the entire range. The suspension response indicates higher magnitudes at the natural frequencies and higher frequencies. Figures 7.11 and 7.12 indicate the system gain factor representation of the leading suspension and unsprung relative displacements with respect to the leading excitation input. The responses in these figures also indicate that the adaptive active suspension closely follows the reference model for the *Excitation mode II*. These figures indicate reduction of the relative displacement responses at the natural frequencies compared to the passive suspension response.

## 7.6 Discussion

Simulation results obtained for the deterministic input are based on the sampling interval of 0.01 seconds. Since the sampling frequency is not very high, the hardware necessary for practical implementation need not be sophisticated. This would also increase the reliability and ruggedness of the hardware that could be used and at the same time would reduce the installation and maintenance costs. A lesser sampling interval would improve the tracking performance further due to faster computer control. The initial controller parameters ($\hat{\Theta}^{'T}$) can be chosen to be of any arbitrary values. Better transient response in model following could be achieved by having some knowledge about the initial values of the gains. The reference model need not be physically realizable and its parameters are coded in the controller. The performance required could be specified by varying the damping and natural frequency parameters of the reference model in the controller. The active suspension results obtained above could be varied by just specifying the reference model parameters. The control law derived

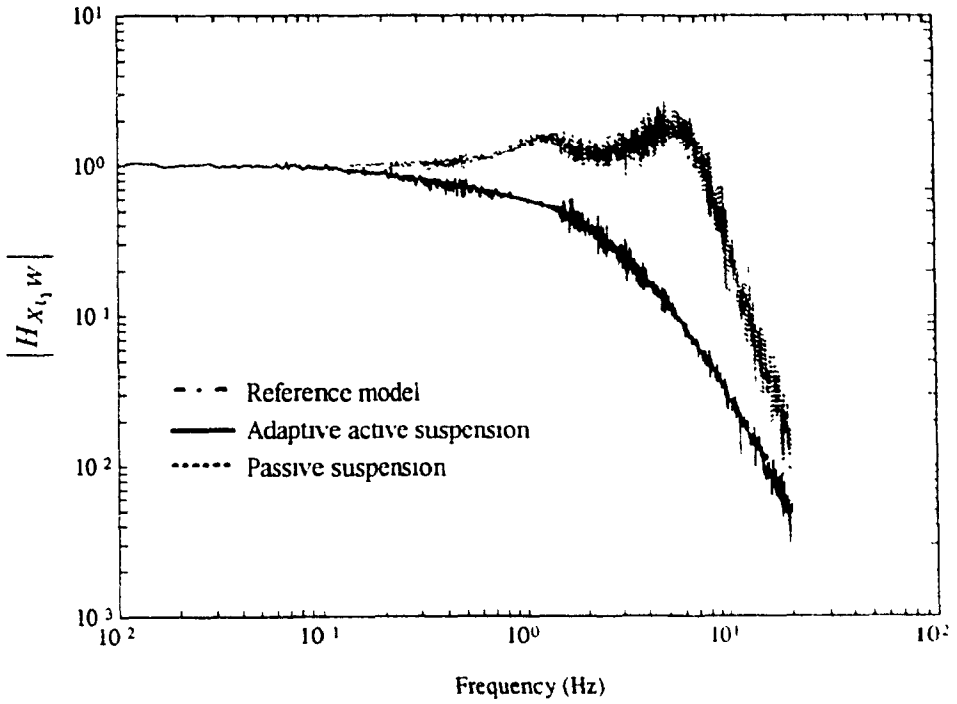


Fig.7.10: System gain factor of leading unsprung mass bounce displacement response with respect to the leading excitation input.

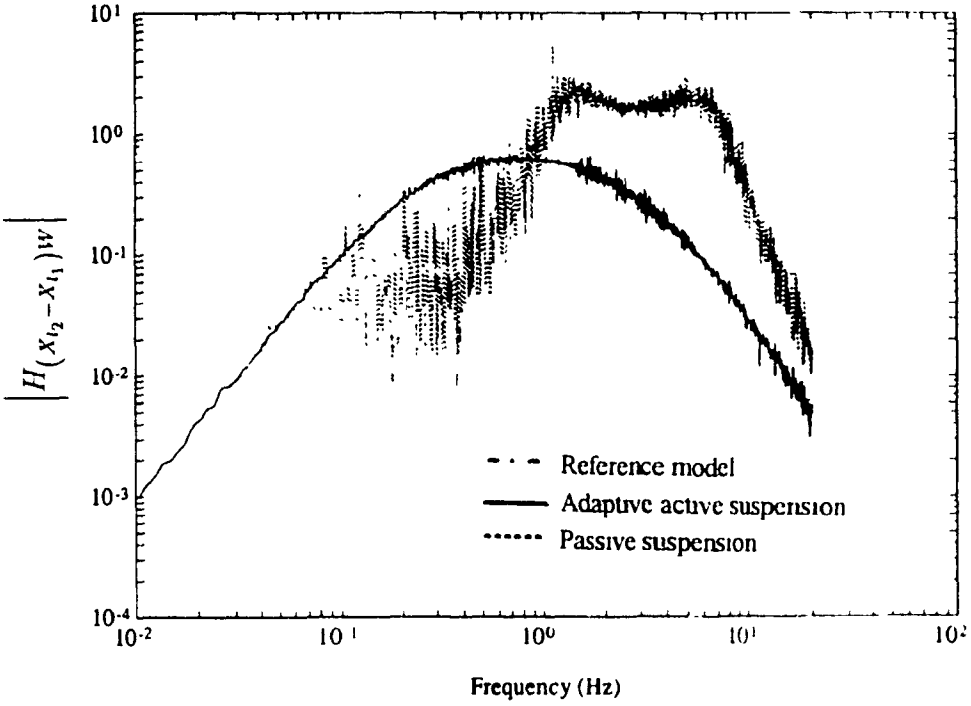


Fig.7.11: System gain factor of leading suspension relative displacement response with respect to the leading excitation input.

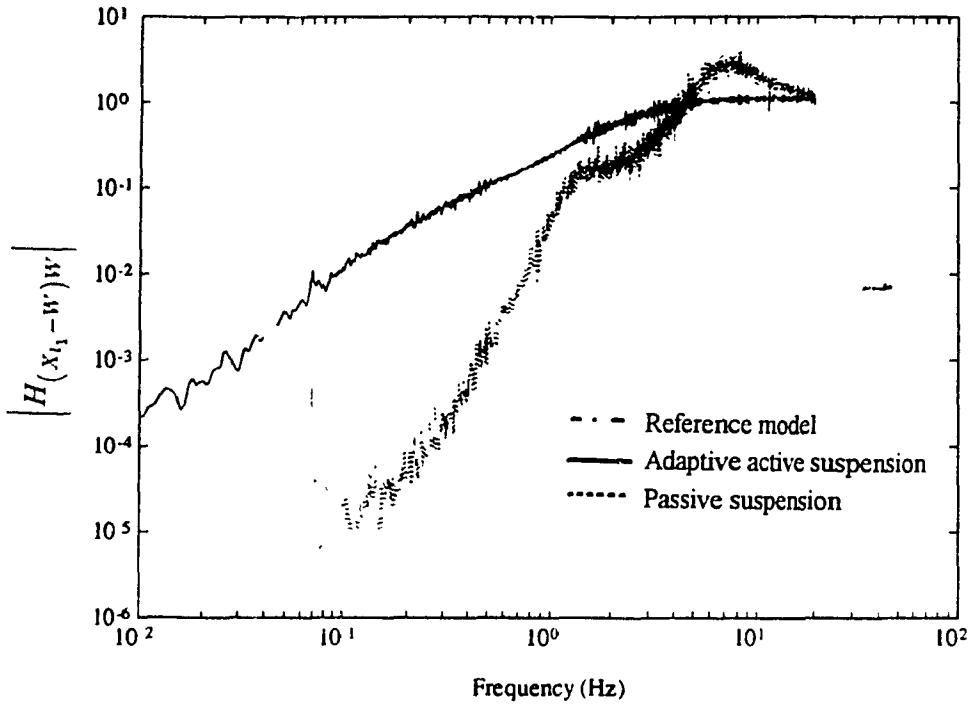


Fig.7.12: System gain factor of leading unsprung mass relative displacement response with respect to the leading excitation input.

in Eq.7.65 indicates that some sort of preview control is necessary. Controllers based on preview sensors have been designed in the past which could achieve some excellent qualities of vehicle performance as discussed in Refs. [1] and [161]. But estimation equations could be developed to estimate these values based on past knowledge. Also, since the controller is adaptive in nature, these terms could be truncated and other gains would be updated depending on the error.

A MDOF MRAC control system with a decoupled and a decentralized controller can be designed. This assigns an independent processing unit for each DOF. The decentralized structure and the simple controller makes the scheme computationally very fast and is amenable to parallel processing implementation within a distributed computing architecture, with a microprocessor dedicated to each DOF. Decoupling of the actuators in the case of MDOF would give an improved performance and at the same time would ease the controller design and implementation.

## 7.7 Summary

The adaptive control of active suspension for a multi-degree of freedom system has been analyzed in the discrete domain. A half-car nonlinear time varying model has been represented by the dynamic equations. A dual skyhook reference model that was used for model following has been represented in terms of the dynamic equations. Deterministic auto regressive moving average (DARMA) models for a linearized half-car and a reference model have been developed and used for DMRAC control involving recursive least square estimation and covariance modification. A modified version of the least square estimation in which the parameters are updated as a matrix thereby reducing the order of the projection operator matrix has been implemented. This reduces the computational efforts in evaluating the adaptive control law and estimating the controller gains. Simulation results in time domain and frequency domain for *Excitation mode I and II* and *Parametric variations mode I* have been presented.

The results indicate good initial adaptation and the adaptive active suspension is very robust for large dynamic load shifts during longitudinal manoeuvres.

# Chapter 8

# Experimental Validation of Failsafe Adaptive Active Suspension Simulation Results

## 8.1 General

This chapter enumerates the efforts made in the experimental validation of single degree of freedom (SDOF) adaptive active suspension. It has been a challenging affair for the research community to validate the theoretical results obtained in active suspension. In the literature, no efforts have been made for experimental validation of adaptive active suspension in general and a failsafe adaptive active suspension that requires less control forces in particular. The force generators being the most important component in the hardware that is required, the state of the art in implementing active suspension in terms of actuators used is briefly itemized below.

**Electromagnetic:** The electromagnetic actuator has been found to be very promising because of its robustness and reliability as it has the advantage of having few moving parts. The frequency response is very good even beyond 50 Hz but its high weight can hinder it for various applications. Prototype actuators

have been constructed and tested, and the results show that acceleration in the vehicle body due to rigid modes can be halved and bogie modes have been very effectively reduced below 8 Hz. Unlike other actuators this does not need high power even at higher frequencies. An improved active magnetic suspension configuration with a position controller was proposed by Sridharan [149]. A BT 10 rail bogie attached with neat double acting magnets between bolster and bogie has been described in Ref.[39]. This reference also describes the results for bogie and pitch modes obtained. Stuart of Aura systems, Los Angeles in Ref [150], described the success of smart magnetic suspensions which consume no more than 0.25 horsepower (hp) under normal conditions and utmost 3 hp in severe manoeuvre such as panic stops from the engine through an alternator.

**Air-pump Actuator:** The air pump actuator replaces the fixed volume reservoir with a variable volume which is varied by moving a diaphragm in and out via a nut and lead screw through an electric motor. The ride height and force transmitted are changed as functions of pressure and volume of the air spring. An air pump actuator was fitted to an Advanced passenger Train (APT) test vehicle and the results for pitch and bounce motions are described in Ref.[39].

**Servo-Hydraulic Actuator:** A servo-hydraulic actuator for lateral suspension control has been placed in parallel with the air springs at each end of the APT test vehicle. The improvement obtained in the lateral oscillations for force levels of 2-3 KN rms and power consumption of 1 kW per actuator is described in [39].

**Electromechanical Actuator:** Here, an electric motor drives through a belt to a leadscrew lying parallel to the motor which operates between the body and the bogie frame. This can be used to replace the lateral damping hence realizing a pure active suspension. The actuator can also be deemed as a failsafe suspension as it acts as an electrical damper in case of a failure of any active component.

**Electro-Pneumatic Actuator:** This has been used successfully for railroad passenger cars where the pneumatic servo elements are mounted parallel to the

conventional air spring and lateral hydraulic damper. About a 50% reduction of lateral vibration was found when tests were performed with the series 485 limited Express Electric cars on the Touhoku line by Okamoto et al. [151] and [152]. Discrete time state space equations incorporating the control valve delay of electropneumatic proportional pressure control valves and the results of a pneumatic active air suspension have been discussed by Matsushita et al. in [153].

Due to the availability of hardware and expertise in the servo controlled electro hydraulic systems in the Mechanical Engineering Department and in particular to vehicle systems at CONCAVE Research Center, Concordia University, a hydraulic force generator has been chosen. The following sections describe various steps which were taken both in terms of hardware and software and their integration to realize a complete setup.

## 8.2 Initial Hardware and Software Setups

In this section, a brief description of various hardware and software tools developed for final implementation of SDOF adaptive active suspension has been given. The components and all the circuitry have been built as modules and are tested independently for the evaluation of their characteristics.

### 8.2.1 Software Modules

For the purpose of practical implementation, the SDOF discrete model reference adaptive controller (DMRAC) developed in chapter 4 has been transformed to a software module. The software has been mainly divided into two capsules which have been designed for a PC based system using C language and Graphical routines. *Capsule A*

provides a Windows based selection of the test parameters. The menu driven Windows prompt for various provisions, collects the information and stores it as data files. This provision would simplify the testing procedure by selecting various excitation inputs, both deterministic and random, and various vehicle model parameter variations. Figure 8.1 shows a complete self explanatory snap shot of the final test data entry screen for the adaptive active suspension simulator. As shown in the final screen, it is an interactive program which accepts various time domain parameters such as simulation interval and time step for the control. It also selects various deterministic or random excitation inputs to check the adaptation capabilities. As shown in Fig.8.1, a wide selection of deterministic inputs are incorporated. The program can also generate random excitations of the nature of Asphalt road, Dirt road and Paved road. The data selection provision incorporates either selection of nominal values, changes whose knowledge is basically used to evaluate a comparative passive suspension response. A priori knowledge of these values or changes are not necessary for the actual controller. Approximate nominal values for the passive suspension simulation and a reference model are required to be given along with the approximate time delay in terms of the time step. Information about the controller status (on/off), type of controller gains estimator are also given. Finally, the program displays complete selected parameters for evaluation and check out.

The second *Capsule B* is the controller module that uses the selected information in *Capsule A* and involves the data acquisition from the actual hardware and control input modulation. Omega (Metrobyte) data acquisition board DAS 20 has been used as a hardware interface. C language server routines have been used for the DAC/ADC operations. The complete vehicle control program contains modules for excitation, state space representation of the reference model, state space representation of a passive suspension model, Runge-Kutta Solver, Controller modules and finally the interface with active suspension hardware. All these modules are independent and could be varied independently for any changes required in that module. DAC ports of the hardware interface unit have been used for sending digital to ana-

log command signals for the primary excitation hydraulic circuit and the secondary actuator to implement the controller output. ADC ports are used for data acquisition and feedback signals. The controller module involving the recursive least square estimation of the controller parameters with covariance modification as described in chapter 4 has been developed to calculate the control force required by the actuator.

As shown in Fig.8.2, the software provides graphical display Windows for on line simulation and animation of the results. The simulation Windows indicate the performance of the controller and allows for comparison with the passive suspension. The suspension parameters which closely coincide with the actual model have been used for the on line passive suspension simulation. The animation Window would incorporate the signals from the feedback sensors and are used for graphical illustration of the experimental results. The provisions of simulation and animation Windows are very advantageous for the demonstration of test results and would increase the portability of the testing procedure.

### 8.2.2 Mechanical Hardware

A servo controlled electro-hydraulic position and force feedback software and mechanical hardware modules which form the excitation and actuator forces for the over all system implementation are described in Appendix D. These systems have been developed independently and are tested to evaluate their characteristics. The mechanical hardware involves a servo controlled electro hydraulic actuator with all the hydraulic accessories and horizontal test bed involving the fixtures and feedback signals monitoring instruments.

Appendix D describes the hydraulic actuator with the servo valve and the analog controller used for implementing the position and force control. The test results with various calibration curves are also documented in Appendix D. These results indicate good performance characteristics of the force controller and could be

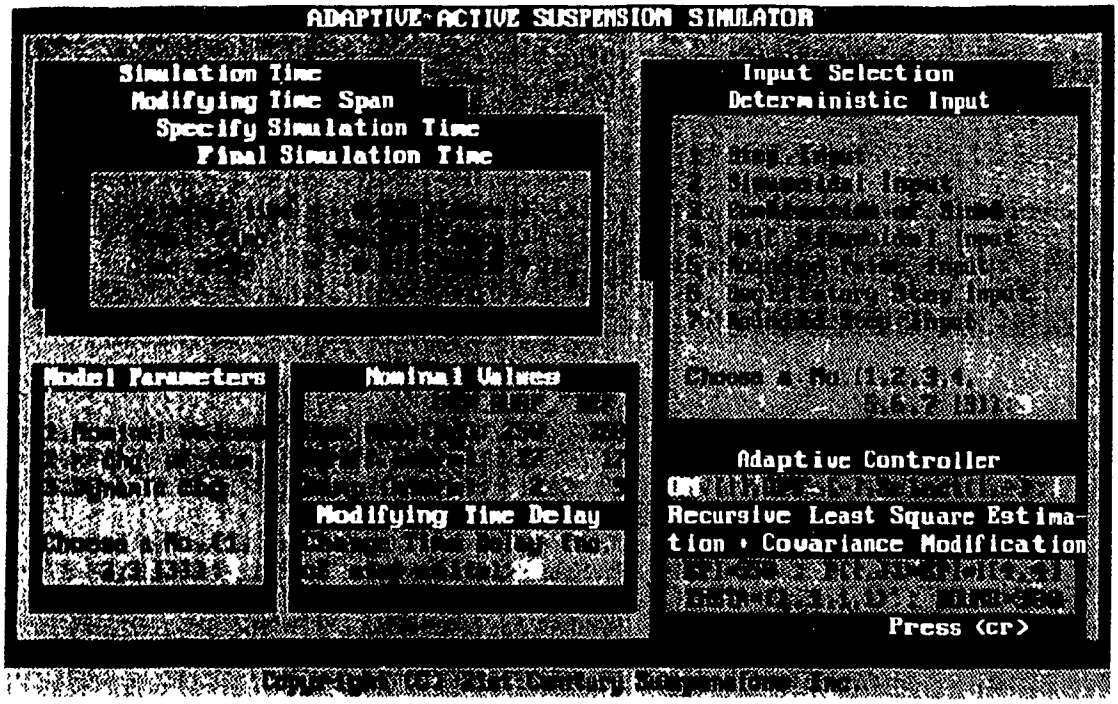


Fig.8.1: Interactive Data Entry for Adaptive Active Suspension Simulator.

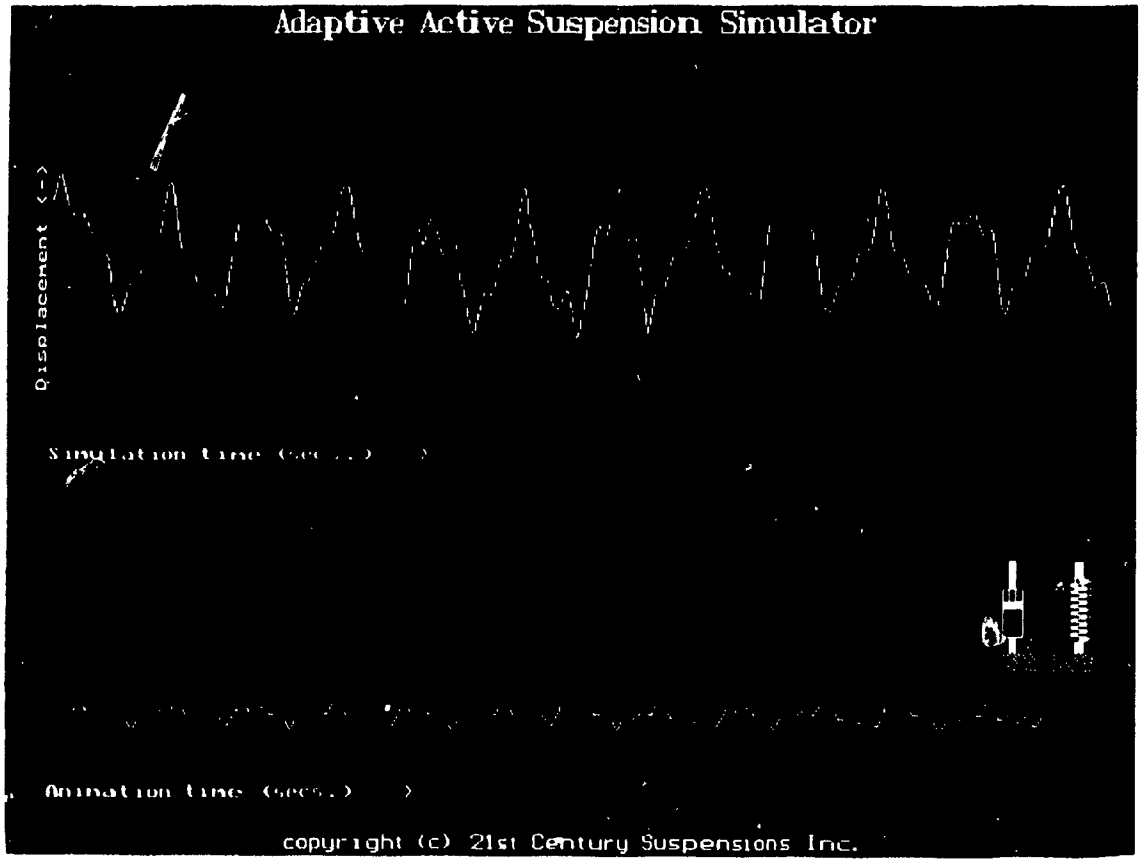


Fig.8.2: Simulation & Animation of the Online Adaptive Active Suspension.

integrated as part of the failsafe active suspension.

## 8.3 Single Degree of Freedom Adaptive Active Suspension Experimental Setup

Various sub setups (discussed in Appendix D) along with some further hardware have been used to realize a complete adaptive active suspension setup.

To experimentally validate the SDOF adaptive active suspension described in chapter 4, various vehicle models have been surveyed. It has been very difficult to obtain detailed information about various individual components such as dampers and coil springs for any particular vehicle. A sports model Porsche 928 has been found to possess some interesting characteristics. This vehicle is considered to be a sports coupe but possess low sprung mass bounce frequency of 1.2 Hz and due to heavy unsprung mass it possess lower wheel hop and tramp modes of 8.6 Hz. But it has very stiff roll stabilizer bars for maintaining the required handling/stability of the vehicle.

The full vehicle specifications for the Porsche 928 vehicle model from reference [160] are as follows.

$$\textit{The Design Sprung mass} = 1385\ kg.$$

$$\textit{Location of C.G.}$$

$$d_1 = 1.275m$$

$$d_2 = 1.225m$$

$$\textit{Coil spring rates}$$

$$\textit{Leading}\ (K_l) = 18.63\ \frac{kN}{m}$$

$$\textit{Trailing}\ (K_t) = 22.55\ \frac{kN}{m}$$

*Shock Viscous Damping Constant*

*Leading* ($C_l$) = 2500 $\frac{Ns}{m}$

*Trailing* ($C_t$) = 2500 $\frac{Ns}{m}$

*Tire Stiffness (vertical)*

$K_{tire}$ = 175 $\frac{kN}{m}$

*Unsprung mass* ($M_{u_l}, M_{u_t}$) = 56 *kg.*

A linear time invariant passive suspension model has been derived from Fig.2.9. This figure shows a half-car model with full failsafe leading and trailing suspensions. Linear equations for the vehicle model with the suspension spring and linear damping between the sprung and unsprung masses have been developed. The homogeneous equations could be written in the form

$$\mathcal{M}\ddot{X} + \mathcal{C}\dot{X} + \mathcal{K}X = 0 \tag{8.1}$$

where,

$$X = \begin{Bmatrix} x_b \\ \theta \\ x_{l_1} \\ x_{t_1} \end{Bmatrix}$$

$$\mathcal{M} = \begin{bmatrix} M_s & 0 & 0 & 0 \\ 0 & I_{MI} & 0 & 0 \\ 0 & 0 & M_{u_l} & 0 \\ 0 & 0 & 0 & M_{u_t} \end{bmatrix}$$

$$\mathcal{C} = \begin{bmatrix} C_l + C_t & C_l d_1 - C_t d_2 & -C_l & -C_t \\ C_l d_1 - C_t d_2 & C_l {d_1}^2 + C_t {d_2}^2 & -C_l d_1 & C_t d_2 \\ -C_l & -C_l d_1 & C_l & 0 \\ -C_t & C_t d_2 & 0 & C_t \end{bmatrix}$$

$$\mathcal{K} = \begin{bmatrix} K_l + K_t & K_l d_1 - K_t d_2 & -K_l & -K_t \\ K_l d_1 - K_t d_2 & K_l {d_1}^2 + K_t {d_2}^2 & -K_l d_1 & K_t d_2 \\ -K_l & -K_l d_1 & K_l + K_{tire} & 0 \\ -K_t & K_t d_2 & 0 & K_t + K_{tire} \end{bmatrix}$$

Eq.8.1 could be written in the eigen value extraction form as

$$\left[\mathcal{K} - \omega^2 \mathcal{M} + \imath\, \omega \mathcal{C}\right] X = 0 \tag{8.2}$$

Eq.8.2 is solved for the complex eigen values using modal analysis and the complex eigen values of the form $(\alpha + i\beta)$ are

$$\lambda_i = \left\{ \begin{array}{c} -2.0745 \pm i\ 5.7535 \\ -3.0492 \pm i\ 6.9389 \\ -21.2712 \pm i\ 51.5119 \\ -21.2925 \pm i\ 50.2778 \end{array} \right\} \tag{8.3}$$

The undamped natural frequencies in Hz. could be extracted from the above equations as $\omega_n = \sqrt{\alpha^2 + \beta^2}$ as

$$\lambda_{n_i} = \left\{ \begin{array}{c} 0.9734 \\ 1.2063 \\ 8.869 \\ 8.69 \end{array} \right\} \tag{8.4}$$

The undamped natural frequencies obtained from the above process for sprung mass bounce and wheel hop as 1.2 Hz. and 8.9 Hz. correspond to the values given in Ref.[160].

The frequencies obtained in the previous analysis of this section are based on a model which has sprung and unsprung mass as derived in Eq.8.1. But for the experimental active suspension model, a SDOF suspension system with only sprung mass and coil spring has been chosen. A study has been performed involving various sprung mass values and coil spring rates to optimize the sprung mass frequency and static deflection for a SDOF suspension model. But with various limitations on the amount of sprung mass that could be made available and incorporated onto the test rig, coil spring rates and free length, a compromise value has been chosen as follows. A mass of 300 kg. with a coil spring stiffness of 100 $\frac{lbf}{in}$ which is 17.63 $\frac{kN}{m}$ has been used to obtain the frequency of 1.2 Hz.

A coil spring was purchased from Rockwell International based on their reputation for quality, spring rate accuracy and good dimensional tolerances. The static deflection of the coil spring for the mass specifications as given above is 6.6 in.. The overall free length of the coil spring is chosen to be 10 in. (9 in. minimum) with the provisions for jounce and other allowances. The sprung mass is simulated with

four steel plates of 24" x 24 " x 1" with corresponding holes for fastners which would weigh a total of 270 kg.. The clevis brackets and other attachments along with the aluminium and steel plates would amount to a total of 300 kg. sprung mass.

A Porsche 928 vehicle shock absorber was purchased to simulate the right conditions for a failsafe active suspension. A damper characterization test as described in Appendix D was performed to evaluate the jounce and rebound characteristics of the damper. A series of tests at various frequencies and amplitudes have been performed. Since the intended test on SDOF involving this damper is performed for a maximum velocity of 0.15 $\frac{m}{sec}$, an average value of 6250 $\frac{Ns}{m}$ has been used as the nominal value for the adaptive active controller.

### 8.3.1 Single Degree of Freedom Adaptive Active Suspension Hardware Integration

The efforts made so far in developing, processing and evaluating various individual components and the respective feedback loops have been finally culminated to realize a complete SDOF adaptive active suspension system. The discussions in the previous sections would enumerate the response characteristics of each component and the circuits which would be integrated into the final setup.

The software modules namely *Capsule A* and *Capsule B* have been modified with the model parameter values such as damping constant of proportionality, sprung mass etc. The software display module has been tuned to show the on line performance of the experiment. The data acquisition routines involving the DAC and ADC ports for various data transfers have been reconfigured to access the respective sensors and actuators. Fig.8.3 shows the schematic diagram for the hardware and signal flow connections. The hardware shown in Fig.8.3 includes all the components discussed in the previous sections, but is integrated to form the adaptive active suspension setup.

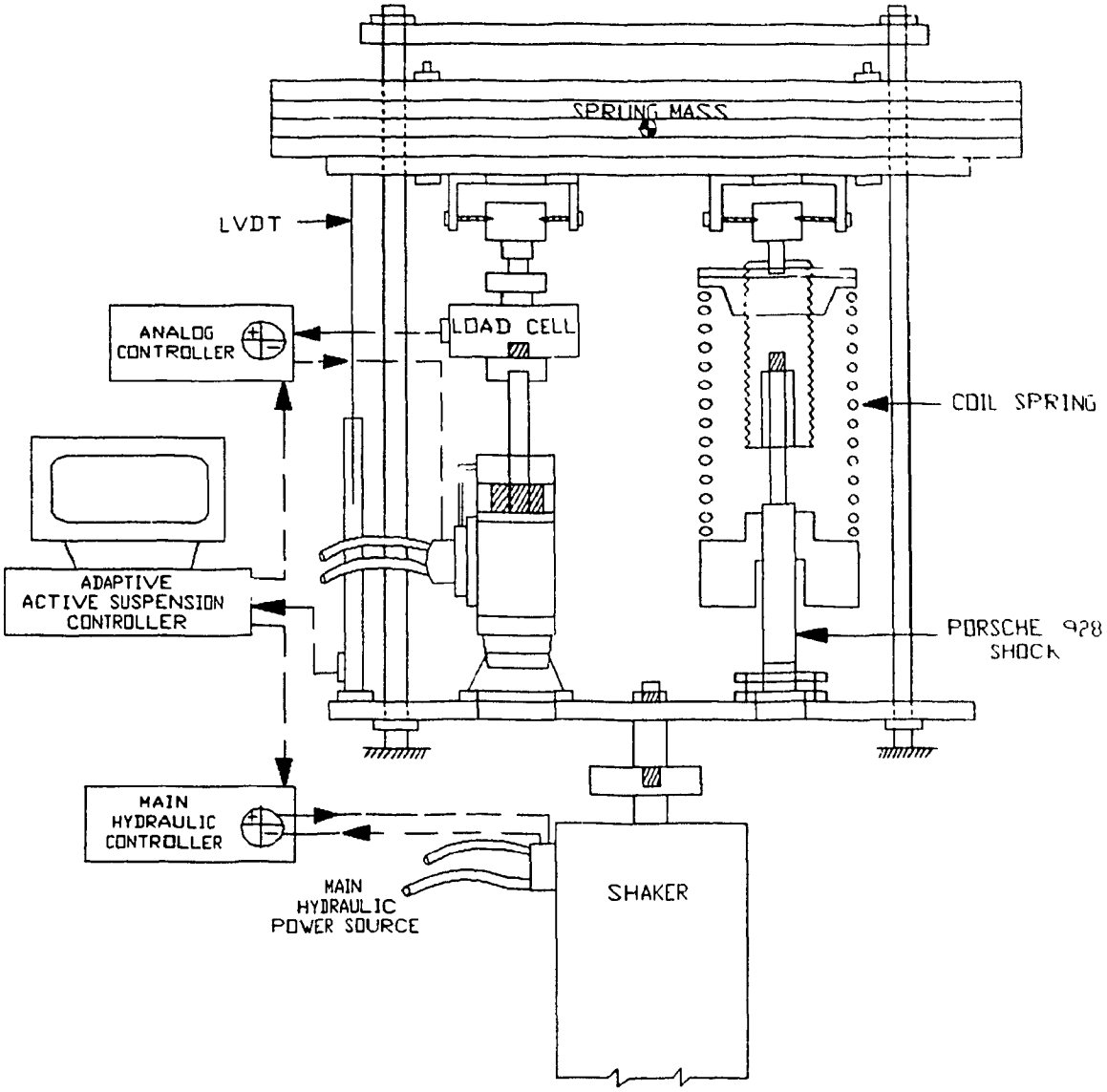


Fig.8.3: Schematic diagram of experimental setup for hardware implementation of adaptive active suspension.

A set of pictures indicating the assembly of the setup are shown in Figs. 8.4, 8.5, 8.6 and 8.7. Fig.8.4 shows the complete setup and gives the dimensional feel of the setup with respect to the main hydraulic circuit controller. Fig.8.5 indicates the front view with sprung mass and subframe attached to the main hydraulic actuator. Details of failsafe active suspension components are shown in Fig.8.6. Fig.8.7 shows the on line adaptive active suspension simulator screen that would show the real time simulation and animation results as the experiment is carried on.

The total sprung mass of 300 kg. including the four (1″ thick) plates, aluminium supporter holding the linear bearings and clevises are guided by a four pole subframe that is rigidly fixed. The subframe is hung from the top from a cross main beam and attached at the bottom to vertical beams. This restricts the sprung mass to have only the bounce DOF and tries to eliminate any moment onto the actuators and shock absorber. The bottom plate which signifies the geometric point of knuckle and axle attachment is attached rigidly to the main hydraulic shaker. The output of the shaker would replicate the excitation at the unsprung mass location of the system. As shown in these figures the active suspension components have been embedded between the top and bottom plates. The Porsche 928 shock has a total stroke of 4″. So the assembly of the suspension along with the coil spring should be adjusted so that the whole setup moves down by 2″ to allow for 2″ stroke both in jounce and rebound. The total sprung mass of 300 kg. with the coil rate of $100\frac{lb}{in}$ would lead to a static deflection of 6.6″ out of the total 10″ free length. To effectively use the free length and obtain the shock piston to half the total stroke, the coil spring is subjected to a pre-tense of 4.6″. The figures 8.4 and 8.5 show mechanism with a lock nut that was used to pre-tense the coil to compensate for the static load. A lower spring seat without an isolator has been designed to have an interference fit with respect to the shock outer tube collars. The bottom of the shock has been fixed through a clevis and a bonded spool bushing to the bottom plate. The shock rod has been fixed to the sprung mass through a clevis and the rod end to allow for misalignment.

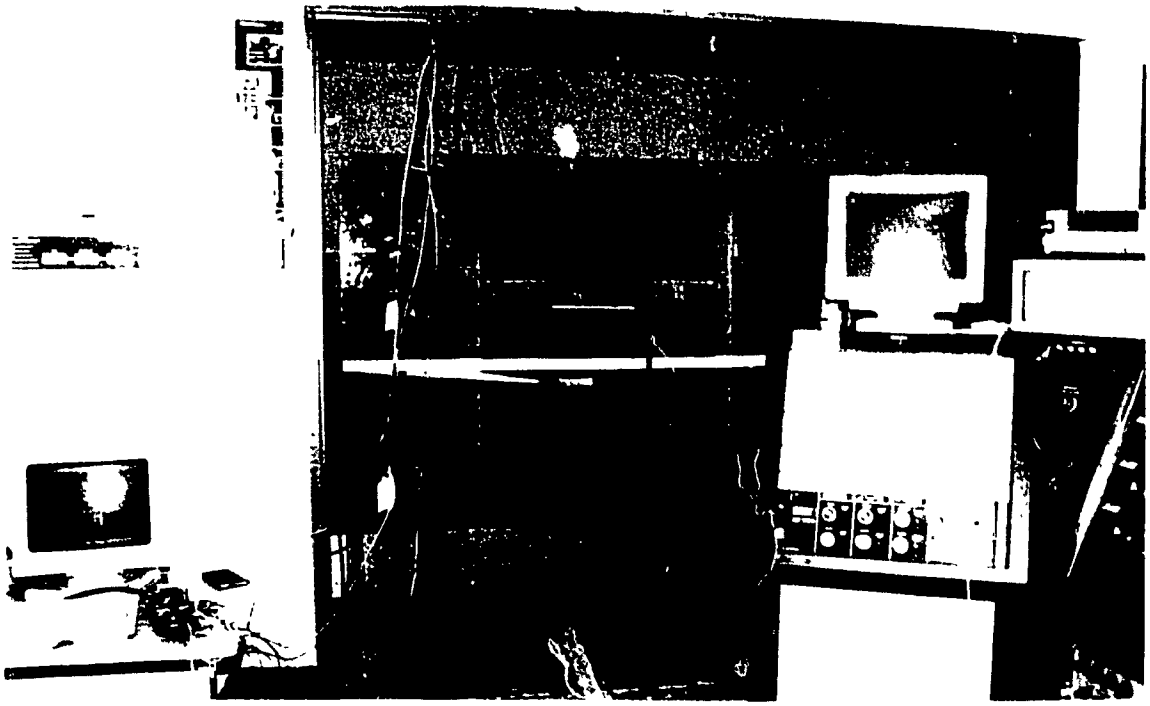

Fig.8.4: Picture of the overall experimental setup.

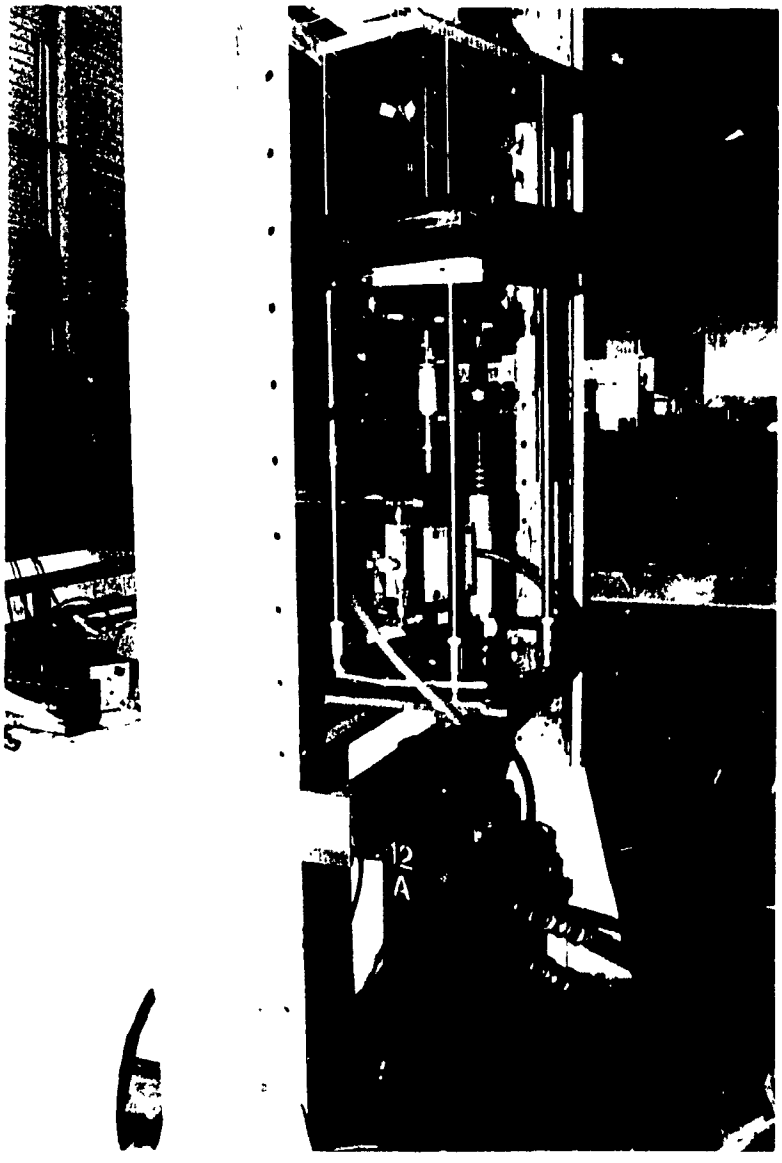


Fig.8.5: Picture indicating the main & auxiliary hydraulic power sources.

Fig.8.6: Picture indicating the actuator & strut assembly.

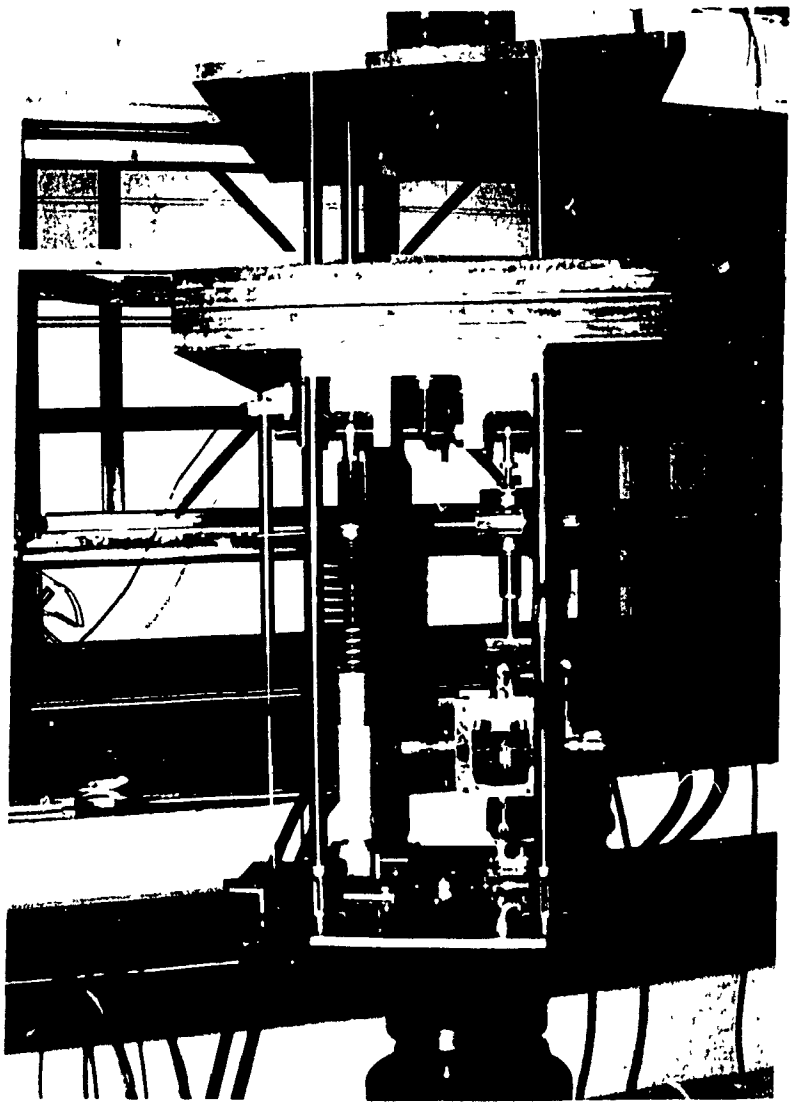

Fig.8.7: The real time simulation & animation for online display.

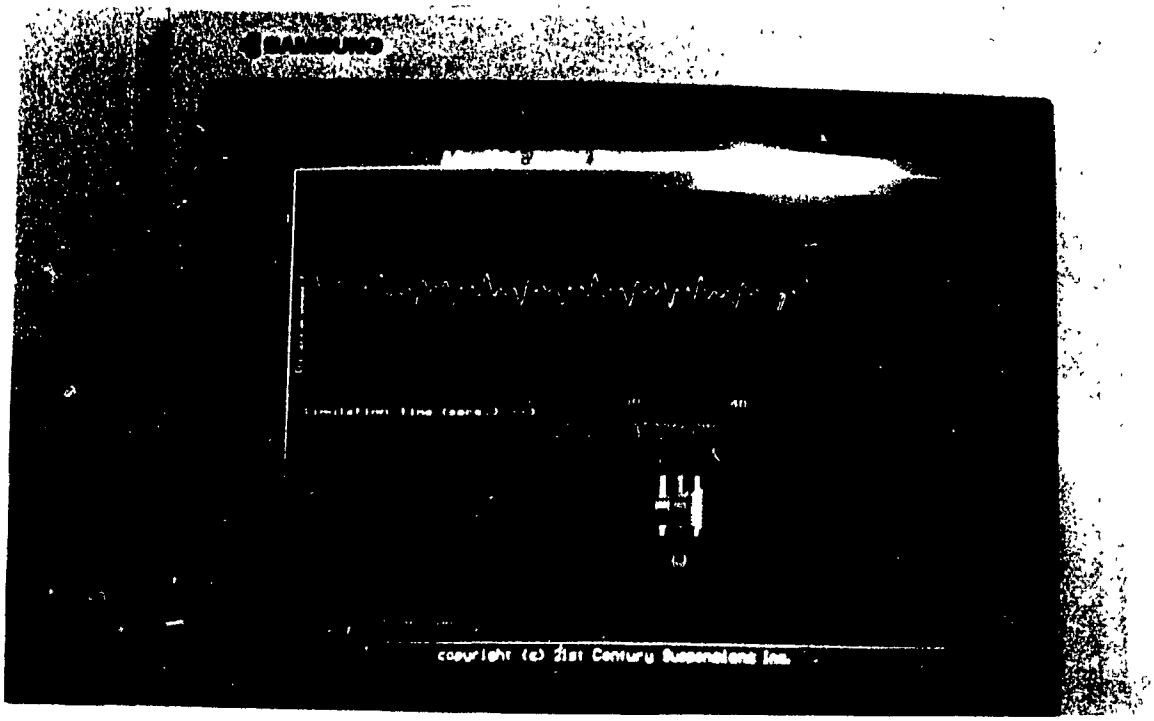

The actuator subsystem along with the calibrated load cell is attached in parallel to the coil and shock assembly. The actuator has a total stroke of 6", but the shock has a 4" stroke p-t-p. The actuator stroke has been reduced to protect the shock from being damaged due to any unstable performance of the system, which might extend the actuator beyond 2" from the center. A safety provision has been incorporated by inserting a $2\frac{1}{4}$ inch thick stop block with diameter less than the inner diameter of the cylinder to maintain normal flow of oil towards the rod end of the actuator. This will provide the hardware safety provision along with the software constraints to safe guard the experimental setup. The other end of the load cell has been attached to the sprung mass through a clevis and a rod end to avoid any misalignment in the setup.

The force feedback circuit has been reinstalled through the analog controller and an Op-Amp is connected to the servo valve. The position feedback circuit has been completed through a main hydraulic shaker circuit as shown in Fig.8.4. The whole setup is being excited by two different hydraulic circuits. The main hydraulic power source has been used for position control of the excitation shaker. The auxiliary low powered hydraulic power source has been used for the actuator force feedback circuit. The command signals for both of the circuits have been given through the same Adaptive Active Simulator Software run on the PC through the DAS-20 data acquisition system. The provision for obtaining the relative displacement (rattle space) from the setup through a LVDT has been made.

### 8.3.2 Adaptive Active Suspension Experimental Results

The complete setup as described earlier in section 8.3.1 and the details of the controller in terms of the analytical results were presented in chapter 4. A sinusoidal excitation has been chosen and is applied at the unsprung mass location. The results indicate that the controller adapts to the reference model and achieves better isolation. Fig.8.8 shows how the active suspension model adapts to the reference model. The figure

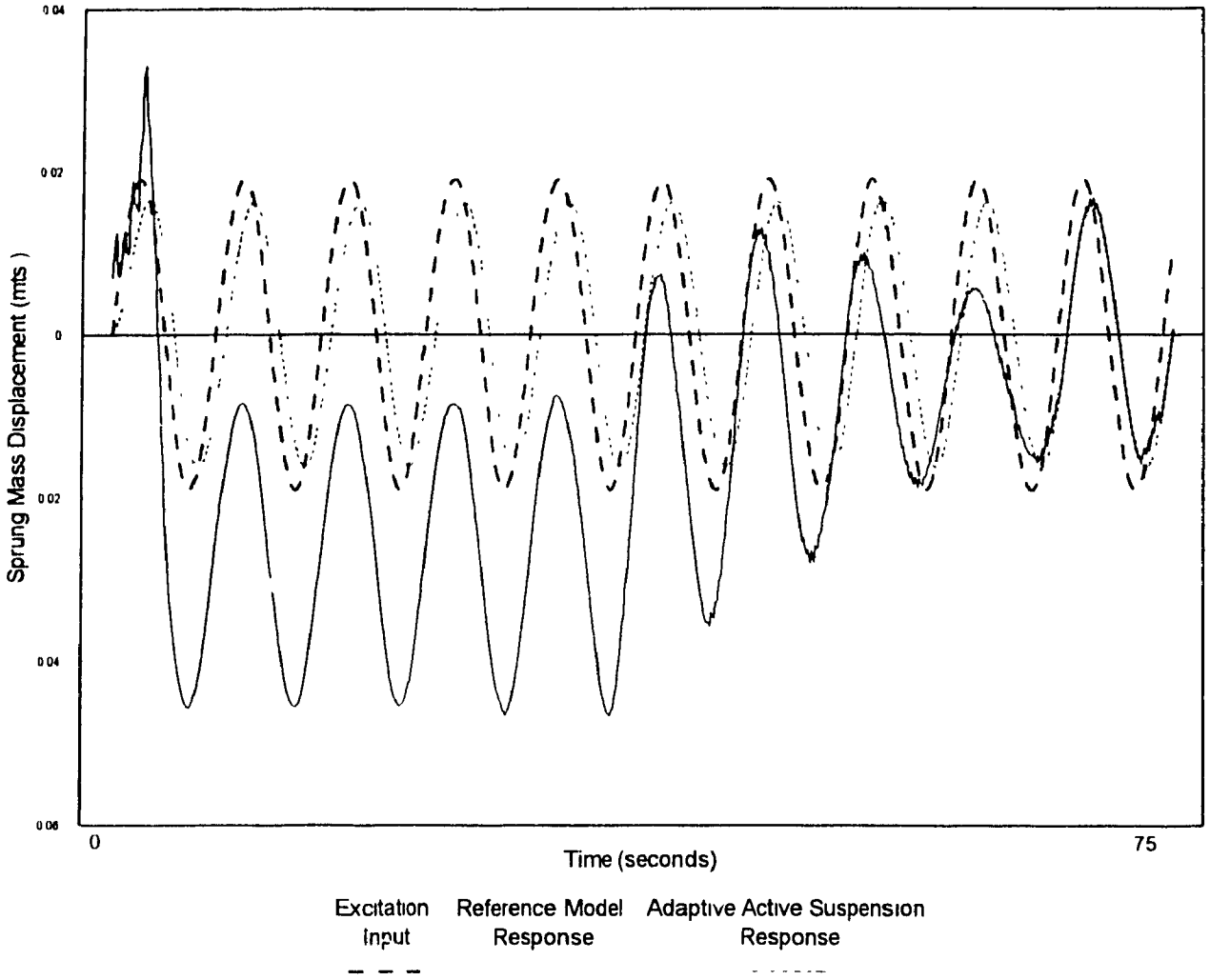


Fig.8.8 The Experimental Adaptive Active Suspension Response.

shows that due to improper initial co ditions the system takes time to adapt to the reference model. The controller initially reaches a large steady state error and gradually adapts the gains to reflect the reference model performance. Despite of the limitations such as the compatibility of the time step of the PC based control with respect to the main hydraulic controller, the test setup responded well. Detailed discussion on the experiment has been described in the following section.

## 8.4 Discussion on the Experimental Results

The analytical results of the discrete adaptive active suspension presented in chapter 4 have been very extensive. This analysis involved complicated deterministic excitation inputs, parametric variations and random excitations. The experimental setup discussed in previous sections involved various sub components, characterization and fool proofing of all the circuits. Due to the limitations of the hardware, the parametric variations could not be implemented. Hence the results indicate only the adaptation to the reference model. Due to the limitations in the setup, the experimental results could not reflect the analytical results in a one-to-one match in terms of adaptation period and model following. Due to the following reasons, the initial adaptation period has been longer when compared to the analytical results.

1. The controller has been designed to accommodate for time step of 0.01 secs but the input to the excitation shaker at this rate has been very coarse. The main hydraulic power source and the shaker circuit are more accurate than the time step chosen for the model formulation.

2. Due to the friction in the system and slight variation of the pressures in the actuator the initial conditions were difficult to maintain. This also contributed to the bad initial adaptation of the system. The relative displacement feedback system from the LVDT was very inconsistent and would not synchronize to the

initial conditions in the controller. This led to a large initial error that has to be compensated.

3. The discrete controller with recursive least square estimator as discussed in chapter 4 estimates gains better when more frequency content is available in the signal. But the hardware with the huge sprung mass and subframe limits the excitation to lower frequencies only.

4. As evident from any adaptive controlled system, the initial adaptation constants play a major role in initial model following. This system could be tuned by varying the adaptation constants to obtain better results.

5. During the testing process it was assumed that the excitation command signals given by the main hydraulic shaker was the same as generated in the controller excitation module. The velocities and acceleration required for evaluation of actuator force were assumed to be just the theoretical derivatives rather than actual measured values. So there might be error in the values which were used in the controller, when compared to the actual accelerations generated at the base.

6. Since an analog controller was used for enforcing the actuator force signal on to the sprung mass, the feedback from the actual force applied has not been used in the recursive least square estimation of controller gains. The estimator uses the calculated values instead of the actual force enforced by the closed loop force feedback circuit.

7. This being a real time control experiment and being implemented on a slower PC and data acquisition system, we have been limited by the control implementation and post processing by the same chip. However, the program was in C language for faster implementation, and it also does data acquisition and post processing of the signals. This would lead to extra time delay in the overall circuit and gives a zero order hold type of data sampling response with a larger time delay. Hence the time delays in the circuit was one of the major

drawbacks of this system. With the advanced dual processor data acquisition in which the data acquisition board processor does the implementation and the PC processor performing the data retrieval and processing [DMA (Direct Memory Access)], the overall implementation would be better. The controller could also be implemented in a faster and easy to debug way by using MATLAB's SIMULINK control software. This would generate the controller code in the low level machine language which could be embedded in the data acquisition chip for faster implementation.

Even with these assumptions and limitations, the adaptive active suspension adapts to the reference model, but takes longer initial time to update itself and to follow the reference model. The actual system when viewed through the playback on video would show that after initial glitches it would stabilize and adapt to the reference model.

## 8.5 Summary

Experimental validation of the analytical results obtained in chapter 4 coded as *Discrete Model Reference Adaptive Control* for a single degree of freedom (SDOF) system have been presented in this chapter. The hardware (Mechanical/Electronics) and software developed for implementation has been quoted as *Adaptive Active Suspension Simulator*. A systematic approach that involves recognization of various individual components and circuits and piece wise characterization and implementation has been performed. A SDOF system model that would resemble (1:1) a Porsche 928 vehicle (quarter car without unsprung mass) has been fabricated and installed. A complete set of the software and the data acquisition system which involve modules for model data entry, controller implementation, graphical display and DAC/ADC routines have been developed. A complete system integration with the hardware hooked up to the dual hydraulic power sources and feedback control circuits has been performed. This

chapter presented the theory behind the selection of various components and their characterization curves by performing actual individual experiments. Finally the results of the controller implementation which showed good adaptation to the reference model were presented. The limitations described for this level of implementation have been enumerated and discussion on the results has been presented. Recommendations for a better system are given in the next chapter.

# Chapter 9

# Conclusions and Suggestions for Future Research

## 9.1 General

In this chapter, the analytical and experimental results obtained are summarized. The conclusions based on these results are also described. The analytical and experimental work on adaptive active suspension which has been described in this thesis lead to a list of suggestions for future research as presented in Section 9.3.

## 9.2 Conclusions

Suspension design has always been a critical factor in vehicle design and is being put to a higher magnitude of importance due to increased demands by customers in terms of safety and comfort. With the increased use of automobiles in the transportation sector, the demand for a comfortable ride has been on the rise. However, at the same time with the speed limits either being raised or removed completely, vehicle highway safety also plays a very important factor. These lead to the requirements of vehicle suspension systems that are pressed for a more optimal performance. The

first chapter described the perspective of active suspension for the vehicle handling and comfort optimization. This chapter also reviewed the present state of the art on the active control applications for vehicle systems. A detailed review on active and semiactive systems in light of concepts and control strategies has also been included. The first chapter also reviewed how an adaptive active suspension concept is relevant to active suspension requirements and could provide a better "bang for the buck".

To emphasize the capabilities of adaptive active suspension and for modelling purposes, various assumptions have been made and were analyzed in chapter 2. Two types of excitations ( deterministic and random ) and parametric variations have been identified for simulation of the results. Various nonlinear properties of the suspension components have been incorporated and they were linearized about an operating point. The discussion made in this chapter has been used in various models and also for computer simulations.

As described in chapter 3, a single degree of freedom (SDOF) adaptive active suspension has been used to illustrate the concept in the continuous time domain. Simulation results for *Excitation mode I* and *Parametric variations mode I* which indicate the time domain results have been presented. The results indicated good adaptation and robustness to very large parametric variations. Results for random input excitation and *Parametric variations mode II* have been discussed in terms of the system gain factors and power spectral density (PSD) curves. The results presented were encouraging and this prompted further research. Chapter 3 concluded that a continuous time controller applied for the adaptive active system would produce all the required results in terms of model following for any excitation and parameter variations. The frequency domain results also indicated how an optimal performance (skyhook reference model) in terms of isolation (for comfort) and suspension travel (handling and stability) could be achieved and would be maintained for any gross parameter variations. These results would substantially validate the requirement of adaptive active suspension to satisfy various requirements as enumerated in section

1.4.2 of chapter 1.

With the advent of new and faster computer chips which have faster digital processing capabilities, the computer based control is becoming more popular. Even though the continuous domain controller structures are strong analytically, the actual computer based implementation leads to the requirement of a discrete domain analysis. A discrete model reference adaptive controller has been implemented for the same SDOF suspension model with all suspension nonlinearities. Discrete Auto Regressive Moving Average (DARMA) models have been derived for the vehicle suspension model and the reference model used. The control input equations with the gains being updated by recursive least squares estimation with covariance modification have been derived. Simulation results for the *Excitation mode I & II* and *Parametric variations mode I & II* have been presented. The results indicated good adaptation to the reference model and the trends are similar to the continuous time domain. Whenever the model parameter variations occur, the controller parameters were estimated to new values as indicated in the time domain results for excitation and parametric variations in mode I. The time delay in the whole circuit could be incorporated in the model in terms of number of sampling intervals. The conclusions as listed above about the continuous time domain results could be extended to the discrete model. The initial adaptation depends on initial values of covariance matrix constants and should be tuned to obtain a good adaptation to the reference model. To adapt to the changes in the model parameters and to achieve robust performance, the controller parameter needs enough frequency content in the signals.

As referred in chapter 1, some of the state of the art publications use an optimal control gain vector calculated off-line for various velocities, excitations and parametric variations. The performance of such a system has been also termed as an adaptive active suspension system. Such an approach would need off-line parameter estimation and the stochastic optimal control evaluations to obtain the required gains for implementation. To show such an approach is not robust to various adaptive char-

acteristics, required a comparison between the adaptive control approach (developed in this dissertation) and a stochastic optimal control approach presented in chapter 5. Stochastic optimal control with random excitation has been formulated and simulation results have been generated. A detailed comparative study between these two approaches has been made which includes a comparison of a linear time invariant (LTI) model and both of them being subjected to parameter variations. A Stochastic Optimal Control is found to perform good for a LTI model but gains were needed to be updated at a faster rate with the assumption that the vehicle model parameter changes are known ahead of occurrence. But the results indicated that even if the gains were updated at a faster rate with the assumption of knowledge of parametric variations, the adaptive controller performance was found to be superior. The frequency domain results of absolute displacement and relative displacement in both the cases indicated the differences between the approaches. A simple optimal controller has been chosen for comparison but a Stochastic optimal controller could be designed to be robust for parameter variations, modelling errors and time delays by designing bounds on the perturbations. A more thorough investigation and comparison to such an approach has to be made to obtain better insight about the differences. The study described in chapter 5 has been very important to give a comparative insight of the adaptive active suspension and off-line gains estimation for stochastic optimal control. As a conclusion for the single degree of freedom (SDOF) analysis, an experimental validation has been conducted in extension to the continuous and discrete domain analysis which was presented in chapter 8.

An analytical study of the multi degree of freedom (MDOF) system has been presented in chapter 6. In consistent with a SDOF system, continuous time and discrete time domain approaches have been used. A MDOF general suspension system equations have been derived with all nonlinearities to the suspension components incorporated. The equations have been extended from a two DOF bounce model with primary and secondary suspension. The general non-linear time varying (NTV) suspension model has been linearized about the operating point and a linear operat-

ing point equations were derived. A reference model for a two DOF bounce model has been used and general equations have been derived from the model. A passive NTV model with discrete harmonic linearization (DHLEM) technique and a reference model performance has been anaiyzed using frequency domain results. A model reference adaptive control (MRAC) approach with feedforward, feedback and auxiliary signals has been used. A detailed description of this approach was given in chapter 6. The adaptation laws and control input equations have been derived as a first order trapezoidal set of equations. The overall general model could be used to deduce any specialized set of equations by putting constraints on any of the terms in the equation. So the general approach could still be valid to any application chosen. A complete set of time domain and frequency domain simulation results for a 2 DOF bounce NTV model have been presented. The frequency domain results very much correlate with the transfer function predictions for both the passive, and active or reference models. A detailed description of the results and a discussion on them was incorporated in chapter 6. The two DOF bounce model chosen could be used to simulate many of the suspension applications such as seat suspensions, rail vehicle applications etc.. The results indicated good robustness and they satisfy the main objectives of obtaining an optimal suspension performance. The results also indicated the complication of tuning the controller and implementing the whole system.

One of the classic examples, where the adaptive active suspension applications could be of significant importance as mentioned in chapter 1 is the prevention of nose dive and squat during longitudinal maneuvers. To address such an issue a detailed study of the MDOF half-car model has been incorporated in chapter 7. A discrete time domain model and the respective controller has been developed anticipating a quick application of the concept for a real prototype. The study in Chapter 7 included a detailed suspension with all nonlinearities along with front and rear actuators to realize a failsafe half-car active suspension. A linearized half-car model and then a DARMA model have been created from the NTV suspension model. A time invariant reference model that has the skyhook damper characteristics to give an optimal

performance has been developed. Initial transfer function comparative studies in the frequency domain has been conducted. This study shows the relative performance of the reference model and the results which are expected from the adaptive active suspension. A discrete model reference adaptive controller has been used for the derivation of the control law and the controller parameters were estimated by recursive least square estimator, with the parameters being updated as a matrix. Previous studies include only a vector estimator, so the global convergence properties with the multi input multi output (MIMO) discrete model reference adaptive control (DMRAC) system have been proved for the matrix approach. The controller parameters estimator has a covariance matrix which was updated using a covariance modification method. The over all controller and the complete model has been tested for various excitation and parametric variations as described in chapter 2. The results in time domain indicated that the approach helps in reducing the bounce and pitch DOF and hence improve the longitudinal manoeuvres. The nose dive and squat during braking and accelerations were found to be mostly eliminated as compared with the passive suspension. Therefore the objectives given in chapter 1 are achieved.

Being encouraged by the analytical results developed in chapters 3,4,6 and 7 an experimental validation as discussed in chapter 8 has been conducted. A SDOF failsafe active suspension as described in chapter 4 has been fabricated. A systematic approach that involves recognization of various individual components and circuits with piece wise characterization and implementation has been performed. A SDOF system model that resembles (1:1) a Porsche 928 vehicle (quarter car without unsprung mass) has been fabricated and installed. A complete set of software and data acquisition system which involves modules for model data entry, controller implementation, graphical display and DAC/ADC routines have been developed. The complete test system described at a greater detail in chapter 8 has been powered up and test runs were also conducted. The suspension adaptation to the reference model has been observed in the test. The system adapted to the reference model with some initial steady state errors takes some time for convergence. Due to various critical

limitations as mentioned in chapter 8 it takes longer time for adaptation compared to the analytical results in chapter 4. The overall experiment validated the analytical results and gave some light for the overall investigation as a "do-able concept". Details about the experiment and the results were discussed in chapter 8.

The dissertation as concluded above presents a series of efforts made to introduce the new concept of Adaptive Active Suspension and showed various advantages of taking the active suspension a step ahead. Efforts have been made to systematically prove the concept by laying a foundation using a SDOF suspension through a MDOF complex system and finally validating it by conducting experiments.

## 9.3 Suggestions for Future Research

The analytical work done on a SDOF system in chapter 3 and 4 could be extended to a quarter car model. The results obtained by extending the adaptive controller in chapters 3 and 4 for a quarter vehicle could be evaluated for proper adaptation at the tire hop and tramp modes. Various initial values of gains and controller factors that would help for better adaptation could be tuned to obtain the required performance characteristic over wide range of handling frequencies. The quarter vehicle model could be extended to incorporate various other suspension components depending on the type, like quadra link, SLA etc.. Such a model could be used to see if the adaptive active suspension influence on longitudinal and lateral manoeuvres would influence any of the toe and camber variations with respect to jounce and rebound.

A new controller design approach which involves feed forward controller gains based on a linear time invariant system and an adaptive controller to compensate for the operational parametric variations could be designed. The feed forward controller contains fixed gains either analytically derived or experimentally measured. The adaptive controller in this case would adapt to the required reference model as

a compensation for finer parametric variations and error in signal processing. This approach would necessitate evaluation of the required feed forward gains for various vehicles and considering the coupling between various vehicle operational conditions. This would also require sensory information about operating conditions such as acceleration, steering input, etc.. Chapter 6 described an overall adaptive controller that involves both feed forward and feed back gains which are adapted to achieve the required reference model performance without much sensory information. A comparative study involving both approaches could be made to bring out limitations and positive benefits of either design.

A more detailed study that could be extended from this thesis includes the packaging of the actuator for various suspension types. The results presented in various chapters indicate a failsafe active suspension configuration that renders benefits in two ways. It helps to take the static load due to very low frequency manoeuvres letting the actuator apply the forces to obtain the required performance. Hence these actuator forces are smaller. This would reduce the hardware dimensions and cost. The failsafe actuator would also have the passive suspension to take care of any malfunctioning of the active suspension circuitry.

A more detailed theoretical and experimental study as an extension to results presented in chapter 2 that involves various load variations due to longitudinal and lateral maneuvers need to be conducted. Such results could be used in theoretical evaluation through simulations to better understand the adaptive characteristics of the controller and to obtain better confidence in the overall system.

Stochastic optimal controller (SOC) has been used to compare with the adaptive active suspension in chapter 5. The results indicated that SOC is not robust enough for any parametric variations. Hence the comparison with other controllers should be explored to show the definite benefits of the adaptive active suspension approach. The adaptive control approach could be compared with a robust optimal controller in which gains are evaluated based on the error bounds imposed on the sus-

pension parameter variations. But generally these controllers normally have a limited bounds for parametric variations. This study would help to shed more light on the positive aspects of both approaches.

The adaptive active suspension model developed in this dissertation is tuned more towards the longitudinal manoeuvres which include the dynamics during braking and acceleration. This concept proved that nose dive and squat can be greatly reduced during these manoeuvres by using the adaptive active suspension control. The actuator hardware at the four suspension (left and right at front and rear) could be effectively used for achieving other different required vehicle dynamic performances.

The adaptive control active suspension discussed in chapter 7 for longitudinal manoeuvres like braking and acceleration alone could change the vehicle design status in terms of over steer or under steer during a cornering and longitudinal manoeuvre. For example if a vehicle is under steer and is accelerating around a curve, then there is load transfer to the rear. In the attempt of giving a constant ride height the adaptive active suspension would apply a tensile load on the rear axle and compressive load on the front axle. This process would increase the normal load on the rear and decrease the load on the front axle. Hence the vehicle might behave as an oversteer vehicle or achieve neutral steer characteristics. Similarly if a vehicle is oversteering and is decelerating when taking a curve, then due to the adaptive active suspension the vehicle can perform as a under steer or neutral steer. Hence a more detailed study is recommended for the complete system model involving interaction due to various critical manoeuvres.

Vehicle roll during lateral maneuvers such as describing a curve or lane changes is an another critical issue that shows the compromise between stability/handling and ride comfort. An adaptive control active suspension designed in chapter 7 and applied for the longitudinal maneuvers could be well extended for a transverse model. Such a study should address mainly two aspects, namely monitoring the static equilibrium conditions due to the lateral load shifts and restoring/improving cornering stiffness of

the vehicle. The centrifugal forces experienced by the suspended vehicle would shift the loads from the inner to outer wheels during the curving maneuvers. The vehicle roll due to this maneuver could be reduced by the adaptive active suspension without hampering the handling of the vehicle. The total cornering stiffness at the tire patches due to rolling of the vehicle is less than the actual total stiffness due to normal vehicle weight. The adaptive control could be used to incorporate the antiroll phenomenon and also restore/improve the cornering stiffness at the tire patches by varying the normal loads. A detailed study based on the above outline is recommended to evaluate the feasibility of the concept.

Even with the advent of many independent control system devices such as Automatic stability control + traction (ASC+T), traction control etc., the results in the previous studies indicated that an active suspension would help in improving the performance of other active control systems. One such potential benefit could be obtained by proper channelizing the braking force or traction on the vehicle. The ideal braking force distribution between the front and rear axles is designed for optimum utilization of the total potential braking capability of the vehicle. An adaptive suspension could be designed to govern the normal loads during the braking conditions and provide the proper traction/braking normal loads to achieve the required objective. Hence the study in this dissertation could be extended to satisfy this criteria and could be designed to be compatible with other active control systems on board.

A MDOF system as analyzed in chapter 6 could be very cumbersome for a full vehicle or any system with a larger number of degrees of freedom. Hence a decentralized adaptive control could be designed so that it would have an independent controller derived from the overall system but evaluates the actuator force independently. Such a system would also facilitate a faster real time control due to smaller independent loops.

Chapter 8 presented in this dissertation validated the adaptation to a reference model. The hardware could be modified to incorporate parametric variations

and robustness of the adaptation could be monitored. Due to robust design of the hardware and software of the experimental setup various other excitations could be tested and fine tuned to obtain the respective results.

# Bibliography


[1] Goodall R. M. and Kortüm W., "Active controls in ground transportation - A review of the state of the art and future potential", *Vehicle system dynamics*, Vol. 12, 1983, pp. 225-257.

[2] Sharp R. S. and Crolla D. A., "Road vehicle suspension system design - a review", *Vehicle system dynamics*, Vol. 16, 1987, pp. 167-192.

[3] Hedrick J. K. and Wormley D. N., "Active suspensions for ground transport vehicles - A state of the art review", *Mechanisms of transport systems*, ASME,AMD - Vol. 15, 1975, pp. 21-40.

[4] "Powertrain and chassis control systems integration," *Automotive engineering*, Vol. 99, No. 1, January 1991, pp. 15-18.

[5] Iguchi M., "Application of active control technology to motor vehicle control", *Int.journal of vehicle design*, 1988, Vol. 9, No. 3.

[6] Nakahara M., Mamiyama F. and Shirai Y., "Steering sensation power steering of trucks and buses," *Journal of the society of automotive engineers of japan*, 1984, Vol. 38, No. 5.

[7] Iitumi S., Koyama T., Okamura H., Ebisawa K. and Maekawa M., "Development of powertard for 8DC9T engine", *Mitsubishi heavy industries, technical journal*, 1985, Vol. 22, No. 4.

[8] Yabuka K., Iizaka H., Yanagishima T., Kakaoka Y. and Seno Y. "The development of drowsiness warning devices", *The 10th international technical conference on ESV*, 1985.

[9] Kawata H., et al., "Study of laser radar", *The 10th international technical conference on ESV*, 1985.

[10] Crosby M. J. and Karnopp D.C., "The active damper - a new concept for and vibration control ", *Vibration bulletin*, 1973, 43, part II.

[11] Karnopp D. C., Crosby M. J. and Harwood R.A., "Vibration controlling semi-active force generators", *J.Engg. for industries*, 1974, 96, Sar.B(2), pp. 619 626.

[12] Margolis D.C. "Semiactive and pitch control for ground vehicles", *Vehicle system dynamics*, 1983, 12, pp. 291-316.

[13] Rakheja S. and Sankar S., "Vibration and shock isolating performance of a semi active "on-off" damper", *Journal of vibration, acoustics, stress and reliability in design*, Vol. 107, October 1955, pp. 398-403.

[14] Sharp R. S. and Hassan S.A., "Performance and design consideration for semi active suspension system for automobiles", *Proc. instr. mech. engrs.*, Vol. 201, No. D2, 1987, pp. 149-153.

[15] Sharp R. S. and Hassan S. A., "The relative performance capabilities of passive, active and semi-active car suspensions systems",*Proc. instr. i mech. engrs.*, Vol. 200, No. D3, 1986, pp. 219-228.

[16] Yokoya Y., Asami K., Hamajima T. and Nakashima N.,"Toyota electronic modulated suspension (TEMS) system for the 1983", *SAE paper 840341*, 1984.

[17] Mituguchi M., Suda T., Chikamosi S. and Kobayashi K. "Chassis electronic control systems for the mitsubushi 1984 galent", *SAE paper*, 840258, 1984.

[18] Crolla D. A., Pitcher R. H. and Lines J.A., "Active suspension control for an off-road vehicle", *Proc. instr. mech. engrr.*, Vol. 201, No. D1, 1987, pp. 1-10.

[19] Clerk R.C., "Fully active suspension by autonomous low-loss hydraulic struts", *Int. journal of vehicle design*, Vol.11, No.415, 1990, pp. 422-438.

[20] Dominy J. and Bulman D. N., "An active suspension for a formula one grand prix racing car", *Journal of dyn. sys. meas. and control*, Vol. 107, March 1985, pp. 73-78.

[21] Elmadany M. M and Abdul Jabbar Z., "On the statistical performance of active and semi-active car suspension systems", *Computers and*, 1989, Vol. 33, No. 3, pp. 785-790.

[22] Sutton H. B., "The potential for active suspension systems", *Automotive Engg. (Lon)*, V4, V2, April-May 1979, pp. 21-24.

[23] Sutton H. B., "Synthesis and development of an experimental active suspension", *Automotive engineer*, Vol. 4, No. 5, Oct.-Nov. 1979, pp. 51-54.

[24] Hall B. B. and Gill K. F., "Performance evaluation of motor vehicle active suspension systems", *Proc. instn. mech. engs.*, Vol. 201, No. D2, 1987, pp. 135-148.

[25] Junker H. and Seewald A., "Theoretical investigation of an active suspension system for wheeled tractors", *International society for terrain vehicle systems, 8th international conference : the performance of off-road vehicles and machines*, Cambridge, England, Aug. 1984, pp. 5-11.

[26] Chalasani R. M., "Ride performance potential of active suspension systems-Part II: Comprehensive analysis based on full-road model", *Symposium on simulation and control of ground vehicles and transportation system presented at the WAM of ASME Anaheim*, California, USA, Dec. 1986, pp. 7-12.

[27] Wright P. G. and Williams D. A., "The application of active suspension to high performance road vehicles", *Proc. instn. mech. engrs.*, Paper c239/84.

[28] "Lotus active suspension", *Automotive Engineer (London)*, Vol. 9, No. 1, Feb.-Mar. 1984, pp. 56-57.

[29] "Active suspension making it happen", *Automotive engineer (London)*, Vol. 14, No. 1, Feb.-Mar. 1989, pp. 60-61.

[30] "Speedy electronics helps cure active suspension's ills", *New electronics*, Z 9, Feb 1989, pp. 26-27.

[31] Sharp R. S. and Hassan S. A., "On the performance capabilities of active automobile suspension systems of limited bandwidth", *Vehicle system dynamics*, Vol. 16, 1987, pp. 213-225.

[32] Osben W. D. and Pertman T. H., "Engineering design study of active ride stabilizer for the department of transportation's high speed test cars", *Report under contract N0. 3-0267, office of high speed ground transportation*, June 1969.

[33] Sarma G. N. and Kozin F., "An active suspension system design for the lateral dynamics of a high speed wheel-rail system", *ASME journal of dynamics, system, measurements and control*, Vol.93, Series G, No. 4, December 1971.

[34] Hullender D. A. and Wormley D. N. and Richardson H. H., "Active control of vehicle air cushion suspensions", *ASME journal of dynamic, system, measurements and control*, Vol. 93, No.1, 1972.

[35] Jeffcoat R. C. and Wormley D. N., "Improvement of rail vehicle lateral dynamics performance through active control", *Vehicle system dynamics*, Vol. 4, No. 2-3, 1975, pp. 169-173.

[36] Sinha P. K., Wormley D. N. and Hedrick J. K., "Rail passenger vehicle lateral dynamics performance improvement through active control", *ASME journal of dynamic, system, measurements and control, series G*, Vol. 100, December 1978, pp. 270-283.

[37] Celinker G. W. and Hedrick J. K., "Rail vehicle active suspensions for lateral ride and stability improvement", *ASME journal of dynamic, system, measurements and control*, Vol. 104, March 1982, pp. 100-106.

[38] Cho. D. and Hedrick J. K., "Performance actuators for vehicle active suspension applications", *ASME journal of dynamic, system, measurements and control*, March 1985, Vol. 107, pp .67-72.

[39] Pollard M. G. and Simons N. J. A., "Passenger comfort - the role of active suspensions", *Proc. instn. mech. engrs.*, Vol. 198D, 1984, pp. 17-31.

[40] Malek K. M. and Hedrick J. K., "Decoupled active suspension design for improved automotive ride quality handling performance", *9th IAVSD symposium, Sweden*, June 1985, N1-3, W14, pp. 383-398.

[41] Usui S., Tani K., Horiuchi E., Shirai R., "Optimal control of an active suspension for a wheeled robotic vehicle (experiment on a one-wheel model)", *Nippon kikai gakkai ronbunshu*, CHEN U55 n 510, Feb. 1989, pp. 354-358.

[42] Tani K., Usui S., Horiuchi E., Shirai N., Hirobe S., "Computers-controlled active suspension for a wheeled terrain robot", *International journal of computer applied technology*, Vol 3, No. 2, 1990, pp. 100-104.

[43] Yoshimura T. and Sugimota M., "Active suspension for a vehicle travelling on flexible beams with an irregular surface", *Journal of sound and vibration*, Vol. 138, No. 3, May 8, 1990, pp. 433-445.

[44] Salm J. R., "Active electromagnetic suspension of an elastic rotor: modelling, control experimental results", *Journal of vibration, acoustics, stress, reliability and design*, Vol. 110, No. 4, Oct. 1988, pp. 493-500.

[45] Allaire P. E., Humphris R. R. and Kelm R. D., "Dynamics of a flexible rotor in magnetic bearings", *4 th Workshop on rotor dynamics instability problems in high performance turbo machinery*, Texas University, Texas, June 1986.

[46] Matsushita O., Takahagi M., Tsumaki N., Yoneyama M., Sugaya T. and Bleuler H.," Flexible rotor vibration analysis combined with active magnetic bearing control", *Int. conf. on rotor dynamics, IFTOMM and JSME*, Tokyo, Sept. 1986.

[47] Nonami K., "Vibration control of rotor shaft systems by active control bearings" , *ASME design engg. division conference*, Cincinnati, Ohio, Sept. 1985.

[48] Zhuravleu Yu. N., "Synthesis of a linear optimum control system for the magnetic suspension of a rigid rotor", *Soviet Mech. Sci* N4 1987, pp. 44-51.

[49] Urusov I. D. and Likhoshvai L. P., "Active magnetic suspension in the working field of an electric motor", *Sov. electrical engg.*, Vol. 56, No. 1, 1985, pp. 68-72.

[50] Goodall R. M., Williams R. A., Canton A. P. and Harborough P. H., "Railway vehicle active suspension in theory and practice", *7th IAVSD-IUTAM symposium Cambridge* , U.K., Sept. 1981.

[51] Williams R. A., "Railway vehicle suspensions enter the electronic age", *IEE conference, railways in the electronic age*, London.

[52] North B. H., "Birmingham airport maglev - the development design of the support structure and guideway," *Track technology nottingham, England*, 1984 July 11-13.

[53] Williams R. A., "Active suspension classical or optimal?", *9th IAVSD symposium 1986, (VSD)*, Vol. 15 supplementary, USA, pp. 607-620.

[54] Thompson A. G., "An active suspension with optimal linear state feedback", *Vehicle system dynamics*, Vol. 5, 1976, pp. 187-203.

[55] Thompson A. G., "Optimal and suboptimal linear active suspensions for road vehicles", *Vehicle system dynamics*, Vol. 13, 1984, pp. 61-72.

[56] Yoshimura T., Ananthanarayana N. and Deepak D., "An active vertical suspension for track/vehicle systems", *Journal of sound and vibration*, 1986, 106(2), pp. 217-225.

[57] Metz D. and Maddock J., "Optimal ride height control for championship race cars, " *Automatica*, 22(5), 1986, pp. 509-520.

[58] Thompson A. G. and Davis B. R., "Optimal linear active suspensions with derivative constraints and output feedback control", *Vehicle system dynamics*, 17, 1988, pp. 179-192.

[59] Davis B. R. and Thompson A. G., "Optimal linear active suspensions with integral constraint", *Vehicle system dynamics*, 17, 1988, pp. 357-366.

[60] Wilson D. A., Sharp. R. S. and Hassan S. A., "The application of linear optimal control theory to the design of active automotive suspensions", *Vehicle system dynamics*, Vol. 15, No. 2, 1986, pp. 105-118.

[61] Hac A., "Suspension optimization of a 2 DOF vehicle model using a stochastic optimal control technique", *Journal of sound and vibration*, 1985, 100(3), pp. 343-357.

[62] Yoshimura T., Ananthanarayana N. and Deepak D., "An active lateral suspension to a track/vehicle system using stochastic optimal control", *Journal of sound and vibration*, 1987, 115(3), pp. 473-482.

[63] Hac. A., "Stochastic optimal control of vehicles with elastic body and active suspension", *Journal of dynamics, systems, measurements and control, Transactions of ASME*, Vol. 108, June 1986, pp. 106-110.

[64] Elmadany M. M., "Stochastic optimal control of highway tractors with active suspensions", *Vehicle system dynamics*, 17, 1988, pp. 193-210.

[65] Frühauf F., Kasper. R. and Lückel. J, "Design of an active suspension for a passenger vehicle model using input processes with time delays", *9th IAVSD Conference Sweden*, 1985 June, No. 1-3, Vol. 14, pp. 115-120.

[66] Louam N., Wilson D. A. and Sharp R. S., "Optimal control of a vehicle suspension incorporating the time delay between front and rear wheel inputs", *Vehicle system dynamics*, Vol. 17, 1988, pp. 317-336.

[67] Elmadany M. M., "Design of an active suspension for a heavy duty truck using optimal control theory", *Computer and structures*, Vol. 31, No. 3, pp 385-393.

[68] Lotus international, "Vehicle active suspension system - control of vehicle dynamics by an on board computers", *Design engg.*, July 1984, pp. 36 37.

[69] Wright P. G. and Williams D. A., "The application of active suspension to high performance road vehicles", *Proc. inst. congress transport electron. (Dearborn, MI)*, Oct, 1986, pp. 333-338.

[70] Corriga G., Sarma S. and Usai G., "An optimal tandem active-passive suspension system for road vehicles with minimum power consumption", *IEEE transactions on industrial electronics*, Vol. 38, No. 3, June 1991, pp. 210 216.

[71] Karnopp D., "Two contrasting versions of the optimal active vehicle suspension", *Transactions of ASME, Journal of dynamic system, measurements and control*, Vol. 108, September 1986, pp. 264-268.

[72] Ghoneim H. and Metwalli S. M., "Optimum vehicle suspension with a damped absorber", *Journal of mechanisms transmissions and automation in design*, 83 DET-42, 1983.

[73] Thompson A. G., Davis B. R. and Salzburn F. J. M., "Active suspensions with vibration absorbers and optimal output feed back control", *Society of automotive engineer, SAE 841253, passenger car meeting*, Dearborn, Michigan USA, Vol 1-4, Oct. 1984.

[74] Thompson A. G. and Davis B. R., "Optimal linear active suspensions with vibration absorbers and integral output feedback control", *Vehicle system dynamics* , 18, 1989, pp. 321-344.

[75] Thompson A. G , "The effect of tyre damping on the performance of vibration absorbers in an active suspension", *Journal of sound and vibration*, 1989, 133(3), pp. 457-465

[76] Allen Y. L. and Salman M. A., "On the design of active suspension using the frequency shaping technique", *ASME Winter annual meeting, Boston, Massachusetts*, Dec. 13-18, 1987.

[77] Allen Y. L. and Salman M. A., "On the design of active suspension incorporating human sensitivity to vibration", *Cptimal control applied methods*, Vol. 10, N2, Apr.-Jun.1989, pp. 189-195.

[78] Cheok K. C., Hu H. X. and Loh N. K "Discrete-time frequency-shaping parametric LQ control with application to active seat suspension control", *IEEE trans. ind. electronics*, Vol. 36, No. 3, Aug. 1989, pp. 383-390.

[79] Salman M. A. and Allen Y. L., "Reduced order design of active suspension control", *27th IEEE Conference on Decision and control*, Texas USA, Dec.7-9 1988.

[80] Tsypkin Ya. Z., "Adaptation, training and self organization in automatic systems.", *Automotive remote control*, 27, 1966, pp. 16-51.

[81] Landau I. D.,"A survey of model reference adaptive techniques - theory and practice", *Automatica*, Vol. 10, pp. 353-379.

[82] Chalam V. V., "Adaptive control-recent trends", *System science*, Vol. 12, No. 1-2, 1986, pp. 55-73.

[83] Sanchez and Edgar N., "Adaptive control robustness in flexible aircraft applications", *Proccedings of the American control conference*, Jun. 18-20 1986, Seattle, WA, USA, pp. 494-496.

[84] Kruise J. and Stein G., "General adaptive control structure with a missile application", *Proceedings of the American control conference*, Jun. 15-17 1988, Atlanta, GA, USA, pp. 561-566.

[85] Sabri T. and Delbet T., "State of the art in adaptive control of robotic systems", *IEEE transactions on aerospace and electronic systems*, Vol. 21, N0. 5, Sept. 1988, pp. 552-561.

[86] Raju G. V. S., Noorinejad A. and Coleman N. P., "Adaptive control of robotic manipulators", *IEEE international conference on systems, man and cybernetics*, Oct. 14-17 1986, Atlanta, GA, USA, pp. 184-188.

[87] Yuh J., Holley W. E., Smith C. E. and Baek Y. S., "Adaptive control of robotic manipulators", *Proceedings of IEEE international conference on systems, man and cybernetics*, Oct. 14-17 1986, Atlanta, GA, USA, pp. 180-183.

[88] Han J. Y., Hemami H. and Yurkovich S., "Nonlinear adaptive control of an N-link robot with unknown load", *International journal of robotic research*, Vol. 6, No. 3, Fall, 1987, pp 71-86.

[89] Yuh J. and Holley W. E., "Application of discrete-time model reference adaptive control to industrial robots: a computer simulation", *Journal of manufacturing systems*, Vol. 7, No. 1, 1988, pp. 47-56.

[90] Skowronski J. M., "Algorithms for adaptive control of two-arm flexible manipulators under uncertainty", *IEEE transactions on aerospace and electronic systems*, Vol. 24, No. 5, Sept. 1988, pp. 562-570.

[91] Unbehauen H. D., "Adaptive systems for process control", *IFAC proceedings series*, 1986, pp. 15-23.

[92] Hahn V., Röck H., Schmid Chr. and Wiener P., "Some experiences with the application of multi-variable adaptive control in chemical and electromechanical plants", *Optimal control applications and methods*, Vol. 6, 1985, pp. 235-248.

[93] Wiener P., Hahn N., Schmid Chr. and Unbehauen H., "Applications of multivariable model reference adaptive control to a binary distillation column", *Adaptive systems in control and signal processing 1983, Proceedings of the IFAC workshop* , San Francisco, California, USA, 1983, June 20-22.

[94] Fernandez D. B., Sanchez E. N., Urbieta R. and Kaufman H.,"Application of a model reference adaptive algorithm to the combustion control of a power unit boiler", *Journal of Dynamics system measurements and control, Trans. of ASME*, Vol.107, No. 4, Dec.1985, pp. 290-291.

[95] Ciccarella G. and Marietti P., "Model reference adaptive control of a thermostatic chamber", *IEEE transactions of industrial electronics*, Vol. 36, No. 1, Feb. 1989, pp. 88-93.

[96] David J. T. S. and Lee T., "Model reference adaptive control of a solenoid valve controlled hydraulic system", *International journal of systems science, 1987*, Vol. 18, No. 11, pp. 2065-2091.

[97] Platzer D. and Kaufman H., "Model reference adaptive control of Thyristor driven DC motor systems subject to current limitations", *IFAC proceedings series 1985*, No. 4, pp. 1991-1995.

[98] Naito H. and Tadakuma S., "Model reference adaptive control based armature current control for DC motors in the discontinuous current mode", *Electrical engg. in Japan*, Vol. 106, NO. 2, 1986, pp. 54-61.

[99] Hori N., Ukrainetz P. R., Nikiforuk P. N. and Bikner D. U., "Simplified adaptive control of an electrohydraulic servosystem", *IEEE proc. part D*, Vol. 137, No. 2, Mar.1990, pp. 107-111.

[100] Ulsoy A. G., "Applications of adaptive control theory to metal cutting", *Dynamic Systems: modelling and control, winter annual meeting of ASME*, Miami beach, Fl, USA, 1985, Nov. 17-22.

[101] Daneshmend L. K. and Pak H. A., "Model reference adaptive control of feed force in turning", *Journal of dynamic systems, measurements and control*, Sept. 1986, Vol. 108, pp. 215-222.

[102] Pak H. A., "Cascaded adaptive controller for CNC lathe spindle drives", *Proceedings of the 1988 American control conference*, Atlanta, GA, USA, Jun. 15-17 1988, pp. 1184-1188.

[103] Fussell B. K. and Srinivasan K., "Model reference adaptive control of force in end milling operations", *Proceedings of the 1988 american control conference*, Atlanta, GA, USA, Jun. 15-17 1988, pp. 1189-1191.

[104] Lauderbaugh L. K. and Ulsoy A. G., "Model reference adaptive force control in milling", *Modelling, sensing and control of manufacturing process, winter annual meeting of ASME*, Anaheim, CA, USA, Dec. 7-12 1986, pp. 165-179.

[105] Suzuki A. and Hardt D., "Application of adaptive control to in process weld geometry regulation", *Proceedings of the american control conference*, Minneapolis, MN, USA, Jun.10-12 1987, pp. 723-728.

[106] Fujii S., Mizuno N. and Nomura Y., "Discrete time multi-variable model reference adaptive control algorithm with application to a real plant", *IFAC proceedings series* 1985, N2, pp. 877-882.

[107] Konishu K., Magava K., Yoshimura T. and Ishihara H., "Multivariable discrete time model reference adaptive control with input smoothing property and its application", *Int. Journal of system science*, Vol. 19, No. 5, May 1988, pp. 761-778.

[108] Li Z., Wang t. and Chen N., "Data model reference adaptive control for linear system", *Advanced modelling simulation*, Vol. 18, No. 1, 1989, pp. 47-56.

[109] M'Saad M., Landany I. D., Duque M. and Saman M., "Example applications of the partial state model reference adaptive design techniques", *Int. journal adaptive control signal process*, Vol. 3, No. 2, June 1989, pp. 155-165.

[110] Liu Y. E., Skormin V. and Liu Z., "Experimental comparison on adaptive control schemes", *Proceedings of the 27th IEEE conference on decision and control*, 1988, Vol. 3, pp. 1960-1961.

[111] Taylor Z. D. and Skormin V., "Design of an adaptive velocity controller for a programmable four wheel vehicle", *Proc. 1988 IEEE south tier tech. conference*, Binghamton, NY, USA, 1988, pp. 234-240.

[112] Zoubeidi M. and Auslander D. M., "Application of learning in adaptive control", *Proceedings of the 1985 american control conference*, Boston, MA, USA, Jun. 19-21 1985, pp. 1495-1500.

[113] Sharp P. S. and Hassan S. A., "An evaluation of passive automotive suspension systems with variable stiffness and damping parameters", *Vehicle system dynamics*, Vol. 15, 1986, pp. 335-350.

[114] Poyser J., "Development of a computer controlled suspension system", *Int. journal of vehicle design*, Vol. 8, 1987, pp. 74-86.

[115] Redfield R. C. and Karnopp D. C., "Optimal performance of variable component suspensions", *Vehicle system dynamics*, 17, 1988, pp. 231-253.

[116] Miller L. R., "Tuning passive, semi-active and fully active suspension systems", *Proceedings of the 27th IEEE conference on decision and control*, Austin, TX, USA, Dec. 7-9 1988, pp. 2047-2053.

[117] Hamilton J. M., "Computer optimized adaptive suspension technology (COAST)," *IEEE transactions on industrial electronics*, Vol. IE-32, No. 4, Nov. 1985, pp. 355-363.

[118] Karnopp D. and Margolis D., "Adaptive suspension concepts for road vehicles", *Vehicle system dynamics*, 13, 1984, pp. 145-160.

[119] Sachs H. K., "An adaptive control for vehicle suspensions", *Vehicle system dynamics*, Vol. 8, no. 2-3, 1979, pp. 210-206.

[120] Hac A., "Adaptive control of vehicle suspension", *Vehicle system dynamics* , 16, 1987, pp. 57-74.

[121] Yeh H., "Application of microprocessor in adaptive suspension systems", *IEEE*

[122] Adaptive suspension control. Technical leaflet, 1985, (Armstrong patents company Limited.).

[123] Patel R. V., Toda M. and Sridhar B., "Robustness of linear quadratic state feedback designs in the presence of system uncertainties", *IEEE. Trans. on automatic control*, Vol. Ac-22, No. 6, Dec. 1977, pp. 945-949.

[124] Leatherwood J. D. and Nixon G. V., "Active vibration isolation for flexible payloads".

[125] Cheok K. C., Mcgee N. H. and Petit T. F., "Optimal model following suspension with microcomputerized damping", *IEEE transactions on industrial electronics*, Vol. IE-32, No.4, Nov. 1985, pp. 364-371.

[126] Vallurupalli S. S., Dukkipati R. V. and Osman M. O. M., "Stable adaptive control of active suspension for nonlinear railway vehicle-plant: a model reference adaptive control approach", *Proceedings of 13th canadian congress of applied mechanics, CANCAM 91*, June 2-6 1991, Winnepeg, Manitoba, Canada, pp. 742-743.

[127] Sunwoo M., Cheok K. C. and Huang N. J., "Model reference adaptive control for vehicle active suspension systems", *IEEE transactions on industrial electronics*, Vol. 38, No. 3, June 1991.

[128] Dukkipati R. V., Vallurupalli S. S. and Osman M. O. M., "Adaptive control of active suspension - a state of the art review", *The archives of transport, journal of Polish academy of sciences*, Vol. IV, No. 1, 1992, pp. 7-17.

[129] Dukkipati R. V., Osman M. O. M., Vallurupalli S. S., "Real time adaptive control compared with stochastic optimal control of active suspension", *Trans*

*actions of Canadian society of mechanical engineering (CSME)*, Vol. 17, No. 4b, 1993, pp. 713-734.

[130] Vallurupalli S. S., Dukkipati R. V. and Osman M. O M., "Adaptive active suspension to attain optimal performance and maintain static equilibrium level", *International journal of vehicle design*, Vol. 14, Nos. 5/6, 1993.

[131] Vallurupalli S. S., Dukkipati R. V. and Osman M. O. M., "Discrete adaptive active suspension for hardware implementation". *Vehicle system dynamics journal*, Vol. 25, 1996.

[132] Vallurupalli S. S., Dukkipati R. V. and Osman M. O. M.,"Robust decentralized model reference adaptive control of active suspension for passenger rail vehicle systems", *12th IAVSD symposium at dynamics of vehicles on roads and tracks, Lyon, France*, August 26-30 1991, pp. 206-209.

[133] Vallurupalli S. S., Dukkipati R. V. and Osman M. O. M., "Adaptive control of an active suspension for nonlinear time varying vehicle-plant: a model reference adaptive control approach", *ASME winter annual meeting, 1991*, RTD-Vol 4, Atlanta, Georgia, USA, pp. 123-130.

[134] Vallurupalli S. S., Dukkipati R. V. and Osman M. O. M., "Adaptive control of active suspension for a general nonlinear time varying vehicle model", *Proceedings of ASME winter annual meeting*, 1992, Nov. 8-13, pp. 89-96.

[135] Vallurupalli S. S., Dukkipati R. V. and Osman M. O. M., "Adaptive vehicle system that maintains static equilibrium during load shifts", *Proceedings of ASME winter annual meeting*, DSC-Vol. 52, Nov. 1993, pp. 175-185.

[136] Vallurupalli S. S., Dukkipati R. V. and Osman M. O. M., "Smart adaptive active suspension the counteracts dynamic parameter variations in critical acceleration and deceleration maneuvers", Proceedings of *ASME winter annual Meeting*, 1994.

[137] Dukkipati R. V., Osman M. O. M. and Vallurupalli S. S., "Real time adaptive control compared with stochastic optimal control of active suspension", *Transport 1992+*, CSME forum 1992, 1-5 June 1992, Montreal, Canada.

[138] Cheok K. C. and Huang N. J., "Lyapunov stability analysis for self learning neural model with application to semi-active suspension control system", *Proceeding of IEEE international symposium on intelligent control* 1989, Albany, NY, USA, Sept. 25-26 1989, pp. 326-331.

[139] De Benito C. D. and Eckert S.J., "Control of an active suspension system subject to random component failures", *Journal of dynamic systems, measurements and control, Trans. of ASME*, Vol. 112, March 1990, pp. 94-99.

[140] Rakheja S. and Sankar S., "Vibration and shock isolation performance of a semi active "on-off" damper", *Journal of vibration, acoustics, stress and reliability in design*, Transactions of ASME, Vol. 107, October 1985, pp. 398-403.

[141] Rakheja S., Van Vliet M. and Sankar S., "A discrete harmonic linearization technique for simulating non-linear mechanical systems", *Journal of sound and vibration*, 100(4), 1985, pp. 511-526.

[142] La Barre R. P., Forbes R. T. and Andrew S., "The measurement and analysis of road surface roughness", *The motor industry research association*, Report No. 1970/5.

[143] Ruf G., "The calculation of the vibrations of a four wheeled vehicle induced by random road roughness of the left and right track", *Vehicle system dynamics*, Vol. 7, 1978, pp. 1-23.

[144] Kreyzig, "Engineering mathematics", Mcgraw Hill publications, pp. 617 624

[145] Astrom K. J. and Wittermark B., "Adaptive control", Addison Wesley Publishing Company.

[146] Goodwin, Sin K. C., "Adaptive filtering, prediction and control", Prentice Hall Inc., ISBN 0-13-0040 69.

[147] "Engi eering Mathematical Hand Book", Mc Graw Hill Publications, 1989, pp. 419-422.

[148] Vogel E. G. and Edgar T. F., "Applications of an adaptive , ole-zero placement controller to chemical processes with variable dead time", American control conference, Washington D.C..

[149] Sridharan G., "Improved active magnetic suspension", *Rev. Sci. Instrum.*, 54(10),October 1983, pp. 1418-1419.

[150] Stuart K., "Smart suspensions for the ideal ride", *Design news (Boston)*, Vol.45, No. 19, Oct. 2, 1989, pp. 104-106.

[151] Okamoto I., Koyamagi S., Higuki K., Terada K., Sebata M. and Takoi H., "Active suspension system for rail road passenger cars", *IEEE technical papers presented at the joint ASME/IEEE/AAR rail road conference*, 1987, pp. 141-146.

[152] Nagai M. and Sawada Y., "Optimal control of active suspension for a high speed ground vehicle (Analysis of a two-dof-model with a pneumatic actuator)", *Nippon kikai gakkai ronbunshu*, C Hen, Vol. 53, No. 487, Mar. 1987, pp. 750-756.

[153] Matushita H., Noritsugu T. and Wada T., "Pneumatic actuators", *Nippon Kikai Gakkai Ronbunshu*, C Hen, Vol. 56, No. 526, June 1990, pp. 1499-1504.

[154] Seraji H., "A new approach to adaptive control of manipulators", *Journal of dynamics, systems, measurements and control*, Vol. 109, Sept. 1987, pp. 193-201.

[155] Patel R. V and Munro N., "Multivariable system theory and design", Pergamon Press, New York.

[156] Wilkinson J. H., "The algebraic eigen value problem", Oxford University Press, Oxford.

[157] Patel R. V. and Misra P., "Numerical algorithms for eigen value assignment by state feedback, "Proceedings of IEEE, Vol.72, No. 12, Dec. 1984.

[158] Varga A. and Sima V., "Numerically stable algorithm for transfer function matrix evaluation", International journal of control, Vol. 33, No. 6, 1981, pp. 1123-1133.

[159] Bryson A. E. and Ho Y. C., "Applied optimal control, optimization, estimation and control", New York, John Wiley and sons, 1975.

[160] Colin, Campbell, "New directions in suspension design", Robert Bentley Inc., ISBN 0-8376-0150-9.

[161] Kortüm W Schichlen W., "General purpose vehicle system dynamics software based on multi-body formalisms", Vehicle system dynamics journal, Vol. 14, 1985, pp. 229-263.

[162] Bender B. K., "Optimization of the random vibration characteristics of vehicle suspensions", D.Sc.Thesis, M.I.T., 1967.

[163] Thompson A. G. and Pearce C. E. M., "An optimal suspension for an automobile on a random road", SAE Paper No. 790478, 1979.

[164] Sunwoo M., "Adaptive Control of Vehicle Active Suspension Systems", Ph.D Dissertation, Oakland University, Michigan, 1990.

# Appendix A

## A.1 Adaptation Laws For Continuous Time Multi-Degree of Freedom Model

The adjustable system derived in Eq.6.31 can be represented in the form

$$\dot{\vartheta} = \begin{bmatrix} 0 & \mathcal{I} \\ -\mathcal{J}_1 & -\mathcal{J}_2 \end{bmatrix} \{ \vartheta \} + \begin{Bmatrix} 0 \\ \mathcal{J}_3 \end{Bmatrix} + \begin{Bmatrix} 0 \\ \mathcal{J}_4 \end{Bmatrix} \ddot{Z}_m + \begin{Bmatrix} 0 \\ \mathcal{J}_5 \end{Bmatrix} \dot{Z}_m + \begin{Bmatrix} 0 \\ \mathcal{J}_6 \end{Bmatrix} Z_m + \begin{Bmatrix} 0 \\ \mathcal{J}_7 \end{Bmatrix} + \begin{Bmatrix} 0 \\ \mathcal{J}_8 \end{Bmatrix} \cdot \begin{Bmatrix} 0 \\ \mathcal{J}_9 \end{Bmatrix} \ddot{w} \quad \text{(A.1)}$$

where the terms $\mathcal{J}_1, \cdots, \mathcal{J}_9$ are given as

$$\begin{aligned} \mathcal{J}_1 &= \mathcal{M}^{*^{-1}} (\mathcal{M}^* + K_p) \\ \mathcal{J}_2 &= \mathcal{M}^{*^{-1}} (C^* + K_v) \\ \mathcal{J}_3 &= -\mathcal{M}^{*^{-1}} U_{ax} \\ \mathcal{J}_4 &= \mathcal{M}^{*^{-1}} (\mathcal{M}^* - \mathcal{M}_0) \\ \mathcal{J}_5 &= \mathcal{M}^{*^{-1}} (C^* - \mathcal{C}_0) \\ \mathcal{J}_6 &= \mathcal{M}^{*^{-1}} (K^* - \mathcal{K}_0) \\ \mathcal{J}_7 &= \mathcal{M}^{*^{-1}} (N^* - \mathcal{N}_0) \\ \mathcal{J}_8 &= \mathcal{M}^{*^{-1}} (L^* - \mathcal{L}_0) \\ \mathcal{J}_9 &= \mathcal{M}^{*^{-1}} (D^* - \mathcal{D}_0) \end{aligned} \quad \text{(A.2)}$$

Eq.A.1 contains the controller adjustable parameter vector $\{K_p, K_v, U_{ax}, \mathcal{M}_0, \mathcal{C}_0, \mathcal{K}_0, \mathcal{N}_0, \mathcal{L}_0, \mathcal{D}_0\}$. This vector contains the auxiliary, feedback and feed forward constants which are to be adapted and adjusted without a priori knowledge of actual vehicle parameters variations. The feed forward adjustable vector contains the information about the operating conditions. Since the changes in the operating conditions are not known, these matrices cannot be calculated and are to be adapted as a function of the model following error. Hence all th e controller parameters should be updated and adjusted in such a way that in spite of the dynamic parameter variations in the actual suspension model the actual error $[\vartheta(t)]$ should follow the desired error $[\vartheta_m(t)]$ as indicated by Eq.6.41 for any excitation $\ddot{w}(t)$ input to the model.

To derive the adaptation laws let the error between the actual error in model following and desired error be defined as

$$e|_{2n\times 1} = \vartheta_m(t)|_{2n\times 1} - \vartheta(t)|_{2n\times 1} \tag{A.3}$$

From Eq.6.39 and 6.41 we can write the error model as

$$\dot{e} = \begin{bmatrix} 0 & \mathcal{I}_n \\ -\cap_1 & -\cap_2 \end{bmatrix} e + \begin{bmatrix} 0 & 0 \\ \mathcal{J}_1 - \cap_1 & \mathcal{J}_2 - \cap_2 \end{bmatrix} \vartheta - \begin{Bmatrix} 0 \\ \mathcal{J}_3 \end{Bmatrix} - \begin{Bmatrix} 0 \\ \mathcal{J}_4 \end{Bmatrix} \dot{Z}_m$$

$$\begin{Bmatrix} 0 \\ \mathcal{J}_5 \end{Bmatrix} \dot{Z}_m - \begin{Bmatrix} 0 \\ \mathcal{J}_6 \end{Bmatrix} Z_m - \begin{Bmatrix} 0 \\ \mathcal{J}_7 \end{Bmatrix} - \begin{Bmatrix} 0 \\ \mathcal{J}_8 \end{Bmatrix} - \begin{Bmatrix} 0 \\ \mathcal{J}_9 \end{Bmatrix} w \tag{A.4}$$

which can be denoted in the form as

$$\dot{e} = \cap e + \mathcal{T}_1\vartheta - \mathcal{T}_2 - \mathcal{T}_3\ddot{Z}_m - \mathcal{T}_4\dot{Z}_m - \mathcal{T}_5 Z_m - \mathcal{T}_6 - \mathcal{T}_7 - \mathcal{T}_8\ddot{w} \tag{A.5}$$

Let the actual but unknown controller parameters vector be represented as

$$\{K_p^*, K_v^*, U_{ax}^*, \mathcal{M}_0^*, \mathcal{C}_0^*, \mathcal{K}_0^*, \mathcal{N}_0^*, \mathcal{L}_0^*, D_0^*\} \tag{A.6}$$

When these unknown controller parameters are substituted in Eq.A.2, we derive the actual but unknown values of the respective terms $\mathcal{J}_1, \cdots, \mathcal{J}_9$ which are represented as $\mathcal{J}_1^*, \cdots, \mathcal{J}_9^*$

$$\begin{aligned}
\mathcal{J}_1^* &= \mathcal{M}^{*-1}(\mathcal{K}^* + K_p^*) \\
\mathcal{J}_2^* &= \mathcal{M}^{*-1}(\mathcal{C}^* + K_v^*) \\
\mathcal{J}_3^* &= -\mathcal{M}^{*-1}U_{ax} \\
\mathcal{J}_4^* &= \mathcal{M}^{*-1}(\mathcal{M}^* - \mathcal{M}_0^*) \\
\mathcal{J}_5^* &= \mathcal{M}^{*-1}(\mathcal{C}^* - \mathcal{C}_0^*) \\
\mathcal{J}_6^* &= \mathcal{M}^{*-1}(\mathcal{K}^* - \mathcal{K}_0^*) \\
\mathcal{J}_7^* &= \mathcal{M}^{*-1}(\mathcal{N}^* - \mathcal{N}_0^*) \\
\mathcal{J}_8^* &= \mathcal{M}^{*-1}(\mathcal{L}^* - \mathcal{L}_0^*) \\
\mathcal{J}_9^* &= \mathcal{M}^{*-1}(\mathcal{D}^* - \mathcal{D}_0^*)
\end{aligned} \tag{A.7}$$

The error as the difference between the actual nonlinear and unknown operating point values in Eq.A.7 and the corresponding differences between the terms at the estimated operating point in Eq.A.2 would yield

$$\{(\mathcal{J}_1 - \mathcal{J}_1^*), (\mathcal{J}_2 - \mathcal{J}_2^*), \cdots, (\mathcal{J}_9 - \mathcal{J}_9^*)\} \tag{A.8}$$

The error vector also indicates the difference between the parameters estimated and the actual unknown controller parameters. Let a Lyapunov function incorporating tracking error represented in Eq.A.3 and controller parameter errors defined in Eq.A.8 be defined in the form

$$\begin{aligned} \mathcal{V} \;=\; & e^T \mathcal{R} e + tr\left\{(\mathcal{J}_1 - \mathcal{J}_1^*)^T \mathcal{Q}_1 (\mathcal{J}_1 - \mathcal{J}_1^*)\right\} \\ & + tr\left\{(\mathcal{J}_2 - \mathcal{J}_2^*)^T \mathcal{Q}_2 (\mathcal{J}_2 - \mathcal{J}_2^*)\right\} + \left\{(\mathcal{J}_3 - \mathcal{J}_3^*)^T \mathcal{Q}_3 (\mathcal{J}_3 - \mathcal{J}_3^*)\right\} \\ & + tr\left\{(\mathcal{J}_4 - \mathcal{J}_4^*)^T \mathcal{Q}_4 (\mathcal{J}_4 - \mathcal{J}_4^*)\right\} + tr\left\{(\mathcal{J}_5 - \mathcal{J}_5^*)^T \mathcal{Q}_5 (\mathcal{J}_5 - \mathcal{J}_5^*)\right\} \\ & + tr\left\{(\mathcal{J}_6 - \mathcal{J}_6^*)^T \mathcal{Q}_6 (\mathcal{J}_6 - \mathcal{J}_6^*)\right\} + \left\{(\mathcal{J}_7 - \mathcal{J}_7^*)^T \mathcal{Q}_7 (\mathcal{J}_7 - \mathcal{J}_7^*)\right\} \\ & + \left\{(\mathcal{J}_8 - \mathcal{J}_8^*)^T \mathcal{Q}_8 (\mathcal{J}_8 - \mathcal{J}_8^*)\right\} + \left\{(\mathcal{J}_9 - \mathcal{J}_9^*)^T \mathcal{Q}_9 (\mathcal{J}_9 - \mathcal{J}_9^*)\right\} \end{aligned} \tag{A.9}$$

where, "$tr$" denotes the trace of the matrix and the nature of matrices $\mathcal{Q}_1, \cdots, \mathcal{Q}_9$ is discussed in the next section.

## A.2 Derivation of Adaptation Laws

This section deals with derivation of the controller laws based on the Lyapunov function described in Eq.A.9. The derivative of Lyapunov function in Eq.A.9 can be written as

$$\begin{aligned} \dot{\mathcal{V}} = \dot{e}^T \mathcal{R} e + e^T \mathcal{R} \dot{e} + \quad & tr\left\{\left(\dot{\mathcal{J}}_1 - \dot{\mathcal{J}}_1^*\right)^T \mathcal{Q}_1 (\mathcal{J}_1 - \mathcal{J}_1^*) + (\mathcal{J}_1 - \mathcal{J}_1^*)^T \mathcal{Q}_1 \left(\dot{\mathcal{J}}_1 - \dot{\mathcal{J}}_1^*\right)\right\} \\ & + tr\left\{\left(\dot{\mathcal{J}}_2 - \dot{\mathcal{J}}_2^*\right)^T \mathcal{Q}_2 (\mathcal{J}_2 - \mathcal{J}_2^*) + (\mathcal{J}_2 - \mathcal{J}_2^*)^T \mathcal{Q}_2 \left(\dot{\mathcal{J}}_2 - \dot{\mathcal{J}}_2^*\right)\right\} \\ & + \left\{\left(\dot{\mathcal{J}}_3 - \dot{\mathcal{J}}_3^*\right)^T \mathcal{Q}_3 (\mathcal{J}_3 - \mathcal{J}_3^*) + (\mathcal{J}_3 - \mathcal{J}_3^*)^T \mathcal{Q}_3 \left(\dot{\mathcal{J}}_3 - \dot{\mathcal{J}}_3^*\right)\right\} \\ & + tr\left\{\left(\dot{\mathcal{J}}_4 - \dot{\mathcal{J}}_4^*\right)^T \mathcal{Q}_4 (\mathcal{J}_4 - \mathcal{J}_4^*) + (\mathcal{J}_4 - \mathcal{J}_4^*)^T \mathcal{Q}_4 \left(\dot{\mathcal{J}}_4 - \dot{\mathcal{J}}_4^*\right)\right\} \end{aligned}$$

$$+tr\left\{\left(\dot{\mathcal{J}}_5 - \dot{\mathcal{J}}_5^*\right)^T Q_5(\mathcal{J}_5 - \mathcal{J}_5^*) + (\mathcal{J}_5 - \mathcal{J}_5^*)^T Q_5\left(\mathcal{J}_5 \quad \mathcal{J}_5^*\right)\right\}$$

$$+tr\left\{\left(\mathcal{J}_6 - \dot{\mathcal{J}}_6^*\right)^T Q_6(\mathcal{J}_6 - \mathcal{J}_6^*) + (\mathcal{J}_6 \quad \mathcal{J}_6^*)^T Q_6\left(\mathcal{J}_6 \quad \mathcal{J}_6^*\right)\right\}$$

$$+\left\{\left(\mathcal{J}_7 - \dot{\mathcal{J}}_7^*\right)^T Q_7(\mathcal{J}_7 - \mathcal{J}_7^*) + (\mathcal{J}_7 \quad \mathcal{J}_7^*)^T Q_7\left(\mathcal{J}_7 \quad \mathcal{J}_7^*\right)\right\}$$

$$+\left\{\left(\mathcal{J}_8 - \dot{\mathcal{J}}_8^*\right)^T Q_8(\mathcal{J}_8 - \mathcal{J}_8^*) + (\mathcal{J}_8 - \mathcal{J}_8^*)^T Q_8\left(\mathcal{J}_8 \quad \mathcal{J}_8^*\right)\right\}$$

$$+\left\{\left(\mathcal{J}_9 - \dot{\mathcal{J}}_9^*\right)^T Q_9(\mathcal{J}_9 - \mathcal{J}_9^*) + (\mathcal{J}_9 \quad \mathcal{J}_9^*)^T Q_9\left(\mathcal{J}_9 \quad \mathcal{J}_9^*\right)\right\}$$

(A.10)

$$\begin{aligned}
\dot{\mathcal{V}} = \; & e^T \Omega^T \mathcal{R} e + e^T \mathcal{R} \Omega e + \left(\vartheta^T \mathcal{T}_1{}^T \mathcal{R} e + e^T \mathcal{R} \mathcal{T}_1 \vartheta\right) + \left(\mathcal{T}_2{}^T \mathcal{R} e \quad e^T \mathcal{R} I\right) + \\
& \left(-\ddot{Z}_m^T \mathcal{T}_3{}^T \mathcal{R} e - e^T \mathcal{R} \mathcal{T}_3 \ddot{Z}_m\right) + \left(-\dot{Z}_m^T \mathcal{T}_4{}^T \mathcal{R} e - e^T \mathcal{R} \mathcal{T}_4 Z_m\right) + \\
& \left(-Z_m{}^T \mathcal{T}_5{}^T \mathcal{R} e - e^T \mathcal{R} \mathcal{T}_5 Z_m\right) + \left(-\mathcal{T}_6{}^T \mathcal{R} e - e^T \mathcal{R} \mathcal{T}_6\right) + \\
& \left(-\mathcal{T}_7{}^T \mathcal{R} e - e^T \mathcal{R} \mathcal{T}_7\right) + \left(-\ddot{w}^T \mathcal{T}_8{}^T \mathcal{R} e - e^T \mathcal{R} \mathcal{T}_8 w\right) + \\
& tr\left\{\left(\dot{\mathcal{J}}_1 - \dot{\mathcal{J}}_1^*\right)^T Q_1(\mathcal{J}_1 - \mathcal{J}_1^*) + (\mathcal{J}_1 - \mathcal{J}_1^*)^T Q_1\left(\mathcal{J}_1 \quad \mathcal{J}_1^*\right)\right\} + \\
& tr\left\{\left(\dot{\mathcal{J}}_2 - \dot{\mathcal{J}}_2^*\right)^T Q_2(\mathcal{J}_2 - \mathcal{J}_2^*) + (\mathcal{J}_2 - \mathcal{J}_2^*)^T Q_2\left(\mathcal{J}_2 \quad \mathcal{J}_2^*\right)\right\} + \\
& \left\{\left(\dot{\mathcal{J}}_3 - \dot{\mathcal{J}}_3^*\right)^T Q_3(\mathcal{J}_3 - \mathcal{J}_3^*) + (\mathcal{J}_3 - \mathcal{J}_3^*)^T Q_3\left(\mathcal{J}_3 - \mathcal{J}_3^*\right)\right\} + \\
& tr\left\{\left(\dot{\mathcal{J}}_4 - \dot{\mathcal{J}}_4^*\right)^T Q_4(\mathcal{J}_4 - \mathcal{J}_4^*) + (\mathcal{J}_4 - \mathcal{J}_4^*)^T Q_4\left(\mathcal{J}_4 \quad \mathcal{J}_4^*\right)\right\} + \\
& tr\left\{\left(\dot{\mathcal{J}}_5 - \dot{\mathcal{J}}_5^*\right)^T Q_5(\mathcal{J}_5 - \mathcal{J}_5^*) + (\mathcal{J}_5 - \mathcal{J}_5^*)^T Q_5\left(\mathcal{J}_5 \quad \mathcal{J}_5^*\right)\right\} + \\
& tr\left\{\left(\dot{\mathcal{J}}_6 - \dot{\mathcal{J}}_6^*\right)^T Q_6(\mathcal{J}_6 - \mathcal{J}_6^*) + (\mathcal{J}_6 \quad \mathcal{J}_6^*)^T Q_6\left(\mathcal{J}_6 - \mathcal{J}_6^*\right)\right\} + \\
& \left\{\left(\dot{\mathcal{J}}_7 - \dot{\mathcal{J}}_7^*\right)^T Q_7(\mathcal{J}_7 - \mathcal{J}_7^*) + (\mathcal{J}_7 - \mathcal{J}_7^*)^T Q_7\left(\mathcal{J}_7 \quad \mathcal{J}_7^*\right)\right\} + \\
& \left\{\left(\dot{\mathcal{J}}_8 - \dot{\mathcal{J}}_8^*\right)^T Q_8(\mathcal{J}_8 - \mathcal{J}_8^*) + (\mathcal{J}_8 \quad \mathcal{J}_8^*)^T Q_8\left(\mathcal{J}_8 \quad \mathcal{J}_8^*\right)\right\} + \\
& \left\{\left(\dot{\mathcal{J}}_9 - \dot{\mathcal{J}}_9^*\right)^T Q_9(\mathcal{J}_9 - \mathcal{J}_9^*) + (\mathcal{J}_9 - \mathcal{J}_9^*)^T Q_9\left(\mathcal{J}_9 - \mathcal{J}_9^*\right)\right\}
\end{aligned}$$

(A.11)

Various terms in Eq.A.11 are simplified and are individually reduced, so that the

derivative of the Lyapunov function can be written in the following form

$$\begin{aligned}
\dot{V} = & -\epsilon^T Q\epsilon + 2tr\left\{\epsilon_1^T \quad E^T + \epsilon_2^T \quad E^T\right\} + \\
& 2tr\left\{\mathcal{J}_1^T[-\quad E^T + Q_1\mathcal{J}_1 - Q_1\mathcal{J}_1^* - \mathcal{J}_1^{*T}Q_1\left[\mathcal{J}_1 - \mathcal{J}_1^*\right]\right\} + \\
& 2tr\left\{\mathcal{J}_2^T[-\quad E^T + Q_2\mathcal{J}_2 \quad Q_2\mathcal{J}_2^* \quad \mathcal{J}_2^{*T}Q_2\left[\mathcal{J}_2 \quad \mathcal{J}_2^*\right]\right\} + \\
& 2\mathcal{J}_3^T[\quad + Q_3\mathcal{J}_3 - Q_3\mathcal{J}_3^* \quad 2\mathcal{J}_3^{*T}Q_3\left[\mathcal{J}_3 - \mathcal{J}_3^*\right] + \\
& 2tr\left\{\mathcal{J}_4^T[-\dot{Z}_m^T - Q_4\mathcal{J}_4 - Q_4\mathcal{J}_4^*] - \mathcal{J}_4^{*T}Q_4\left[\mathcal{J}_4 \quad \mathcal{J}_4^*\right]\right\} + \\
& 2tr\left\{\mathcal{J}_5^T[-\dot{Z}_m^T - Q_5\mathcal{J}_5 - Q_5\dot{\mathcal{J}}_5^*] - \mathcal{J}_5^{*T}Q_5\left[\mathcal{J}_5 \quad \mathcal{J}_5^*\right]\right\} + \\
& 2tr\left\{\mathcal{J}_6^T[\quad Z_m^T + Q_6\mathcal{J}_6 - Q_6\dot{\mathcal{J}}_6^*] - \mathcal{J}_6^{*T}Q_6\left[\mathcal{J}_6 \quad \mathcal{J}_6^*\right]\right\} + \\
& 2\mathcal{J}_7^T[\quad + Q_7\mathcal{J}_7 - Q_7\mathcal{J}_7^*] - 2\mathcal{J}_7^{*T}Q_7\left[\mathcal{J}_7 - \mathcal{J}_7^*\right] + \\
& 2\mathcal{J}_8^T[\quad + Q_8\mathcal{J}_8 - Q_8\mathcal{J}_8^*] - 2\mathcal{J}_8^{*T}Q_8\left[\mathcal{J}_8 \quad \mathcal{J}_8^*\right] + \\
& 2\mathcal{J}_9^T[-\dot{w} - Q_9\dot{\mathcal{J}}_9 - Q_9\mathcal{J}_9^*] - 2\mathcal{J}_9^{*T}Q_9\left[\mathcal{J}_9 - \mathcal{J}_9^*\right]
\end{aligned} \tag{A.12}$$

where, $\cdot = \mathcal{R}_2 E + \mathcal{R}_3 E$. Simplification of the term $"2tr\left\{\epsilon_1^T \quad E^T + \epsilon_2^T \quad E^T\right\}"$ in the above equation, would result in the form of a summation as

$$\sum_{i=1}^{n}\left\{\omega_i^2\mathcal{R}_{2i}E_i^2 + \left(\omega_i^2\mathcal{R}_{3i} + 2\zeta_i\omega_i\mathcal{R}_{2i}\right)E_i\dot{E}_i + 2\zeta_i\omega_i\mathcal{R}_{3i}\left(\dot{E}_i\right)^2\right\} \tag{A.13}$$

$\mathcal{R}_{2i}$ and $\mathcal{R}_{3i}$ in the above expression represent the diagonal elements of matrices $R_2$ and $\mathcal{R}_3$ respectively. The expression in Eq A.13 is a summation of squares of $E$ or $\dot{E}$. Since the error at the initial condition and on adaptation is small, the product is smaller and hence this term can be considered to be zero. For the adaptation error ($\epsilon$) to asymptotically approach zero (i.e $\vartheta(t) \to \vartheta_m(t)$ or $\vartheta(t) \to 0$ as $t \to \infty$), $\dot{V}$ should be negative definite in $\epsilon$. Hence, on choosing the following terms as zeros in Eq.A.12, we have

$$\begin{aligned}
-\epsilon E^T \quad + \quad & Q_1\dot{\mathcal{J}}_1 - Q_1\dot{\mathcal{J}}_1^* = 0 \\
-\epsilon \dot{E}^T \quad + \quad & Q_2\dot{\mathcal{J}}_2 - Q_2\dot{\mathcal{J}}_2^* = 0 \\
\epsilon \quad + \quad & Q_3\dot{\mathcal{J}}_3 - Q_3\dot{\mathcal{J}}_3^* = 0 \\
\epsilon\ddot{Z}_m^T \quad + \quad & Q_4\dot{\mathcal{J}}_4 - Q_4\dot{\mathcal{J}}_4^* = 0 \\
\epsilon\dot{Z}_m^T \quad + \quad & Q_5\mathcal{J}_5 - Q_5\dot{\mathcal{J}}_5^* = 0 \\
\epsilon Z_m^T \quad + \quad & Q_6\mathcal{J}_6 - Q_6\dot{\mathcal{J}}_6^* = 0
\end{aligned}$$

$$
\begin{aligned}
+ \quad & Q_7 \mathcal{J}_7 - Q_7 \mathcal{J}_7^* = 0 \\
+ \quad & Q_8 \mathcal{J}_8 - Q_8 \mathcal{J}_8^* = 0 \\
+ \quad & Q_9 \mathcal{J}_9 - Q_9 \dot{\mathcal{J}}_9^* = 0
\end{aligned}
\tag{A.14}
$$

Sub equations in the above equation would consequently yield equations of the form

$$
\begin{aligned}
Q_1 \left( \mathcal{J}_1 - \mathcal{J}_1^* \right) &= E^I \\
Q_2 \left( \mathcal{J}_2 - \mathcal{J}_2^* \right) &= F^I \\
Q_3 \left( \mathcal{J}_3 - \mathcal{J}_3^* \right) &= - \\
Q_4 \left( \mathcal{J}_4 - \dot{\mathcal{J}}_4^* \right) &= - \quad Z_m^I \\
Q_5 \left( \mathcal{J}_5 - \mathcal{J}_5^* \right) &= - \quad \dot{Z}_m^I \\
Q_6 \left( \mathcal{J}_6 - \dot{\mathcal{J}}_6^* \right) &= - \quad Z_m{}^I \\
Q_7 \left( \mathcal{J}_7 - \dot{\mathcal{J}}_7^* \right) &= - \\
Q_8 \left( \mathcal{J}_8 - \mathcal{J}_8^* \right) &= - \\
Q_9 \left( \dot{\mathcal{J}}_9 - \dot{\mathcal{J}}_9^* \right) &= - \quad \dot{w}
\end{aligned}
\tag{A.15}
$$

Substituting the above conditions into Eq.A.12 we obtain

$$
\dot{\mathcal{V}} = -\epsilon^T Q \epsilon - 2tr \left\{ \mathcal{J}_1^{*T} \quad E^T \right\} - 2tr \left\{ \mathcal{J}_2^{*T} \dot{E}^I \right\} + 2\mathcal{J}_3^{*T} + 2\mathcal{J}_4^{*T} \quad \dot{Z}_m^T + 2\mathcal{J}_5^{*T} \quad \dot{Z}_m^I + 2\mathcal{J}_6^{*T} \quad Z_m{}^T + 2\mathcal{J}_7^{*T} + 2\mathcal{J}_8^{*T} + 2\mathcal{J}_9^{*T} \ddot{w}
\tag{A.16}
$$

since $tr \left\{ \mathcal{J}_i^{*T} \quad E^I \right\} = E^I \mathcal{J}_i^{*I}$ where, $i = 1,9$. we can write Eq.A.16 as

$$
\begin{aligned}
\dot{\mathcal{V}} = -\epsilon^T Q \epsilon \; & - 2E^I \mathcal{J}_1^{*T} - 2\dot{E}^I \mathcal{J}_2^{*T} + 2\mathcal{J}_3^{*T} + 2\ddot{Z}_m^T \mathcal{J}_4^{*T} + \\
& 2\dot{Z}_m^I \mathcal{J}_5^{*I} + 2Z_m{}^T \mathcal{J}_6^{*T} + 2\mathcal{J}_7^{*T} + 2\mathcal{J}_8^{*T} + 2\mathcal{J}_9^{*T} \ddot{w}
\end{aligned}
\tag{A.17}
$$

Let us choose the unknown but constant controller parameters described in Eqs.A.2

as

$$
\begin{aligned}
\mathcal{J}_1^* &= -\mathcal{Q}_1 E^T \\
\mathcal{J}_2^* &= \mathcal{Q}_2 E^T \\
\mathcal{J}_3^* &= \mathcal{Q}_3 \\
\mathcal{J}_4^* &= -\mathcal{Q}_4 Z_m^T \\
\mathcal{J}_5^* &= \mathcal{Q}_5 Z_m^T \\
\mathcal{J}_6^* &= -\mathcal{Q}_6 Z_m^T \\
\mathcal{J}_7^* &= -\mathcal{Q}_7 \\
\mathcal{J}_8^* &= -\mathcal{Q}_8 \\
\mathcal{J}_9^* &= -\dot{w}\mathcal{Q}_9
\end{aligned}
\tag{A.18}
$$

The matrices $\mathcal{Q}_1 \cdots \mathcal{Q}_9$ are chosen to be some positive semi definite symmetric constant $(n \times n)$ matrices. Substituting the sub-equations in Eq A.18 and in Eq A.17 we obtain

$$
\begin{aligned}
\dot{\mathcal{V}} = -\epsilon^T \mathcal{Q}_\epsilon - 2\left(E^T E\right) \tilde{\mathcal{J}}_1^T \mathcal{Q}_1 - 2\left(\dot{E}^T E\right) \tilde{\mathcal{J}}_2^T \mathcal{Q}_2 - 2 \tilde{\mathcal{J}}_3^T \mathcal{Q}_3 \\
- 2\left(\ddot{Z}_m^T \dot{Z}_m\right) \tilde{\mathcal{J}}_4^T \mathcal{Q}_4 - 2\left(\dot{Z}_m^T Z_m\right) \tilde{\mathcal{J}}_5^T \mathcal{Q}_5 - 2\left(Z_m^T Z_m\right) \tilde{\mathcal{J}}_6^T \mathcal{Q}_6 \\
- 2 \tilde{\mathcal{J}}_7^T \mathcal{Q}_7 - 2 \tilde{\mathcal{J}}_8^T \mathcal{Q}_8 - 2(\dot{w})^2 \tilde{\mathcal{J}}_9^T \mathcal{Q}_9
\end{aligned}
\tag{A.19}
$$

All the terms in Eq.A.19 are negative definite, hence $\dot{\mathcal{V}}$ is negative definite in terms of the error $(\epsilon)$ and the error in controller parameters. Hence, the model following error $(\epsilon)$ and the controller parameter error vector in Eq A.8 would asymptotically go to zero (i.e. $\epsilon \to 0$, $K_p \to K_p^*, K_v \to K_v^*, \ldots, \mathcal{D}_0 \to D^*$ as $t \to \infty$).

Substituting Eqs.A.18 in the corresponding equations in Eqs.A.14, we obtain the adaptation laws as

$$
\begin{aligned}
\dot{\mathcal{J}}_1 &= \mathcal{Q}_1^{-1} \left[ E^T + \dot{\mathcal{Q}}_1 \frac{d\left(E^T\right)}{dt} \right] \\
\dot{\mathcal{J}}_2 &= \mathcal{Q}_2^{-1} \left[ \dot{E}^T + \dot{\mathcal{Q}}_2 \frac{d\left(\dot{E}^T\right)}{dt} \right]
\end{aligned}
$$

$$
\begin{aligned}
\dot{J}_1 &= -Q_1^{-1} \quad -\dot{Q}_1 \frac{d(\quad)}{dt} \\
\dot{J}_2 &= -Q_2^{-1} \quad Z_m^I - \dot{Q}_2 \frac{d\left(-Z_m^I\right)}{dt} \\
\dot{J}_3 &= -Q_3^{-1} \quad Z_m^I - \dot{Q}_3 \frac{d\left(-Z_m^I\right)}{dt} \\
\dot{J}_4 &= -Q_4^{-1} \cdot Z_m{}^T - \dot{Q}_4 \frac{d\left(-Z_m{}^T\right)}{dt} \\
\dot{J}_5 &= -Q_5^{-1} \cdot \quad -\dot{Q}_5 \frac{d(\quad)}{dt} \\
\dot{J}_6 &= -Q_6^{-1} \quad -\dot{Q}_6 \frac{d(\quad)}{dt} \\
\dot{J}_7 &= -Q_7^{-1} \quad -\dot{Q}_7 \frac{d(-\ddot{w})}{dt}
\end{aligned}
\tag{A.20}
$$

Since the controller laws are simple first order differential equations, the controller could be implemented with small step size. As the vehicle model parameters are assumed to vary slowly compared to the controller dynamics, it is assumed that dynamic equation matrices $\mathcal{M}^*, \mathcal{C}^*, \mathcal{K}^*, \mathcal{N}^*, \mathcal{L}^*, \mathcal{D}^*$ are constants about an operating point. Taking the derivative on both sides of Eqs.A.2 would yield

$$
\begin{aligned}
\dot{J}_1 &= \mathcal{M}^{*-1}\dot{K}_p \\
\dot{J}_2 &= \mathcal{M}^{*-1}\dot{K}_v \\
\dot{J}_3 &= -\mathcal{M}^{*-1}\dot{I}_{ax} \\
\dot{J}_4 &= -\mathcal{M}^{*-1}\dot{\mathcal{M}}_0 \\
\dot{J}_5 &= -\mathcal{M}^{*-1}\dot{\mathcal{C}}_0 \\
\dot{J}_6 &= -\mathcal{M}^{*-1}\dot{\mathcal{K}}_0 \\
\dot{J}_7 &= -\mathcal{M}^{*-1}\dot{\mathcal{N}}_0 \\
\dot{J}_8 &= -\mathcal{M}^{*-1}\dot{\mathcal{L}}_0 \\
\dot{J}_9 &= -\mathcal{M}^{*-1}\dot{\mathcal{D}}_0
\end{aligned}
\tag{A.21}
$$

Substituting the equations in Eq.A.20 into corresponding sub-equations in Eq.A.21, we obtain the adaptation laws as

$$
\begin{aligned}
\dot{K}_p &= \mathcal{M}^* Q_1^{-1} \ominus E^T + \mathcal{M}^* \dot{Q}_1 \frac{d\left(\ominus E^T\right)}{dt} \\
\dot{K}_v &= \mathcal{M}^* Q_2^{-1} \ominus \dot{E}^T + \mathcal{M}^* \dot{Q}_2 \frac{d\left(\ominus \dot{E}^T\right)}{dt}
\end{aligned}
$$

$$
\begin{aligned}
\dot{I}_{zz} &= \mathcal{M}^{*}\mathcal{Q}_{1}^{-1} \quad + \mathcal{M}^{*}\dot{\mathcal{Q}}_{1}\frac{d(\quad)}{dt} \\
\dot{\mathcal{M}}_{0} &= \mathcal{M}^{*}\mathcal{Q}_{4}^{-1} \quad \mathcal{Z}_{m}^{I} + \mathcal{M}^{*}\dot{\mathcal{Q}}_{4}\frac{d\left(\quad \mathcal{Z}_{m}^{I}\right)}{dt} \\
\dot{\mathcal{C}}_{0} &= \mathcal{M}^{*}\mathcal{Q}_{5}^{-1} \quad \mathcal{Z}_{m}^{I} + \mathcal{M}^{*}\dot{\mathcal{Q}}_{5}\frac{d\left(\quad \mathcal{Z}_{m}^{I}\right)}{dt} \\
\dot{\mathcal{K}}_{0} &= \mathcal{M}^{*}\mathcal{Q}_{6}^{-1} \quad \mathcal{Z}_{m}^{I} + \mathcal{M}^{*}\dot{\mathcal{Q}}_{6}\frac{d\left(\quad \mathcal{Z}_{m}^{I}\right)}{dt} \\
\dot{\mathcal{N}}_{0} &= \mathcal{M}^{*}\mathcal{Q}_{7}^{-1} \quad + \mathcal{M}^{*}\dot{\mathcal{Q}}_{7}\frac{d(\quad)}{dt} \\
\dot{\mathcal{L}}_{0} &= \mathcal{M}^{*}\mathcal{Q}_{8}^{-1} \quad + \mathcal{M}^{*}\dot{\mathcal{Q}}_{8}\frac{d(\quad)}{dt} \\
\dot{\mathcal{D}}_{0} &= \mathcal{M}^{*}\mathcal{Q}_{9}^{-1} - \ddot{w} + \mathcal{M}^{*}\dot{\mathcal{Q}}_{9}\frac{d(\quad\dot{w})}{dt}
\end{aligned}
\tag{A.22}
$$

The controller laws in Eq.A.22 could be implemented easily with the knowledge of $\mathcal{M}^{*}$. If $\mathcal{M}^{*}$ is time varying some sort of identification could be used to estimate the matrix $\mathcal{M}^{*}$. But as proved earlier by the adaptation $\mathcal{M}_{0} \rightarrow \mathcal{M}^{*}$ as $t \rightarrow \infty$, $\mathcal{M}_{0}$ could be used as an estimate for a better result. In this case since $\mathcal{M}_{0}$ is positive definite, $\mathcal{M}^{*}$ could be replaced by $\mathcal{M}_{0}$. If the matrices $(\mathcal{Q}_{1}, \quad , \mathcal{Q}_{9})$ and $\left(\dot{\mathcal{Q}}_{1}, \quad , \dot{\mathcal{Q}}_{9}\right)$ in sub-equations in Eq.A.22 are chosen such that

$$
\begin{aligned}
\mathcal{M}_{0}\mathcal{Q}_{1}^{-1} &= \alpha_{1} \;:\; \mathcal{M}_{0}\dot{\mathcal{Q}}_{1} = \beta_{1} \\
\mathcal{M}_{0}\mathcal{Q}_{2}^{-1} &= \alpha_{2} \;:\; \mathcal{M}_{0}\dot{\mathcal{Q}}_{2} = \beta_{2} \\
\mathcal{M}_{0}\mathcal{Q}_{3}^{-1} &= \alpha_{3} \;:\; \mathcal{M}_{0}\dot{\mathcal{Q}}_{3} = \beta_{3} \\
\mathcal{M}_{0}\mathcal{Q}_{4}^{-1} &= \alpha_{4} \;:\; \mathcal{M}_{0}\dot{\mathcal{Q}}_{4} = \beta_{4} \\
\mathcal{M}_{0}\mathcal{Q}_{5}^{-1} &= \alpha_{5} \;:\; \mathcal{M}_{0}\dot{\mathcal{Q}}_{5} = \beta_{5} \\
\mathcal{M}_{0}\mathcal{Q}_{6}^{-1} &= \alpha_{6} \;:\; \mathcal{M}_{0}\dot{\mathcal{Q}}_{6} = \beta_{6} \\
\mathcal{M}_{0}\mathcal{Q}_{7}^{-1} &= \alpha_{7} \;:\; \mathcal{M}_{0}\dot{\mathcal{Q}}_{7} = \beta_{7} \\
\mathcal{M}_{0}\mathcal{Q}_{8}^{-1} &= \alpha_{8} \;:\; \mathcal{M}_{0}\dot{\mathcal{Q}}_{8} = \beta_{8} \\
\mathcal{M}_{0}\mathcal{Q}_{9}^{-1} &= \alpha_{9} \;:\; \mathcal{M}_{0}\dot{\mathcal{Q}}_{9} = \beta_{9}
\end{aligned}
\tag{A.23}
$$

then substituting Eq.A.23 in Eq.A.22, we derive the following equations.

$$
\dot{K}_{p} = \alpha_{1} \quad E^{T} + \beta_{1}\frac{d\left(\quad E^{T}\right)}{dt}
$$

$$
\begin{aligned}
\dot{K}_1 &= \alpha_2 \quad E^T + \beta_2 \frac{d\left(\quad \dot{E}^T\right)}{dt} \\
\dot{\Gamma}_{12} &= \alpha_3 \quad + \beta_3 \frac{d(\quad)}{dt} \\
\dot{\mathcal{M}}_0 &= \alpha_4 \quad \dot{Z}_m^T + \beta_4 \frac{d\left(\quad \ddot{Z}_m^T\right)}{dt} \\
\dot{\mathcal{C}}_0 &= \alpha_5 \quad \dot{Z}_m^T + \beta_5 \frac{d\left(\quad Z_m^T\right)}{dt} \\
\dot{\mathcal{K}}_0 &= \alpha_6 \quad Z_m{}^T + \beta_6 \frac{d\left(\quad Z_m{}^T\right)}{dt} \\
\dot{\mathcal{N}}_0 &= \alpha_7 \quad + \beta_7 \frac{d(\quad)}{dt} \\
\dot{\mathcal{L}}_0 &= \alpha_8 \quad + \beta_8 \frac{d(\quad)}{dt} \\
\dot{\mathcal{D}}_0 &= \alpha_9 \quad \ddot{w} + \beta_9 \frac{d(\quad \ddot{w})}{dt}
\end{aligned}
\tag{A.24}
$$

Sub equations in Eq.A.24 represent the desired adaptation rates for feed forward, feed back and auxiliary signal controller parameters as first order differential equations.

# Appendix B

## B.1 Linearization of Half-Car Suspension Model

The nonlinear and discontinuous functions in the elastic stops namely $S_l^*$ and $S_r^*$ are converted to nonlinear but continuous (analytic) functions as

$$S_l^*(x_b + d_1\theta - x_{t_1}) = 1 - \frac{2}{\pi}\int_0^\infty \frac{\sin\left(\omega\frac{D}{2}\right)\cos\left[\omega(x_b + d_1\theta - x_{t_1})\right]}{\omega}d\omega$$

$$S_r^*(x_b - d_2\theta - x_{t_1}) = 1 - \frac{2}{\pi}\int_0^\infty \frac{\sin\left(\omega\frac{D}{2}\right)\cos\left[\omega(x_b - d_2\theta - x_{t_1})\right]}{\omega}d\omega \qquad \text{(B.1)}$$

The other terms in the elastic stops that are discontinuous in nature are $sgn(x_b + d_1\theta - x_{t_1})$ and $sgn(x_b - d_2\theta - x_{t_1})$. These could be replaced by continuous functions of the form

$$sgn(x_b + d_1\theta - x_{t_1}) = \frac{2}{\pi}\int_0^\infty \left(\frac{1 - \cos\left(\omega\dot{D}\right)}{\omega}\right)\sin\left[\omega(x_b + d_1\theta - x_{t_1})\right]d\omega$$

$$sgn(x_b - d_2\theta - x_{t_1}) = \frac{2}{\pi}\int_0^\infty \left(\frac{1 - \cos\left(\omega\dot{D}\right)}{\omega}\right)\sin\left[\omega(x_b - d_2\theta - x_{t_1})\right]d\omega \qquad \text{(B.2)}$$

The discontinuity in the Coulomb friction terms could be made analytic by Fourier integral and the terms $sgn\left(\dot{x}_b + d_1\dot{\theta} - \dot{x}_{t_1}\right)$ and $sgn\left(\dot{x}_b - d_2\dot{\theta} - \dot{x}_{t_1}\right)$ could be written as

$$sgn\left(\dot{x}_b + d_1\dot{\theta} - \dot{x}_{t_1}\right) = \frac{2}{\pi}\int_0^\infty \left(\frac{1 - \cos\left(\omega\dot{D}\right)}{\omega}\right)\sin\left[\omega\left(\dot{x}_b + d_1\dot{\theta} - \dot{x}_{t_1}\right)\right]d\omega$$

$$sgn\left(\dot{x}_b - d_2\dot{\theta} - \dot{x}_{t_1}\right) = \frac{2}{\pi}\int_0^\infty \left(\frac{1 - \cos\left(\omega\dot{D}\right)}{\omega}\right)\sin\left[\omega\left(\dot{x}_b - d_2\dot{\theta} - \dot{x}_{t_1}\right)\right]d\omega \qquad \text{(B.3)}$$

where $\dot{D}$ and $\dot{D}$ are some large numbers much greater than $D$.

For the development of the controller, the terms in the nonlinear discontinuous model described in Eq.7.3 are made nonlinear but continuous, hence analytic at all

points is linearized about the operating point $\mathcal{OP}(t_o, Z_o, U_o, W_o)$. At the operating point various vectors are defined as

$$Z_o = \begin{Bmatrix} x_{b_o} \\ \theta_o \\ x_{t_{1_o}} \\ x_{t_{1_o}} \end{Bmatrix} \quad U_o = \begin{Bmatrix} u_{t_o} \\ u_{t_o} \end{Bmatrix} \quad W_o = \begin{Bmatrix} w_o \\ w_o(t-\tau) \end{Bmatrix} \tag{B.4}$$

Let $(\Delta t, \Delta Z, \Delta U, \Delta W)$ be the variation of the parameters $(t, Z, U, W)$ about the operating point $\mathcal{OP}$ which satisfy the following equations

$$\begin{aligned} t &= t_o + \Delta t \\ Z &= Z_o + \Delta Z \\ U &= U_o + \Delta U \\ W &= W_o + \Delta W \end{aligned} \tag{B.5}$$

The nonlinear and discontinuous equations as described in Eq.7.3 and Eq. 7.4 could be represented as a nonlinear continuous equation whose terms are analytic at all points. This could be written as

$$\mathcal{M}(t)\ddot{Z} + F_s(Z,t) + F_d(\dot{Z},t) + F_c(\dot{Z},t) + F_k(Z,t) = \mathcal{G}U(t) + \mathcal{H}(t)W(t) + \mathcal{S}(t) \tag{B.6}$$

where, various force vectors are defined in Eq.7.4 and the discontinuous terms in $F_s(Z,t)$ and $F_c(\dot{Z},t)$ are substituted as continuous approximations described in Eqs.B.1, B.2 and B.3. From the Eq.B.6, the dynamic equation at the operating point can be written as

$$\begin{aligned} \mathcal{M}(t_o)\ddot{Z}_o + F_s(Z_o,t_o) + F_d(\dot{Z}_o,t_o) + F_c(\dot{Z}_o,t_o) + F_k(Z_o,t_o) = \mathcal{G}U_o + \\ \mathcal{H}(t_o)W_o + \mathcal{S}(t_o) \end{aligned} \tag{B.7}$$

The nonlinear and time varying terms in Eq.B.6 are all analytic at every point and could be expanded by the Taylor series about the operating point as

$$\begin{aligned} \mathcal{M}(t) &= \mathcal{M}(t_o) + \frac{\partial \mathcal{M}}{\partial t}\Big|_{\mathcal{OP}} \Delta t + \cdots \\ &= \mathcal{M}(t_o) + \dot{\mathcal{M}}(t_o)\Delta t + \cdots \end{aligned} \tag{B.8}$$

The discontinuous terms $F_s(Z,t)$ and $F(\dot{Z},t)$ which have been transformed into the continuous functions are expanded using Taylor series as follows

$$F_s(Z,t) = F_s(Z_o,t_o) + \left.\frac{\partial F_s}{\partial Z}\right|_{OP} \Delta Z + \left.\frac{\partial F_s}{\partial t}\right|_{OP} \Delta t + \cdots$$

$$F\left(\dot{Z},t\right) = F\left(\dot{Z}_o,t_o\right) + \left.\frac{\partial F_s}{\partial \dot{Z}}\right|_{OP} \Delta Z + \left.\frac{\partial F}{\partial t}\right|_{OP} \Delta t + \qquad \text{(B 9)}$$

The damping and stiffness force terms could also be expanded by the Taylor series as follows

$$F_d\left(\dot{Z},t\right) = F_d\left(\dot{Z}_o,t_o\right) + \left.\frac{\partial F_d}{\partial \dot{Z}}\right|_{OP} \Delta \dot{Z} + \left.\frac{\partial F_d}{\partial t}\right|_{OP} \Delta t + \cdots$$

$$F_k(Z,t) = F_k(Z_o,t_o) + \left.\frac{\partial F_k}{\partial Z}\right|_{OP} \Delta Z + \left.\frac{\partial F_k}{\partial t}\right|_{OP} \Delta t + \qquad \text{(B 10)}$$

Since $\mathcal{G}$ is a constant it remains the same at all operating conditions but other vectors $\mathcal{H}(t)$ and $\mathcal{S}(t)$ could be expanded as

$$\mathcal{H}(t) = \mathcal{H}(t_o) + \left.\frac{d\mathcal{H}(t)}{dt}\right|_{OP} \Delta t + \cdots$$

$$\mathcal{S}(t) = \mathcal{S}(t_o) + \left.\frac{d\mathcal{S}(t)}{dt}\right|_{OP} \Delta t + \cdots \qquad \text{(B 11)}$$

Various terms in Taylor series in Eqs.B.9, B.10 and B.11 could be simplified as

$$\left.\frac{\partial F_s(Z,t)}{\partial Z}\right|_{OP} = \begin{bmatrix} K_{es_l}(t_o)[\vartheta_1\vartheta_5+\vartheta_2\vartheta_6]+ & K_{es_l}(t_o)\,d_1[\vartheta_1\vartheta_5+\vartheta_2\vartheta_6]- \\ \quad K_{es_t}(t_o)[\vartheta_3\vartheta_7+\vartheta_4\vartheta_8] & \quad K_{es_t}(t_o)\,d_2[\vartheta_3\vartheta_7+\vartheta_4\vartheta_8] \\ K_{es_l}(t_o)\,d_1[\vartheta_1\vartheta_5+\vartheta_2\vartheta_6]- & K_{es_l}(t_o)\,d_1^{\,2}[\vartheta_1\vartheta_5+\vartheta_2\vartheta_6]+ \\ \quad K_{es_t}(t_o)\,d_2[\vartheta_3\vartheta_7+\vartheta_4\vartheta_8] & \quad K_{es_t}(t_o)\,d_2^{\,2}[\vartheta_3\vartheta_7+\vartheta_4\vartheta_8] \\ -K_{es_l}(t_o)[\vartheta_1\vartheta_5+\vartheta_2\vartheta_6] & -K_{es_l}(t_o)\,d_1[\vartheta_1\vartheta_5+\vartheta_2\vartheta_6] \\ -K_{es_t}(t_o)[\vartheta_3\vartheta_7+\vartheta_4\vartheta_8] & K_{es_t}(t_o)\,d_2[\vartheta_3\vartheta_7+\vartheta_4\vartheta_8] \end{bmatrix}$$

$$\begin{bmatrix} -K_{es_l}(t_o)[\vartheta_1\vartheta_5+\vartheta_2\vartheta_6] & -K_{es_t}(t_o)[\vartheta_3\vartheta_7+\vartheta_4\vartheta_8] \\ -K_{es_l}(t_o)\,d_1[\vartheta_1\vartheta_5+\vartheta_2\vartheta_6] & K_{es_t}(t_o)\,d_2[\vartheta_3\vartheta_7+\vartheta_4\vartheta_8] \\ K_{es_l}(t_o)[\vartheta_1\vartheta_5+\vartheta_2\vartheta_6] & 0 \\ 0 & K_{es_t}(t_o)[\vartheta_3\vartheta_7+\vartheta_4\vartheta_8] \end{bmatrix}$$

$$\left.\frac{\partial F_s(Z,t)}{\partial t}\right|_{OP} = \begin{Bmatrix} K_{es_l}(t_o)\,\vartheta_1\vartheta_2+\dot{K}_{es_t}(t_o)\,\vartheta_3\vartheta_4 \\ \dot{K}_{es_l}(t_o)\,\vartheta_1\vartheta_2 d_1-\dot{K}_{es_t}(t_o)\,\vartheta_3\vartheta_4 d_2 \\ -\dot{K}_{es_l}(t_o)\,\vartheta_1\vartheta_2 \\ -\dot{K}_{es_t}(t_o)\,\vartheta_3\vartheta_4 \end{Bmatrix}$$

$$\left.\frac{\partial F_t(Z,t)}{\partial Z}\right|_{OP} = \begin{bmatrix} F_l(t_o)\vartheta_9+F_t(t_o)\dot{\vartheta}_{10} & F_l(t_o)d_1\vartheta_9-F_t(t_o)d_2\dot{\vartheta}_{10} & -F_l(t_o)\vartheta_9 & -F_l(t_o)\dot{\vartheta}_{10} \\ F_l(t_o)d_1\vartheta_9-F_t(t_o)d_2\vartheta_{10} & F_l(t_o){d_1}^2\vartheta_9+F_t(t_o){d_2}^2\dot{\vartheta}_{10} & -F_l(t_o)d_1\vartheta_9 & F_t(t_o)d_2\dot{\vartheta}_{10} \\ -F_l(t_o)\dot{\vartheta}_9 & -F_l(t_o)d_1\dot{\vartheta}_9 & F_l(t_o)\vartheta_9 & 0 \\ -F_t(t_o)\dot{\vartheta}_{10} & F_t(t_o)d_2\dot{\vartheta}_{10} & 0 & F_t(t_o)\vartheta_{10} \end{bmatrix}$$

$$\left.\frac{\partial F_t(Z,t)}{\partial t}\right|_{OP} = \begin{Bmatrix} F_l(t_o)\dot{\vartheta}_{11}+F_t(t_o)\dot{\vartheta}_{12} \\ F_l(t_o)\dot{\vartheta}_{11}d_1-F_t(t_o)\dot{\vartheta}_{12}d_2 \\ -F_l(t_o)\dot{\vartheta}_{11} \\ -F_t(t_o)\dot{\vartheta}_{12} \end{Bmatrix}$$

$$\frac{\partial F_d(Z,t)}{\partial Z}\Big|_{\mathcal{OP}} = \begin{bmatrix} C_l(t_o)\vartheta_{13} + C_t(t_o)\vartheta_{14} & C_l(t_o)\vartheta_{13}d_1 \quad C_t(t_o)\vartheta_{14}d_2 \\ C_l(t_o)\vartheta_{13}d_1 - C_t(t_o)\vartheta_{14}d_2 & C_l(t_o)\vartheta_{13}d_1^2 + C_t(t_o)\vartheta_{14}d_2^2 \\ -C_l(t_o)\vartheta_{13} & C_l(t_o)\vartheta_{13}d_1 \\ -C_t(t_o)\vartheta_{14} & C_t(t_o)\vartheta_{14}d_2 \end{bmatrix}$$

$$\begin{bmatrix} -C_l(t_o)\vartheta_{13} & C_t(t_o)\vartheta_{14} \\ -C_l(t_o)\vartheta_{13}d_1 & C_t(t_o)\vartheta_{14}d_2 \\ C_l(t_o)\vartheta_{13} & 0 \\ 0 & C_t(t_o)\vartheta_{14} \end{bmatrix}$$

$$\frac{\partial F_d(Z,t)}{\partial t}\Big|_{\mathcal{OP}} = \begin{Bmatrix} C_l(t_o)\vartheta_{13} + C_t(t_o)\vartheta_{14} \\ C_l(t_o)\vartheta_{13}d_1 - C_t(t_o)\vartheta_{14}d_2 \\ -\dot{C}_l(t_o)\vartheta_{13} \\ -\dot{C}_t(t_o)\vartheta_{14} \end{Bmatrix}$$

$$\frac{\partial F_{k_t}(Z,t)}{\partial Z}\Big|_{\mathcal{OP}} = \begin{bmatrix} K_l(t_o) + K_t(t_o) & l_1K_l(t_o) - l_2K_t(t_o) & -K_l(t_o) & K_t(t_o) \\ d_1K_l(t_o) - d_2K_t(t_o) & l_1^2K_l(t_o) + d_2^2K_t(t_o) & -d_1K_l(t_o) & l_2K_t(t_o) \\ -K_l(t_o) & -d_1K_l(t_o) & K_l(t_o) + K(t_o) & 0 \\ -K_t(t_o) & d_2K_t(t_o) & 0 & K_t(t_o) + K(t_o) \end{bmatrix}$$

$$\frac{\partial F_{k_t}(Z,t)}{\partial t}\Big|_{\mathcal{OP}} = \begin{Bmatrix} K_l(t_o)\left(x_{b_0} + d_1\theta_0 - x_{t_{1_0}}\right) + K_t(t_o)\left(x_{b_0} - l_2\theta_0 \quad x_{t_{1_0}}\right) \\ K_l(t_o)\left(x_{b_0} + d_1\theta_0 - x_{t_{1_0}}\right)d_1 - K_t(t_o)\left(x_{b_0} - d_2\theta_0 - x_{t_{1_0}}\right)d_2 \\ -K_l(t_o)\left(x_{b_0} + d_1\theta_0 - x_{t_{1_0}}\right) + x_{t_{1_0}}K_{tire}(t_o) \\ -K_t(t_o)\left(x_{b_0} - d_2\theta_0 - x_{t_{1_0}}\right) + x_{t_{1_0}}K_{tire}(t_o) \end{Bmatrix}$$

$$\frac{d\mathcal{H}(t)}{dt}\Big|_{\mathcal{OP}} = \begin{Bmatrix} 0 & 0 \\ 0 & 0 \\ \dot{K}_{tire}(t_o) & 0 \\ 0 & \dot{K}_{tire}(t_o) \end{Bmatrix}$$

$$\frac{d\mathcal{S}(t)}{dt}\Big|_{\mathcal{OP}} = \begin{Bmatrix} \dot{K}_t(t_o)\delta_{st_t} + \dot{K}_l(t_o)\delta_{st_l} - \dot{M}_s(t_o)g \\ \dot{K}_l(t_o)\delta_{st_l}d_1 - \dot{K}_t(t_o)\delta_{st_t}d_2 + \dot{M}_s(t_o)ah \\ \dot{K}_{tire}(t_o)\delta_{t_l} - \dot{K}_l(t_o)\delta_{st_l} \\ \dot{K}_{tire}(t_o)\delta_{t_t} - \dot{K}_t(t_o)\delta_{st_t} \end{Bmatrix}$$

(B.12)

where, the terms $\vartheta_1, \ldots, \vartheta_{14}$ are represented as follows

$$\vartheta_1 = 1 - \frac{2}{\pi}\int_0^R \frac{\sin(\omega\frac{D}{2})\cos\left[\omega\left(x_{b_o} + d_1\theta_o - x_{t_{1_o}}\right)\right]}{\omega} d\omega$$

$$\vartheta_2 = \left[\left(x_{b_o} + d_1\theta_o - x_{t_{1_o}}\right) - \frac{D}{\pi}\int_0^R \left(\frac{1-\cos(\omega D)}{\omega}\right) \sin\left[\omega\left(x_{b_o} + d_1\theta_o - x_{t_{1_o}}\right)\right] d\omega\right]$$

$$\vartheta_3 = 1 - \frac{2}{\pi}\int_0^R \frac{\sin(\omega\frac{D}{2})\cos\left[\omega\left(x_{b_o} - d_2\theta_o - x_{t_{1_o}}\right)\right]}{\omega} d\omega$$

$$\vartheta_4 = \left[\left(x_{b_o} - d_2\theta_o - x_{t_{1_o}}\right) - \frac{D}{\pi}\int_0^R \left(\frac{1-\cos(\omega D)}{\omega}\right) \sin\left[\omega\left(x_{b_o} - d_2\theta_o - x_{t_{1_o}}\right)\right] d\omega\right]$$

$$\vartheta_5 = 1 - \frac{D}{\pi}\int_0^R \left(1 - \cos\left(\omega\dot{D}\right)\right) \cos\left[\omega\left(x_{b_o} + d_1\theta_o - x_{t_{1_o}}\right)\right] d\omega$$

$$\vartheta_6 = \frac{2}{\pi}\int_0^R \sin\left(\omega\frac{D}{2}\right) \sin\left[\omega\left(x_{b_o} + d_1\theta_o - x_{t_{1_o}}\right)\right] d\omega$$

$$\vartheta_7 = 1 - \frac{D}{\pi}\int_0^R \left(1 - \cos\left(\omega\dot{D}\right)\right) \cos\left[\omega\left(x_{b_o} - d_2\theta_o - x_{t_{1_o}}\right)\right] d\omega$$

$$\vartheta_8 = \frac{2}{\pi}\int_0^R \sin\left(\omega\frac{D}{2}\right) \sin\left[\omega\left(x_{b_o} - d_2\theta_o - x_{t_{1_o}}\right)\right] d\omega$$

$$\vartheta_9 = \frac{2}{\pi}\int_0^R \left(1 - \cos\left(\omega\dot{D}\right)\right) \cos\left[\omega\left(\dot{x}_{b_o} + d_1\dot{\theta}_o - x_{t_{1_o}}\right)\right] d\omega$$

$$\vartheta_{10} = \frac{2}{\pi}\int_0^R \left(1 - \cos\left(\omega\dot{D}\right)\right) \cos\left[\omega\left(\dot{x}_{b_o} - d_2\dot{\theta}_o - x_{t_{1_o}}\right)\right] d\omega$$

$$\vartheta_{11} = \frac{2}{\pi}\int_0^R \frac{\left(1-\cos(\omega\dot{D})\right)}{\omega} \sin\left[\omega\left(\dot{x}_{b_o} + d_1\dot{\theta}_o - x_{t_{1_o}}\right)\right] d\omega$$

$$\vartheta_{12} = \frac{2}{\pi}\int_0^R \frac{\left(1-\cos(\omega\dot{D})\right)}{\omega} \sin\left[\omega\left(\dot{x}_{b_o} - d_2\dot{\theta}_o - x_{t_{1_o}}\right)\right] d\omega$$

$$\vartheta_{13} = \left[\left|\dot{x}_{b_o} + d_1\dot{\theta}_o - \dot{x}_{t_{1_o}}\right| + \left(\dot{x}_{b_o} + d_1\dot{\theta}_o - \dot{x}_{t_{1_o}}\right)\right]$$

$$\vartheta_{14} = \left[\left|\dot{x}_{b_o} - d_2\dot{\theta}_o - \dot{x}_{t_{1_o}}\right| + \left(\dot{x}_{b_o} - d_2\dot{\theta}_o - \dot{x}_{t_{1_o}}\right)\right] \tag{B.13}$$

For simplification of the linearized equations, the following assumptions are made. Linearization is assumed to be performed about a small operating region which implies $\Delta t$ is very small. The variation of vehicle parameters at a slow rate along with close operating points would result in very small values of $\dot{M}_s(t_o)$, $\dot{I}_{MI}(t_o)$,

$M_{ij}(t)$, $\dot{M}_{ij}(t)$, $k_1(t)$, $k_2(t)$, $k_{3f}(t)$, $k_{3r}(t)$, $k_{4f}(t)$, $k_{4r}(t)$, $C_1(t)$, $C_2(t)$, $F_1(t)$ and $F_2(t)$. Neglecting the product of $\Delta t$ and rate of variation in the vehicle parameters, the above Taylor series expansions could be simplified as

$$\begin{aligned}
\mathcal{M}(t) &= \mathcal{M}(t_o) \\
F_1(Z,t) &= F_1(Z_o,t_o) + \left.\frac{\partial F_1}{\partial Z}\right|_{\mathcal{O}_p} \Delta Z \\
F_2(Z,t) &= F_2(Z_o,t_o) + \left.\frac{\partial F_2}{\partial Z}\right|_{\mathcal{O}_p} \Delta Z \\
F_3(Z,t) &= F_3(Z_o,t_o) + \left.\frac{\partial F_3}{\partial Z}\right|_{\mathcal{O}_p} \Delta Z \\
F_4(Z,t) &= F_4(Z_o,t_o) + \left.\frac{\partial F_4}{\partial Z}\right|_{\mathcal{O}_p} \Delta Z \\
\mathcal{H}(t) &= \mathcal{H}(t_o) \\
\mathcal{S}(t) &= \mathcal{S}(t_o)
\end{aligned}$$

and

$$\begin{aligned}
Z &= Z_o + \Delta Z \\
U(t) &= U(t_o) + \Delta U \\
W(t) &= W(t_o) + \Delta W
\end{aligned} \tag{B.14}$$

On substituting the above linearized terms in Eq.B.6 and subtracting the dynamic equation at the operating point (Eq.B.7), we obtain the linearized equation of the form

$$\mathcal{M}(t_o)\Delta\ddot{Z} + \left[\left.\frac{\partial F_d}{\partial \dot{Z}}\right|_{\mathcal{O}_p} + \left.\frac{\partial F_c}{\partial \dot{Z}}\right|_{\mathcal{O}_p}\right]\Delta\dot{Z} + \left[\left.\frac{\partial F_s}{\partial Z}\right|_{\mathcal{O}_p} + \left.\frac{\partial F_k}{\partial Z}\right|_{\mathcal{O}_p}\right]\Delta Z = \mathcal{G}(t_o)\Delta U + \mathcal{H}(t_o)\Delta W \tag{B.15}$$

This equation forms a LTI (Linear Time Invariant) equation in the operating region and could be written in the following simplified form

$$\mathcal{M}_o\Delta\ddot{Z} + \mathcal{C}_o\Delta\dot{Z} + \mathcal{K}_o\Delta Z = \mathcal{G}_o\Delta U + \mathcal{H}_o\Delta W \tag{B.16}$$

where,

$$\mathcal{M}_o = \begin{bmatrix} M_l(t_o) & 0 & 0 & 0 \\ 0 & I_{Ml}(t_o) & 0 & 0 \\ 0 & 0 & M_{ut}(t_o) & 0 \\ 0 & 0 & 0 & M_{ut}(t_o) \end{bmatrix}$$

$$\mathcal{C}_o = \begin{bmatrix} F_l(t_o)\vartheta_9 + F_t(t_o)\vartheta_{10} + C_l(t_o)\vartheta_{13} + C_t(t_o)\vartheta_{14} & F_l(t_o)d_1\vartheta_9 - F_t(t_o)d_2\vartheta_{10} + C_l(t_o)d_1\vartheta_{13} - C_t(t_o)d_2\vartheta_{14} & -F_l(t_o)\vartheta_9 - C_l(t_o)\vartheta_{13} & -F_t(t_o)\vartheta_{10} - C_t(t_o)\vartheta_{14} \\ F_l(t_o)d_1\vartheta_9 - F_t(t_o)d_2\vartheta_{10} + C_l(t_o)d_1\vartheta_{13} - C_t(t_o)d_2\vartheta_{14} & F_l(t_o)d_1{}^2\vartheta_9 + F_t(t_o)d_2{}^2\vartheta_{10} + C_l(t_o)d_1{}^2\vartheta_{13} + C_t(t_o)d_2{}^2\vartheta_{14} & -F_l(t_o)d_1\vartheta_9 - C_l(t_o)d_1\vartheta_{13} & F_t(t_o)d_2\vartheta_{10} + C_t(t_o)d_2\vartheta_{14} \\ -F_l(t_o)\vartheta_9 - C_l(t_o)\vartheta_{13} & -F_l(t_o)d_1\vartheta_9 - C_l(t_o)d_1\vartheta_{13} & F_l(t_o)\vartheta_9 + C_l(t_o)\vartheta_{13} & 0 \\ -F_t(t_o)\vartheta_{10} - C_t(t_o)\vartheta_{14} & F_t(t_o)d_2\vartheta_{10} + C_t(t_o)d_2\vartheta_{14} & 0 & F_t(t_o)\vartheta_{10} + C_t(t_o)\vartheta_{14} \end{bmatrix}$$

$$\mathcal{K}_o = \begin{bmatrix} K_{est}(t_o)[\vartheta_1\vartheta_5 + \vartheta_2\vartheta_6] + K_{est}(t_o)[\vartheta_3\vartheta_7 + \vartheta_4\vartheta_8] + K_l(t_o) + K_t(t_o) & K_{est}(t_o)d_1[\vartheta_1\vartheta_5 + \vartheta_2\vartheta_6] - K_{est}(t_o)d_2[\vartheta_3\vartheta_7 + \vartheta_4\vartheta_8] + K_l(t_o)d_1 - K_t(t_o)d_2 & -K_{est}(t_o)[\vartheta_1\vartheta_5 + \vartheta_2\vartheta_6] - K_l(t_o) & -K_{est}(t_o)[\vartheta_3\vartheta_7 + \vartheta_4\vartheta_8] - K_t(t_o) \\ K_{est}(t_o)d_1[\vartheta_1\vartheta_5 + \vartheta_2\vartheta_6] - K_{est}(t_o)d_2[\vartheta_3\vartheta_7 + \vartheta_4\vartheta_8] + K_l(t_o)d_1 - K_t(t_o)d_2 & K_{est}(t_o)d_1{}^2[\vartheta_1\vartheta_5 + \vartheta_2\vartheta_6] + K_{est}(t_o)d_2{}^2[\vartheta_3\vartheta_7 + \vartheta_4\vartheta_8] + K_l(t_o)d_1{}^2 + K_t(t_o)d_2{}^2 & -K_{est}(t_o)d_1[\vartheta_1\vartheta_5 + \vartheta_2\vartheta_6] - K_l(t_o)d_1 & K_{est}(t_o)d_2[\vartheta_3\vartheta_7 + \vartheta_4\vartheta_8] + K_t(t_o)d_2 \\ -K_{est}(t_o)[\vartheta_1\vartheta_5 + \vartheta_2\vartheta_6] - K_l(t_o) & -K_{est}(t_o)d_1[\vartheta_1\vartheta_5 + \vartheta_2\vartheta_6] - K_l(t_o)d_1 & K_{est}(t_o)[\vartheta_1\vartheta_5 + \vartheta_2\vartheta_6] + K_l(t_o) + K_{tire}(t_o) & 0 \\ -K_{est}(t_o)[\vartheta_3\vartheta_7 + \vartheta_4\vartheta_8] - K_t(t_o) & K_{est}(t_o)d_2[\vartheta_3\vartheta_7 + \vartheta_4\vartheta_8] + K_t(t_o)d_2 & 0 & K_{est}(t_o)[\vartheta_3\vartheta_7 + \vartheta_4\vartheta_8] + K_t(t_o) + K_{tire}(t_o) \end{bmatrix}$$

$$\mathcal{G}_o = \begin{bmatrix} 1 & 1 \\ d_1 & -d_2 \\ -1 & 0 \\ 0 & -1 \end{bmatrix} \qquad \mathcal{H}_o = \begin{bmatrix} 0 & 0 \\ 0 & 0 \\ K_{tire}(t_o) & 0 \\ 0 & K_{tire}(t_o) \end{bmatrix}$$

# Appendix C

## C.1 Convergence Properties of Least Square Approximation Estimator Updating as a Matrix

Theorem: To prove the convergence properties of the least square approximation (LSA) estimator derived in Eq.7.64, where the parameters are being updated as a matrix.

An error vector of the following form derived from the estimator in Eq.7.64 is defined as

$$e[k] = \Delta U[k-d] - \hat{\breve{\Theta}}[k-1]^T \bar{\phi}[k-d] \tag{C.1}$$

But we know that the true value of the control input is given by

$$\Delta U[k-d] = \breve{\Theta}_o^T \bar{\phi}[k-d] \tag{C.2}$$

On substituting Eq.C.2 into Eq.C.1 we could express the error term in the form

$$\begin{aligned} e[k] &= \left[\breve{\Theta}_o^T - \hat{\breve{\Theta}}[k-1]^T\right] \bar{\phi}[k-d] \\ &= -\hat{\breve{\Theta}}'[k-1]^T \bar{\phi}[k-d] \end{aligned} \tag{C.3}$$

*where,*

$$\hat{\breve{\Theta}}'[k-1]^T = \hat{\breve{\Theta}}[k-1]^T - \breve{\Theta}_o^T$$

From Eq.7.64, on subtracting $\hat{\breve{\Theta}}_o^T$ from both the sides and on substituting $\left[\Delta U[k-d] - \hat{\breve{\Theta}}[k-1]^T \bar{\phi}[k-d]\right]$ as $\left[-\hat{\breve{\Theta}}'[k-1]^T \bar{\phi}[k-d]\right]$ we have

$$\hat{\breve{\Theta}}'[k]^T = \hat{\breve{\Theta}}'[k-1]^T - \frac{\hat{\breve{\Theta}}'[k-1]^T \bar{\phi}[k-d] \bar{\phi}[k-d]^T \mathcal{P}^*[k-d-1]^T}{\left[r + \bar{\phi}[k-d]^T \mathcal{P}^*[k-d-1]^T \bar{\phi}[k-d]\right]} \tag{C.4}$$

Taking the transpose of the Projection operator update equation 7.64 we obtain

$$\mathcal{P}^*[k-d]^T = \mathcal{P}^*[k-d-1]^T - \frac{\mathcal{P}^*[k-d-1]^T\bar{\phi}[k-d]\bar{\phi}[k-d]^T\mathcal{P}^*[k-d-1]^T}{\left[r+\bar{\phi}[k-d]^T\mathcal{P}^*[k-d-1]^T\bar{\phi}[k-d]\right]} \tag{C.5}$$

Equations C.4 and C.5 could be written in the form

$$\hat{\xi}'[k]^T = \hat{\xi}'[k-1]^T\left[\mathcal{I} - \frac{\hat{\xi}'[k-1]^T\bar{\phi}[k-d]\bar{\phi}[k-d]^T\mathcal{P}^*[k-d-1]^T}{\left[r+\bar{\phi}[k-d]^T\mathcal{P}^*[k-d-1]^T\bar{\phi}[k-d]\right]}\right] \tag{C.6}$$

$$\mathcal{P}^*[k-d]^T = \mathcal{P}^*[k-d-1]^T\left[\mathcal{I} - \frac{\mathcal{P}^*[k-d-1]^T\bar{\phi}[k-d]\bar{\phi}[k-d]^T\mathcal{P}^*[k-d-1]^T}{\left[r+\bar{\phi}[k-d]^T\mathcal{P}^*[k-d-1]^T\bar{\phi}[k-d]\right]}\right] \tag{C.7}$$

From equations C.6 and C.7 we obtain

$$\hat{\Xi}'[k]^T = \hat{\Xi}'[k-1]^T\left[\mathcal{P}^*[k-d-1]^T\right]^{-1}\mathcal{P}^*[k-d]^T \tag{C.8}$$

*where,*

$$\hat{\Theta}'[k]^T = \left\{\begin{array}{c}\hat{\Theta}_1'[k]^T\\ \vdots \\ \hat{\Theta}_i'[k]^T\\ \vdots \\ \hat{\Theta}_m'[k]^T\end{array}\right\}_{(m\times mn)}$$

Any general term in Eq.C.8 could be written as

$$\hat{\Theta}_i'[k]^T = \hat{\Theta}_i'[k-1]^T\left[\mathcal{P}^*[k-d-1]^T\right]^{-1}\mathcal{P}^*[k-d]^T \tag{C.9}$$

*where,* $i \in \{1,\cdots,m\}$

Introducing a positive function of the form for any $i^{th}$ element

$$\bigvee_i[k] = \hat{\Theta}_i'[k]^T\left[\mathcal{P}^*[k-d]^T\right]^{-1}\hat{\Theta}_i'[k] \tag{C.10}$$

Then for $i = 1,m$ the total summation of the elemental positive functions could be written as

$$\bigvee[k] = \sum_{i=1}^{m}\bigvee_i[k] \tag{C.11}$$

Substituting Eq.C.10 in Eq.C.11 we obtain

$$\begin{aligned} V[k] &= \hat{\Theta}_1'[k]^T \left[\mathcal{P}^*[k-d]^T\right]^{-1} \hat{\Theta}_1'[k] + \cdots + \hat{\Theta}_m'[k]^T \left[\mathcal{P}^*[k-d]^T\right]^{-1} \hat{\Theta}_m'[k] \\ V[k-1] &= \hat{\Theta}_1'[k-1]^T \left[\mathcal{P}^*[k-d-1]^T\right]^{-1} \hat{\Theta}_1'[k-1] + \cdots + \hat{\Theta}_m'[k-1]^T \\ &\quad \left[\mathcal{P}^*[k-d-1]^T\right]^{-1} \hat{\Theta}_m'[k-1] \end{aligned} \tag{C.12}$$

On evaluating the difference between the positive functions at $[k]$ and $[k-1]$ from Eq.C.12 and substituting for $\hat{\Theta}_i'[k]^T$ from Eq.C.9 we obtain

$$\begin{aligned} V[k] - V[k-1] = \hat{\Theta}_1'[k-1]^T \left[\mathcal{P}^*[k-d-1]^T\right]^{-1} \left[\hat{\Theta}_1'[k] - \hat{\Theta}_1'[k-1]\right] + \cdots + \\ \hat{\Theta}_m'[k-1]^T \left[\mathcal{P}^*[k-d-1]^T\right]^{-1} \left[\hat{\Theta}_m'[k] - \hat{\Theta}_m'[k-1]\right] \end{aligned} \tag{C.13}$$

Taking the transpose of the controller parameters estimation equation C.4, it could be written as

$$\hat{\Theta}'[k] = \hat{\Theta}'[k-1] - \frac{\mathcal{P}^*[k-d-1]\bar{\phi}[k-d]\phi[k-d]^T \hat{\Theta}'[k-1]}{\left[r + \phi[k-d]^T \mathcal{P}^*[k-d-1]\bar{\phi}[k-d]\right]} \tag{C.14}$$

*where,* $\hat{\Theta}'[k] = \left[\hat{\Theta}_1'[k], \cdots, \hat{\Theta}_i', \cdots, \hat{\Theta}_m'\right]$

From Eq.C.14 we could derive a general $i^{th}$ term of the form

$$\hat{\Theta}_i'[k] - \hat{\Theta}_i'[k-1] = -\frac{\mathcal{P}^*[k-d-1]\bar{\phi}[k-d]\phi[k-d]^T \hat{\Theta}_i'[k-1]}{\left[r + \phi[k-d]^T \mathcal{P}^*[k-d-1]\phi[k-d]\right]} \tag{C.15}$$

Substituting the respective terms from Eq.C.15 in Eq.C.13 we can express the difference in the positive quadratic function as

$$\begin{aligned} V[k] - V[k-1] = \hat{\Theta}_1'[k-1]^T \left[\mathcal{P}^*[k-d-1]^T\right]^{-1} \left[-\frac{\mathcal{P}^*[k-d-1]\bar{\phi}[k-d]\phi[k-d]^T \hat{\Theta}_1'[k-1]}{\left[r+\phi[k-d]^T \mathcal{P}^*[k-d-1]\phi[k-d]\right]}\right] \\ + \cdots + \hat{\Theta}_m'[k-1]^T \left[\mathcal{P}^*[k-d-1]^T\right]^{-1} \left[-\frac{\mathcal{P}^*[k-d-1]\phi[k-d]\phi[k-d]^T \hat{\Theta}_m'[k-1]}{\left[r+\phi[k-d]^T \mathcal{P}^*[k-d-1]\phi[k-d]\right]}\right] \end{aligned} \tag{C.16}$$

Since the function assumed in Eq.C.10 is positive definite, the matrix $\mathcal{P}^*[k-d-1]$ is symmetric in nature. So the inverse of the transpose is equal to inverse of the matrix itself as $\left[\mathcal{P}^*[k-d-1]^T\right]^{-1} = [\mathcal{P}^*[k-d-1]]^{-1}$. On substituting this in Eq.C.16 and simplifying we obtain

$$\bigvee[k] - \bigvee[k-1] = -\sum_{i=1}^{m} \frac{\hat{\Xi}_i'[k-1]^T \bar{\phi}[k-d]\bar{\phi}[k-d]^T \hat{\Xi}_i'[k-1]}{\left[r + \phi[k-d]^T \mathcal{P}^*[k-d-1]\bar{\phi}[k-d]\right]} \tag{C.17}$$

The term within the summation for any $i$ in the above equation is a positive quantity, hence the overall sum for all $i \in \{1, \cdots, m\}$ is also positive, which implies that the left hand side is a negative quantity. So the positive quadratic function $\bigvee[k]$ at any $k$ is always decreasing from $\bigvee[k-1]$ which in turn is always less than $\bigvee[0]$. But from the definition of the total positive function defined in Eqs.C.11 and C.12 we have $\bigvee[k]$ defined as a non-negative function. Hence $\bigvee[k]$ for any value of [k] is a non-negative, non increasing function as defined in the following equation

$$\left[\sum_{i=1}^{m} \hat{\Xi}_i'[k]^T \left[\mathcal{P}^*[k-d]^T\right]^{-1} \hat{\Xi}_i'[k]\right] \leq \left[\sum_{i=1}^{m} \hat{\Xi}_i'[0]^T \left[\mathcal{P}^*[-d]^T\right]^{-1} \hat{\Xi}_i'[0]\right] \tag{C.18}$$

But on applying the Matrix Inversion lemma as defined in Ref.[146], we have

$$\left[\mathcal{P}^*[k-d]^T\right]^{-1} = \left[\mathcal{P}^*[k-d-1]^T\right]^{-1} + \bar{\phi}[k-d]\bar{\phi}[k-d]^T \tag{C.19}$$

From the above equation we can deduce that

$$\lambda_{min}\left[\mathcal{P}^*[k-d]^T\right]^{-1} \geq \lambda_{min}\left[\mathcal{P}^*[k-d-1]^T\right]^{-1} \tag{C.20}$$

But we know from the Eq.7.64 that

$$\begin{aligned} \hat{\Xi}[k]^T &= \mathcal{FN}\left(\hat{\Xi}[k-1]^T, \bar{\phi}[k-d], \mathcal{P}^*[k-d-1]^T\right) \\ \mathcal{P}^*[k-d-1]^T &= \mathcal{FN}\left(\mathcal{P}^*[k-d-2]^T, \bar{\phi}[k-d-1]\right) \end{aligned} \tag{C.21}$$

On evaluating the initial conditions from the previous equation for the estimates of the controller parameters we obtain

$$\begin{aligned} \hat{\Xi}[1]^T &= \mathcal{FN}\left(\hat{\Xi}[0]^T, \bar{\phi}[-d], \mathcal{P}^*[-d-1]^T\right) \\ \textit{where,} \qquad \mathcal{P}^*[-d]^T &= \mathcal{FN}\left(\mathcal{P}^*[-d-1]^T, \bar{\phi}[-d]\right) \end{aligned} \tag{C.22}$$

Also on assuming the initial conditions on the projection operator submatrix $\mathcal{P}^*[k - d]^T$ as

$$\mathcal{P}^*[-d-1]^T = \mathcal{P}^*[-d]^T = \mathcal{P}^*[-d+1]^T = \cdots = \mathcal{P}^*[0]^T \qquad (C.23)$$

and extending the result of the Matrix Inversion Lemma as indicated in Eq.C.20 we could write the inequalities as

$$\begin{aligned} \lambda_{min}\left[\mathcal{P}^*[k]^T\right]^{-1} &\geq \lambda_{min}\left[\mathcal{P}^*[k-d]^T\right]^{-1} \\ &\geq \lambda_{min}\left[\mathcal{P}^*[k-d-1]^T\right]^{-1} \\ &\vdots \\ &\geq \lambda_{min}\left[\mathcal{P}^*[-d]^T\right]^{-1} \end{aligned} \qquad (C.24)$$

$$\Rightarrow$$

$$\lambda_{min}\left[\mathcal{P}^*[k]^T\right]^{-1} \geq \lambda_{min}\left[\mathcal{P}^*[-d]^T\right]^{-1}$$

For any arbit row $i$ in the controller parameters matrix $\hat{\Theta}'[k]$ and using Eq C.24 we obtain

$$\lambda_{min}\left[\mathcal{P}^*[-d]^T\right]^{-1} \| \hat{\Theta}_i'[k]\|^2 \leq \lambda_{min}\left[\mathcal{P}^*[k-d]^T\right]^{-1} \| \hat{\Theta}_i'[k]\|^2 \qquad (C.25)$$

$$where, \qquad i = 1, m$$

Equation C.25 could be modified to involve various row vectors as

$$\sum_{i=1}^{m} \lambda_{min}\left[\mathcal{P}^*[-d]^T\right]^{-1} \| \hat{\Theta}_i'[k]\|^2 \leq \sum_{i=1}^{m} \lambda_{min}\left[\mathcal{P}^*[k-d]^T\right]^{-1} \| \hat{\Theta}_i'[k]\|^2 \qquad (C.26)$$

On substituting the Eq.C.10 we could write the above equation in the form

$$\sum_{i=1}^{m} \lambda_{min}\left[\mathcal{P}^*[-d]^T\right]^{-1} \| \hat{\Theta}_i'[k]\|^2 \leq \sum_{i=1}^{m} \hat{\Theta}_i'[k]^T \left[\mathcal{P}^*[k-d]^T\right]^{-1} \hat{\Theta}_i'[k] \qquad (C.27)$$

But from the derivation in Eq.C.17 we have inferred that the positive function satisfies the condition $V[k] < V[k-1] < \cdots < V[0]$. On applying this condition and substituting in the right hand side of Eq.C.27 we obtain

$$\sum_{i=1}^{m} \lambda_{min}\left[\mathcal{P}^*[-d]^T\right]^{-1} \| \hat{\Theta}_i'[k]\|^2 \leq \sum_{i=1}^{m} \hat{\Theta}_i'[0]^T \left[\mathcal{P}^*[-d]^T\right]^{-1} \hat{\Theta}_i'[0] \qquad (C.28)$$

Reformating equation C.28 similarly to equation C.25. we have

$$\sum_{i=1}^{m} \lambda_{min}\left[\mathcal{P}^{*}[-d]^{T}\right]^{-1} \| \hat{\tilde{\Theta}}_{i}'[k]\|^{2} \leq \sum_{i=1}^{m} \lambda_{max}\left[\mathcal{P}^{*}[-d]^{T}\right]^{-1} \| \hat{\tilde{\Theta}}_{i}'[0]\|^{2} \tag{C.29}$$

which could be simplified as

$$\lambda_{min}\left[\mathcal{P}^{*}[-d]^{T}\right]^{-1} \sum_{i=1}^{m} \| \hat{\tilde{\Theta}}_{i}'[k]\|^{2} \leq \lambda_{max}\left[\mathcal{P}^{*}[-d]^{T}\right]^{-1} \sum_{i=1}^{m} \| \hat{\tilde{\Theta}}_{i}'[0]\|^{2} \tag{C.30}$$

$\Rightarrow$

$$\frac{\sum_{i=1}^{m} \| \hat{\tilde{\Theta}}_{i}'[k]\|^{2}}{\sum_{i=1}^{m} \| \hat{\tilde{\Theta}}_{i}'[0]\|^{2}} \leq \frac{\lambda_{max}\left[\mathcal{P}^{*}[-d]^{T}\right]^{-1}}{\lambda_{min}\left[\mathcal{P}^{*}[-d]^{T}\right]^{-1}} \tag{C.31}$$

$\Rightarrow$

$$\frac{\| \hat{\tilde{\Theta}}_{1}[k] - \check{\tilde{\Theta}}_{o_1}\|^{2} + \cdots + \| \hat{\tilde{\Theta}}_{i}[k] - \check{\tilde{\Theta}}_{o_i}\|^{2} + \cdots + \| \hat{\tilde{\Theta}}_{m}[k] - \check{\tilde{\Theta}}_{o_m}\|^{2}}{\| \hat{\tilde{\Theta}}_{1}[0] - \check{\tilde{\Theta}}_{o_1}\|^{2} + \cdots + \| \hat{\tilde{\Theta}}_{i}[0] - \check{\tilde{\Theta}}_{o_i}\|^{2} + \cdots + \| \hat{\tilde{\Theta}}_{m}[0] - \check{\tilde{\Theta}}_{o_m}\|^{2}} \leq \kappa_{1} \tag{C.32}$$

where, $\kappa_{1} = \frac{\lambda_{max}\left[\mathcal{P}^{*}[-d]^{T}\right]^{-1}}{\lambda_{min}\left[\mathcal{P}^{*}[-d]^{T}\right]^{-1}}$ called the condition number of the matrix $\left[\mathcal{P}^{*}[-d]^{T}\right]^{-1}$. From Eq.C.32 the total error is reduced by $\kappa_{1}$ times the initial error. Hence for proper estimation of the controller parameters the condition number of the projection operator submatrix should be less than 1. If $\kappa_{1} = \frac{1}{2}$ then Eq.C.31 could be written as

$$\sum_{i=1}^{m} \| \hat{\tilde{\Theta}}_{i}[k] - \check{\tilde{\Theta}}_{o_i}\|^{2} \leq \frac{1}{2} \sum_{i=1}^{m} \| \hat{\tilde{\Theta}}_{i}[0] - \check{\tilde{\Theta}}_{o_i}\|^{2} \tag{C.33}$$

Eq.C.17 which represents the difference in the positive function could be written as a sequence of recursive equations of the form

$$\begin{array}{lcll}
V[k] & = & V[k-1] & - \sum_{i=1}^{m} \frac{\hat{\tilde{\Theta}}_{i}'[k-1]^{T}\bar{\phi}[k-d]\bar{\phi}[k-d]^{T}\hat{\tilde{\Theta}}_{i}'[k-1]}{\left[r+\bar{\phi}[k-d]^{T}\mathcal{P}^{*}[k-d-1]\bar{\phi}[k-d]\right]} \\
V[k-1] & = & V[k-2] & - \sum_{i=1}^{m} \frac{\hat{\tilde{\Theta}}_{i}'[k-2]^{T}\bar{\phi}[k-d]\bar{\phi}[k-d-1]^{T}\hat{\tilde{\Theta}}_{i}'[k-2]}{\left[r+\bar{\phi}[k-d-1]^{T}\mathcal{P}^{*}[k-d-2]\bar{\phi}[k-d-1]\right]} \\
\vdots & & \vdots & \vdots \\
V[1] & = & V[0] & - \sum_{i=1}^{m} \frac{\hat{\tilde{\Theta}}_{i}'[0]^{T}\bar{\phi}[k-d]\bar{\phi}[1-d]^{T}\hat{\tilde{\Theta}}_{i}'[0]}{\left[r+\bar{\phi}[1-d]^{T}\mathcal{P}^{*}[-d]\bar{\phi}[1-d]\right]} \\
(+) & & & \\
\hline
V[k] & = & V[0] & - \sum_{k=1}^{N}\sum_{i=1}^{m} \frac{\hat{\tilde{\Theta}}_{i}'[k-1]^{T}\bar{\phi}[k-d]\bar{\phi}[k-d]^{T}\hat{\tilde{\Theta}}_{i}'[k-1]}{\left[r+\bar{\phi}[k-d]^{T}\mathcal{P}^{*}[k-d-1]\bar{\phi}[k-d]\right]}
\end{array} \tag{C.34}$$

We know from Eq.C.10 and Eq.C.11 that the assumed initial positive function at $k = 0$ could be written as

$$\bigvee[0] = \sum_{i=1}^{m} \hat{\tilde{\Theta}}_i'[0]^T \left[\mathcal{P}^*[-d]^T\right]^{-1} \hat{\tilde{\Theta}}_i'[0] \;\Rightarrow\; \sum_{i=1}^{m} \hat{\tilde{\Theta}}_i'[0]^T \left[\mathcal{P}_0^{*T}\right]^{-1} \hat{\tilde{\Theta}}_i'[0] \qquad (C.35)$$

The function on the right hand side of Eq.C.35 is a positive quantity and could be written as some positive real value less than $\infty$ i.e. $(\bigvee[0] < \infty)$. From Eq C.34 which implies $\bigvee[k] < \bigvee[0]$, it could be deduced that the quantity within the summation on the right hand side of Eq.C.35 is a positive real value less than $\infty$. The above discussion could be summarized as the following inequality

$$\lim_{N \to \infty} \sum_{k=1}^{N} \sum_{i=1}^{m} \left[ \frac{\hat{\tilde{\Theta}}_i'[k-1]^T \bar{\phi}[k-d] \bar{\phi}[k-d]^T \hat{\tilde{\Theta}}_i'[k-1]}{\left[r + \bar{\phi}[k-d]^T \mathcal{P}^*[k-d-1] \bar{\phi}[k-d]\right]} \right] < \infty \qquad (C.36)$$

But we know from the initial error equation C.3 that

$$\begin{aligned} e[k] = & -\hat{\tilde{\Theta}}'[k-1]^T \bar{\phi}[k-d] \\ = & \begin{Bmatrix} -\hat{\tilde{\Theta}}_1'[k-1]^T \bar{\phi}[k-d] \\ \vdots \\ -\hat{\tilde{\Theta}}_i'[k-1]^T \bar{\phi}[k-d] \\ \vdots \\ -\hat{\tilde{\Theta}}_m'[k-1]^T \bar{\phi}[k-d] \end{Bmatrix} = \begin{Bmatrix} e_1[k] \\ \vdots \\ e_i[k] \\ \vdots \\ e_m[k] \end{Bmatrix} \end{aligned} \qquad (C.37)$$

the inequality in Eq.C.36 could be expressed in terms of the error derived in Eq.C.37 as follows

$$\lim_{N \to \infty} \sum_{k=1}^{N} \sum_{i=1}^{m} \left[ \frac{e_i[k] e_i[k]}{\left[r + \bar{\phi}[k-d]^T \mathcal{P}^*[k-d-1] \bar{\phi}[k-d]\right]} \right] < \infty$$

$$\lim_{N \to \infty} \sum_{k=1}^{N} \frac{1}{\left[r + \bar{\phi}[k-d]^T \mathcal{P}^*[k-d-1] \bar{\phi}[k-d]\right]} \left\{ e_1[k], \cdots, \right.$$

$$\left. e_i[k], \cdots, e_m[k] \right\} \begin{Bmatrix} e_1[k] \\ \vdots \\ e_i[k] \\ \vdots \\ e_m[k] \end{Bmatrix} < \infty$$

$$\lim_{N \to \infty} \sum_{k=1}^{N} \left[ \frac{e[k]^T e[k]}{\left[ r + \bar{\phi}[k-d]^T \mathcal{P}^*[k-d-1] \bar{\phi}[k-d] \right]} \right] < \infty \qquad \text{(C.38)}$$

We know that from Eq.C.17 and further explanation that $V[k] \to 0$ as $k \to \infty$, hence $[V[k] - V[k-1]] \to 0$ as $k \to \infty$. This condition can be expressed as

$$\lim_{N \to \infty} \left[ \sum_{i=1}^{m} \frac{\hat{\Xi}_i'[k-1]^T \bar{\phi}[k-d] \bar{\phi}[k-d]^T \hat{\Xi}_i'[k-1]}{\left[ r + \phi[k-d]^T \mathcal{P}^*[k-d-1] \bar{\phi}[k-d] \right]} \right] \longrightarrow 0$$

$$\lim_{N \to \infty} \left[ \frac{e[k]^T e[k]}{\left[ r + \bar{\phi}[k-d]^T \mathcal{P}^*[k-d-1] \bar{\phi}[k-d] \right]} \right] \longrightarrow 0$$

$$\lim_{N \to \infty} \left[ \frac{e[k]}{\sqrt{r + \bar{\phi}[k-d]^T \mathcal{P}^*[k-d-1] \bar{\phi}[k-d]}} \right] = 0 \qquad \text{(C.39)}$$

But from the equation C.20 we can write

$$\begin{aligned}
\lambda_{min}[\mathcal{P}[k-d]] &\leq \lambda_{min}[\mathcal{P}[k-d-1]] \\
\lambda_{max}[\mathcal{P}[k-d]] &\leq \lambda_{max}[\mathcal{P}[k-d-1]] \\
&\leq \lambda_{max}[\mathcal{P}[k-d-2]] \\
&\leq \vdots \\
&\leq \lambda_{max}[\mathcal{P}[-d]] \\
\\
\lambda_{max}[\mathcal{P}[k-d-1]] &\leq \lambda_{max}[\mathcal{P}[-d]]
\end{aligned} \qquad \text{(C.40)}$$

Hence, the Eq.C.39 could be written as

$$\lim_{N \to \infty} \left[ \frac{e[k]}{\sqrt{r + \bar{\phi}[k-d]^T \mathcal{P}^*[k-d-1] \bar{\phi}[k-d]}} \right] = 0$$

$$\lim_{N \to \infty} \left[ \frac{e[k]}{\sqrt{r + \kappa_2 \bar{\phi}[k-d]^T \bar{\phi}[k-d]}} \right] = 0$$

$$where, \qquad \kappa_2 = \lambda_{max}[\mathcal{P}[-d]] = \lambda_{max}[\mathcal{P}_0] \qquad \text{(C.41)}$$

Also from the result in Eq.C.38, on multiplying the numerator and denominator by $\left[r + \bar{o}[k-d]^T \mathcal{P}^*[k-d-1]\bar{o}[k-d]\right]$ and resubstituting Eq.C.38 we obtain

$$\lim_{N \to \infty} \sum_{k=1}^{N} \left[ \frac{\left[\bar{o}[k-d]^T \mathcal{P}^*[k-d-1]\bar{o}[k-d]\right] e[k]^T e[k]}{\left[r + o[k-d]^T \mathcal{P}^*[k-d-1]o[k-d]\right]} \right] < \infty \qquad (C.42)$$

Eq.7.62 which represents row wise controller parameters estimation equation can be modified as

$$\left[\hat{\bar{\Theta}}_i[k] - \hat{\bar{\Theta}}_i[k-1]\right] = \frac{\mathcal{P}^*[k-d-1]\bar{\phi}[k-d]e_i[k]}{\left[r + \phi[k-d]^T \mathcal{P}^*[k-d-1]\phi[k-d]\right]} \qquad (C.43)$$

On squaring the above equation we obtain

$$\|\hat{\bar{\Theta}}_i[k] - \hat{\bar{\Theta}}_i[k-1]\|^2 = \frac{e_i[k]\,\bar{\phi}[k-d]^T \mathcal{P}^*[k-d-1]^T \mathcal{P}^*[k-d-1]\bar{\phi}[k-d]e_i[k]}{\left[r + \bar{\phi}[k-d]^T \mathcal{P}^*[k-d-1]\bar{\phi}[k-d]\right]^2} \qquad (C.44)$$

summing the above equation for various values of $i \in \{1, \cdots, m\}$ we obtain

$$\sum_{i=1}^{m} \|\hat{\bar{\Theta}}_i[k] - \hat{\bar{\Theta}}_i[k-1]\|^2 = \frac{\bar{\phi}[k-d]^T \mathcal{P}^*[k-d-1]^T \mathcal{P}^*[k-d-1]\bar{\phi}[k-d]e_i[k]^T e_i[k]}{\left[r + \bar{\phi}[k-d]^T \mathcal{P}^*[k-d-1]\phi[k-d]\right]^2} \qquad (C.45)$$

on substituting the results from Eq.C.40 we can write the right hand side of Eq.C.45 as

$$\frac{\bar{\phi}[k-d]^T \mathcal{P}^*[k-d-1]^T \mathcal{P}^*[k-d-1]\bar{\phi}[k-d]e_i[k]^T e_i[k]}{\left[r + \bar{\phi}[k-d]^T \mathcal{P}^*[k-d-1]\bar{\phi}[k-d]\right]^2} \leq \frac{\bar{\phi}[k-d]^T \mathcal{P}^*[k-d-1]\bar{\phi}[k-d]e_i[k]^T e_i[k]\lambda_{max}\left[\mathcal{P}^*[-d]\right]}{\left[r + \bar{\phi}[k-d]^T \mathcal{P}^*[k-d-1]\bar{\phi}[k-d]\right]^2}$$

$\Rightarrow$

$$\sum_{i=1}^{m} \|\hat{\bar{\Theta}}_i[k] - \hat{\bar{\Theta}}_i[k-1]\|^2 \leq \frac{\bar{\phi}[k-d]^T \mathcal{P}^*[k-d-1]\bar{\phi}[k-d]e_i[k]^T e_i[k]}{\left[r + \bar{\phi}[k-d]^T \mathcal{P}^*[k-d-1]\phi[k-d]\right]^2} \lambda_{max}\left[\mathcal{P}_0^*[-d]\right] \qquad (C.46)$$

Taking limits on both sides as $N \rightarrow \infty$ we obtain

$$\lim_{N \rightarrow \infty} \sum_{k=1}^{N} \sum_{i=1}^{m} \|\hat{\bar{\Theta}}_i[k] - \hat{\bar{\Theta}}_i[k-1]\|^2 \leq \lim_{N \rightarrow \infty} \sum_{k=1}^{N} \frac{\phi[k-d]^T \mathcal{P}^*[k-d-1]\bar{\phi}[k-d]e_i[k]^T e_i[k]}{\left[r + \phi[k-d]^T \mathcal{P}^*[k-d-1]\bar{\phi}[k-d]\right]^2} \lambda_{max}[\mathcal{P}_0^*[-d]] \tag{C.47}$$

substituting the right hand side of the inequality C.47 in Eq.C.42 we obtain

$$\lim_{N \rightarrow \infty} \sum_{k=1}^{N} \sum_{i=1}^{m} \|\hat{\bar{\Theta}}_i[k] - \hat{\bar{\Theta}}_i[k-1]\|^2 < \infty \tag{C.48}$$

For any finite value of $k_0$, the controller parameters convergence term in Eq.C.48 could be written as

$$\|\hat{\bar{\Theta}}_i[k] - \hat{\bar{\Theta}}_i[k-k_0]\|^2 = \|\hat{\bar{\Theta}}_i[k] - \hat{\bar{\Theta}}_i[k-1] + \hat{\bar{\Theta}}_i[k-1] - \cdots + \hat{\bar{\Theta}}_i[k-k_0+1] - \hat{\bar{\Theta}}_i[k-k_0]\|^2 \tag{C.49}$$

But by using the Schwarz inequality [146] we can represent Eq.C.49 as

$$\|\hat{\bar{\Theta}}_i[k] - \hat{\bar{\Theta}}_i[k-k_0]\|^2 \leq k_0 \left[\|\hat{\bar{\Theta}}_i[k] - \hat{\bar{\Theta}}_i[k-1]\|^2 + \cdots + \|\hat{\bar{\Theta}}_i[k-k_0+1] - \hat{\bar{\Theta}}_i[k-k_0]\|^2\right] \tag{C.50}$$

Hence from Eq.C.48 and Eq.C.50 we derive the inequality as

$$\lim_{N \rightarrow \infty} \sum_{k=k_0}^{N} \sum_{i=1}^{m} \|\hat{\bar{\Theta}}_i[k] - \hat{\bar{\Theta}}_i[k-k_0]\|^2 < \infty \tag{C.51}$$

To satisty the inequality in Eq.C.51 as $k \rightarrow \infty$ it has to satisfy the condition

$$\lim_{k \rightarrow \infty} \sum_{i=1}^{m} \|\hat{\bar{\Theta}}_i[k] - \hat{\bar{\Theta}}_i[k-k_0]\|^2 = 0 \tag{C.52}$$

The results derived above are used in the next section to prove the global convergence properties for the model reference adaptive control problem.

## C.2 Global Convergence Properties of the Multi-Input Multi-Output Discrete Model Reference Adaptive Control System with Least Square Approximation Estimator

Theorem: To prove the Global convergence properties of the multi-input multi output (MIMO) discrete model reference adaptive control (DMRAC) system and least square approximation (LSA) estimation with the parameters being updated as a matrix.

The lemmas presented in the previous section which deal with the underlying properties of the Least square parameter estimator [ as a matrix ] are used here to prove the global convergence of the controller.

We know the error term from the least square estimator from Eq.C.1 as

$$e[k] = \Delta U[k-d] - \hat{\Theta}[k-1]^T \phi[k-d] \tag{C.53}$$

But from the control law in Eq.7.65 we obtain

$$\begin{aligned} e[k] &= \hat{\Theta}[k-d]^T \phi'[k-d] - \hat{\Theta}[k-1]^T \bar{\phi}[k-d] \\ &= \hat{\Theta}[k-d]^T \phi'[k-d] - \hat{\Theta}[k-1]^T \phi'[k-d] + \hat{\Theta}[k-1]^T \phi'[k-d] - \\ &\qquad \hat{\Theta}[k-1]^T \phi[k-d] \\ &= \hat{\Theta}[k-1]^T \left[\phi'[k-d] - \bar{\phi}[k-d]\right] + \left[\hat{\Theta}[k-d]^T - \hat{\Theta}[k-1]^T\right] \phi'[k-d] \end{aligned} \tag{C.54}$$

On substituting the terms $\phi'[k-d]$ and $\bar{\phi}[k-d]$ from the equations 7.15, 7.16 and

7.49 and on simplifying we obtain

$$\begin{aligned}
\epsilon[k] &= \hat{\Theta}[k-1]^T \left[0, 0, \cdots, \left[\tilde{Y}_m[k]^T - \tilde{Y}[k]^T\right]\right]^T + \tilde{\epsilon}[k] \\
&= \left[\alpha_0', \alpha_1', \cdots \alpha_{d_{min}}', \beta_1^{1'}, \cdots, \beta_{d_{min}}^{1'}, \beta_{[-d_{max}+1]}^{2'}, \cdots, \beta_{[-1]}^{2'}, \right. \\
&\quad \left. \beta_0^{2'}, \cdots, \beta_{d_{min}}^{2'}, \frac{1}{\beta_0^1}\right] \left[0, 0, \cdots, \left[\tilde{Y}_m[k]^T - \tilde{Y}[k]^T\right]\right]^T + \tilde{\epsilon}[k] \\
&= \left[\frac{1}{\beta_0^1}[k-1]\right] \left[\tilde{Y}_m[k]^T - \tilde{Y}[k]^T\right] + \tilde{\epsilon}[k] \\
&= -\hat{\Theta}[k-1]^T_{[n]} \epsilon[k] + \tilde{\epsilon}[k]
\end{aligned} \tag{C.55}$$

where,

$$\begin{aligned}
\epsilon[k] &= \tilde{Y}[k]^T - \tilde{Y}_m[k]^T \\
&= E(q^{-1})\mathcal{U}(q)Y[k] - H(q^{-1})W[k] \\
&= E(q^{-1})\left[\bar{Y}[k] - \bar{Y}_m[k]\right]
\end{aligned}$$

The parameter estimation equation 7.64 indicates that the controller parameters $\left(\hat{\Theta}[k]^T\right)$ at any instant $[k]$ is a function of the parameters at $[k-1]$ i.e. $\left(\hat{\Theta}[k-1]^T\right)$, the error term ($e[k]$) in Eq.C.55, $\bar{\phi}[k-d]^T$ and $\mathcal{P}^*[k-d-1]^T$. On substituting Eq.C.55 in Eq.7.64 we obtain

$$\hat{\Theta}[k]^T = \hat{\Theta}[k-1]^T + \frac{-\hat{\Theta}[k-1]^T_{[n]} E(q^{-1})\left[\bar{Y}[k] - \bar{Y}_m[k]\right]\bar{\phi}[k-d]^T\mathcal{P}^*[k-d-1]^T}{\left[r + \bar{\phi}[k-d]^T\mathcal{P}^*[k-d-1]^T\bar{\phi}[k-d]\right]} + \frac{\tilde{\epsilon}[k]\bar{\phi}[k-d]^T\mathcal{P}^*[k-d-1]^T}{\left[r + \bar{\phi}[k-d]^T\mathcal{P}^*[k-d-1]^T\bar{\phi}[k-d]\right]} \tag{C.56}$$

The terms $E(q^{-1})$, $Y[k]$ and $\bar{Y}_m[k]$ in the error term $\epsilon[k]$ in Eq.C.55 are given as

$$\begin{aligned}
E(q^{-1}) &= \begin{bmatrix} e_0 + e_1q^{-1} + \cdots + e_8q^{-8} & 0 \\ 0 & e_0 + e_1q^{-1} + \cdots + e_8q^{-8} \end{bmatrix} \\
\bar{Y}[k] &= \begin{Bmatrix} \bar{Y}_1[k] \\ \bar{Y}_2[k] \end{Bmatrix} \quad \bar{Y}_m[k] = \begin{Bmatrix} \bar{Y}_{m_1}[k] \\ \bar{Y}_{m_2}[k] \end{Bmatrix}
\end{aligned} \tag{C.57}$$

On substituting the above matrices in the error term in Eq.C.55 we obtain

$$\epsilon[k] = \left\{ \begin{array}{l} \epsilon_0 \left[ Y_1[k] - Y_{m_1}[k] \right] + \cdots + \epsilon_8 \left[ Y_1[k-8] - Y_{m_1}[k-8] \right] \\ \\ \epsilon_0 \left[ Y_2[k] - Y_{m_2}[k] \right] + \cdots + \epsilon_8 \left[ Y_2[k-8] - Y_{m_2}[k-8] \right] \end{array} \right\} \qquad (C.58)$$

The error term $\epsilon[k]$ as shown in the Eq.C.58 is a vector with the summation of the error between the actual response and the desired reference model response until the past eight data points. This $\epsilon[k]$ is the governing error that makes the system follow the reference model. But the second term $\tilde{\epsilon}[k]$ is an auxiliary error input which is the difference between the parameters at different instants and is not significant. Also the term $\hat{\underline{\xi}}[k-1]^T_{[n]}$ in the Eq.C.56 is an estimate of $\frac{1}{\beta_0^1}$ which is represented as $\beta_0^*$. Hence the controller parameters update equation in terms of errors could be written as

$$\hat{\underline{\xi}}[k]^T = \hat{\underline{\xi}}[k-1]^T + \frac{-\beta_0^* \epsilon[k] \bar{\phi}[k-d]^T \mathcal{P}^*[k-d-1]^T}{\left[ r + \phi[k-d]^T \mathcal{P}^*[k-d-1]^T \phi[k-d] \right]} + \frac{\tilde{\epsilon}[k] \bar{\phi}[k-d]^T \mathcal{P}^*[k-d-1]^T}{\left[ r + \bar{\phi}[k-d]^T \mathcal{P}^*[k-d-1]^T \phi[k-d] \right]} \qquad (C.59)$$

The middle term in the above equation is a function of error vector $\epsilon[k]$ and the coefficient matrix $\beta_0^*$. The gain matrix $\beta_0^*$ is restricted by modified constraint equations so that it would not be zero and prevent further convergence as follows

$$\begin{array}{lll} If & & \beta^*_{0_{ij}}[k] \; sign \left[ \left( \frac{1}{\beta_0^1} \right)_{ij} \right] > |\beta_0|_{min} \\ & then & \beta^*_{0_{ij}}[k-1] = \beta^*_{0_{ij}}[k-1] \\ else & & \beta^*_{0_{ij}}[k-1] = |\beta_0|_{min} \; sign \left[ \left( \frac{1}{\beta_0^1} \right)_{ij} \right] \end{array} \qquad (C.60)$$

$$where, \quad i, j \in \{1, \cdots, m\}$$

Here it is assumed that the sign of every element of $\left[ \beta_0^{1^{-1}} \right]$ hence, the initial matrix $\beta_0^1$ is known and it is non-singular.

The driving error equation C.55 could be modified by dividing throughout by $\sqrt{r + \kappa_2 \bar{\phi}[k-d]^T \bar{\phi}[k-d]}$, which is the denominator in Eq.C.41 to obtain

$$\frac{e[k]}{\sqrt{r + \kappa_2 \bar{\phi}[k-d]^T \bar{\phi}[k-d]}} = \frac{-\beta_0^* \epsilon[k]}{\sqrt{r + \kappa_2 \bar{\phi}[k-d]^T \phi[k-d]}} + \frac{\tilde{\epsilon}[k]}{\sqrt{r + \kappa_2 \bar{\phi}[k-d]^T \phi[k-d]}}$$

(C.61)

Taking limits on both sides as $k \rightarrow \infty$ Eq.C.61 can be represented as

$$\underbrace{\lim_{k \rightarrow \infty} \frac{e[k]}{\sqrt{r + \kappa_2 \bar{\phi}[k-d]^T \bar{\phi}[k-d]}}}_{I} = \underbrace{\lim_{k \rightarrow \infty} \frac{-\beta_0^* \epsilon[k]}{\sqrt{r + \kappa_2 \bar{\phi}[k-d]^T \bar{\phi}[k-d]}}}_{II} + \underbrace{\lim_{k \rightarrow \infty} \frac{\tilde{e}[k]}{\sqrt{r + \kappa_2 \bar{\phi}[k-d]^T \bar{\phi}[k-d]}}}_{III} \quad \text{(C.62)}$$

the three terms in Eq.C.61 could be analyzed separately as follows.

From the result in Eq.C.41 we conclude that the first term in Eq.C.62 is

$$\underbrace{\lim_{k \rightarrow \infty} \frac{e[k]}{\sqrt{r + \kappa_2 \bar{\phi}[k-d]^T \bar{\phi}[k-d]}}}_{I} = 0 \quad \text{(C.63)}$$

The auxiliary error term in Eq.C.62 could be written as

$$\begin{aligned} \tilde{e}[k] &= \left[\hat{\bar{\Theta}}[k-d]^T - \hat{\bar{\Theta}}[k-1]^T\right] \\ &= -\left[\hat{\bar{\Theta}}[k-1+1]^T - \hat{\bar{\Theta}}[k-d+1]^T\right] \quad \text{(C.64)} \\ &= -\left[\hat{\bar{\Theta}}[k]^T - \hat{\bar{\Theta}}[k-\iota]^T\right] \\ &\textit{where,} \qquad \iota = d-1 \ (\textit{finite quantity}) \end{aligned}$$

But from the derivation in the previous section and the resulting equation C.52, if $k_0 = \iota$ then

$$\lim_{N \rightarrow \infty} \sum_{i=1}^{m} \hat{\bar{\Theta}}_i[k] - \hat{\bar{\Theta}}_i[k-\iota] = 0 \quad \text{(C.65)}$$

From the above equation we can deduce that the third term in Eq.C.62 is equal to zero as shown below

$$\underbrace{\lim_{k \rightarrow \infty} \frac{\left[\hat{\bar{\Theta}}[k-d]^T - \hat{\bar{\Theta}}[k-1]^T\right] \phi'[k-d]}{\sqrt{r + \kappa_2 \bar{\phi}[k-d]^T \bar{\phi}[k-d]}}}_{III} = 0 \quad \text{(C.66)}$$

Substituting the independent results from Eqs.C.63 and C.66 in Eq.C.62 we obtain

$$\underbrace{\lim_{k \to \infty} \frac{-\beta_0^* \epsilon[k]}{\sqrt{r + \kappa_2 \bar{\phi}[k-d]^T \phi[k-d]}}}_{II} = 0 \qquad (C.67)$$

The conditions described in equation C.60 are substituted in the above equation to derive

$$\lim_{k \to \infty} \frac{|\beta_0|_{min} \mathcal{I}_m \epsilon[k]}{\sqrt{r + \kappa_2 \bar{\phi}[k-d]^T \bar{\phi}[k-d]}} = 0 \qquad (C.68)$$

from Eq.C.68 it could be established that the error vector $\epsilon[k]$ is equal to zero, hence it could be rewritten as

$$\lim_{k \to \infty} \frac{[|\beta_0|_{min} \mathcal{I}_m \epsilon[k]]^T [|\beta_0|_{min} \mathcal{I}_m \epsilon[k]]}{\sqrt{r + \kappa_2 \bar{\phi}[k-d]^T \bar{\phi}[k-d]}} = 0 \qquad (C.69)$$

On applying the standard key technical lemma for the above discrete-time adaptive control algorithm to check the uniformity and linear boundedness conditions [146] the above equation can be transformed to the following standard form.

$$\lim_{k \to \infty} \frac{s[k]^2}{b_1[k] + b_2[k] \sigma[k]^T \sigma[k]} = 0 \qquad (C.70)$$

where,

$$\begin{aligned} s[k] &= \sqrt{[|\beta_0|_{min} \mathcal{I}_m \epsilon[k]]^T [|\beta_0|_{min} \mathcal{I}_m \epsilon[k]]} \\ b_1[k] &= r \\ b_2[k] &= \kappa_2 \\ \sigma[k] &= \bar{\phi}[k-d] \end{aligned}$$

From the result in Eq.C.70 and the standard result as described in Ref.[146] we can state the following conclusions:

1. closed loop stability is achieved,
2. the output tracking error asymptotically goes to zero (perfect tracking is achieved),
3. and the convergence rate is better than $\frac{1}{k}$.

# Appendix D

## D.1 Hardware Components

A hydraulic actuator from the Parker-Hennifen series with the following specifications has been used.

| | |
|---|---|
| *Model* : | $2BB2HLT14A-6$ |
| *Bore* : | $2''$ |
| *Stroke* : | $6''$ |
| *Rod dia.* : | $1''$ |
| *Style* : | *Parker style BB* |
| | *NFPA style MP1* |
| | *with pivot pin and mounting plate* |

The actuator has been modified to incorporate cross port leakage by fitting a flow control orifice for differential pressure control across the piston to achieve smaller pressure gain. This provision is incorporated to tune the force feedback for the actuator control force of the adaptive active suspension. This valve could be closed completely for a faster response in the position feedback control.

An electro-hydraulic MOOG servo valve (model 760-102A) has been used to achieve the position and force feedback control. The 760 series is a high performance, two stage design that covers the range of 1 to 15 gpm rated flows at 1000 psi valve pressure drop. The output stage is a closed center, four-way and sliding spool. The pilot stage is a symmetrical double-nozzle and flapper driven by a double air gap and dry torque motor. Mechanical feedback of spool position is provided by a cantilever spring. A list of servo valve specifications are quoted as follows.

| | |
|---|---|
| *Model* : | $760 - 102\ A$ |
| *Rated Flow* : | $5\ gpm, < 0.35\ gpm\ internal\ leakage$ |
| *Torque Motor Coil* : | *Parallel Coil Configuration* |
| | *Rated current* : $15\ mA$ |
| *Coil Resistance* : | $200\ ohm$ |
| *Supply Pressure* : | *Minimum* : $200\ psi$ |
| | *Maximum* : $5000\ psi$ |
| | *Standard* : $3500\ psi$ |

The servo valve is rigidly mounted on the actuator to attain good hydraulic stiffness between servo valve and ports (pressure and return) of the actuator which improves the overall response of the actuator and servo valve as a single unit during the actual test setup. A manifold and mounting plate has been designed and fabricated with the configuration and dimensions which attache the servo valve rigidly to the actuator and provides rigid hosing connections. This would enhance the dynamic response between the output and input of the servo valve over wide range of frequencies.

An analog controller board is used to maintain the feedback at a faster rate and apply the command signal faster than the overall digital adaptive controller loop. An analog controller which has a fast response to maintain the command signal is used to reduce the time delay of the overall system. The analog controller used has built in proportional, integral and derivative (PID) gain adjustable pots and summing junctions. This system would act as a very fast constant gain closed loop local feedback system to implement the actuator force signal from the adaptive controller. By adjusting the PID pots, the controller can be tuned to achieve the critical damping response and also could be optimized to achieve the stable tracking of the command signal. The servo valve torque motor has its coils limited to a maximum of 15 mA current. The command signal from the digital controller which has been passed through DAC port of the data acquisition system has been conveniently limited to a maximum of $\pm$ 10 volts. The individual torque motor coil resistance is 200 ohms. Hence when connected in parallel it has a resultant resistance of 100 ohms. For

a resistance of 100 ohm and maximum current of 15 mA the voltage is limited to a maximum of 1.5 Volts. An Op-Amp circuit that is capable of reducing the $\pm$ 10 *Volts* to $\pm$ 1.5 *Volts* at the servo valve has been added to the circuit. The Op-Amp circuit has been calibrated and tuned to obtain this step down transformation. Fig.D.1 shows the Mechatronix Systems servo controller card coupled with the Op-Amp circuit made compatible with the servo valve chosen. The card shows the summing junction for the command and feedback signals. The Op-Amp is powered from 15 volt power supply and the output from the board is fed to the Op-Amp circuit. The step down signal is connected to the servo valve with appropriate polarity.

## D.2 Electro Hydraulic Position Feedback Circuit (Excitation)

As discussed earlier in section 8.2.1, the adaptive controller software incorporates a module which would send the selected excitation to the main hydraulic circuit to simulate the road input. The hydraulic circuit with the servo valve mounted actuator has been used to create a position feedback controller that is completely controlled by the software through data acquisition system. The analog controller has been used as the fast feedback loop within the over all position control circuit. The software incorporates a selection Window which shows the command signal that is being issued and the feedback position signal from the actuator. Fig.D.2 shows the schematic diagram of the complete position control feedback circuit.

A rigid base with appropriate mounting blocks for connecting the actuator has been fabricated and the actuator assembly is fixed to the base with appropriate freedom of rotation. Figs.D.3 and D.4 show the actual pictures of the setup. The above figures indicate how the servo valve is mounted and rigidly connected to the actuator as discussed earlier. The circuit is powered by a hydraulic power source with various subcomponents such as pump, pressure regulators etc.. The hydraulic pressure chosen for this setup is 1000 psi. The digital controller with the position control module sends a command signal to the analog controller through a DAC

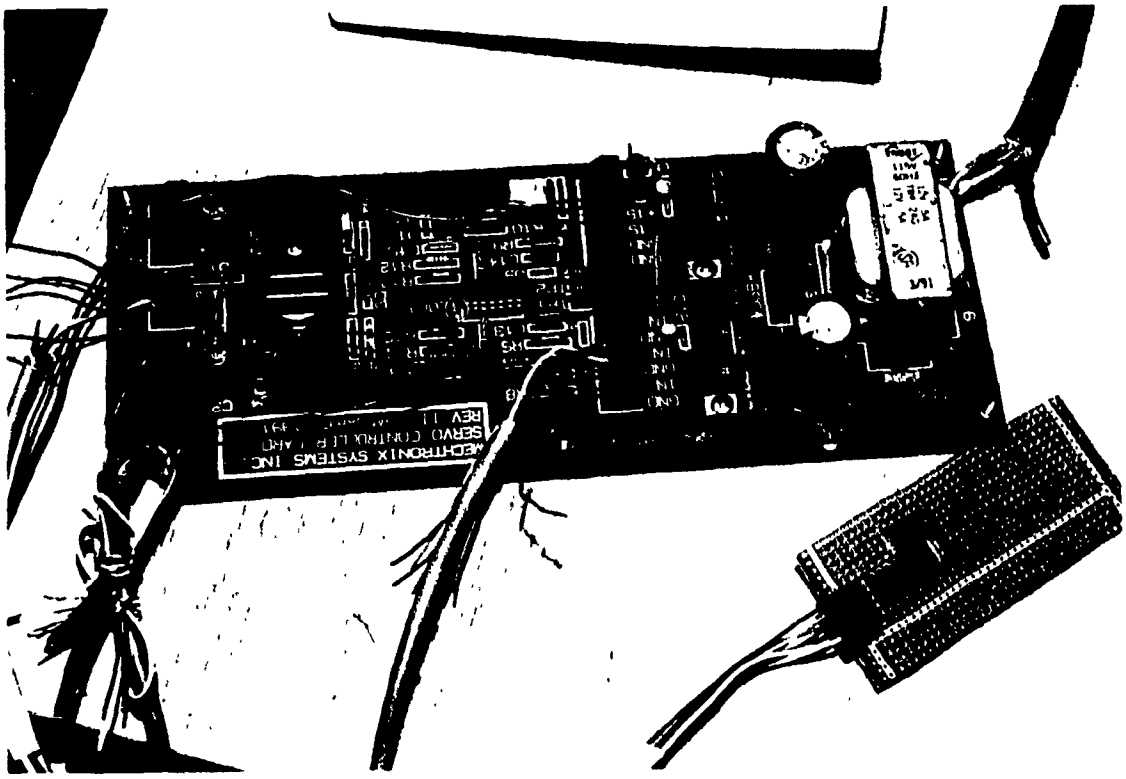

Fig.D.1: Analog servo controller with OP-Amp circuit for position, force and active suspension control implementation.

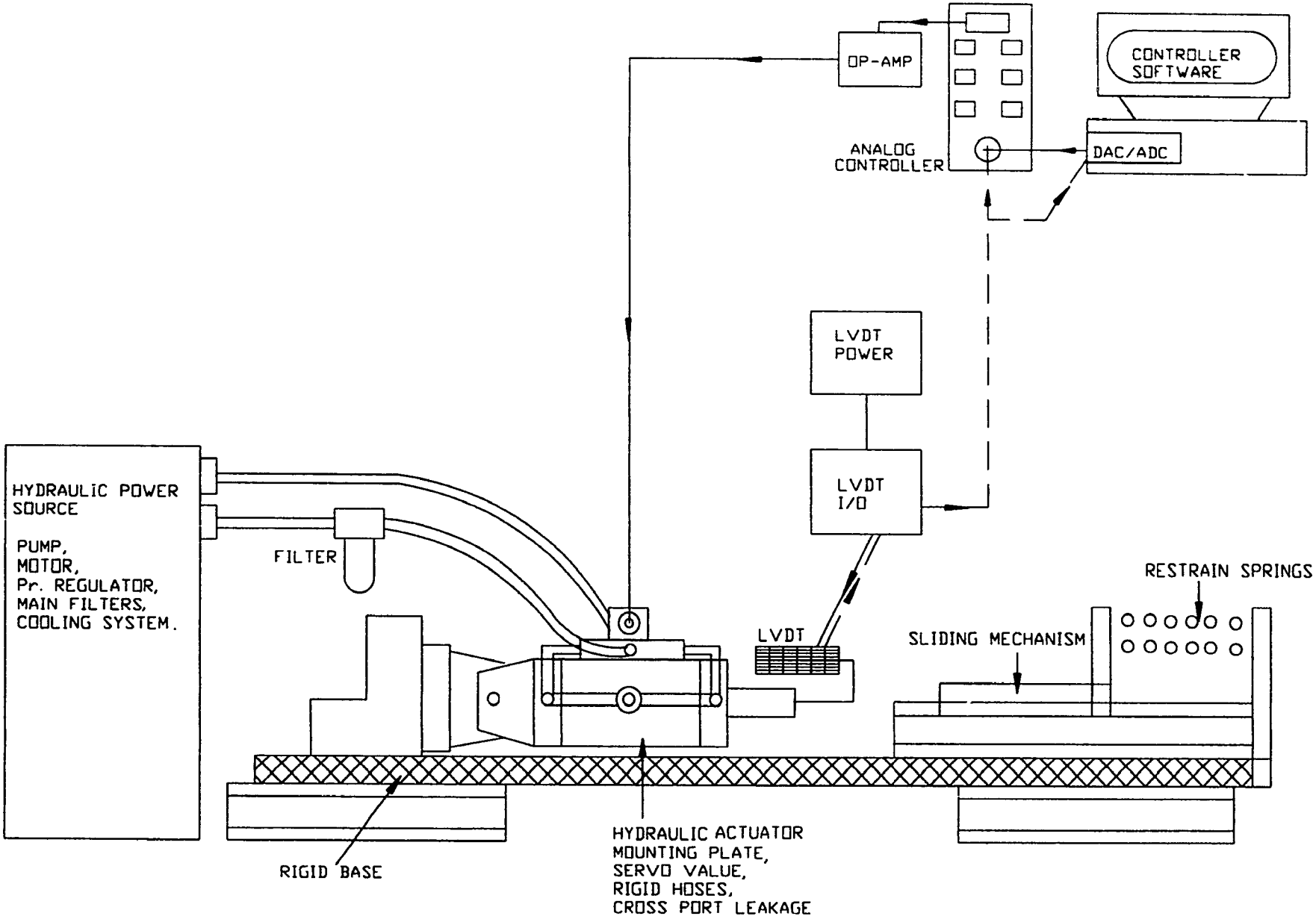


Fig.D.2: Position feedback control implementation to be used as the adaptive active suspension excitation signal.

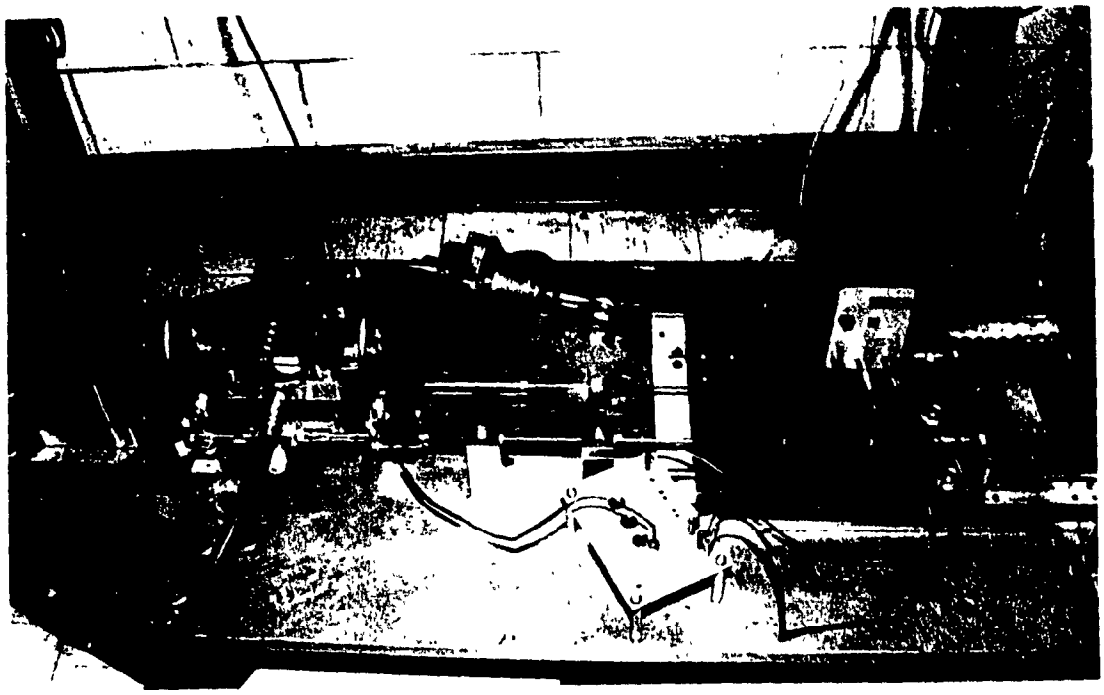

Fig.D.3: The mechanical hardware for the position control feedback loop

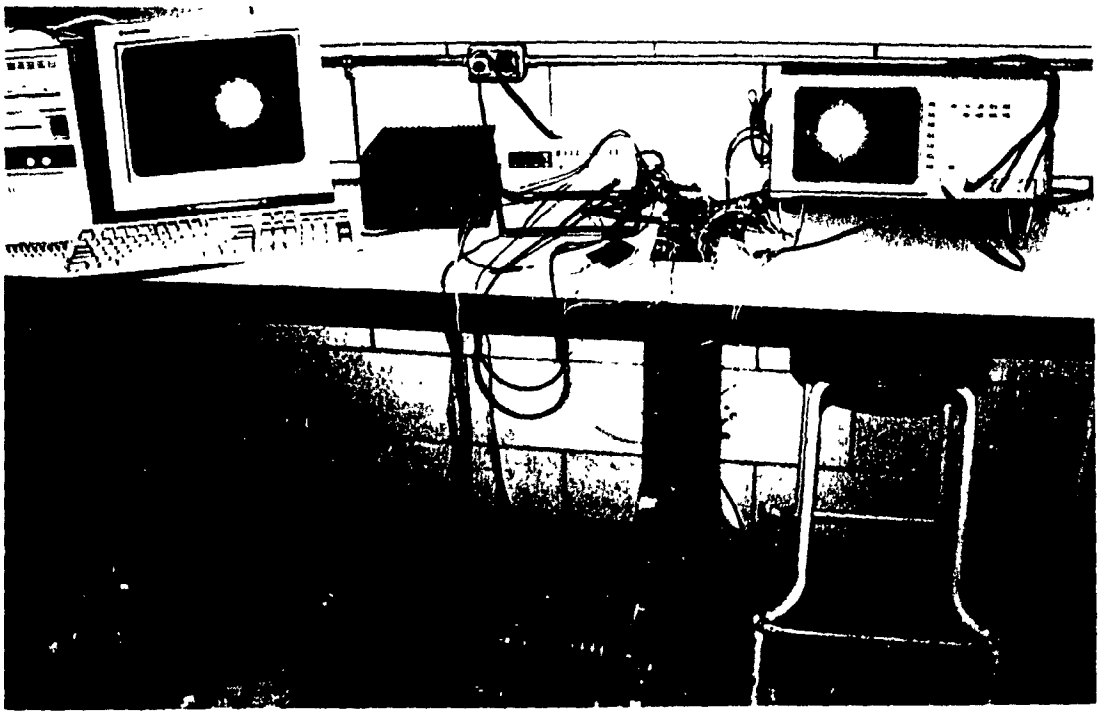

Fig.D.4: Position feedback control circuit.

port. The feedback signal for the position of the actuator is collected through an appropriately calibrated LVDT. The software displays the controller performance by displaying the command and the feedback signals. Fig.D.5 shows the objective performance of the complete position control setup for simulating the excitation to the actual adaptive active suspension. The results indicate that the feedback signal tracks the command signal very closely. Fig.D.5 shows the time delay involved and the limitation of overall system when the actuator fully retracts.

## D.3 Electro Hydraulic Force Feedback Control (Actuator Force)

A separate force feedback control system which would act as an actual force circuitry in the Adaptive Active Suspension has been implemented. An actuator force signal as calculated by the Adaptive Active Suspension Simulator Software has to be imposed on the sprung mass to realize the adaptively controlled system. The actuator setup with cross port leakage as discussed earlier has been used. Fig.D.6 shows the schematic representation of the force feedback control that has been used for implementation.

On the rod end of the actuator the piston has been connected to a Aries load cell (Series 8100) of maximum capacity $\pm$ 1000 $kgf$.. The application of the load cell is minimized to half of its capacity. Hence it is calibrated to $\pm$ 10 $Volts$ to $\pm$ 500 $kgf$.. The load cell has been calibrated using a MTS system against MTS force reading. The load cell is connected to an Aries signal conditioner and the voltage reading is taken from its display. The connections to the signal conditioner are adjusted so that we could extract a feedback signal with negative polarity. Fig.D.7 show the load cell calibration curve with table showing the actual values. Once the load cell is calibrated the gain setting of 1024 is extracted and this would produce a calibration line of slope $500\frac{N}{Volt}$.

A sliding plate on linear bearings has been attached to the actuator through a

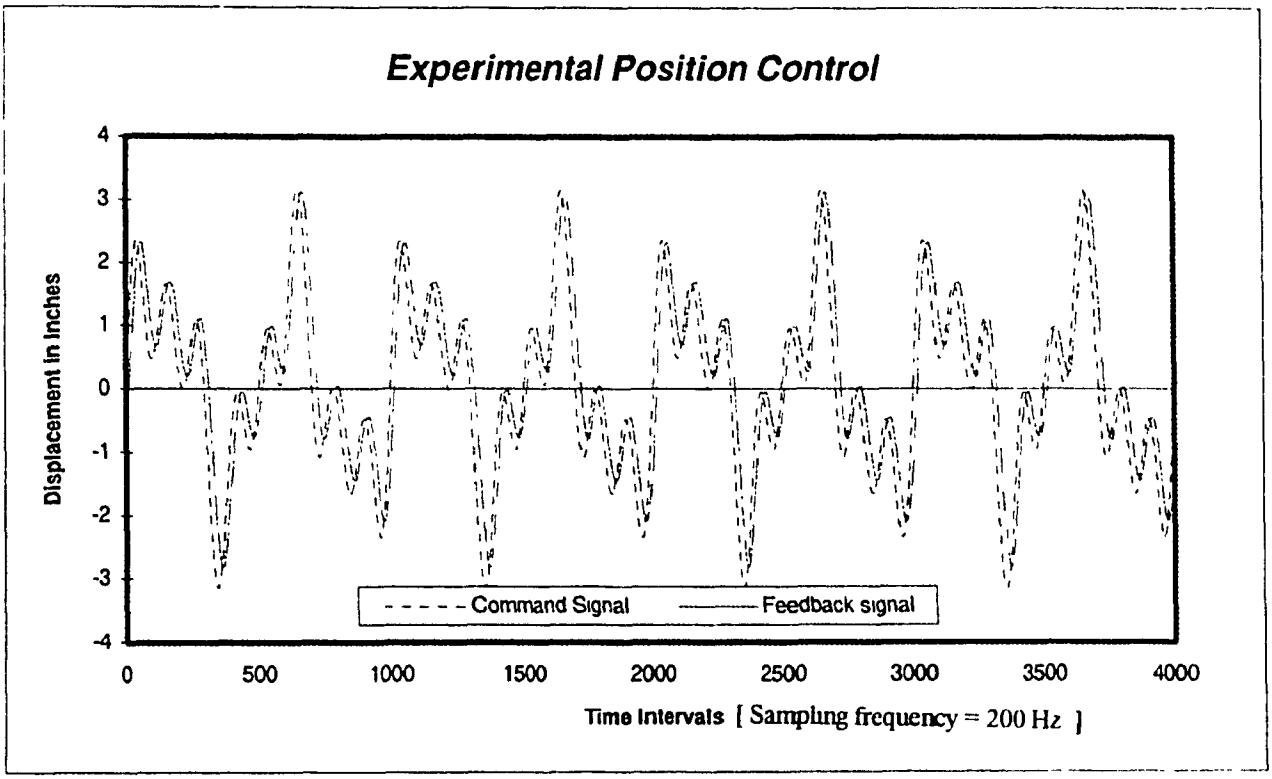


Fig.D.5: Experimental position control results.

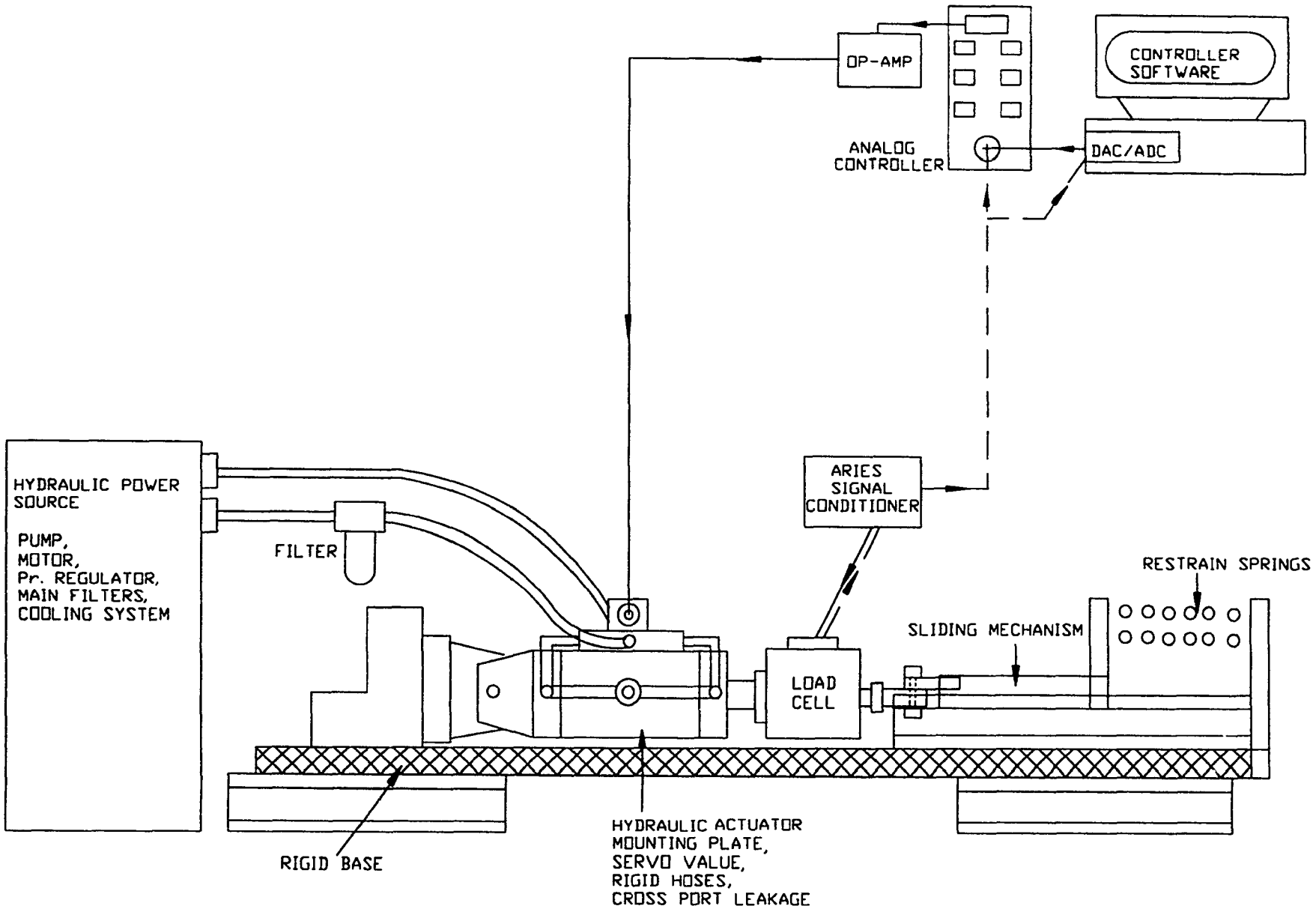


Fig.D.6: Force feedback control implementation to be used as the adaptive active suspension actuator force signal.

| Applied force (N) | Aries Signal Analyzer (volts) | MTS Reading (volts) |
|---|---|---|
| -4990 | 9.97 | 9.98 |
| -3995 | 7.99 | 8 |
| -3020 | 6.04 | 6.04 |
| -2030 | 4.04 | 4.04 |
| -1000 | 2 | 2 |
| -520 | 1.15 | 1.15 |
| 0 | 0 | 0 |
| 570 | -1.14 | -1.15 |
| 1000 | -2 | -2.02 |
| 2010 | -4.04 | -4.0[illegible] |
| 3030 | -6.08 | -6.1 |
| 4000 | -8.07 | -8.05 |
| 5020 | -10.07 | -10.1 |

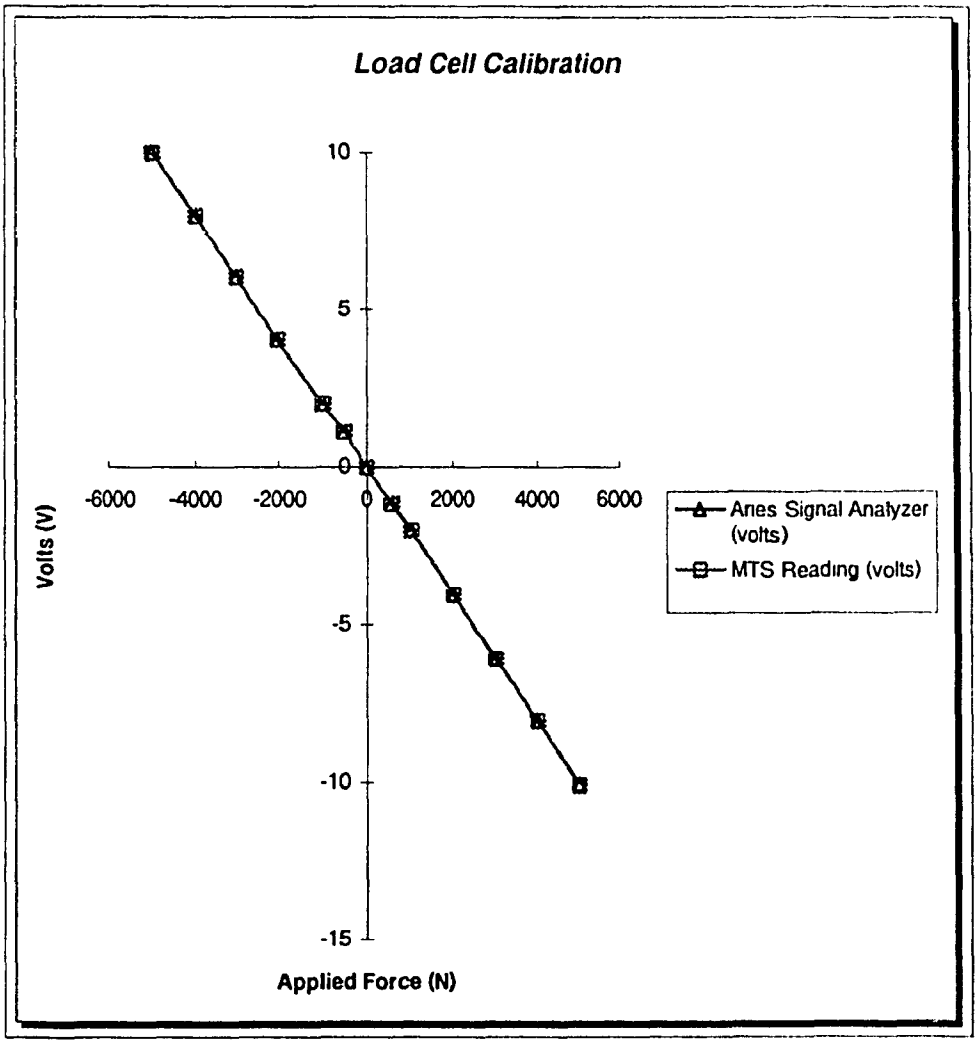


Fig.D.7: Load cell calibration against MTS system readings.

load cell on one end and compressed against a set of springs on the other end. Three springs in parallel with a total stiffness of $100\frac{lb}{in}$ or $17000\frac{N}{m}$ which is approximately the stiffness of the coil spring has been used on the other end. These along with the sliding mechanism have been fixed to the rigid base. Figures D.8 and D.9 show the pictures with the mechanical hardware setup and the overall force feedback control loop. Fig.D.8 indicates the setup involving the actuator attached to the sliding mechanism through a load cell and coil springs on the other end. Complete feedback mechanism from the load cell through the signal conditioners and the analog controller has been shown in this figure.

The controller actuator force evaluation module of the software has been used for evaluating a command signal with a DC shift. The force feedback display that includes the command signal and the feedback from the load cell has been used to show the feedback control. Fig.D.10 shows the command signal and the feedback signal for a test run. The static component of command signal is used to test capability of the actuator force feedback to maintain static equilibrium condition for the adaptive active suspension. The response indicates the effect of time delay and improper tracking upon a sudden change in the direction of the command signal. Appropriate care has been taken to tune the analog controller PID gains so that we could obtain stable performance without damaging the springs in the setup.

## D.4 Damper Test For Component Characterization

The damper was loaded on the damping test rig as shown in Fig.D.11. The damper was suspended through a load cell that was calibrated earlier for force feedback control. The rubber spool bushing that is shot between the outer and inner sleeves of the damper has been included throughout the test to simulate actual vehicle assembly situation. The independent test setup as shown in this figure would develop the damping forces relative to the absolute velocity of the excitation at the lower end, as the top end is fixed in the bounce DOF. But in the actual adaptive active suspension

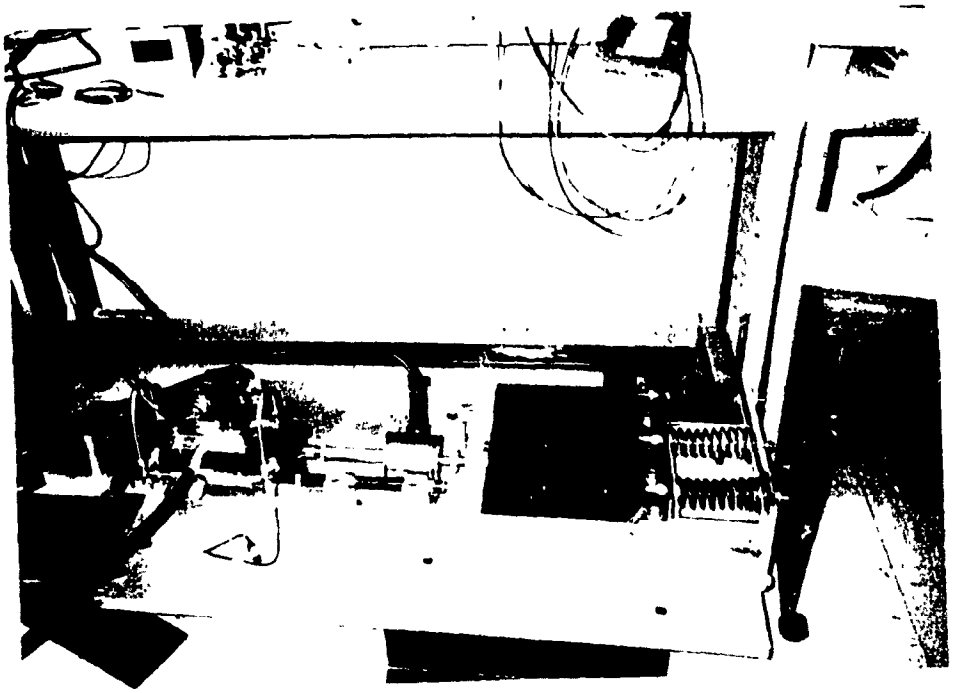

Fig.D.8: The mechanical hardware connections for the force feedback loop

Fig.D.9: Force feedback control circuit.

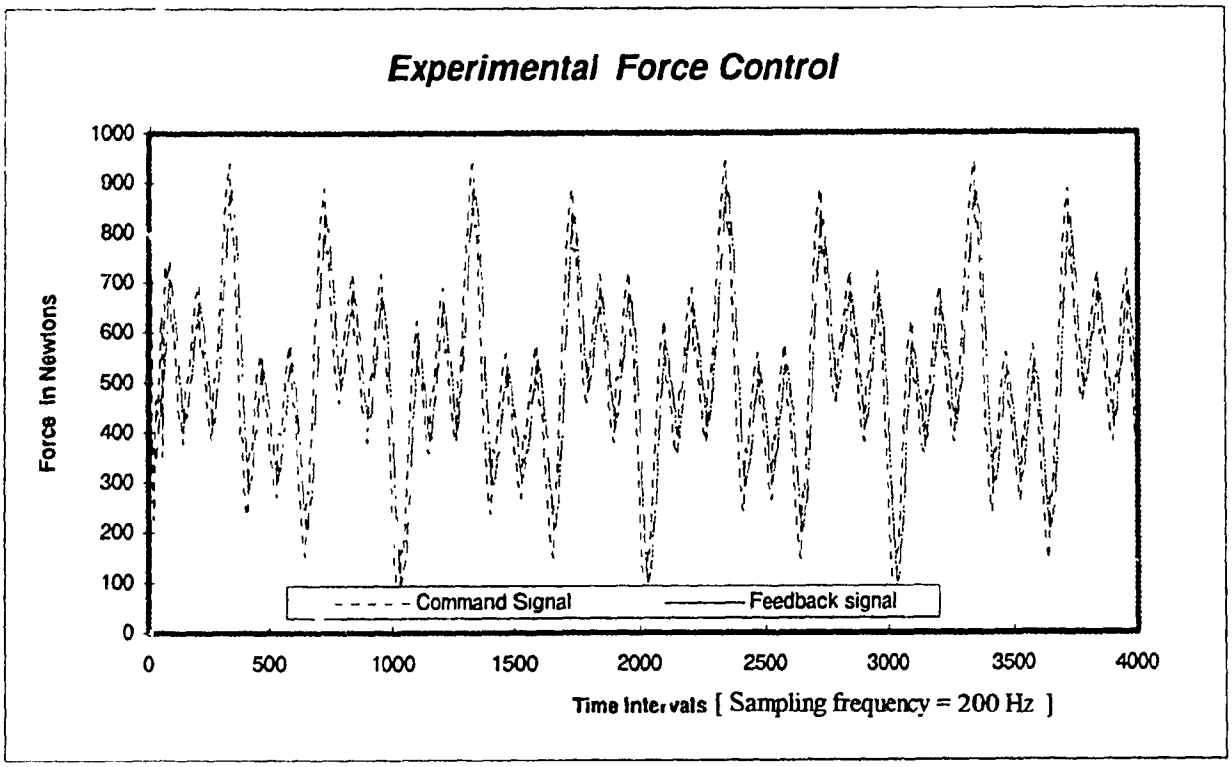


Fig.D.10: Experimental force feedback control results.

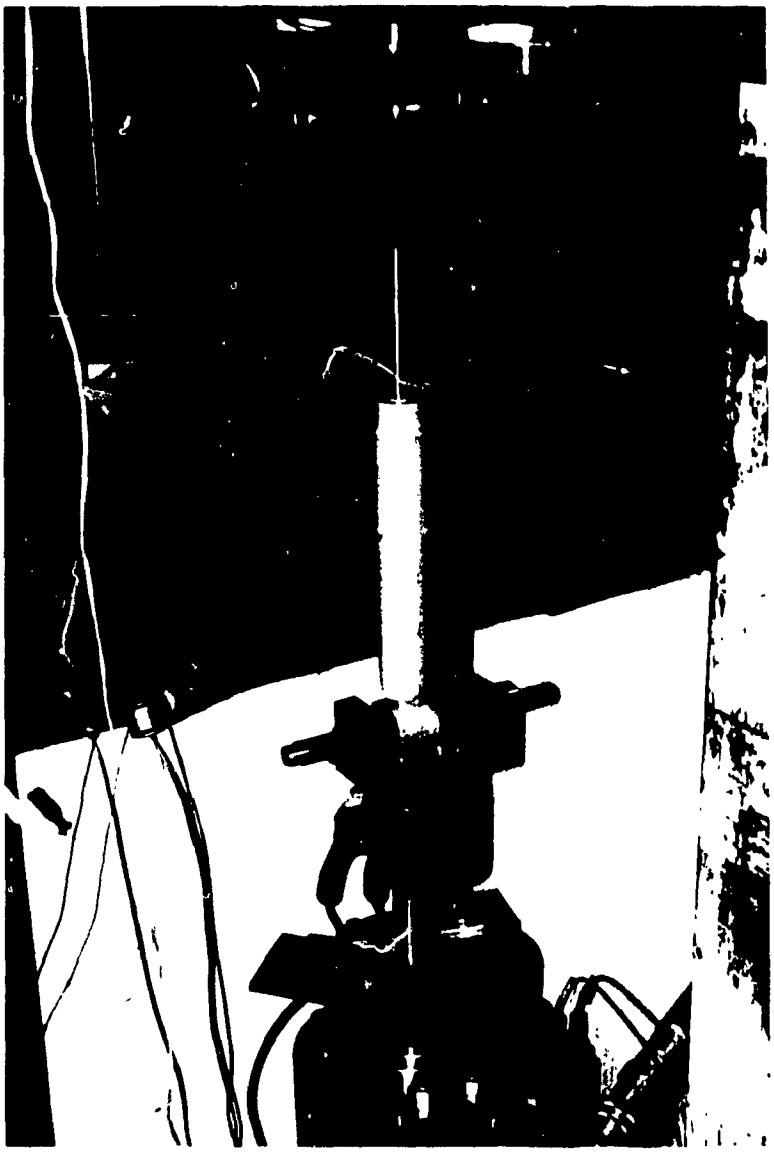

Fig.D.11: Pictures indicating Porsche 928 front shock in the damper test rig

test setup the damper forces are proportional to the relative velocity between the sprung and unsprung masses. The tests for various frequencies and amplitudes, and hence for various velocities are performed and the damping values are read from the test curves to obtain the values with respect to the peak operating velocities.

A series of 30 tests at different frequencies and amplitudes have been conducted. The damper has a total of 4″ stroke which is smaller than the regular 5-6″ stroke peak-to-peak. This also shows that the handling and stability performance has been given higher priority relative to the ride comfort in this type of vehicle. The damper and the load cell were loaded and at no initial deflection the load cell is zeroed. Then the damper is statically compressed to 0.25″ which gave a gas spring force of 35 N. The compression was varied at equistatic conditions and the gas spring force was found to vary from 35 to 55 N, which were calculated from the load cell reading. The gas spring force was not zeroed to simulate the final test setup conditions. The tests enable the evaluation of the damper performance over a wide range of velocities which would be suitable for final test operating conditions.

The loads exerted by the damper at various excitation inputs (different amplitudes and frequencies) have been extracted from the test at the steady state. Two different types of plots have been used for characterization of the damper. The Lissajous curves which show the jounce and rebound forces with the relative displacement have been plotted from the test data. These indicate the distinction between jounce and rebound performance governed by the orifice size. Figs.D.12 and D.13 shows the Lissajous curves for different strokes in terms of peak to peak (p-t-p) values and at different frequencies. Tests at different strokes 0.5″, 1.0″, 2″, and 3″ p-t-p at different frequencies 0.25 Hz., 0.5 Hz., 1.0 Hz., 1.5 Hz. and 3.0 Hz. have been performed for the analysis. Since the adaptive active suspension experiment is the validation for the sprung mass modes, the frequencies and strokes chosen are justifiable. At the lower velocities the curves are shifted towards the compression side due to gas spring force of the damper and it is more clear in the 0.25 Hz. and 0.5″ p-t-p as shown in Fig.D.12.

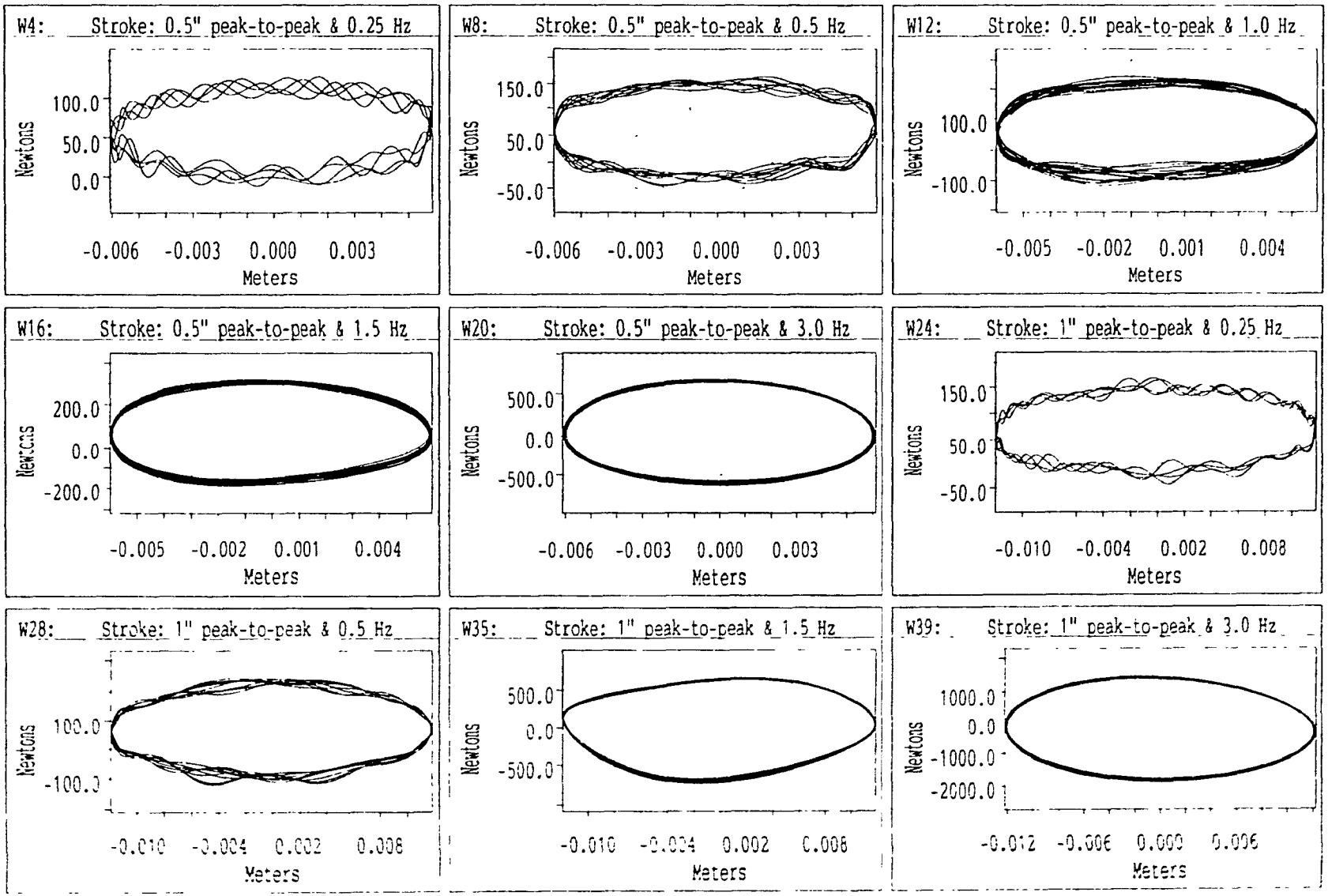


Fig.D.12: Lissajous curves for the damper test (Page 1).

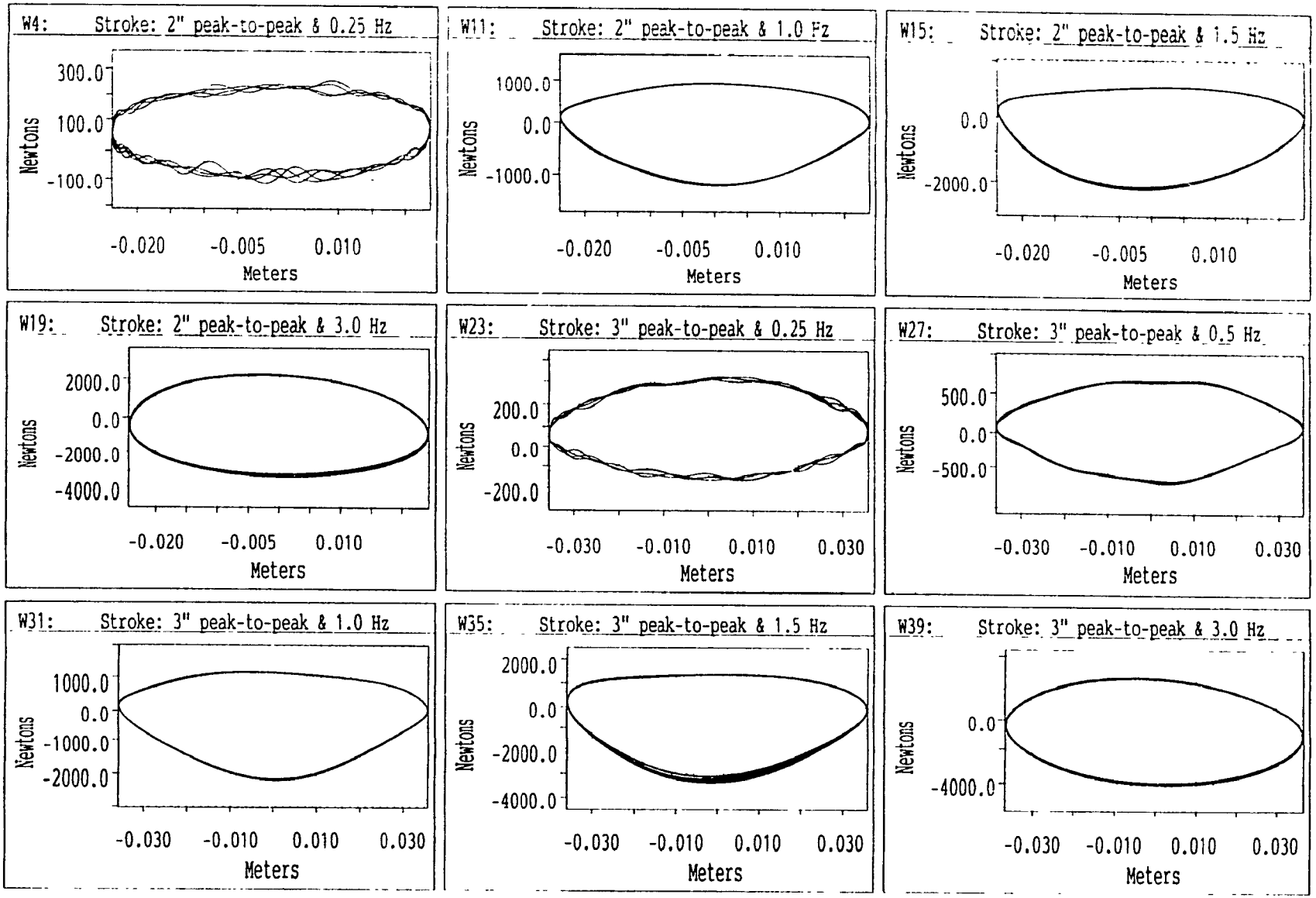


Fig.D.13: Lissajous curves for the damper test (Page 2).

The curves indicate that at high amplitude and high frequencies, the rebound forces are higher than the jounce. This is very critical for the road handling during rebound from pot holes and bump excitations. But the lower jounce forces are needed for ride comfort at large bumps. The curves at the lower velocities which predominantly dictate the performance for the handling like pitch and roll manoeuvres show that the jounce forces are more predominant than the rebound. This would help to stabilize the roll when taking a turn and at the same time does not snap back when returning to neutral position. A higher rebound under these conditions would act in parallel with the recoil forces of the spring and might give an under damped performance of the roll back manoeuvre. Figs. D.14 and D.15 show the Lissajous curves for different p-t-p amplitudes at constant frequency and for different frequencies at constant amplitudes. Both the curves indicate that at lower velocities the jounce forces are higher and as the velocities increase the rebound forces are higher than the jounce. Fig.D.15 shows the damper performance at sprung mass bounce degree of freedom.

The orifice type dampers could be well represented by the force Vs. velocity curves which indicate the constant of proportionality for the dampers. The force extracted by the damper at different frequencies for two different extreme strokes has been indicated in the Fig.D.16. This figure indicates the bleed and blow off characteristics of the damper both in the jounce and rebound strokes. The curves also indicate the threshold velocity at which the blow off occurs. At low velocities the damper indicates the bleed characteristics and hence the higher slope of the curve. But at higher velocity it indicates the blow off characteristics with a larger orifice and hence smaller constant of proportionality. This figure also indicates that damper is designed to give digressive natured characteristics at higher velocities after blow off where the slope increases again. Since the intended test on SDOF involving this damper is performed for a maximum velocity of 0.15 m/sec, an average value of 6250 $\frac{Ns}{m}$ has been used as a nominal value for the adaptive active controller.

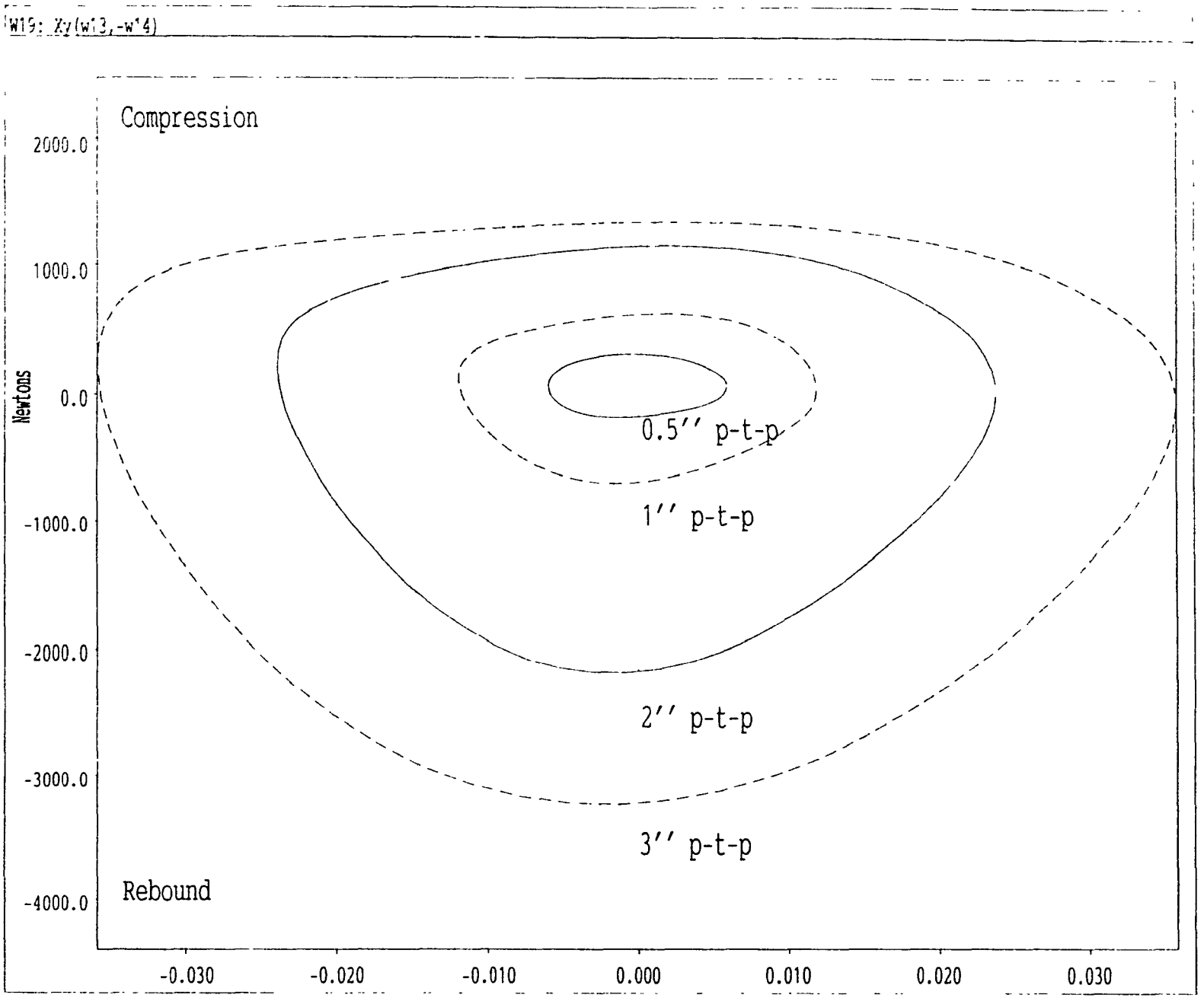


Fig.D.14: Damper force response at constant frequency and different peak-to-peak (p-t-p) amplitudes.

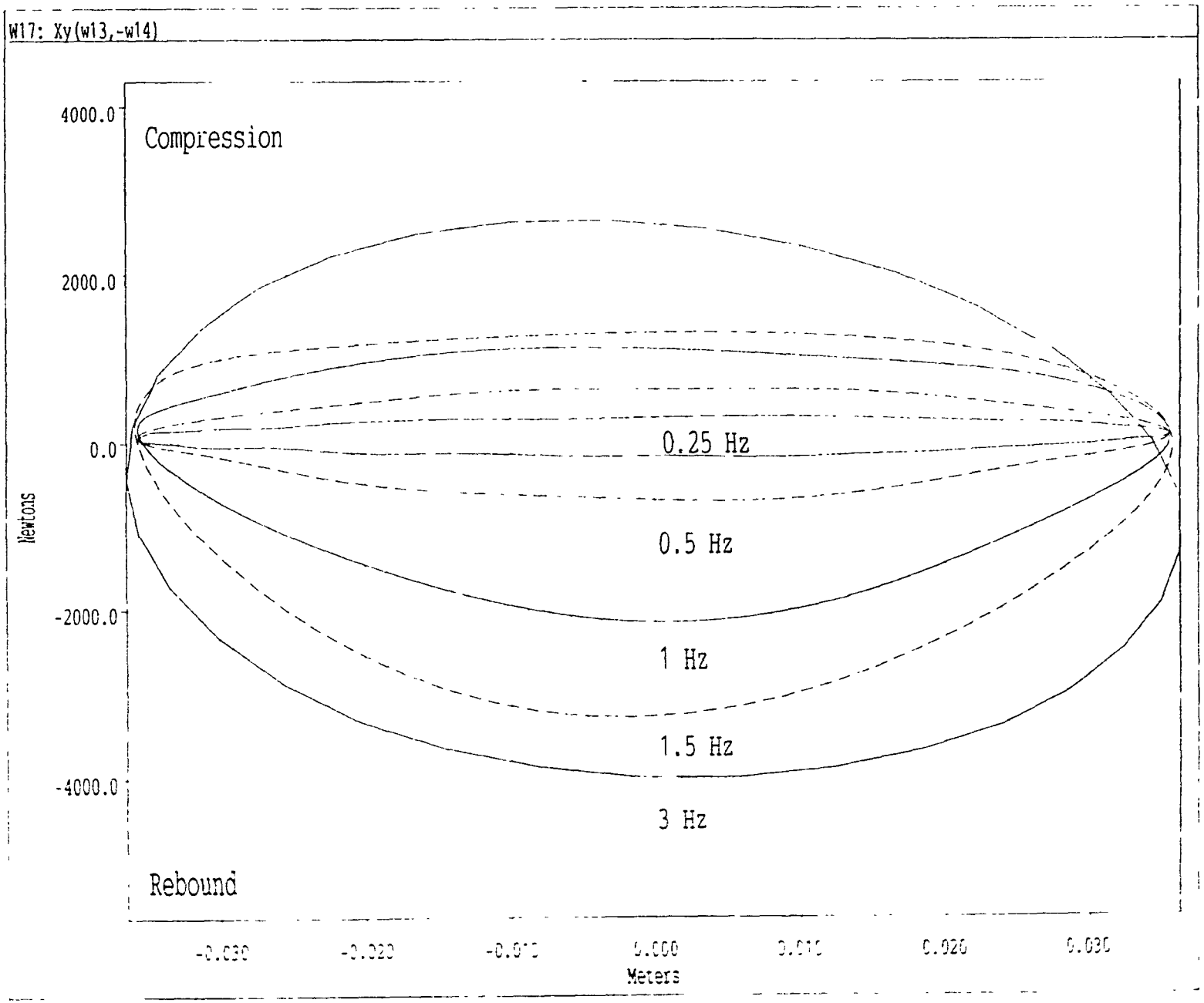


Fig.D.15: Damper force response at constant amplitude and different frequencies.

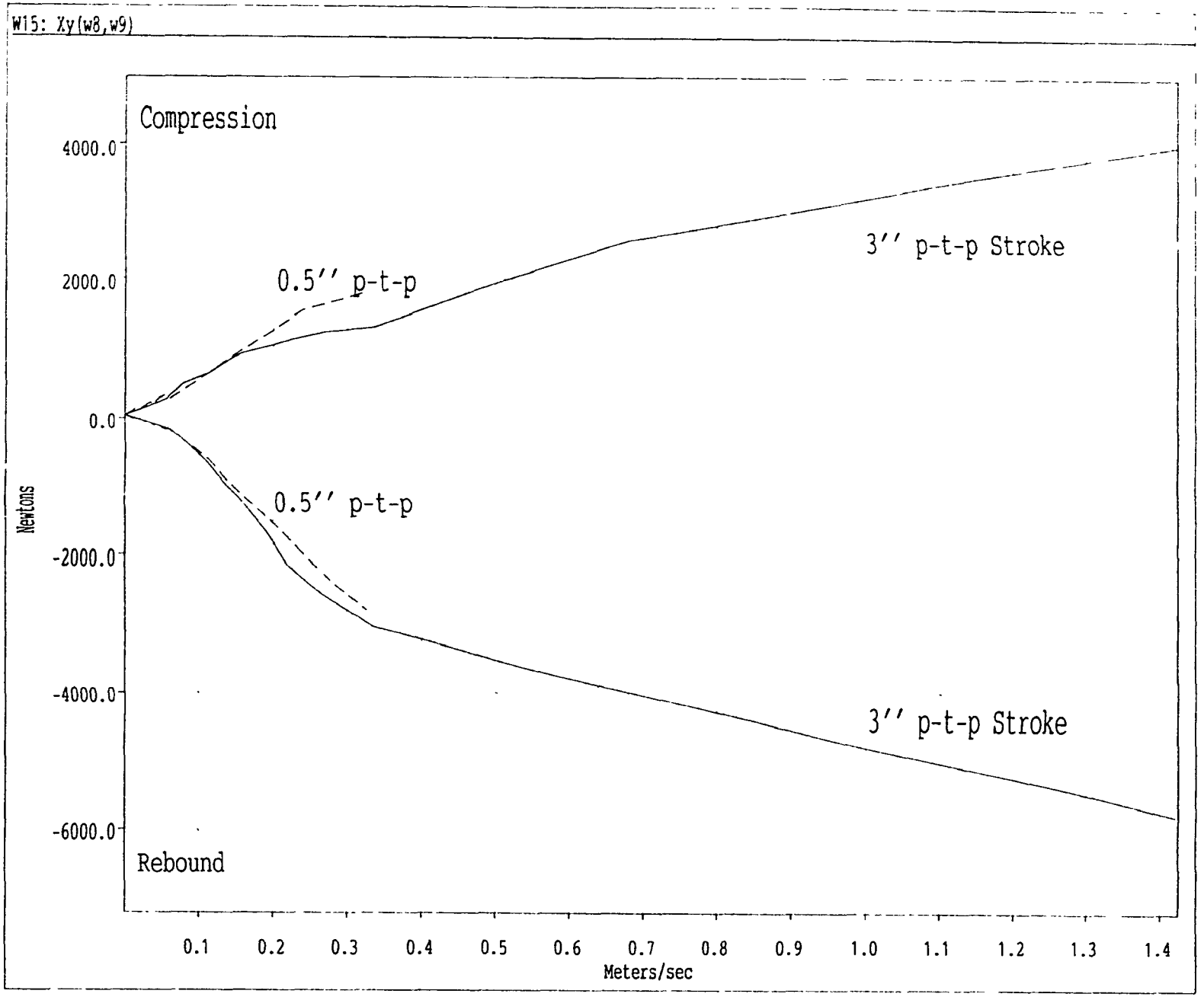


Fig.D.16: Damper force Vs. relative velocity for jounce and rebound.